2023-2024 CALIFORNIA CURRENT ECOSYSTEM STATUS REPORT

A report of the NOAA California Current Integrated Ecosystem Assessment Team (CCIEA) to the Pacific Fishery Management Council

Andrew Leising, Mary Hunsicker, Nick Tolimieri, Greg Williams, Abigail Harley

2024-01-31

TABLE OF CONTENTS

Main Report

Supplementary Materials

1 INTRODUCTION

The 2013 and 2022 Fishery Ecosystem Plans (FEPs) establish a reporting process wherein NOAA provides the Pacific Fishery Management Council (Council) with a yearly update on the status of the California Current Ecosystem (CCE), as derived from environmental, biological, economic and social indicators. NOAA's California Current Integrated Ecosystem Assessment (CCIEA) team is responsible for this report. This is our 12th report, with prior reports in 2012 and 2014-2023.

This report summarizes CCE status based on data and analyses that generally run through 2023 and some that extend into 2024. Highlights are summarized in Box 1.1. Appendices provide additional information or clarification, as requested by the Council and its committees and advisory bodies.

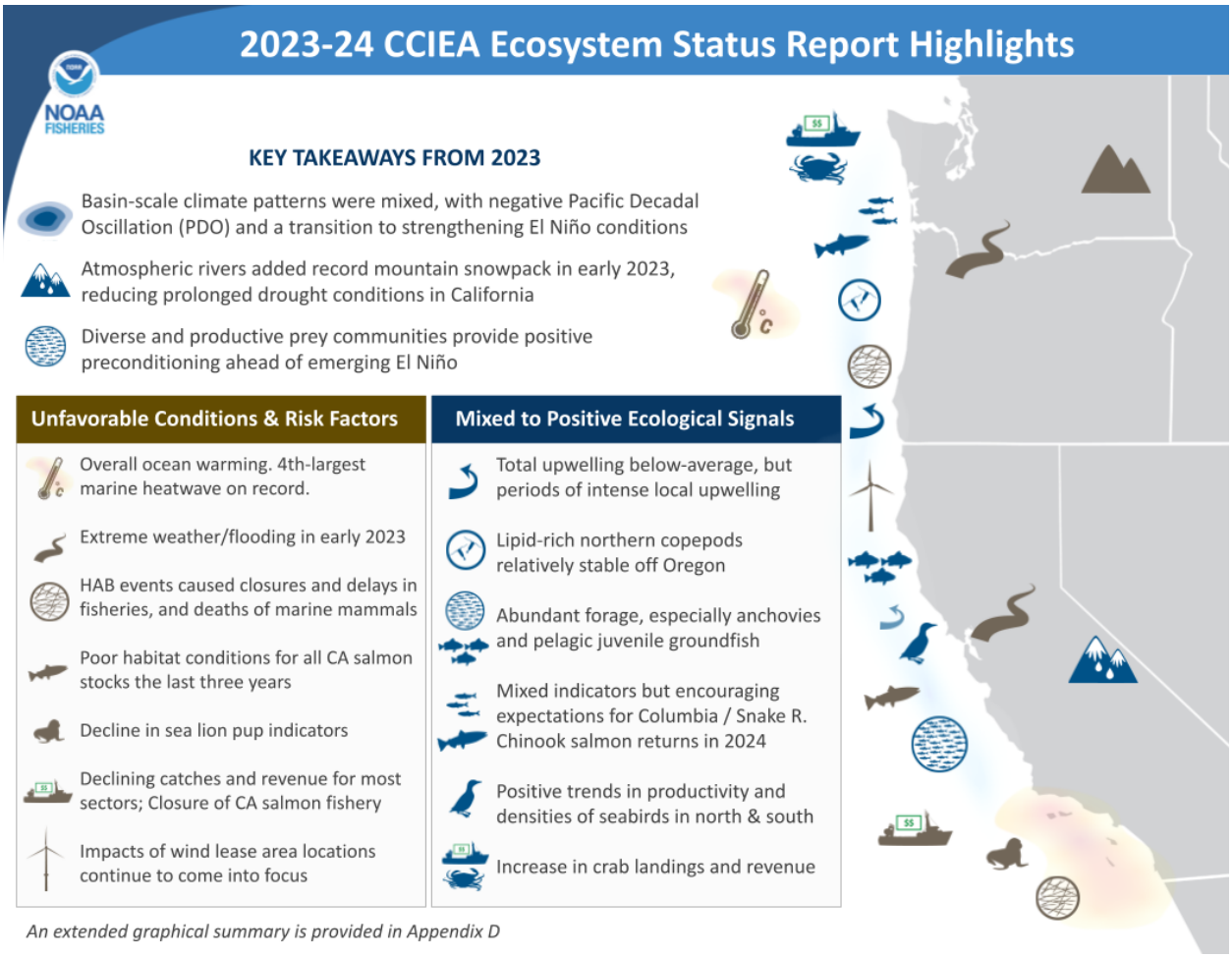

Box 1.1 Highlights of the Ecosystem Status Report indicating major trends and takeaways.

1.1 Sampling Locations

We refer to areas north of Cape Mendocino as the "Northern CCE," Cape Mendocino to Point Conception as the "Central CCE", and south of Point Conception as the "Southern CCE."

Figure 1.1 shows sampling areas for most regional data. Key oceanographic transects are the Newport Line off Oregon, the Trinidad Head Line off northern California, and CalCOFI lines further south, while shaded marine regions indicate sampling areas for surveys. This sampling is complemented by basin-scale oceanographic observations and outputs from models. Figure 1.1 also shows sampling areas for most biological indicators. The shaded terrestrial areas represent freshwater ecoregions in the CCE, and are the basis for summarizing indicators of snowpack, flows, and stream temperatures.

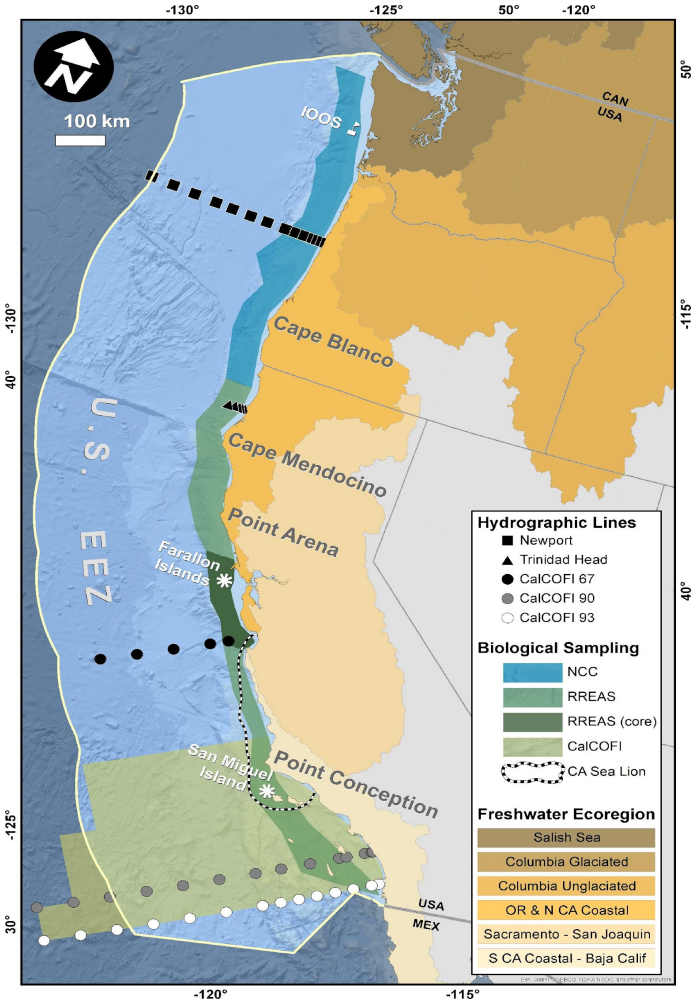

Figure 1.1: Map of most sampling efforts in the California Current Ecosystem (CCE) and U.S. west coast Exclusive Economic Zone (EEZ). Symbols indicate hydrographic line sampling stations for oceanographic data. Shaded ocean regions represent biological sampling areas for the Northern CCE (NCC), which includes the Juvenile Salmon and Ocean Ecology Survey (JSOES); the Rockfish Recruitment and Ecosystem Assessment Survey (RREAS), including its Core Area; and the CalCOFI sampling region. The NCC and RREAS shaded areas, combined, also approximate the survey footprints for NOAA's coastwide CPS acoustic/trawl and groundfish bottom trawl surveys. Dashed line approximates foraging area for adult female California sea lions from the San Miguel colony. Shaded terrestrial areas represent the six freshwater ecoregions in the CCE.

2 CLIMATE AND OCEAN DRIVERS

Since the unprecedented marine heatwave of 2014-16 ("The Blob"), the waters of the Northeast Pacific and most of the California Current have been warmer than normal. One of the larger El Niños on record occurred in late 2015-2016, followed by a brief respite during 2017 and 2018 when conditions were more "normal." Since 2019, there have been large heatwaves offshore each year, typically lasting through late fall, with occasional penetrations into coastal waters in summer through fall. These often have ecological consequences (e.g. HAB events). In 2023, environmental conditions in the CCE again followed this pattern: the heatwave mostly was held offshore by coastal upwelling, which led to cool coastal conditions and high local productivity, although some regions saw significant periods of upwelling relaxation and warming during the summer. In fall 2023, as predicted, we transitioned to a moderately strong El Niño, following three years of La Niña conditions. On land, 2023 again saw high air temperatures and warmer streamflows, but with some temporary drought relief due to high early-year snowpack. These observations are detailed in the following sections.

2.1 Basin-Scale Indicators

We use three indices to characterize large-scale physical ecosystem states in the North Pacific. The Oceanic Niño Index (ONI) describes the equatorial El Niño Southern Oscillation (ENSO). An ONI above 0.5°C indicates El Niño conditions, which often lead to lower primary production, weaker upwelling, poleward transport of equatorial waters and species, and more southerly storm tracks in the CCE. An ONI below -0.5°C means La Niña conditions, which create atmospheric pressure conditions that lead to upwelling-favorable winds that drive productivity in the CCE. The Pacific Decadal Oscillation (PDO) describes North Pacific sea surface temperature (SST) anomalies that may persist for many years. Positive PDOs are associated with warmer SST and lower productivity in the CCE, while negative PDOs indicate cooler SST and are associated with higher productivity. The North Pacific Gyre Oscillation (NPGO), an index of sea surface height, indicates changes in circulation that affect source waters for the CCE. Positive NPGOs are associated with strong equatorward flow and higher salinity, nutrients, and chlorophyll-a in the CCE. Negative NPGOs are associated with decreased subarctic source water and lower CCE productivity.

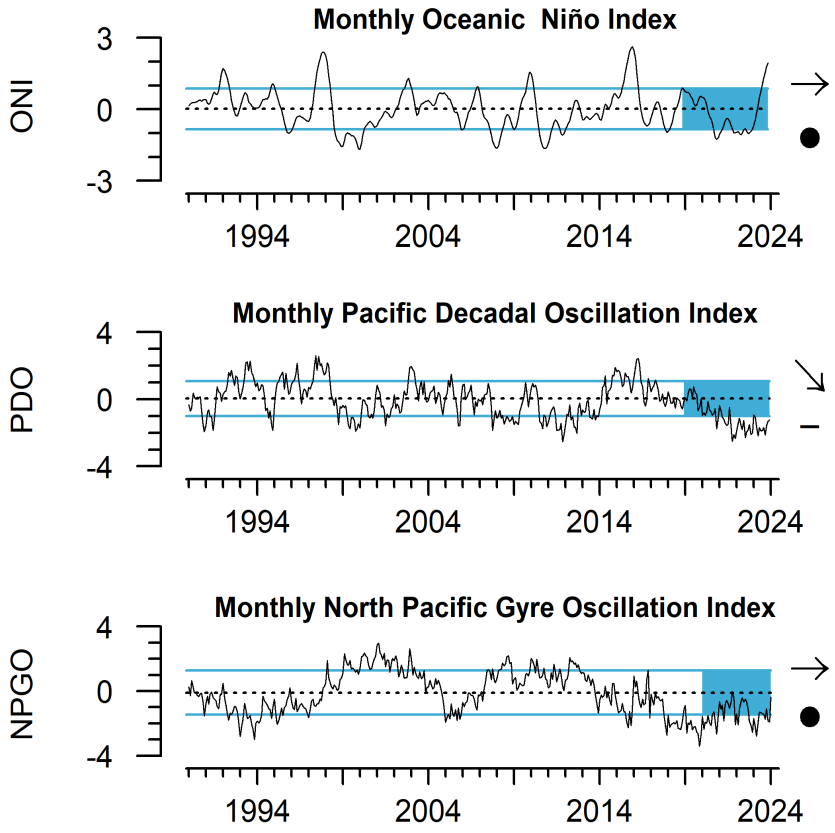

Figure 2.1: Monthly values of the Oceanic Niño Index (ONI), Pacific Decadal Oscillation (PDO), and North Pacific Gyre Oscillation (NPGO) from 1990 - 2024 relative to the mean (dashed line) ±1 s.d. (blue lines) from 1991-2020. The blue shaded area is the most recent 5 years of data. Arrows indicate if the recent 5-year trend is positive (↗), neutral (→), or negative (↘). Symbols indicate if the recent 5-year mean is above the upper blue line (+), within the blue lines (●), or below the lower blue line (−).

Basin-scale indices suggest average conditions for productivity in 2023: the ONI and PDO were negative for most of the year, while the NPGO remained neutral to negative. The negative ONI at the beginning and middle of the year illustrates the La Niña conditions that continued into early 2023 (Fig. 2.1, top), with a transition to strongly positive ONI towards the end of 2023, signaling the incoming El Niño. As of January 2024, we are firmly into what is likely to become a "strong" El Niño state (https://www.cpc.ncep.noaa.gov/). The PDO remained negative for a 4th consecutive year (Fig. 2.1, middle), however, given the most recent distribution of sea surface temperatures, the PDO may shift to positive values (January 2024 values not yet available). After reaching relatively low values in 2019-2020, the NPGO has remained neutral to low (Fig. 2.1, bottom). This indicates that the general circulation in the CCE is likely weaker than average. Taken together, these indices indicate average overall productivity. Seasonal values for all indices are in Appendix F.1.

The northeast Pacific continues to experience large marine heatwaves in surface waters. Far offshore (> 1000km), significant heatwave activity remained from 2022 until April 2023 (Fig. 2.2, left). The 2023 marine heatwave formed in May far offshore, grew in size and proceeded towards the coast during late spring-summer, and reached its maximum size (~7.5 million km^2) on August 29 (Fig. 2.2). It was the 4th largest heatwave by area and the 5th longest in duration since monitoring began in 1982 (Fig. F.9). Note, however, that these recent heatwaves are not as impactful as "The Blob" of 14-16, since recent events do not penetrate as deep (~40-50m vs 140m), and spend less time within the EEZ (weeks to a month vs. months to a year), and our indicator of heatwave size is based solely on surface expression. Similar to 2022, 2023 had many heatwave intrusions into coastal regions during summer and fall, particularly along the WA and OR coasts (Fig. 2.2). These intrusions were related to widespread relaxations in upwelling winds (Fig. 2.4). A short yet significant warming event also occurred off south-central California during late May and into June 2023 (Fig. 2.2; Fig. F.8), which was not connected to the larger offshore marine heatwave, but was driven by similar large-scale atmospheric patterns. This heatwave coincided with the marine mammal mortality event in that area (Section 3.8, Appendix O). Additional information on the 2023 marine heatwave is in Appendix F.2.

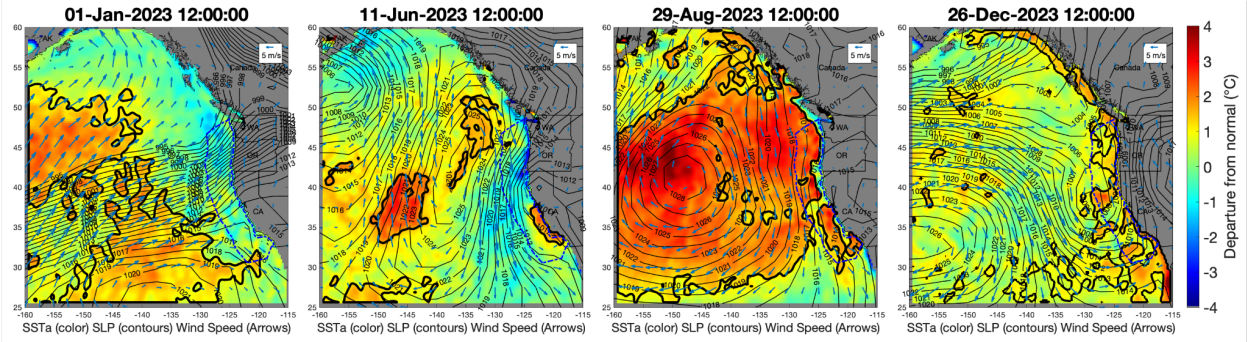

Figure 2.2: Progression of the 2023 marine heatwave in the northeast Pacific Ocean. Colors represent standardized SST anomalies. Heavy black lines denote regions that meet the criteria for a marine heatwave (see Appendix F.2). Gray contours represent sea level pressure (in hectoPascals) and arrows represent wind speed and direction.

Subsurface temperatures (>50m depth) were average in 2023 along much of the West Coast, supporting the observations that the heatwave this year did not penetrate very deeply in the water column, and thus lessening its potential impacts. Off Newport, Oregon, temperatures in the upper 50 m were ~2 to 3.0°C warmer than average on a few very brief occasions during summer (Fig. 2.3, top), coinciding with intrusions of the marine heatwave. Off Monterey and within the CalCOFI sampling region off southern California, surface temperatures followed a similar pattern, with relatively cooler water in the winter and spring, followed by warmer than average temperatures during the summer and fall due primarily to heatwaves (Fig. F.5), whereas subsurface temperatures remained near average.

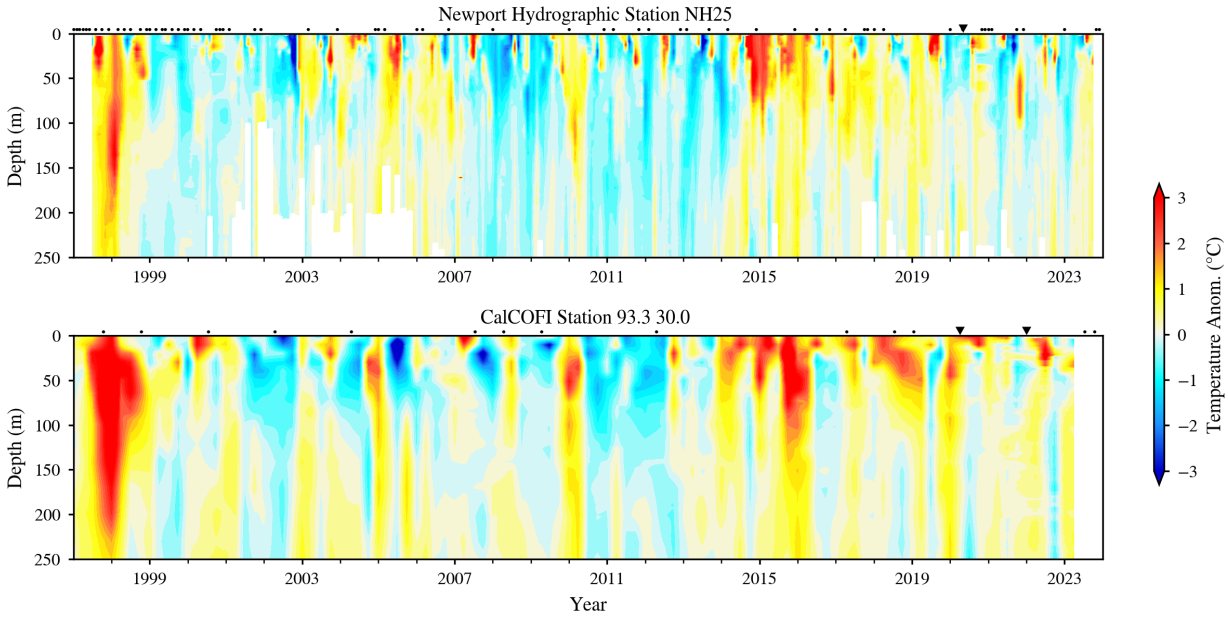

Figure 2.3: Time-depth temperature anomalies at Newport station NH25 and CalCOFI station 90.30, from 1997 through early-mid 2023. Transect locations are in Fig. 1.1.

2.2 Upwelling and Habitat Compression

Upwelling is a major driver of coastal productivity in the CCE. It occurs when equatorward coastal winds force deep, cold, nutrient-rich water to the surface. The greatest upwelling in the CCE occurs off central California and typically peaks in June. Here, we present two upwelling indices: vertical flux of water (Cumulative Upwelling Transport Index; CUTI) and of nitrate (Biologically Effective Upwelling Transport Index; BEUTI) (Jacox et al. 2018).

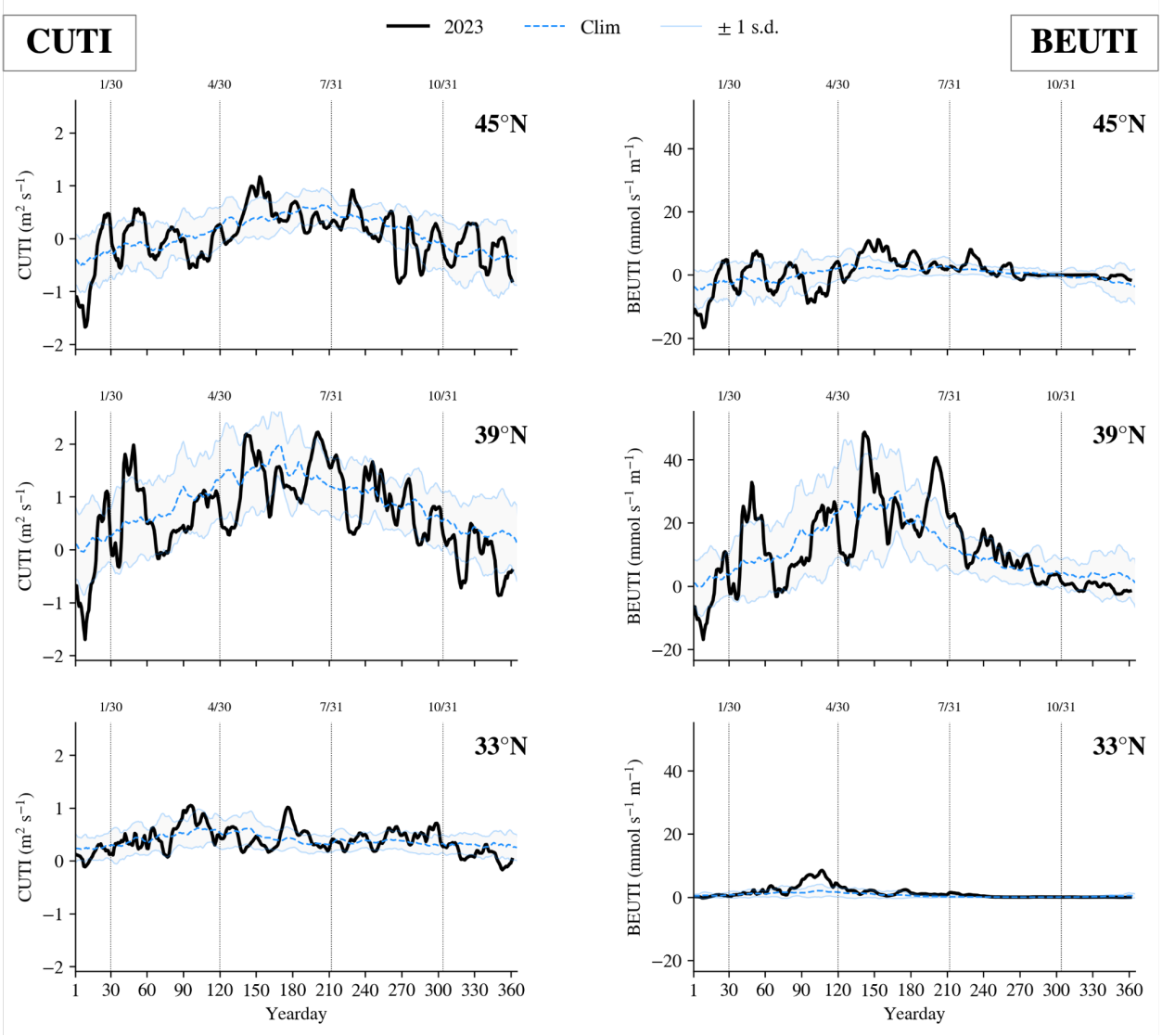

Figure 2.4: Daily estimates of vertical transport of water (CUTI, left) and nitrate (BEUTI, right) in 2023, relative to the 1988-2023 climatological average (blue dashed line) ±1 s.d. (shaded area), at latitudes 33°N (San Diego), 39°N (Pt. Arena), and 45°N (Newport).

Overall, 2023 saw lower total integrated upwelling compared to previous years (Fig. F.8), except for the southernmost region. However, upwelling events were highly variable in strength and timing, consisting of periods of strong upwelling interspersed with periods of significant upwelling relaxation, or even downwelling (Fig. 2.4). For example, in the central region, total upwelling was below average, but there was a period in the late winter with prolonged, strong upwelling 1 s.d. above the climatological average (Fig. 2.4), and then several additional periods of strong upwelling during late spring and summer. In the south, upwelling was slightly higher in the spring, but average during the remainder of the year. This is in contrast to 2022, when upwelling totals were average or above average, but with a higher frequency of relaxation events. Upwelling relaxation events allow for retention of

nutrients that can spur coastal production, but also during the summer and fall allow for offshore marine heatwaves to penetrate into the nearshore coastal waters. The strong early upwelling during 2023 likely led to a spike in early productivity.

Santora et al. (2020) developed the habitat compression index (HCI) to describe how much cool, productive water is available adjacent to the coast. HCI ranges from 0 (poor = complete coverage of warm offshore water in the region) to 1 (good = cool water fully extending 150 km from the coast). In general, cool coastal habitat has been expanding off central California in winter and spring since 2016 (Fig. 2.5). During 2023, there was a decrease in HCI (less cool, productive water) during summer and into fall, marking the arrival of the heatwave into the coastal regions, and presaging the arrival of El Niño conditions (Appendix F.3).

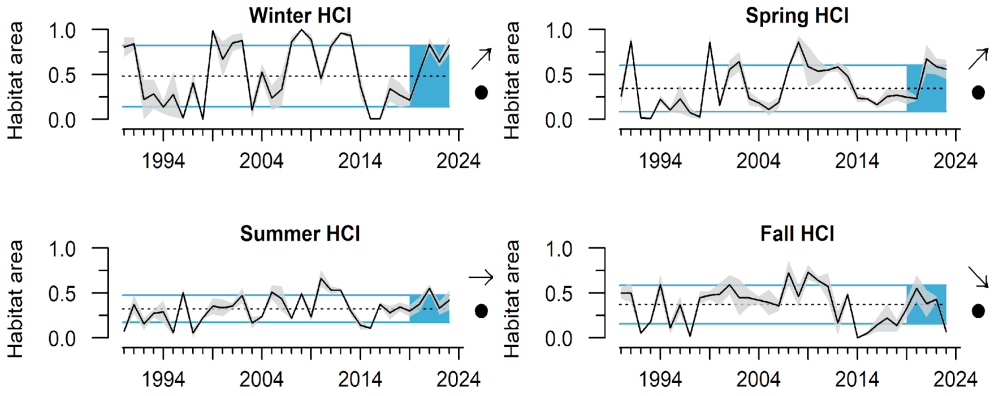

Figure 2.5: Mean habitat compression index (HCI) off central California in winter (Jan-Mar), spring (Apr-Jun), summer (Jul-Sep), and fall (Oct-Dec) for 1990 - 2023. Habitat area is the fraction of coastal habitat that is cooler than the threshold (higher values indicate less compression). Gray envelope indicates ±1 s.e. Lines, colors, and symbols are as in Fig. 2.1.

2.3 Hypoxia and Ocean Acidification

Dissolved oxygen (DO) is influenced by processes such as currents, upwelling, air-sea exchange, primary production, and respiration. Low DO (aka hypoxia, concentrations < 1.4 ml DO/l) can compress habitat and cause stress or die-offs in sensitive species (Chan et al. 2008). Expanding our coverage of near-bottom DO conditions, this year we added a new location to our analysis; CE07, a bottom moored instrument on the shelf off coastal WA, (denoted by IOOS symbol on Fig. 1.1), maintained by the NSF Ocean Observatories Initiative (2024). This location typically shows hypoxic conditions during the summer. During 2023, the hypoxic period began earlier than normal, but was not as sustained as in 2021 or 2022 (Fig. 2.6, top). Conditions were better to the south, as the nearshore station NH05 off Newport, Oregon did not experience hypoxic conditions as it did during previous years (Fig. 2.6, bottom). This highlights the value of adding the WA shelf location: viewing only the OR data could lead to the conclusion that bottom DO was suitable throughout this region. Additional DO data including the CalCOFI region are in Appendix F.4.

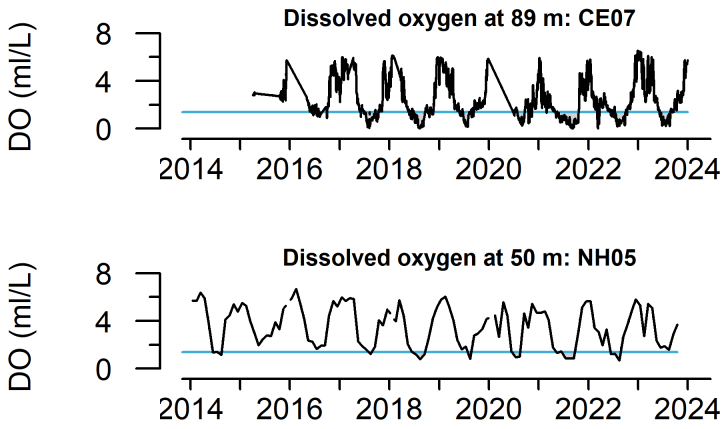

Figure 2.6: Near-bottom dissolved oxygen off Grays Harbor, WA (CE07) and Newport, OR (NHO5), from 2014 - 2023. Blue lines indicate the hypoxia threshold (1.4 ml DO/L).

Ocean acidification, caused by increased anthropogenic CO_2, reduces pH and dissolved carbonate in seawater and is stressful to many marine species (Feely et al. 2008; Busch and McElhany 2016). Aragonite saturation, an indicator of pH, showed the typical seasonal pattern off coastal OR during 2023 (Fig. 2.7, further details in Appendix F.4).

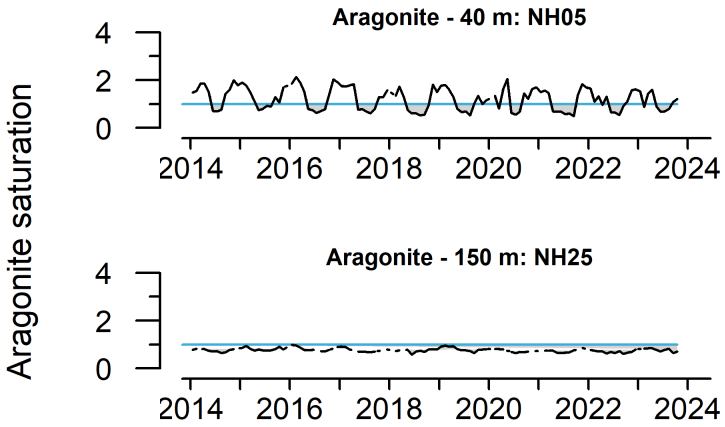

Figure 2.7: Aragonite saturation states off of Newport, OR from 2014 - 2023. Blue lines indicate the biological threshold for aragonite saturation state (1.0).

2.4 Snowpack and Hydrology

Snow-water equivalent (SWE) is the water content in snowpack, supplying cool freshwater to streams from spring through fall that is critical for salmon production (Appendix J, Appendix G). Snowpack in 2023 in California mountain ranges was immense. Winter storms created very high snowpack (>200% of the 30-year median) in California, and subsequent snowmelt replenished reservoirs and removed drought conditions. Snowmelt also caused major flooding, and resulted in the reformation of Tulare Lake in the southern

Central Valley. Oregon also experienced high snowpack, resulting in > 200% median SWE at most Oregon monitoring stations. Snowpack was more moderate in Washington and Idaho, ranging from 75%-over 200% of median SWE (Fig. 2.8). High snowpack persisted into May and led to large declines in drought conditions for much of the Pacific Coast. During a warm summer, however, portions of the Pacific Northwest experienced increasing drought conditions. By the end of the water year in September 2023, 44% of Washington, Oregon, and Idaho was experiencing at least moderate drought conditions (D1 or higher levels of the U.S. Drought Monitor index), while California levels had declined to <0.2% from a high of nearly 100% in December 2022.

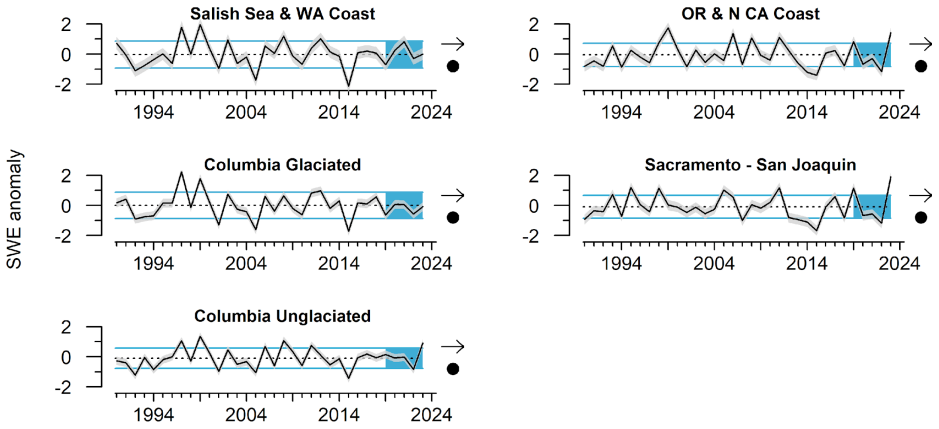

Figure 2.8: Anomalies of April 1st snow-water equivalent (SWE) in freshwater ecoregions of the CCE, 1990 - 2023. Error envelopes represent 95% credible intervals. Lines, colors and symbols are as in Fig. 2.1. Ecoregions are mapped in Fig. 1.1.

As of January 30, 2024, SWE outlook for the West is uncertain: with a strong El Niño, winter precipitation forecasts are above normal for California and normal to below normal for the Pacific Northwest. Recent winter storms have boosted precipitation in Washington and Oregon, but due to the warm El Niño conditions, much of the precipitation is not falling as snow or leading to snow accumulation. Additional details on SWE and drought outlooks for 2024 are available in Appendix G.

Across ecoregions, freshwater conditions were mixed in 2023; both minimum and maximum streamflows remained within one standard deviation of average levels, while summer temperatures were warm in all regions but the Salish Sea (Appendix G). Both maximum and minimum flows show evidence of widespread recent lows (Fig. 2.9), although the recent average was significant (did not overlap with 0) for only two ecoregions for minimum flows. Recent trends have largely been positive for maximum flows, but minimum flows have trended negative. Recent average maximum August temperatures were significantly above average in five of six ecoregions, and have trended higher in recent years, illustrating widespread challenging summer stream conditions for salmon and other freshwater species.

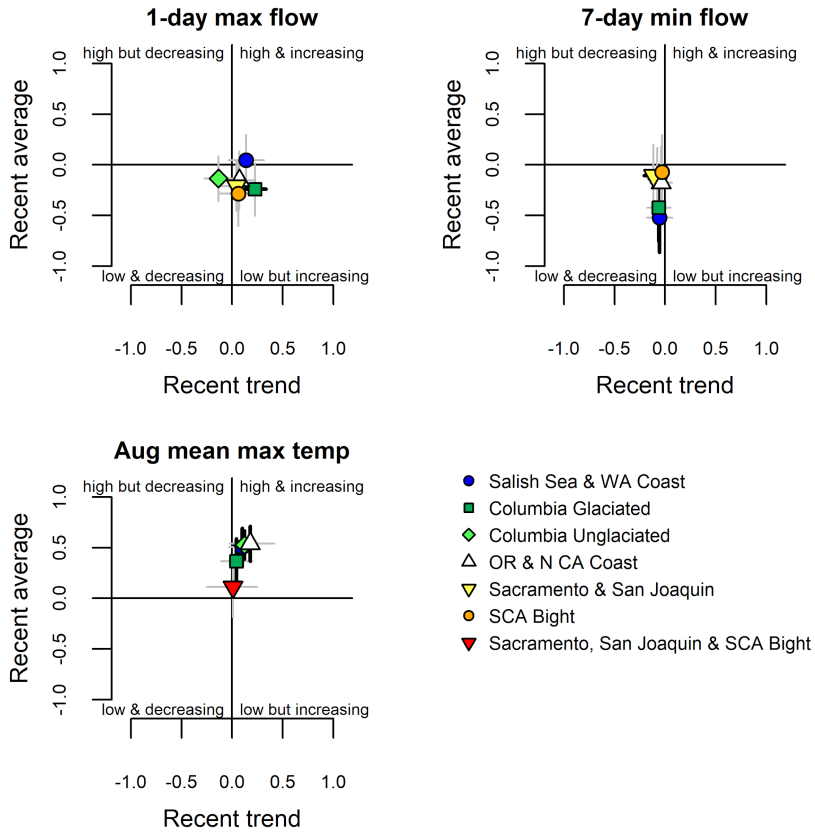

Figure 2.9: Recent (2019-2023) averages and trends in maximum and minimum flow in streams within six freshwater ecoregions. Symbols for each ecoregion fall into quadrants based on recent average (high or low) and recent trend (increasing or decreasing) relative to long-term data (1980-present). Error bars represent 95% credible intervals. Heavy black error bars represent significant differences from zero. Ecoregions are mapped in Fig. 1.1.

3 FOCAL COMPONENTS OF ECOLOGICAL INTEGRITY

La Niña and negative PDO conditions persisted into early 2023 supporting mixed to good conditions for marine productivity, though some ecological indicators reflect less favorable conditions. The forage community was diverse and productive. Anchovy remained highly abundant in the Central and Southern CCE and were a key prey source for many top predators. Juvenile groundfishes were also abundant, with notable increases in young rockfishes in the Central and Northern CCE. Recent ocean conditions for Chinook salmon returning to the Columbia Basin indicate average returns in 2024, while less-favorable indicators for adult salmon returning to California river basins suggest low returns for some cohorts. Impacts of ENSO were not obvious in the ecological indicator time series, as these surveys are from before (spring-fall 2023) the CCE typically would be impacted by El Niño (winter 23/24).

3.1 Copepods and Krill

Copepod biomass anomalies represent variation in northern copepods (cold-water crustacean zooplankton species rich in wax esters and fatty acids) and southern copepods (smaller species with lower fat content and nutritional quality). Northern copepods usually dominate the summer zooplankton community along the Newport Line (Fig. 1.1), while southern species dominate winter. Positive northern copepod anomalies generally correlate with stronger returns of Chinook salmon to Bonneville Dam and coho salmon to coastal Oregon (Peterson et al. 2014). Historically, northern copepods typically have been favored by La Niña and negative PDO conditions (Keister et al. 2011; Fisher et al. 2015).

Lipid-rich northern copepods were relatively stable along the Newport Hydrographic Line throughout 2023. However, their biomass was not as high as in recent years, and the spring-summer northern biomass anomaly was average compared to the overall 26-year time series (Fig. 3.1, top). Southern copepod biomass was below average during spring-summer of 2023, however negative biomass anomalies were not as strong as in the previous two years (Fig. 3.1, bottom). These indicators suggest average feeding conditions for pelagic fishes off central Oregon in 2023.

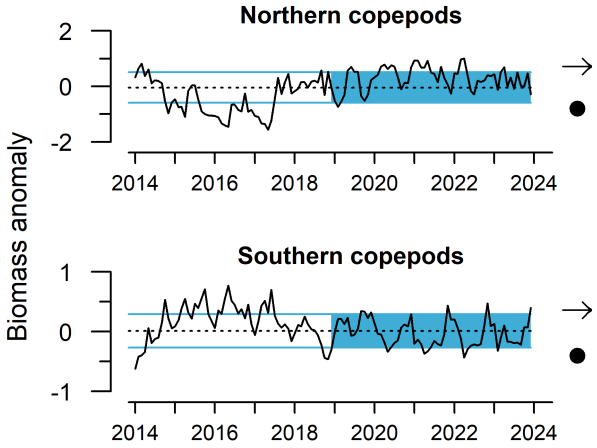

Figure 3.1: Monthly northern and southern copepod biomass anomalies from station NH05 off Newport, OR from 2014 - 2023. Positive values indicate above-average biomass, and negative values indicate below-average biomass. Lines, colors, and symbols are as in Fig. 2.1.

Krill are among the most important prey in the CCE. The krill *Euphausia pacifica* is sampled year-round along the Trinidad Head Line off northern California (Fig. 1.1). Mean adult length and total biomass of *E. pacifica* indicate productivity at the base of the food web, krill condition, and energy content for predators (Robertson and Bjorkstedt 2020). Despite the presence of large krill on one cruise in early 2023, krill length varied around the long-term mean and, similar to 2022, did not exhibit any strong seasonal trends (Fig. 3.2, top). Biomass of *E. pacifica* was low throughout winter 2022/23 and peaks during spring and summer were intermittent and brief (Fig. 3.2, bottom).

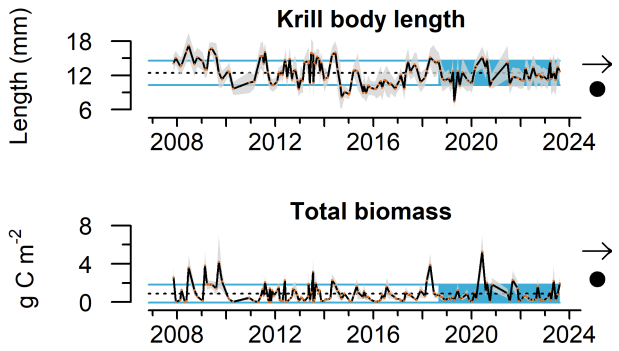

Figure 3.2: Monthly mean E. pacifica length (top) and total E. pacifica biomass (bottom) off Trinidad Head, CA, 2007 - 2023. Gray envelopes indicate ± 1.0 s.d. Lines, colors, and symbols are as in Fig. 2.1.

Krill were also quantified using acoustic backscatter data (see Phillips et al. 2022) during the biennial Joint U.S.-Canada Pacific Hake Ecosystem and Acoustic Trawl (PHEAT) Survey, conducted June-September 2023 from Point Conception to British Columbia. The nautical-area-backscattering coefficient (NASC), which represents relative krill abundance between 50-300 m depth, indicated that most krill were located near the 200-m shelf break off northern California and Oregon (Eureka and Columbia regions), with less krill observed south of Cape Mendocino (Fig. 3.3, Appendix H.). Total krill abundances in 2023 were the second lowest since the start of the time series in 2007 (Fig. 3.3).

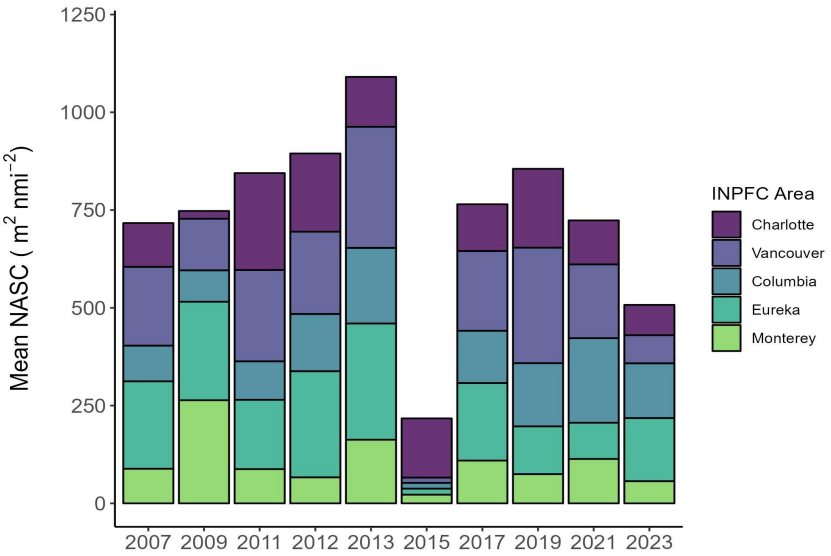

Figure 3.3: Regional abundance of krill in the California Current, based on biannual hydroacoustic sampling. Relative krill abundance is proportional to the mean nautical-area-backscattering coefficient (NASC) plotted by five historic International North Pacific Fishery Council management areas.

3.2 CPS and Regional Forage Availability

3.2.1 Coastwide Coastal Pelagic Species (CPS)

The NOAA CPS survey estimates the abundance and distribution of CPS in the coastal region from Vancouver Island to San Diego, and at times to Baja California. The central stock of anchovy resurged in 2015, reaching ~2.75 million tons in 2021 and remains highly abundant through 2023 (Fig. 3.4; Stierhoff et al. 2023a, Stierhoff et al., in prep). The northern stock of Pacific sardine dominated CPS biomass from 2008-2013 and has been fluctuating at low levels since then, while the southern stock increased to above 100 kilotons in recent years (Fig. 3.4). Jack mackerel abundance trended up from 2017 through 2022 and declined in 2023 (but see Appendix I). Pacific mackerel remained low throughout the time series. Information on spatial distributions and other CPS data are in Appendix I.

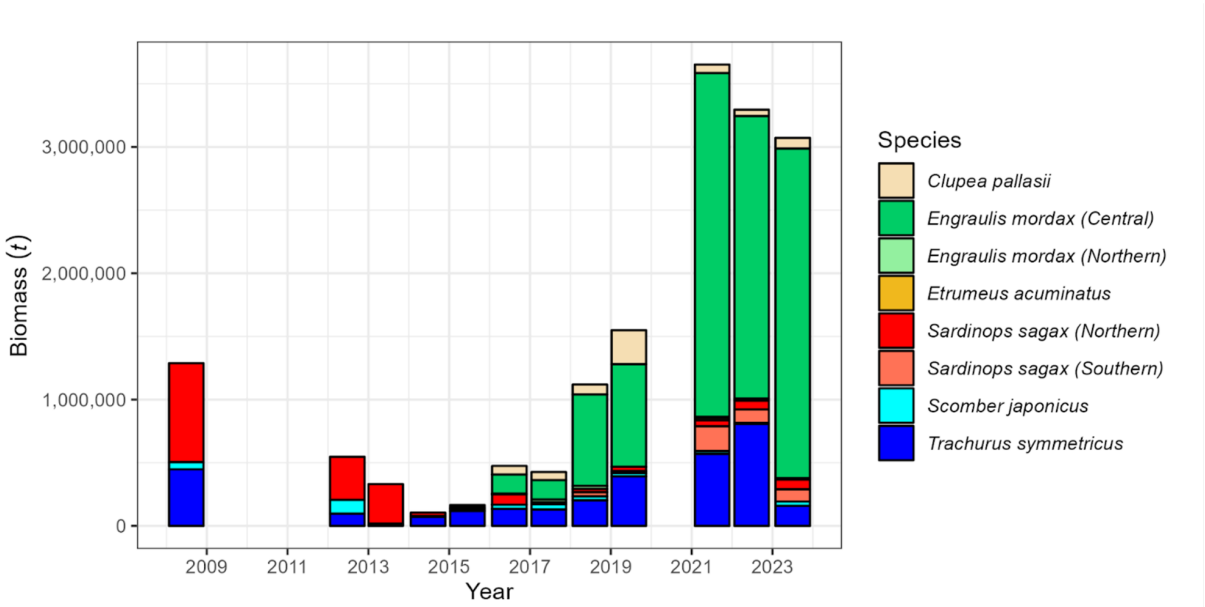

*Figure 3.4: Cumulative estimated biomass for Pacific herring (*Clupea pallasii*), northern anchovy (*Engraulis mordax*), round herring (*Etrumeus acuminatus*), Pacific sardine (*Sardinops sagax*), Pacific mackerel (*Scomber japonicus*), and jack mackerel (*Trachurus symmetricus*) within the summer CPS survey areas, 2008-2023. Note: 2023 data are preliminary and subject to change.*

3.2.2 Regional forage composition

The regional surveys that produce CCE forage data use different gears and survey designs, making regional comparisons difficult. Thus, cluster analysis methods are used to identify regional shifts in forage composition (Thompson et al. 2019a). 2023 data indicate that regional forage assemblages have been consistent over the past five years.

Northern CCE: The JSOES survey off Washington and Oregon (Fig. 1.1) targets juvenile salmon in surface waters, and also samples surface-oriented fishes, squid, and jellies. The composition of this near-surface community has changed since the onset of marine

heatwaves in 2014-2016, but has remained relatively similar since 2018 (Fig. 3.5). The 2023 assemblage was characterized by moderate abundances of sea nettle, moon jelly, market squid and pompano, and high abundances of water jelly, 'young-of-year' (YOY) sablefish and juvenile salmon. This excludes yearling Chinook and juvenile sockeye salmon which were low in abundance. Juvenile salmon time series are discussed further in Section 3.3, and data for the remaining species are in Appendix H.1. The northern portion of the RREAS survey (Fig 1.1) also observed high abundances of YOY rockfishes and relatively low abundances of market squid and krill.

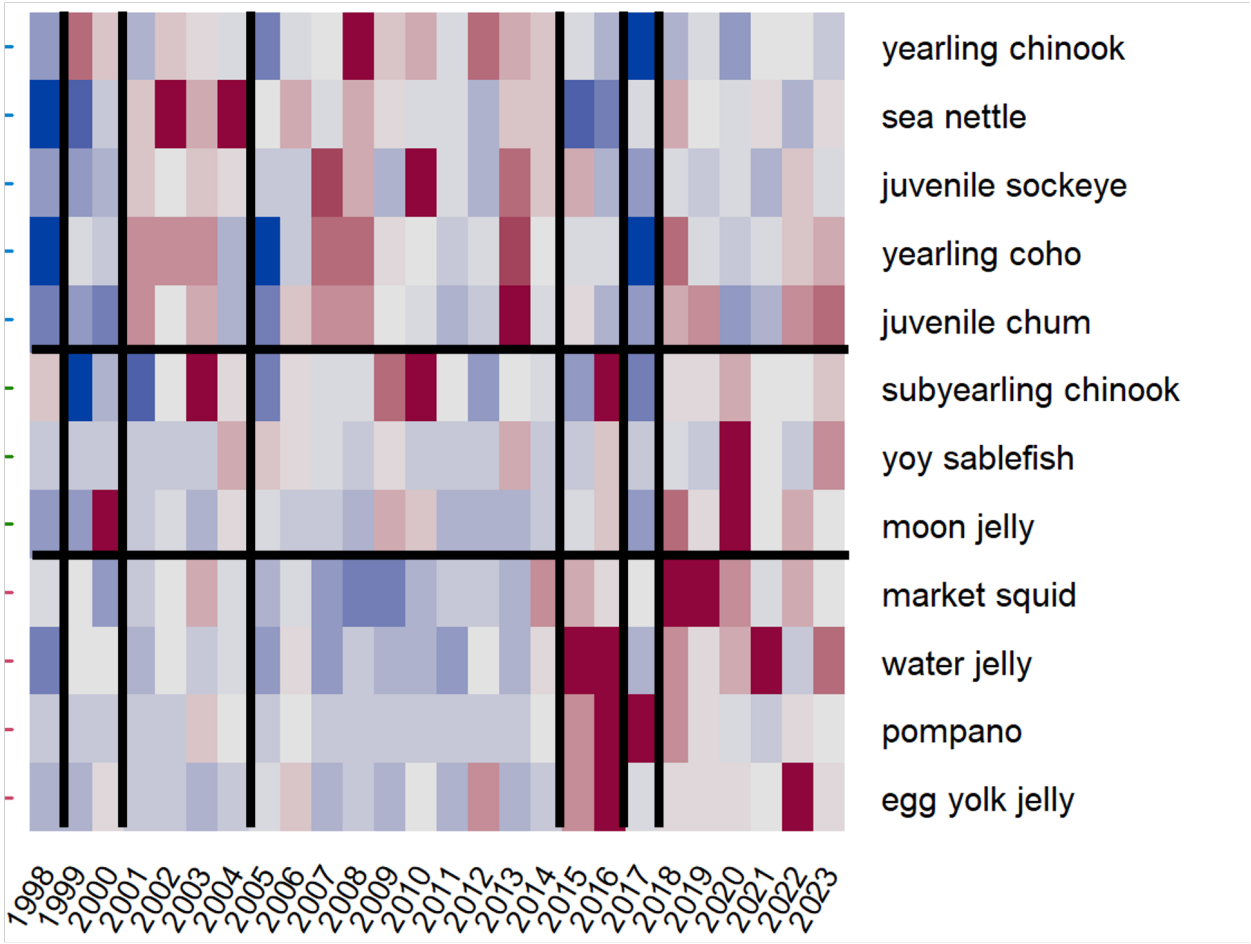

Figure 3.5: Cluster analysis of pelagic community indicators in the Northern CCE, 1998-2023. Colors indicate relative catch per unit effort (red = abundant, blue = rare). Horizontal bars separate clusters of typically co-occurring species. Vertical bars demarcate breaks in assemblage structure between years.

Central CCE: Data in Figure 3.6 are from the "Core Area" of the nearly coastwide RREAS survey (Fig. 1.1) that targets pelagic YOY rockfishes, and samples other pelagic species. The forage assemblage in this area, centered just off Monterey Bay, has been relatively consistent since 2019 (Fig. 3.6). In 2023, adult anchovy continued to be highly abundant, and adult sardine increased to moderate abundance levels. The anchovy and sardine results in this region are consistent with findings from the coastwide CPS survey in 2023

(Fig. 3.4). Catches of YOY anchovy were below average and YOY sardine continued a four-year trend of low abundance. Catches of juvenile rockfish, which were high from 2013-2017 and declined between 2018-2021, increased to above average abundance in 2023. Time series of these data are in Appendix H.2. Also notable in this survey was the high abundance of pyrosomes and crab megalopae; other surveys noted abundant crab megalopae in northern regions of the CCE as well (see Appendix H).

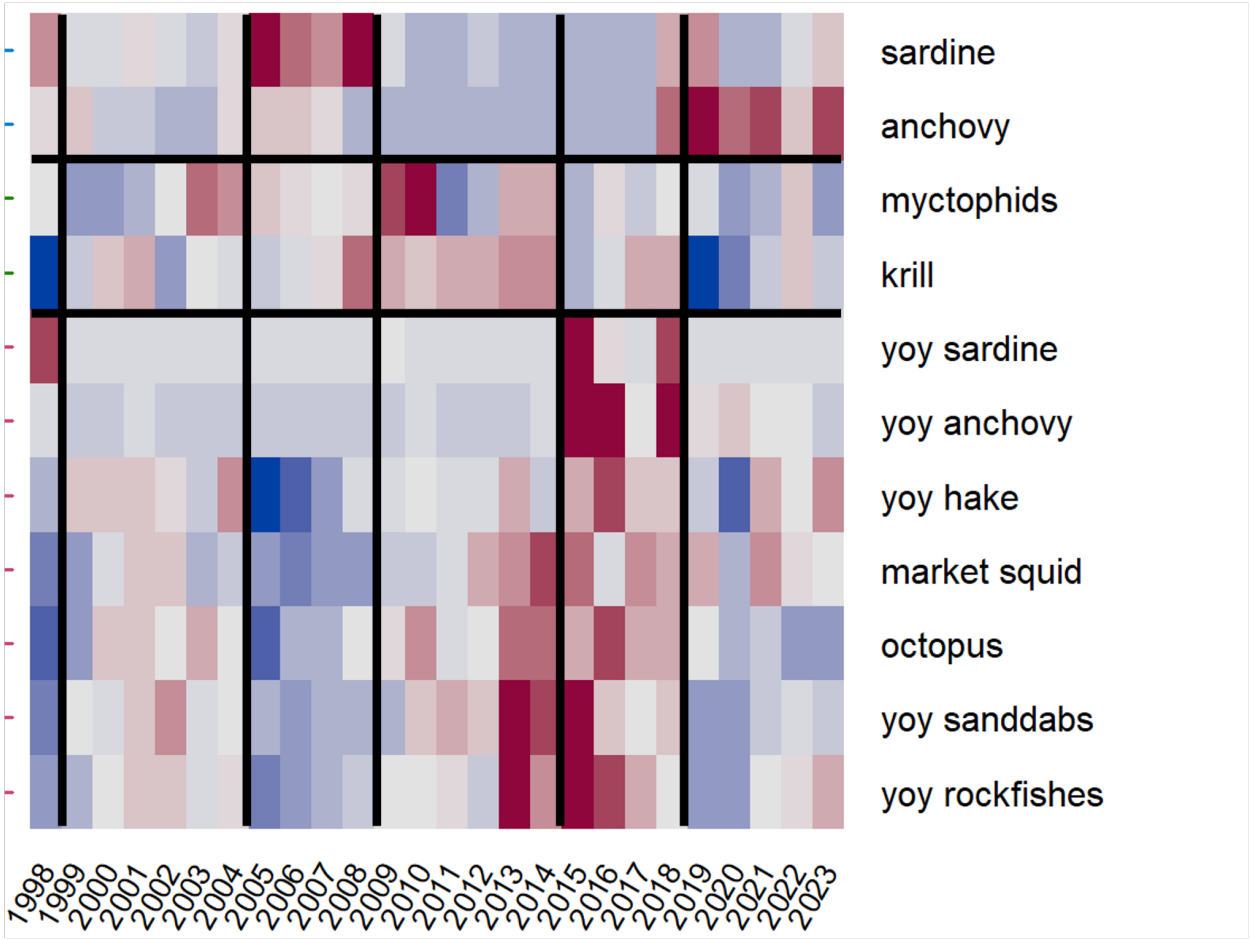

Figure 3.6: Cluster analysis of forage indicators in the Core Area of the Central CCE, 1998-2023. See Figure 3.4 for how to interpret the plot.

Southern CCE: Forage data for the Southern CCE are from spring CalCOFI larval fish surveys (Fig. 1.1). The spring 2023 assemblage clustered with assemblages of 2017-2022 (Fig. 3.7; no data for 2020). These years were characterized by very high abundances of larval anchovy, California smoothtongue, and southern mesopelagics. Sardine have been rare since 2011 and larval abundance remained below average in 2023, despite recent increases of adult sardine in the nearshore in the Southern California Bight (Fig. 3.4). In contrast, hake larvae were above average for the second consecutive year and at their highest abundance since 2011. Market squid and jack mackerel were both highly abundant in 2022, but declined to below average and average levels, respectively, in 2023. Time series of CalCOFI data are available in Appendix H.3.

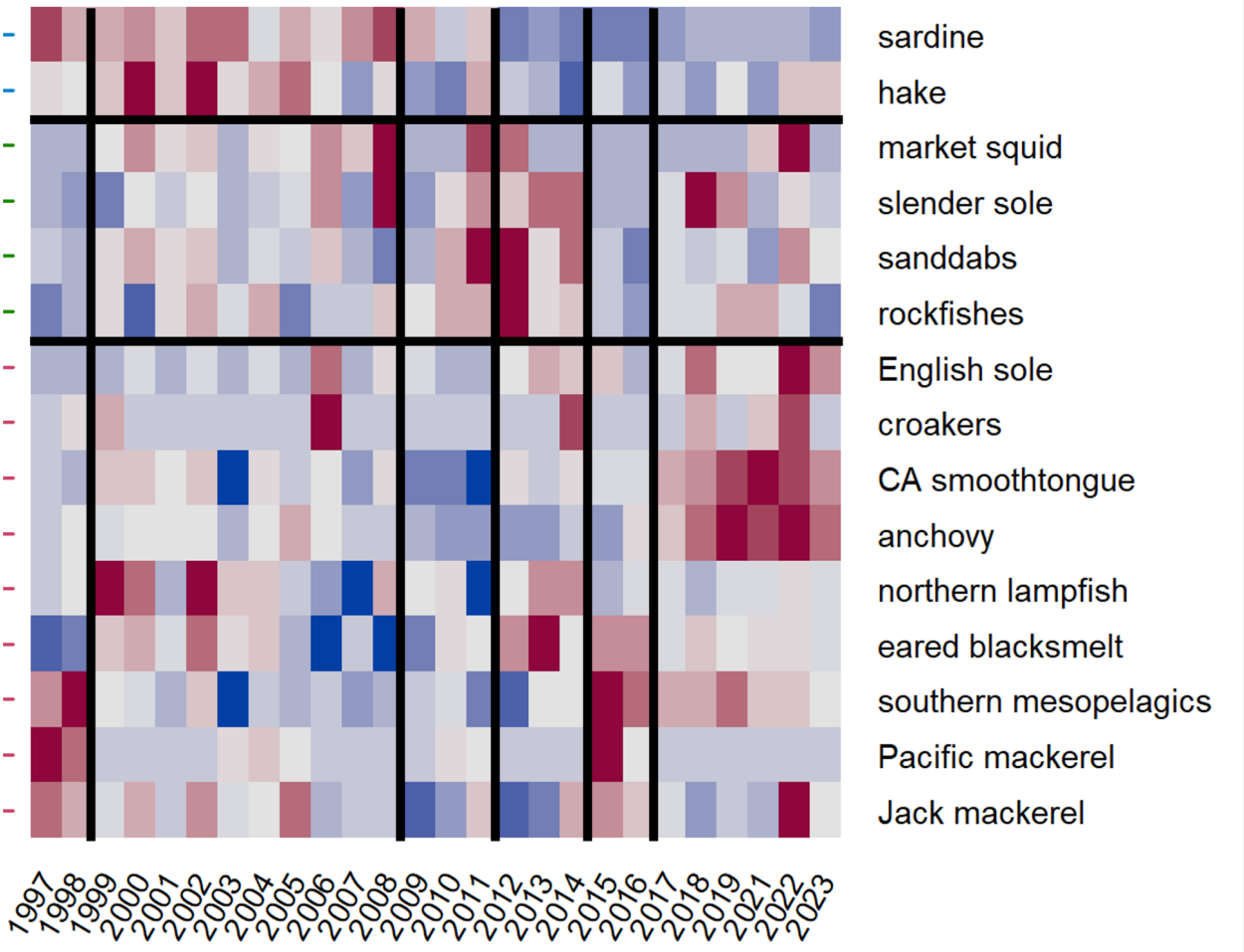

Figure 3.7: Cluster analysis of forage indicators in the Southern CCE, 1998-2023 (no data in 2020). See Figure 3.4 for how to interpret the plot.

3.3 Salmon

Juvenile salmon abundance: Catches of juvenile coho and Chinook salmon from June surveys in the Northern CCE (Fig. 1.1) indicate salmon survival during their first few weeks at sea. In 2023, catch-per-unit-effort (CPUE) of juvenile subyearling Chinook salmon and juvenile yearling Chinook salmon were close to time series averages, whereas catches of juvenile yearling coho salmon increased to above average (Fig. 3.8). Catches of juvenile coho salmon in these surveys over the past five years show an increasing short-term trend.

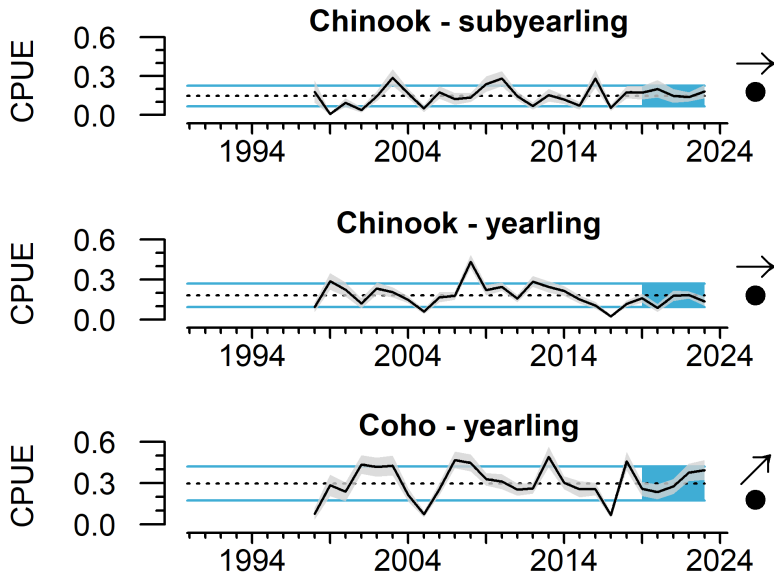

Figure 3.8: Catch per unit effort of juvenile salmon off Oregon and Washington in June, 1998 - 2023. Gray envelope indicates ±1 s.e. Lines, colors, and symbols are as in Fig. 2.1.

Stoplight tables: Long-term associations between oceanographic conditions, food web structure, and salmon productivity support qualitative outlooks of Chinook salmon returns to the Bonneville Dam and smolt-to-adult survival of Oregon Coast coho salmon (Burke et al. 2013; Peterson et al. 2014). The "stoplight table" (Table 3.1) summarizes many indicators shown elsewhere in this report (PDO, ONI, SST, deep temperature, copepods, juvenile salmon catch) relevant to salmon returns.

In 2023, most of the physical and biological indicators were near-average, suggesting moderate ocean conditions for juvenile salmon. Basin-scale climate and atmospheric indicators were above average and consistent with cool and productive conditions that are typically favorable for juvenile salmon. However, as in 2022, local physical conditions were moderate or less favorable, and out of sync with the large-scale climate indices (Table 3.1)

Marine conditions in 2023 indicate average survival for coho salmon returning to this area in 2024, however the inconsistency of ecosystem drivers, a marine heatwave, and the current El Niño warrant additional care when interpreting this qualitative outlook. For Chinook salmon returning to the Columbia Basin in 2024, indicators for the dominant smolt year (2022) reflect a mix of good, poor, and intermediate conditions. A quantitative model that uses the stoplight indicators in Table 3.1 estimates slightly above-average smolt-to-adult survival for most Chinook salmon returning to the Snake and Upper Columbia rivers in 2024 relative to the prior ten cohorts (Appendix J). The model suggests almost identical survival for smolts that went to sea in 2023 (most of which will return in 2025); ecosystem indicators were close to average in both 2022 and 2023 and had similar mean ranks.

Table 3.1: Stoplight table of conditions for smolt years 1998-2023 for coho salmon originating in coastal Oregon and Chinook salmon from the Columbia Basin. Colors represent a given year's indicator relative to the reference period (1998-2020). Blue: >2 s.d. above the mean; green: >1 s.d. above the mean; yellow: ±1 s.d. of the mean; orange: >1 s.d. below the mean; red: >2 s.d. below the mean. Chinook salmon from smolt year 2022 and coho salmon from smolt year 2023 (outlined in blue box) represent the dominant adult age classes in 2024.

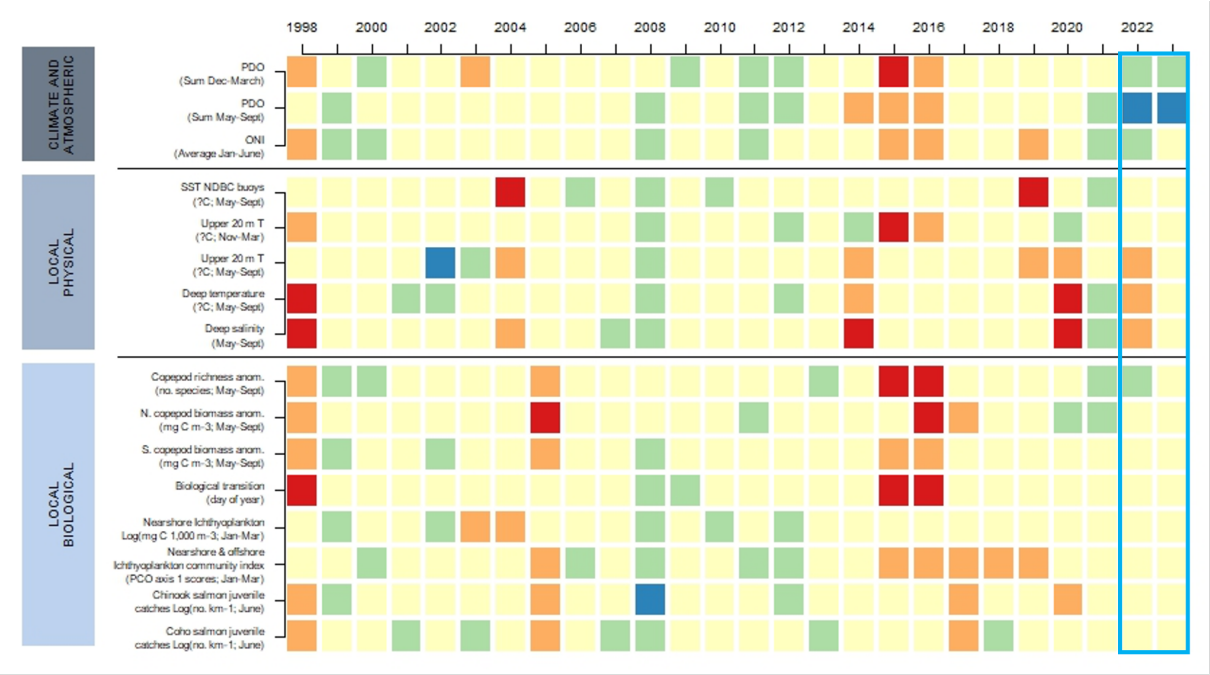

Table 3.2 is another indicator-based table that provides ecosystem context for returns of natural-area Central Valley Fall Chinook salmon. This year we added an egg thiamine concentration indicator based on samples collected from Central Valley fall run hatchery programs.

For adult salmon returning in 2024, the indicators are poor for most age classes. Each of the 2020-2022 brood years has at least one indicator suggesting very poor freshwater productivity (Table 3.2). The dominant age class (age-3, from the 2021 brood year) had low parent spawning escapement, very poor egg incubation temperatures that could result in cohort failure, low egg thiamine concentrations, and very poor rearing and outmigration flows. The older cohorts also had unfavorably warm incubation temperatures and very poor flow for rearing and outmigration. Despite a low February flow indicator, juveniles from the 2022 brood year experienced very good rearing flows in January 2023 and very good outmigration flows in spring 2023. Direct estimates from acoustically tagged smolts indicate much higher (5 to 56%) outmigration survival in 2023 under these flow conditions, compared with the very low outmigration survival (< 5%) of 2020-2022 smolts (see CalFishTrack 2023). However, parent spawning escapement in 2022 was much lower compared to prior cohorts.

Estimates of egg thiamine concentrations were adequate in 2020 but low in 2021 and 2022. Thiamine deficiency is linked with the recent dominance of anchovy in the marine

food web that supports these salmon (e.g., Fig. 3.5) and can lead to high mortality in early life stages of Chinook salmon (Mantua et al. 2021). We suspect that thiamine deficiency has negatively impacted early life stage survival for natural-origin Central Valley Chinook salmon from brood years 2019-2023, with the least impact on fall run and most impact on winter run and late fall run populations. In 2023, all but Coleman hatchery smolts received thiamine supplements to limit impacts on hatchery populations. With respect to predation on juvenile salmon, highly abundant anchovies in the Central CCE may buffer salmon from murre predation; anchovy/sardine have comprised roughly 50-75% of murre diets in the past five years (Fig 3.5, Appendix N). However, the proportion of salmon observed in the diet of common murres in central California in 2023 was well above the long-term mean (Appendix N).

Table 3.2 is best viewed as general qualitative context, as some of the underlying assumptions and descriptors require further data and validation (Appendix J.3). We note that the age-4 class may make a larger contribution to the 2024 adult abundance than normal due to the salmon fisheries closures in California in 2023 (see Council report).

*Table 3.2: Conditions for natural-area Central Valley fall Chinook salmon returning in 2024, from brood years 2019-2022. Indicators include parent spawning escapement, fall stream temperature (during spawning and egg incubation), egg thiamine concentration, and February streamflow (during juvenile rearing and smolt outmigration) (**Friedman et al. 2019**; details in **Appendix J.3**). Dark black box indicates age-3 Chinook salmon, the dominant age class returning to the Central Valley. [1]While median stream flow in the Sacramento River at Colusa was relatively low in February 2023, flows were much higher in January and March-May 2023, with cool stream temperatures throughout this period. These conditions were likely very favorable for juvenile rearing and outmigration success in winter/spring 2023.*

Spawning Escapement (t=0)	Incubation Temperature (Oct-Dec t=0)	Egg thiamine concentration (nmol/g)	February Median Flow (t+1)	Chinook Age in Fall 2024
2019: 121,600 (met goal)	11.3°C (suboptimal)	No data	6,030 cfs **(very low)**	5
2020: 100,100 (low)	11.5°C (poor)	11.0 **(good)**	6,015 cfs **(very low)**	4
2021: 73,230 (low)	13.0°C **(very poor)**	6.6 (low)	4,925 cfs **(very low)**	3
2022: 35,782 **(very low)**	11.7°C (poor)	8.1 (low)	9,005 cfs **(low[1])**	2

The Council's Habitat Committee, Salmon Technical Team, and others including CCIEA scientists have developed more comprehensive stoplight tables for Central Valley spring Chinook salmon, Sacramento River fall Chinook salmon, and Klamath River Fall Chinook salmon. These tables feature indicators from throughout the stocks' life histories, spanning 1983-2022 brood years. Indicators for recent brood years suggest that across California, Chinook salmon stocks encountered relatively poor conditions during spawning in 2022, but much better outmigration conditions in 2023 (Appendix J). Marine indicators for 2023 were mixed but below average. In terms of risk, as defined by the Ecosystem Workgroup's risk classification rubric (EWG 2023), 2022-2023 demonstrated "substantially increased concerns" for ecosystem considerations for salmon going to sea in 2023. In addition, habitat conditions for multiple life stages have been relatively poor for the last three years in all three stocks (Appendix J), which could lead to poor productivity across multiple cohorts and reduced resilience to future ecosystem variability (Munsch et al. 2022).

3.4 Groundfish

3.4.1 Groundfish juvenile abundance

Strong year classes can determine age structure and stock size for marine fishes, and may also indicate favorable environmental conditions, future harvest conditions, and impending potential bycatch issues. The DTS assemblage (Dover sole, thornyheads, and sablefish) is a valuable assemblage for West Coast groundfish fisheries, and bycatch of some species can affect other fisheries.

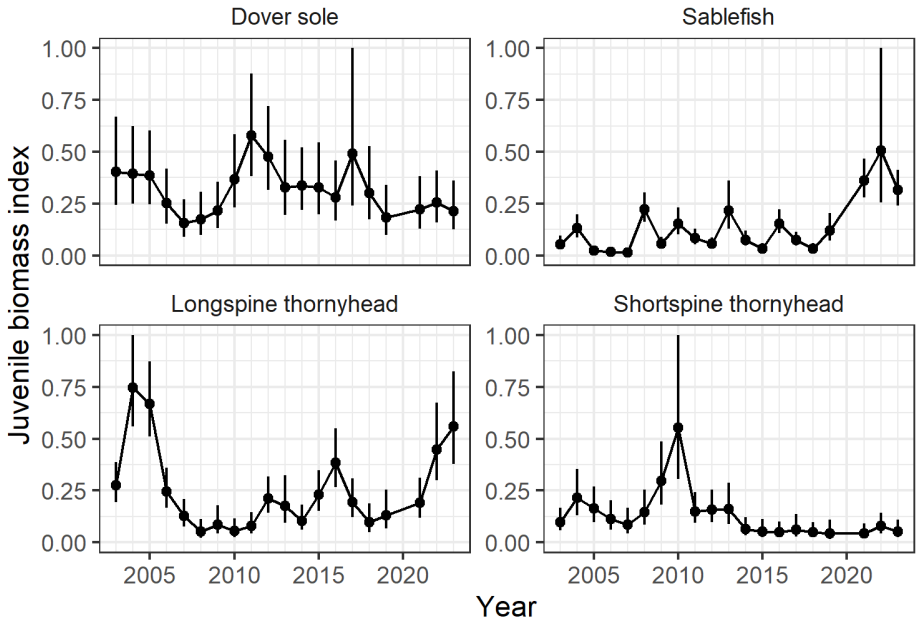

Figure 3.9: Abundance (total biomass) of selected juvenile groundfishes from the WCGBTS for 2002- 2023. The WCGBTS was not completed in 2020 due to COVID restrictions. See Appendix K for statistical details.

Juvenile sablefish abundance was high in 2023 suggesting the recruitment of a particularly strong year class (Fig. 3.9). High sablefish abundance was also observed on the JSOES survey (Fig. H.1). Longspine thornyhead showed a large increase in 2022 and 2023, while Dover sole and shortspine thornyhead showed only minor changes in recent years.

The juvenile biomass index for sablefish initially suggests strong recruitment in the 2021-2023 period (Fig. 3.9). However, size-structure data suggests that the high juvenile biomass in 2022 was due to slow growth of the 2021 cohort, while the values in 2021 and 2023 reflect strong year classes (Fig. K.4, Appendix K). The current status of biomass and fishing pressure for sablefish, shortspine thornyhead, and additional groundfish species based on the most recent stock assessments can be found in Appendix K.

3.4.2 Groundfish distribution

Shifts in groundfish spatial distributions can impact the availability of target species to fisheries as well as bycatch rates. To evaluate potential shifts in groundfish distributions over time, we tracked changes in the center of gravity (CoG) of groundfish stock biomass distributions using the WCGBTS data (Keller et al. 2017). We applied these analyses to 12 species that compose a large component of groundfish landings, or that have broader management interest. Here we highlight findings for three species from the DTS complex (see Section 3.4.1) as well as petrale sole. Information on additional groundfish and methodology is in Appendix K.

The CoG of sablefish, petrale sole, and shortspine thornyhead biomass has shifted to the north over time (Fig. 3.10). For sablefish, the northern shift over the past 10 years returned the CoG to approximately 41.5°N, similar to its distribution in 2003 but with a slight northern shift in 2023, possibly due to strong recruitment in that year. The CoG of Dover sole and several other groundfish species varied over time with no clear latitudinal trend (Fig. 3.10, Fig. K.8). Estimates of the relative availability of groundfish biomass to fishing ports over the same period are in Appendix K and long-term projections of groundfish species distributions under climate change are included in Appendix E.

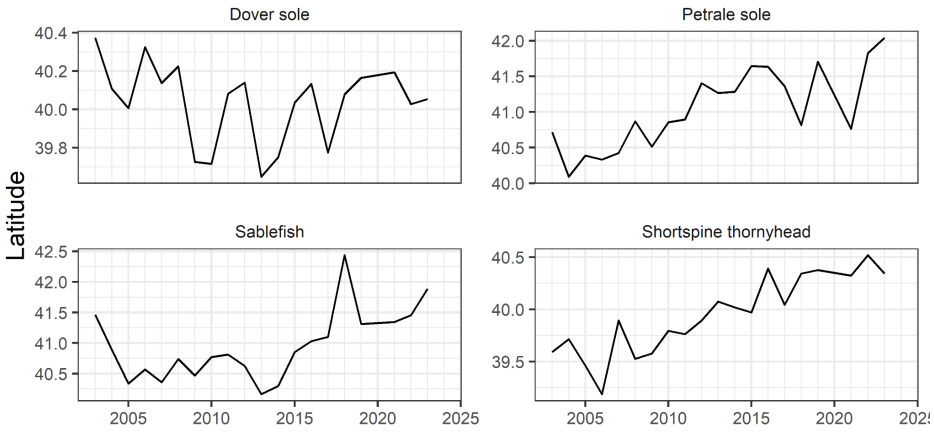

Figure 3.10: Center of gravity of biomass of four groundfish species along the West Coast, 2003-2023.

3.5 Highly Migratory Species (HMS)

3.5.1 Spawning stock biomass and recruitment

Recent ESRs have featured stock assessment-based biomass and recruitment estimates for several HMS stocks that occur in the CCE. The only updates this year are for North Pacific albacore and North Pacific swordfish (see Appendix L). Albacore spawning stock biomass estimates are relatively stable and their recent recruitment estimates are above average. Swordfish show a recent increase in spawning stock biomass but their recruitment estimates are below average. Time series of biomass and recruitment estimates for all available HMS stocks through their most recent assessments are in Appendix L.

3.5.2 HMS diet

HMS are opportunistic predators and information on their diets complement forage surveys, lend insight into how forage varies in space and time, and provide direct measures of forage use by HMS. An updated analysis of albacore stomachs provided by commercial and recreational fishers in Washington, Oregon and northern California reveals that sardines were a major prey item for albacore in 2022. The proportion of sardine in albacore diets had been <10% since 2009 and increased to 56% in 2022 (Fig. 3.11). Sardine have also been an important prey for bluefin tuna in the north; consumption was well above average in 2023 and previous years, excluding 2022. Anchovy importance has been relatively high for swordfish and bluefin tuna in recent years, with record high consumption by bluefin in 2022 (Fig. 3.11). Consumption of hake was well above average for bluefin and swordfish in both 2021 and 2022. Consumption by bluefin declined to the long-term average in 2023. See Appendix L for more information.

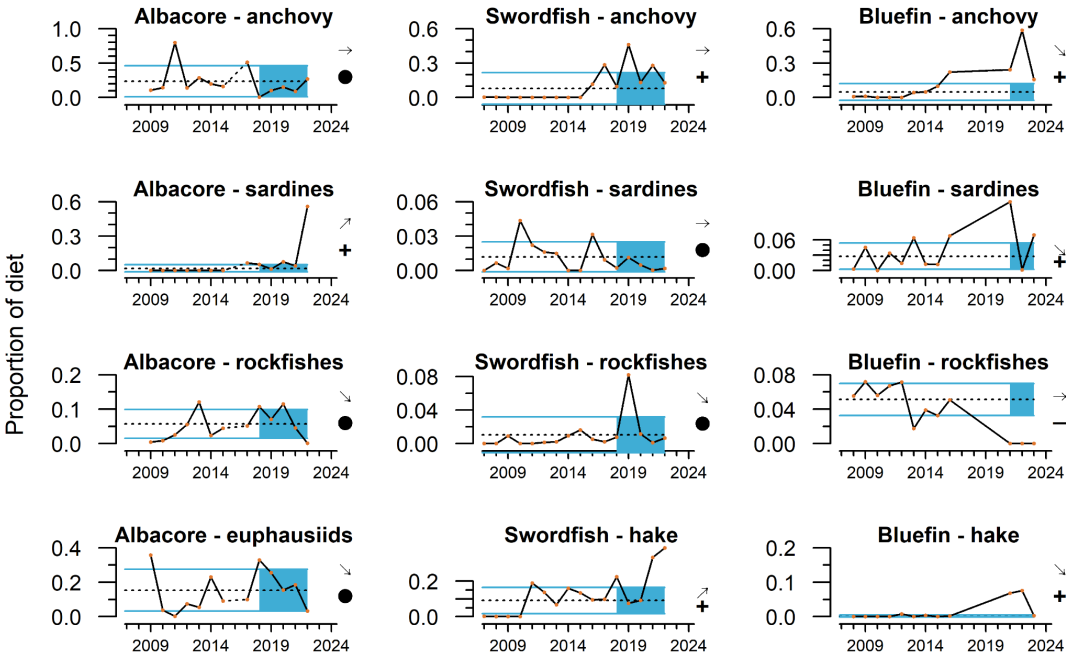

Figure 3.11: Diets of albacore tuna, swordfish, and bluefin tuna sampled from commercial and recreational fisheries in the Northern and Central CCE. Data are proportional contributions of four key prey classes. Data have been updated through 2022 for albacore and swordfish and through 2023 for bluefin. Lines, colors, and symbols are as in Fig. 2.1.

3.6 Marine Mammals

3.6.1 Sea lion productivity

California sea lion pup counts and condition at San Miguel Island are positively correlated with prey availability in the Central and Southern CCE, and are high when energy-rich prey like sardines, anchovy or mackerel have high occurrence in adult female sea lion diets (Melin et al. 2012, see also Appendix M). In 2023, NOAA scientists conducted counts of sea lion pups via Uncrewed Aerial Systems (UAS) for the first time. The preliminary count of the colony indicates a 19% decline in pup births from 2021, reversing a six-year positive trend (data not shown). Sea lion pups were in moderate condition: September pup weight was close to average for the time series, but ~15% lower than 2022 (Fig. 3.12). The lower number of births and moderate condition of pups indicates that foraging conditions for adult female sea lions may have declined over the past year. This result is unexpected as estimated abundances of anchovy and other prey were average to above average in the Central and Southern CCE in 2023 (Section 3.2). Pup growth through February 2024 has not been measured as of this writing and will be provided in the March 2024 presentation to the Council if data are available.

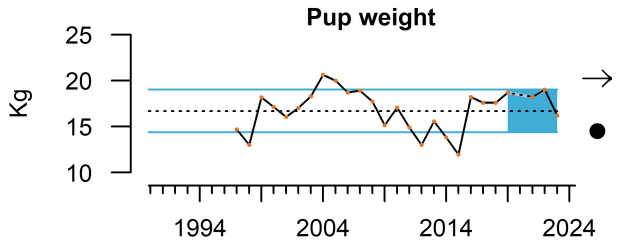

Figure 3.12: California sea lion pup weight in September on San Miguel Island for the 1997 - 2023 cohorts. Lines, colors, and symbols are as in Fig. 2.1.; dashed line indicates years of missing data.

3.6.2 Whale entanglements

Reports of whale entanglements along the West Coast increased in 2014 and even more over subsequent years. Based on preliminary data, West Coast entanglement reports were higher in 2023 than pre-2014, but below the peak years of 2015-2018 and slightly lower than 2022 (Fig. 3.13). Humpback whales continued to be the most common species reported. Most reports were in California, although reports involved gear from all three West Coast states, including confirmed reports from Mexico. Entanglements in 2023 involved a range of sources, including: commercial and recreational Dungeness crab gear; commercial spot prawn, halibut longline, and sablefish pot gear; groundfish trawl; and unidentified gillnet fisheries. No entanglements in large mesh drift gillnet gear were confirmed in 2023.

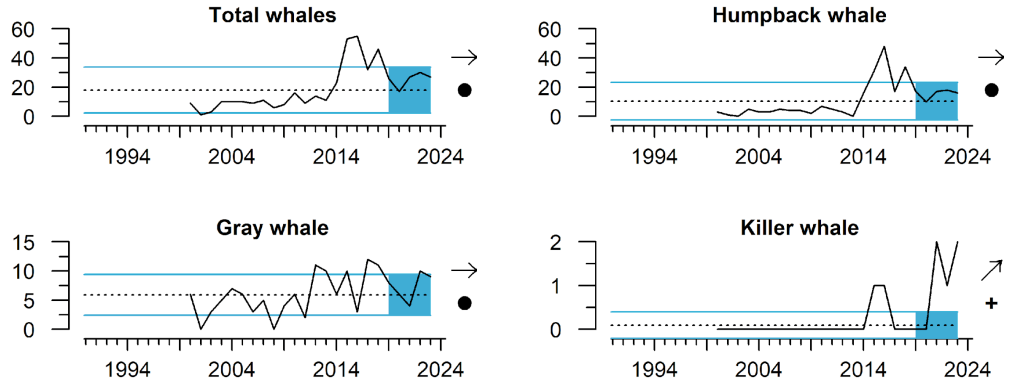

Figure 3.13: Numbers of whales (for selected species) reported as entangled in fishing gear along the West Coast from 2000 - 2023. 2023 data are preliminary. See Appendix M for entanglement information on other whales.

Multiple actions were taken in 2023 to reduce entanglement risk, and despite those actions which have reduced fishing effort, confirmed entanglement reports have been relatively consistent (Figure M.1). Additional factors continue to present obstacles to risk reduction, including derelict gear, foraging by whales in nearshore waters under certain ecosystem conditions, and growth of some whale populations.

3.7 Seabirds

Seabird indicators (productivity, density, diet, and mortality) reflect population health and condition of seabirds, as well as links to lower trophic levels and other conditions in the CCE. The species we report on here and in Appendix N represent a breadth of foraging strategies, life histories, and spatial ranges.

3.7.1 Fledgling production and diet

Seabird colonies on Southeast Farallon Island off central California experienced mostly above-average fledgling production in 2023 (Fig. 3.14). Short-term trends increased for Cassin's auklet, common murre, and rhinoceros auklet and were neutral for two other species. Just south at Año Nuevo Island, fledgling productivity among Brandt's cormorant and rhinoceros auklet were more mixed (Appendix N). Anchovies again dominated diets of piscivorous birds at these two sites, and the proportions of juvenile salmon in the diets of common murre and rhinoceros auklet were well above long-term means. Consumption of juvenile rockfish by Brandt's cormorants was also well above average and showed an increasing trend over the last five years, but was near average for other seabirds (Appendix N).

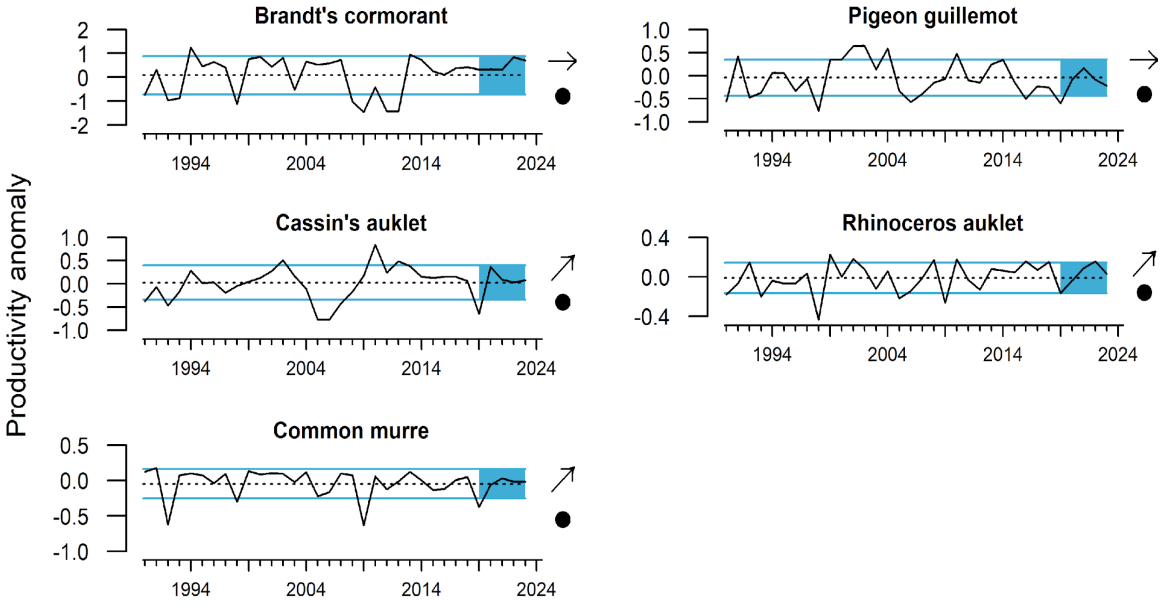

Figure 3.14: Standardized productivity anomalies (annual number of fledglings per pair of breeding adults, minus the long-term mean) for five seabird species on Southeast Farallon Island, 1990 - 2023. Lines, colors, and symbols are as in Fig. 2.1

Further north, fledgling production in 2023 was also above average for seabird colonies at Yaquina Head, Oregon and Destruction Island, Washington (Appendix N). Smelts continued to dominate the diets of rhinoceros auklets and common murre in the Northern CCE, and the proportion of juvenile rockfishes consumed by these species has increased significantly over the last five years (Appendix N).

3.7.2 At-sea densities

At-sea estimates of sooty shearwater densities were again extremely low in the Northern CCE (Appendix N). The sooty shearwater density estimate was the lowest of the time series for the second consecutive year, while the estimated density for Cassin's auklet was the highest of the time series. The opposite pattern was observed in the Central CCE, where at-sea densities of sooty shearwater were the highest of the time series for the third straight year and Cassin's auklet density remained below average. Common murre densities were near average in both regions (Appendix N).

3.7.3 Mortality

Unusual mortality events were not evident in seabird indicator time series from the West Coast beach monitoring programs in 2023 (Appendix N). However, a large die-off of Caspian terns occurred in the Columbia River estuary and adjacent areas in June to August 2023 likely due to an outbreak of a highly-pathogenic avian flu at the East Sand Island colony.

3.8 Harmful Algal Blooms (HABS)

Blooms of the diatom genus *Pseudo-nitzschia* can produce domoic acid, a toxin that can affect coastal food webs and lead to shellfish fishery closures when shellfish tissue levels exceed regulatory limits. In 2023, such blooms were problematic for shellfish fisheries, particularly razor clam, and marine life (Fig. 3.15). The year began with closures in place for the razor clam fishery for Washington, Oregon, and northern California due to high tissue levels of domoic acid remaining from a toxic bloom in the fall of 2022. In southern Oregon, elevated levels of domoic acid delayed the opening of the 2022-23 commercial Dungeness crab fishery, with some areas opening under evisceration orders or requiring in-season evisceration (see Appendix O).

The first major *Pseudo-nitzschia* bloom of 2023 began in late spring in southern California. The bloom lasted ~3 months and resulted in the strandings of >1,000 California sea lions and other pinnipeds and >100 long-beaked common dolphins. This bloom also delayed the opening of portions of the recreational and commercial spiny lobster fisheries by about two weeks. A second major bloom developed in late July/ early August in Washington and northern Oregon and closed or delayed the fall opening of beaches for razor clam harvesting. In mid to late October, bloom activity in the southern Oregon/ northern California "hot spot" continued a pattern of persistent elevated levels of domoic acid in razor clams that began in 2015. State-level details of HAB dynamics and fishery impacts are in Appendix O.

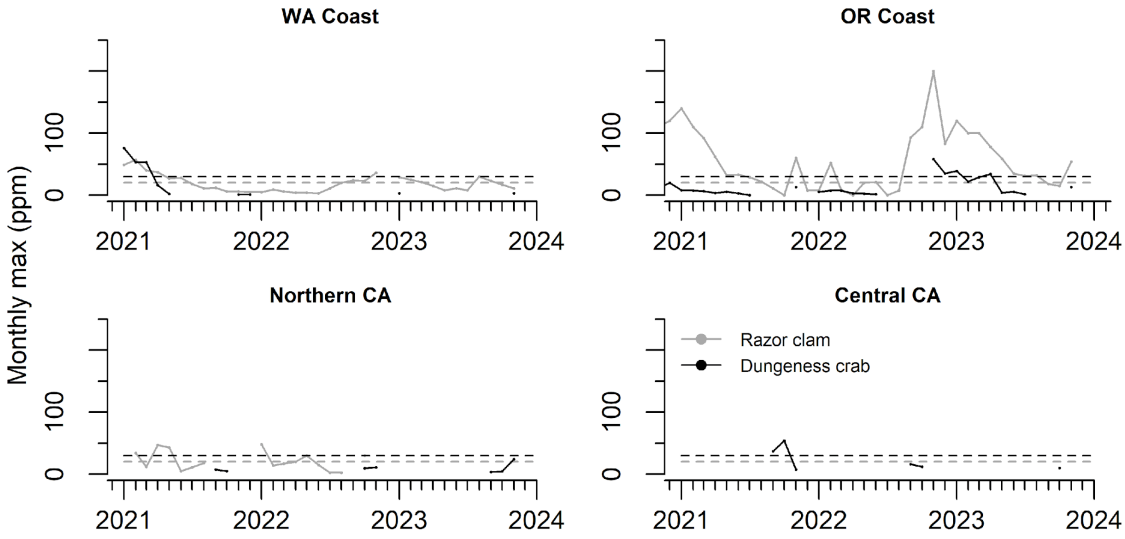

Figure 3.15: Monthly maximum domoic acid concentration in razor clams (gray) and Dungeness crab viscera (black) through 2023 for WA, OR, northern CA (Del Norte to Mendocino counties), and central CA (Sonoma to San Luis Obispo counties). Dashed lines are the management thresholds of 20 ppm (clams, gray) and 30 ppm (crabs, black).

4 Fishing and Non-fishing Human Activities

4.1 Coastwide Landings and Revenue by Major Fisheries

Fishery landings are indicators of ecosystem services and also reflect removals from the CCE. In 2023, coastwide total landings were below the long-term average and decreased 20% from 2022 (Fig. 4.1). Landings from 7 of 9 commercial fisheries decreased in 2023: market squid (-64%), HMS (-61%), salmon (-59%), Pacific whiting (-18%), Other species (-16%), shrimp (-11%) and non-whiting groundfish (-7%). In contrast, landings from crab (65%) and CPS finfish (12%) fisheries increased in 2023. Over the past five years, Pacific whiting landings were above the long-term average, while salmon, CPS finfish, HMS and Other species landings were below long-term averages (Fig. 4.1). Landings from crab fisheries show an increasing trend over the last five years, while Pacific whiting and HMS fisheries show decreasing trends (Fig. 4.1). State-by-state landings and revenues are in Appendix P. There were no commercial landings of salmon in California in 2023, as the fishery was closed.

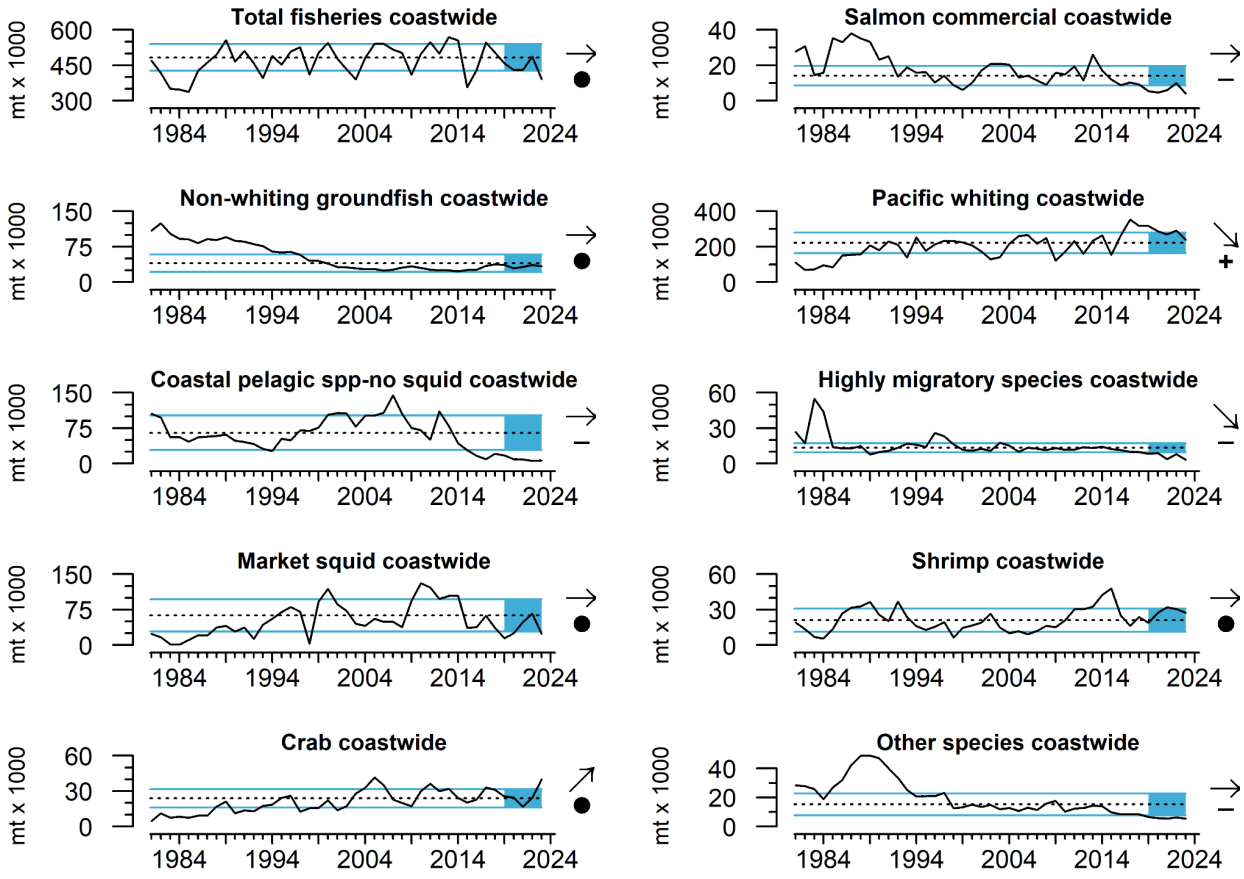

Figure 4.1: Annual landings from West Coast commercial fisheries (data from PacFIN and NORPAC), including total landings across all fisheries, from 1981 - 2023. Data were downloaded from PacFIN on January 10, 2024. Lines, colors, and symbols are as in Fig. 2.1.

Overall, recreational landings declined from 2015 to 2020, then increased from 2021 to 2023 to the long-term average (Fig. 4.2). These patterns can be attributed to increases for 6 of the top 10 most landed recreational species since 2020 (lingcod; albacore; California halibut; black, vermilion and yellowtail rockfish). Recreational salmon landings have been steadily increasing since 2016 (except 2020). Notably, the salmon fishery in California was closed in 2023 though landings data were unavailable for this report. State-level recreational landings are in Appendix P.

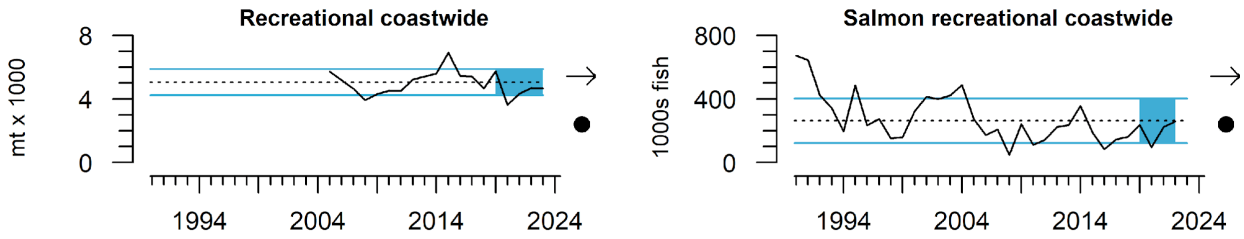

Figure 4.2: Annual landings from most West Coast recreational fisheries from 2005 - 2023 (data from RecFIN) and from recreational salmon fisheries from 1990-2022 (data from PFMC). Data from 2023 are incomplete (see text). Estimates of recreational salmon landings in 2020 may be biased due to COVID-related restrictions on sampling. Lines, colors, and symbols are as in Fig. 2.1.

4.2 Potential Interactions Between Offshore Wind and Ecosystem Indicators

New ocean-use sectors are becoming a reality in the CCE, particularly with two proposed offshore wind energy (OWE) areas off southern Oregon and five lease areas off northern and central California. This highlights the need for a portfolio of indicators that can identify ocean areas important to the overall structure and function of the CCE, and that can track potential ecosystem impacts across all stages of OWE development.

We developed six broad-scale ecosystem indicators, focused on areas being considered for OWE development along the northern California coast. The indicators reflect long-term, spatial variation in upwelling, primary and secondary productivity, juvenile rockfishes and hake, and juvenile groundfish habitat (see Appendix Q). We then developed a gridded map of integrated suitability scores based on the six indicators, ranging from 0 (least suitable for OWE) to 1 (most suitable for OWE) (see Appendix Q for more information about methods). Figure 4.3 identifies a hotspot of productivity offshore from Humboldt Bay, which may signify this area is less suitable for OWE than areas further to the north or south as a function of all six ecosystem indicators. In addition to being applicable to siting of new areas, these indicators could establish baseline conditions that could be used to identify potential effects resulting from OWE development. Indicators of potential interactions with fisheries are in Appendix Q.

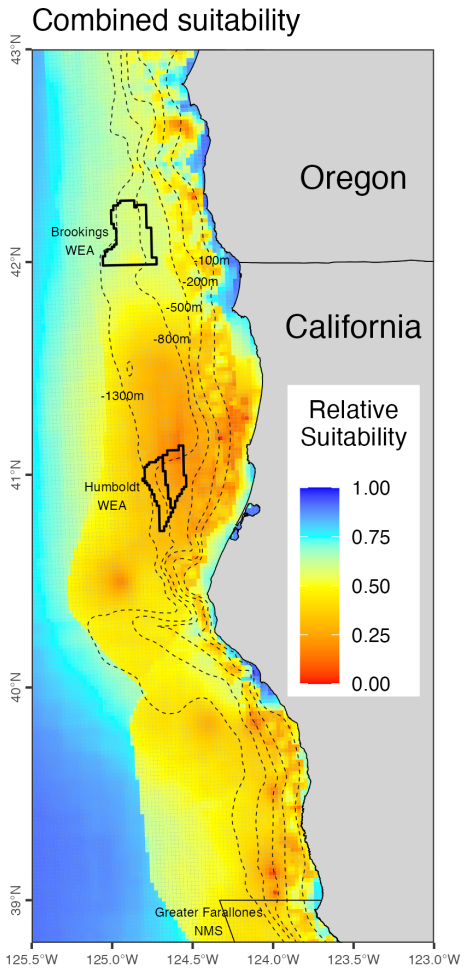

Figure 4.3: Relative suitability scores of 2x2-km grid cells offshore of northern CA based on six broad-scale ecosystem indicators. Scores near 1.00 (blue cells) are most suitable for offshore wind energy development relative to the six ecosystem indicators, while scores near zero (red cells) are less suitable due to overlap with important areas for ecosystem structure and function.

5 HUMAN WELLBEING

Coastal communities depend on marine ecosystems for environmental, economic, social, and cultural wellbeing. This section features indicators and analyses of human wellbeing, relating to the risk profiles and adaptive capacities of coastal communities in the face of environmental and socio-economic pressures, to help track progress toward meeting National Standard 8 (NS-8) of the Magnuson-Stevens Act, as well as monitoring these communities with an interest in environmental justice and fisheries management.

5.1 *Social Vulnerability*

The Community Social Vulnerability Index (CSVI) is a measure of generalized socioeconomic vulnerability at the community scale. CSVI is derived from social vulnerability data (demographics, personal disruption, poverty, housing characteristics, housing disruption, labor force structure, etc.; see Jepson and Colburn 2013), in communities that depend upon commercial fishing. We also maintain the commercial fishing engagement index, based on an analysis of variables reflecting commercial fishing (e.g., fishery landings, revenues, permits, and processing) as well as the commercial fishing reliance index, reflecting per capita commercial fishing engagement. After a multiyear pause in data availability, recreational fishing reliance is once again included, which is a per capita index of a community's recreational fishing engagement (e.g., number of marinas, bait and tackle shops, and charter and guide licenses).

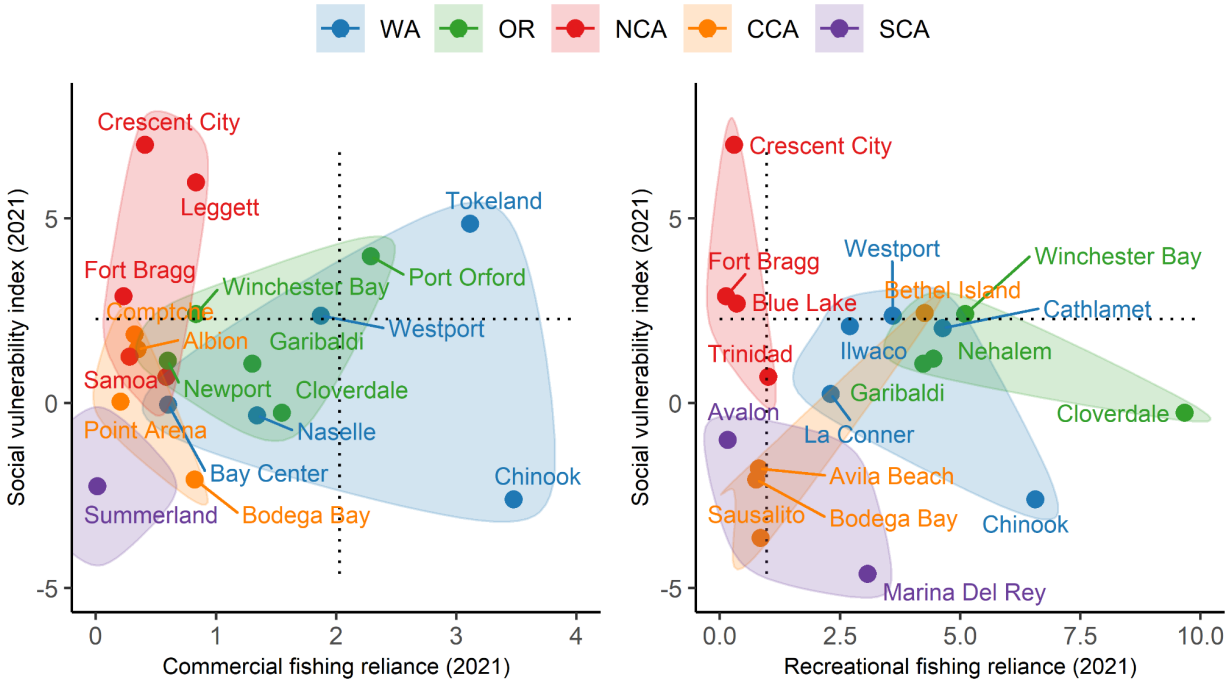

Figure 5.1: Community social vulnerability scores for commercial (left) and recreational fisheries (right) in 2021 for communities in Washington, Oregon, and northern, central and southern California. The five highest-scoring communities for both forms of fishing reliance are shown for each region. Dotted lines indicate 1 s.d. above the means for all communities. Colored polygons within the figures group the five community points from each region together to represent cross-regional differences. Note the difference in x-axis scaling between the two panels.

Figure 5.1 plots CSVI values for 2021 (latest year available) against commercial and recreational fishing reliance for the communities with the highest reliance on commercial fishing across the different regions of the West Coast. Communities in the upper right quadrant of both plots are those with relatively high social vulnerability (vertical axis) and either high commercial fishing reliance (horizontal axis, Fig. 5.1 left), or high recreational

fishing reliance (horizontal axis, Fig. 5.1 right). In 2021, Port Orford, OR and Tokeland, WA had high commercial reliance, followed closely by Westport, WA. Commercial fishing reliance increased in Port Orford, OR from 2020 to 2021 relative to other West Coast communities. Among the communities identified as highly reliant on recreational fishing, the communities with the highest social vulnerability measures were Bethel Island, CA, Winchester Bay, OR and Westport, WA. Of these highly reliant communities, social vulnerability also increased in Winchester Bay in 2021. These results should be interpreted with care; additional details are in Appendix R. The overall higher vulnerability of commercial and recreational fisheries in Oregon and Washington foreshadows anticipated risk due to climate change for groundfish fleets in more northern ports (Appendix E).

5.2 Diversification of Fishery Revenues

Interannual variability in fishing revenue can be reduced by diversifying activities across multiple fisheries or regions, and more diversified fishers also tend to have higher total revenue (Kasperski and Holland 2013). Revenue diversification, which is measured by how revenue is spread across species groups, was unchanged from the 2021 level for current vessels fishing on the U.S. West Coast and in Alaska (those that fished in 2022) (Fig. 5.2a-d). California, Oregon and Washington fleets saw 2%, 10% and 4% increases in average diversification in 2022 relative to 2021, respectively. The overall result is a moderate decline in average diversification since the mid-1990s or earlier for most vessel groupings. Further information on diversification, including port-level and temporal diversification, can be found in Appendix S. We also present levels and trends in non-fishery income diversification for the first time (see Appendix S).

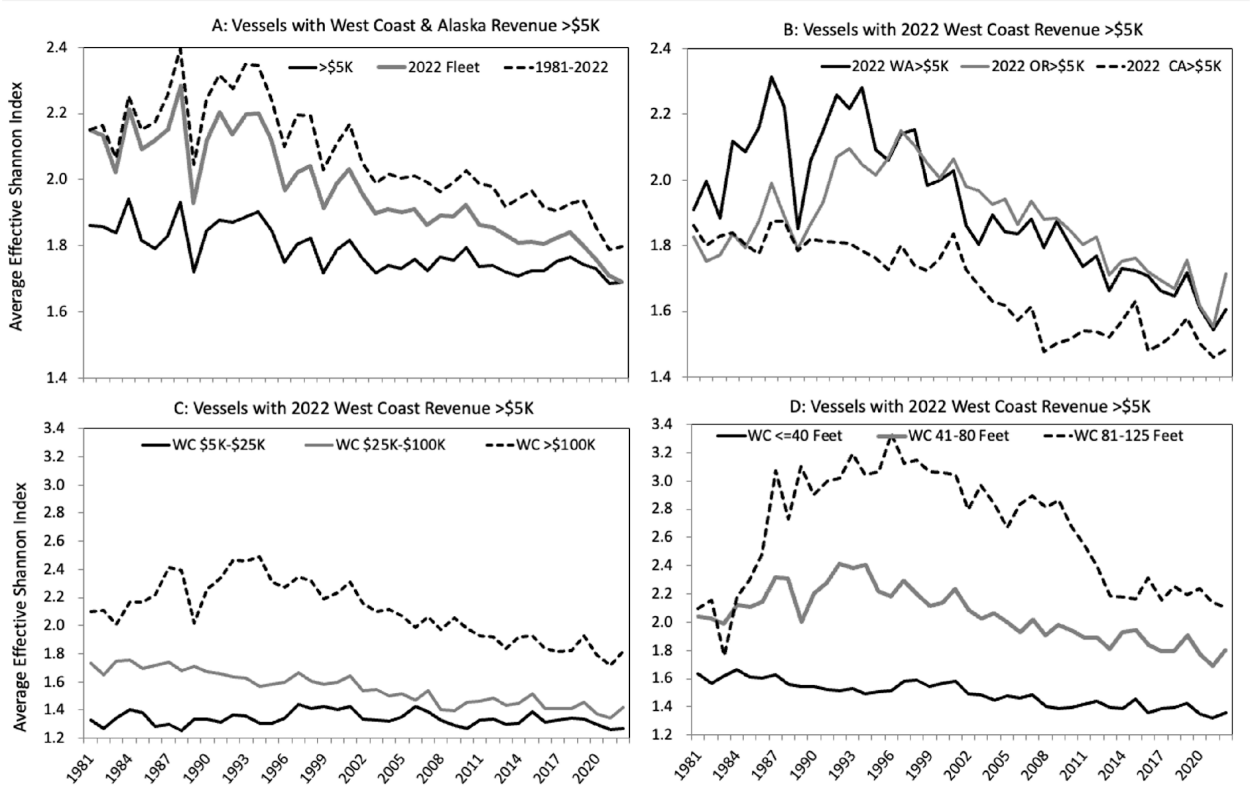

Figure 5.2: Average diversification for West Coast and Alaskan fishing vessels (top left) and for vessels in the 2022 West Coast Fleet, grouped by state (top right), average gross revenue class (bottom left) and vessel length class (bottom right).

Another indicator to track progress toward NS-8 is a Theil Index, used to assess the geographic concentration of fishing revenues. Annually, the Theil Index is calculated for all fisheries and specific management groups, at the scale of the 21 port groups previously established for the economic Input-Output model for Pacific Coast fisheries (Leonard and Watson 2011). See Appendix T.

5.3 Fishery Participation Networks

Fisheries participation networks (FPNs) represent how diversified harvest portfolios create connections between fisheries (Fuller et al 2017, Fisher et al 2021). Last year, we conducted a FPN analysis focused on salmon and examined the vulnerability of West Coast port groups to future shocks to salmon fishing, based on economic dependence (a measure of sensitivity) and a resilience index based on fisheries connectivity (a measure of adaptive capacity) (Harvey et al 2023, Appendix U). Here we compare the number of active salmon vessels and the revenue of commercial salmon vessels between two periods (2017-2022 and 2022-2023) and explore whether our vulnerability framework offered predictive insights into port-level impacts of salmon fisheries closures in California in 2023. We highlight findings for four California fishing ports below and present findings for additional West Coast ports in Appendix U.

Across the California port groups shown in Figure 5.3, participation in commercial fisheries by salmon vessels that were active from 2017-2022 fell by as little as 5% (Santa Barbara) to more than 70% (Bodega Bay) during the 2022-2023 fishing season, when the California salmon fishery was closed. The total revenue from commercial fishing in 2022-2023 for these salmon vessels declined as well (54-64%) in all of these port groups except Santa Barbara, where commercial fishing revenue increased >90%. These outcomes suggest that vulnerability of a port to a fishery closure is greatest when economic dependence on that fishery is high (Bodega Bay, Monterey). However, when economic dependence on a fishery is relatively low (Morro Bay, Santa Barbara), fisheries connectivity is also informative for predicting a port's response to fishery closures (see Fig. U.2).

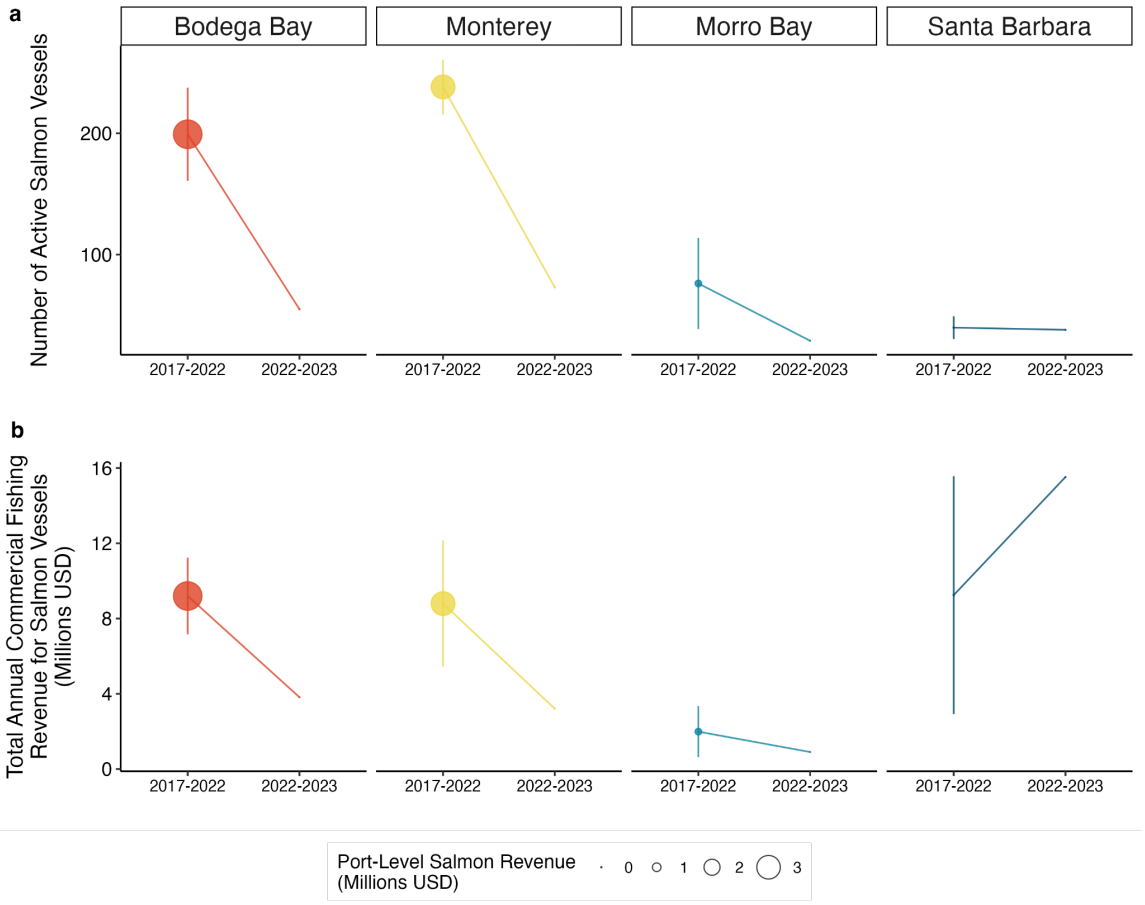

Figure 5.3: (a) Mean (± 1SD) number of active salmon vessels from November 2016 through October 2022 compared to the total number of active salmon vessels from November 2022 to October 2023 for four fishing ports in California. Active salmon vessels are those that had commercial salmon landings anytime between November 2016 and October 2022, and participated in the salmon fishery or any other commercial fishery during both time periods. (b) Total annual revenue (mean ± 1SD) of commercial fishing vessels for salmon vessels (includes revenue from any fishery) for the same time periods and ports described in (a). Diameter of points represents average yearly port-level salmon revenue. See Appendix U for details, and for results for 13 additional West Coast fishing ports.

6 SYNTHESIS

Ecosystem signals in the California Current in 2023 were mixed, with many favorable signs (Box 1.1, Appendix D). The year began in a La Niña state with negative PDO values, which typically indicate cool, productive conditions. Periods of strong upwelling provided expansive cool and productive coastal waters and mitigated offshore heatwaves. Surveys

found abundant anchovies and juvenile groundfishes, and good productivity at several seabird colonies. Higher abundances of sardine have also been observed in nearshore southern California and in albacore diets.

These positive signs are encouraging as we enter a potentially strong El Niño that will likely continue through spring. The moderately strong El Niño of 2015/16 was prefaced by the unprecedented large marine heatwave of 2013-2015, which brought mostly unfavorable conditions to the CCE. Conditions leading into the current El Niño are much more favorable, and the ecosystem appears resilient to the recent surface-oriented and offshore heatwaves. This positive "preconditioning" prior to the current El Niño may help buffer the system against some of the anticipated negative impacts (see Appendix E).

While we are encouraged by these signs of preconditioning, other indicators raise concern. As the year progressed, lengthy upwelling relaxation events reduced total upwelling in most of the CCE and allowed intrusions of warm, less productive water, particularly in the north. The system also experienced lower krill biomass, declines in sea lion pup indicators, and multiple HAB events that caused marine mammal strandings and disrupted shellfish fisheries. Landings for most commercial fisheries declined, California salmon fisheries were closed, and the outlook for adult salmon returning to the Central Valley in 2024 is poor. While improvements in freshwater indicators and smolt outmigration survival are promising signs, marine conditions are less promising.

The salmon stoplight tables and interpretations thereof exemplify the value of considering ecosystem conditions in identifying risk for West Coast fisheries. Downturns in stock abundance and availability negatively impact fishing communities, especially those most vulnerable due to their high dependence on particular stocks or low adaptive capacity (see Section 5.3). Efforts such as the FEP ecosystem initiative (EWG 2023) that aim to assess risk associated with ecosystem conditions can support decision-making to mitigate such impacts. The CCIEA team is well poised to inform these efforts through the existing suite of indicators and by developing new indicators specific to particular species or species complexes.

While the CCE proved reasonably robust to climate and ocean conditions in 2023, this resilience is not likely to be sustained indefinitely. The changes described in this report are happening against a backdrop of rapid and accelerating climate change. Continued ocean warming and ancillary impacts suggest that our methods for interpreting anomalous conditions must evolve. This need is particularly pronounced as species and habitats are confronted with new combinations of conditions, the information conveyed by familiar indicators changes, and "new normals" replace historic expectations. The CCIEA team is well positioned to support efforts aimed at addressing different types of shifting baselines, while also quantifying risk posed to West Coast species, fisheries, and fishing communities from climate variability, climate extremes, and long-term climate change (Appendix E). This work can provide a scientific basis for approaches the Council uses to help individuals and communities within the CCE adapt to an uncertain future.

7 REFERENCES

Abbott JK, Sakai Y, Holland DS (2023) Species, space and time: A quarter century of fishers' diversification strategies on the US West Coast. Fish and Fisheries 24:93–110

Abell R, Thieme ML, Revenga C, et al (2008) Freshwater ecoregions of the world: A new map of biogeographic units for freshwater biodiversity conservation. BioScience 58:403–414

Ainley DG, Dugger KM, La Mesa M, et al (2018) Post-fledging survival of Adélie penguins at multiple colonies: Chicks raised on fish do well. Marine Ecology Progress Series 601:239–251

Amaya DJ, Jacox MG, Fewings MR, et al (2023) Marine heatwaves need clear definitions so coastal communities can adapt. Nature 616:29–32.

Anderson SC, Ward EJ, English PA, Barnett LA (2022) sdmTMB: An R package for fast, flexible, and user-friendly generalized linear mixed effects models with spatial and spatiotemporal random fields. bioRxiv 2022–03. https://doi.org/10.1101/2022.03.24.485545

Burke BJ, Peterson WT, Beckman BR, et al (2013) Multivariate models of adult Pacific salmon returns. PLoS One 8:e54134

Busch DS, McElhany P (2016) Estimates of the direct effect of seawater pH on the survival rate of species groups in the California Current Ecosystem. PLoS One 11:e0160669

Calambokidis J, J Barlow J (2020) Updated abundance estimates for blue and humpback whales along the U.S. West Coast using data through 2018, U.S. Department of Commerce, NOAA Technical Memorandum NMFS-SWFSC-634.

Chan F, Barth J, Lubchenco J, et al (2008) Emergence of anoxia in the California Current large marine ecosystem. Science 319:920–920

Cimino MA, Santora JA, Schroeder I, et al (2020) Essential krill species habitat resolved by seasonal upwelling and ocean circulation models within the large marine ecosystem of the California Current system. Ecography 43:1536–1549

Cushing DH (1990) Plankton production and year-class strength in fish populations: an update of the match/mismatch hypothesis. In: Advances in Marine Biology 26:249-293

Devincenzi D, Beck T, Beck J, et al (2023) Año Nuevo Island seabird conservation annual report 2023. Unpublished Report to California Dept. of Parks and Recreation, Año Nuevo State Park. 2023-Oikonos-Ano-Nuevo-Annual-Report_final.pdf

Dyson K, Huppert DD (2010) Regional economic impacts of razor clam beach closures due to harmful algal blooms (HABs) on the Pacific Coast of Washington. Harmful Algae 9:264–271

EWG (2023) Ecosystem Workgroup report on the ecosystem and climate information initiative. Agenda item f.1.a, september 2023 briefing book, https://www.pcouncil.org/documents/2023/08/f-1-a-ewg-report-1-with-edit.pdf

FDA (2011) Fish and Fishery Products Hazards and Controls Guidance (fourth ed.) Appendix 5: FDA and EPA Safety Levels in Regulations and Guidance. Department of Health and Human Services, Food and Drug Administration. pp 439-442. https://www.fda.gov/media/80637/download

Feely RA, Sabine CL, Hernandez-Ayon JM, et al (2008) Evidence for upwelling of corrosive" acidified" water onto the continental shelf. Science 320:1490–1492

Fiechter J, Edwards CA, Moore AM (2018) Wind, circulation, and topographic effects on alongshore phytoplankton variability in the California Current. Geophysical Research Letters 45:3238–3245

Fiechter J, Santora JA, Chavez F, et al (2020) Krill hotspot formation and phenology in the California Current Ecosystem. Geophysical Research Letters 47:e2020GL088039

Field JC, Miller RR, Santora JA, Tolimieri N, et al (2021) Spatiotemporal patterns of variability in the abundance and distribution of winter-spawned pelagic juvenile rockfish in the California Current. PloS one 16(5):e0251638.

Fisher JL, Peterson WT, Rykaczewski RR (2015) The impact of El Niño events on the pelagic food chain in the northern California Current. Global Change Biology 21:4401–4414

Fisher MC, Moore SK, Jardine SL, et al (2021) Climate shock effects and mediation in fisheries. Proceedings of the National Academy of Sciences 118:e2014379117

FitzGerald AM, John SN, Apgar TM, Mantua NJ, Martin BT (2021) Quantifying thermal exposure for migratory riverine species: phenology of Chinook salmon populations predicts thermal stress. Global Change Biology. 27(3):536-49.

Free CM, Moore SK, Trainer VL (2022) The value of monitoring in efficiently and adaptively managing biotoxin contamination in marine fisheries. Harmful Algae 114:102226.

Friedman WR, Martin BT, Wells BK, et al (2019) Modeling composite effects of marine and freshwater processes on migratory species. Ecosphere 10:e02743

Fuller EC, Samhouri JF, Stoll JS, et al (2017) Characterizing fisheries connectivity in marine social–ecological systems. ICES Journal of Marine Science 74:2087–2096

Hall JE, Greene CM, Stefankiv O, Anderson JH, Timpane-Padgham B, Beechie TJ, Pess GR (2018) Large river habitat complexity and productivity of Puget Sound Chinook salmon. PLoS One 13(11):e0205127.

Haltuch J M. A., Castillo-Jordán CA (2019) Status of the sablefish stock in U.S. Waters in 2019. Pacific Fisheries Management Council, 7700 Ambassador Place NE, suite 200, Portland, OR. 398 p.

Harvey CJ, Garfield NT, Williams GD, Tolimieri N (2020) California Current Integrated Ecosystem Assessment (CCIEA) California Current Ecosystem Status Report, 2020. Report to the Pacific Fishery Management Council. March 2020, agenda item I.1.a.

Harvey CJ, Garfield NT, Williams GD, Tolimieri N (2022) California Current Integrated Ecosystem Assessment (CCIEA) California Current Ecosystem Status Report, 2022. Report to the Pacific Fishery Management Council. March 2022, agenda item I.1.a.

Harvey CJ, Leising A, Tolimieri N, Williams GD (2023) California Current Integrated Ecosystem Assessment (CCIEA) California Current Ecosystem Status Report, 2023. Report to the Pacific Fishery Management Council. March 2023, agenda item i.1.a.

Hobday AJ, Alexander LV, Perkins SE, et al (2016) A hierarchical approach to defining marine heatwaves. Progress in Oceanography 141:227–238

Holland DS, Leonard J (2020) Is a delay a disaster? Economic impacts of the delay of the California Dungeness crab fishery due to a harmful algal bloom. Harmful Algae 98:101904

ISC (2022) Stock assessment of Pacific bluefin tuna in the Pacific Ocean in 2022. Annex 13, 22nd Meeting of the International Scientific Committee for Tuna and Tuna-Like Species in the North Pacific Ocean, Kona, Hawai'i, U.S.A., July 12-18, 2022.

ISC (2023) Stock assessment of albacore tuna in the North Pacific Ocean in 2023. Annex 08, 23rd Meeting of the International Scientific Committee for Tuna and Tuna-Like Species in the North Pacific Ocean, Kanazawa, Japan, July 12-17, 2023.

Jacox MG, Edwards CA, Hazen EL, Bograd SJ (2018) Coastal upwelling revisited: Ekman, Bakun, and improved upwelling indices for the US West Coast. Journal of Geophysical Research: Oceans 123:7332–7350

Jager HI, Cardwell HE, Sale MJ, Bevelhimer MS, Coutant CC, Van Winkle W (1997) Modelling the linkages between flow management and salmon recruitment in rivers. Ecological Modelling 103(2-3):171-91.

Jepson M, Colburn LL (2013) Development of social indicators of fishing community vulnerability and resilience in the US Southeast and Northeast regions. NOAA Tech. Memo. NMFS-F/SPO; 129. https://repository.library.noaa.gov/view/noaa/4438

Jordan MS (2012) Hydraulic predictors and seasonal distribution of *Manayunkia speciosa* density in the Klamath river, CA, with implications for ceratomyxosis, a disease of salmon and trout. : Oregon State University.

Kasperski S, Holland DS (2013) Income diversification and risk for fishermen. Proceedings of the National Academy of Sciences 110:2076–2081

Keister JE, Di Lorenzo E, Morgan C, et al (2011) Zooplankton species composition is linked to ocean transport in the northern California Current. Global Change Biology 17:2498–2511

Keller AA, Wallace JR, Methot RD (2017) The Northwest Fisheries Science Center's West Coast Groundfish Bottom Trawl Survey: History design, and description. NOAA Tech. Memo. NMFS-NWFSC-136. https://repository.library.noaa.gov/view/noaa/14179/noaa_14179_DS1.pdf

Lefebvre KA, Bargu S, Kieckhefer T, Silver MW (2002) From sanddabs to blue whales: The pervasiveness of domoic acid. Toxicon 40:971–977

Leising AW (in revision) Phenology of large marine heatwaves in the Northeast Pacific

Leonard J, Watson P (2011) Description of the input-output model for Pacific Coast fisheries. U.S. Department of Commerce, NOAA Technical Memorandum NMFS-NWFSC-111, 64 p.

Limm MP, Marchetti MP (2009) Juvenile Chinook salmon (*Oncorhynchus tshawytscha*) growth in off-channel and main-channel habitats on the Sacramento River, CA using otolith increment widths. Environmental Biology of Fishes 85:141-51.

Lindgren F, Rue H (2015) Bayesian spatial modelling with r-INLA. Journal of Statistical Software 63:1–25

Mantua N, Johnson R, Field J, et al (2021) Mechanisms, impacts, and mitigation for thiamine deficiency and early life stage mortality in California's Central Valley Chinook salmon. North Pacific Anadromous Fish Commission 92–93

Marshall KN, Kaplan IC, Hodgson EE, et al (2017) Risks of ocean acidification in the California Current food web and fisheries: Ecosystem model projections. Global Change Biology 23:1525–1539

McCabe RM, Hickey BM, Kudela RM, et al (2016) An unprecedented coastwide toxic algal bloom linked to anomalous ocean conditions. Geophysical Research Letters 43:10–366

McKibben SM, Peterson W, Wood AM, et al (2017) Climatic regulation of the neurotoxin domoic acid. Proceedings of the National Academy of Sciences 114:239–244

Melin SR, Orr AJ, Harris JD, et al (2012) California sea lions: An indicator for integrated ecosystem assessment of the California Current system. California Cooperative Oceanic Fisheries Investigations Reports 53:140–152

Messié M, Sancho-Gallegos DA, Fiechter J, et al (2022) Satellite-based lagrangian model reveals how upwelling and oceanic circulation shape krill hotspots in the California Current system. Frontiers in Marine Science 9:835813

Michel CJ (2019). Decoupling outmigration from marine survival indicates outsized influence of streamflow on cohort success for California's Chinook salmon populations. Canadian Journal of Fisheries and Aquatic Sciences 76:1398-410.

Moore SK, Cline MR, Blair K, et al (2019) An index of fisheries closures due to harmful algal blooms and a framework for identifying vulnerable fishing communities on the US West Coast. Marine Policy 110:103543

Moore SK, Dreyer SJ, Ekstrom JA, et al (2020) Harmful algal blooms and coastal communities: Socioeconomic impacts and actions taken to cope with the 2015 US West Coast domoic acid event. Harmful Algae 96:101799

Morgan CA, Beckman BR, Weitkamp LA, Fresh KL (2019) Recent ecosystem disturbance in the northern California Current. Fisheries 44:465–474

Munsch SH, Greene CM, Johnson RC, et al (2019) Warm, dry winters truncate timing and size distribution of seaward-migrating salmon across a large, regulated watershed. Ecological Applications 29:e01880.

Munsch SH, Greene CM, Johnson RC, et al (2020) Science for integrative management of a diadromous fish stock: interdependencies of fisheries, flow, and habitat restoration. Canadian Journal of Fisheries and Aquatic Sciences. 77:1487-504.

Munsch SH, Greene CM, Mantua NJ, Satterthwaite WH (2022) One hundred-seventy years of stressors erode salmon fishery climate resilience in California's warming landscape. Global Change Biology 28:2183–2201

Magnuson-Stevens Act Provisions National Standard 8—Communities. 50 CFR 600.345, 2008.https://www.ecfr.gov/current/title-50/chapter-VI/part-600/subpart-D/section-600.345. Accessed on 2024-01-25.

Neveu E, Moore AM, Edwards CA, et al (2016) An historical analysis of the California Current circulation using ROMS 4D-var: System configuration and diagnostics. Ocean Modelling 99:133–151

NSF Ocean Observatories Initiative. (2024). Stable dissolved oxygen (CE07SHSM-MFD37-03-DOSTAD000) data from the Washington Shelf Surface Mooring from 2015-04-05 to 2023-12-31. Data Portal. https://ooinet.oceanobservatories.org/. Accessed on 2024-01-02.

Perry RW, Plumb JM, Fielding SD, Adams NS, Rondorf DW (2013) Comparing effects of transmitters within and among populations: application to swimming performance of juvenile Chinook Salmon. Transactions of the American Fisheries Society. 142(4):901-11.

Peterson WT, Fisher JL, Peterson JO, et al (2014) Applied fisheries oceanography: Ecosystem indicators of ocean conditions inform fisheries management in the California Current. Oceanography 27:80–89

Phillips EM, Chu D, Gauthier S, et al (2022) Spatiotemporal variability of euphausiids in the California Current ecosystem: Insights from a recently developed time series. ICES Journal of Marine Science 79:1312–1326

R Core Team (2023) R: A language and environment for statistical computing. R Foundation for Statistical Computing, Vienna, Austria

Raghukumar K, Nelson T, Jacox M, et al (2023) Projected cross-shore changes in upwelling induced by offshore wind farm development along the California coast. Communications Earth & Environment 4:116

Reis GJ, Howard JK, Rosenfield JA (2019) Clarifying effects of environmental protections on freshwater flows to—and water exports from—the San Francisco Bay Estuary. San Francisco Estuary and Watershed Science 17(1).

Renfree JS, Beittel A, Bowlin NM, et al (In prep) Report on the Summer 2023 California Current Ecosystem Survey (CCES) (2307RL), 5 July to 25 October 2023, conducted aboard NOAA ship *Reuben Lasker*, NOAA ship *Bell M. Shimada*, fishing vessels *Lisa Marie* and *Long Beach Carnage*, and uncrewed surface vehicles. U.S. Dep. Commer., NOAA Tech. Memo.

Riley KL, Wickliffe LC, Jossart JA, MacKay JK, et al (2021) An aquaculture opportunity area atlas for the US Gulf of Mexico. NOAA technical memorandum NOS NCCOS 299. 545 p. DOI:10.25923/8cb3-3r66

Ritzman J, Brodbeck A, Brostrom S, et al (2018) Economic and sociocultural impacts of fisheries closures in two fishing-dependent communities following the massive 2015 US West Coast harmful algal bloom. Harmful Algae 80:35–45

Robertson RR, Bjorkstedt EP (2020) Climate-driven variability in *Euphausia pacifica* size distributions off northern California. Progress in Oceanography 188:102412

Santora JA, Mantua NJ, Schroeder ID, et al (2020) Habitat compression and ecosystem shifts as potential links between marine heatwave and record whale entanglements. Nature Communications 11:1–12

Santora JA, Rogers TL, Cimino MA, et al (2021) Diverse integrated ecosystem approach overcomes pandemic-related fisheries monitoring challenges. Nature Communications 12:1–10

Satterthwaite WH, Mohr MS, O'Farrell MR, Anderson EC, Banks MA, Bates SJ, Bellinger MR, Borgerson LA, Crandall ED, Garza JC, Kormos BJ (2014) Use of genetic stock identification data for comparison of the ocean spatial distribution, size at age, and fishery exposure of an untagged stock and its indicator: California Coastal versus

Klamath River Chinook Salmon. Transactions of the American Fisheries Society 143:117-33.

Selden RL, Thorson JT, Samhouri JF, et al (2020) Coupled changes in biomass and distribution drive trends in availability of fish stocks to US West Coast ports. ICES Journal of Marine Science 77:188–199. https://doi.org/10.1093/icesjms/fsz211

Shaftel DD (2022) Managing uncertainty: Forecasting ocean abundance of Klamath River fall-run Chinook salmon (*Oncorhynchus tshawytscha*). Capstone Projects - *UC San Diego: Center for Marine Biodiversity and Conservation*. Retrieved from https://escholarship.org/uc/item/70s0n2zj

Shanks AL, Rasmuson LK, Watts MW (in prep) Changing climate and the mechanisms behind larval success, recruitment, and commercial catch for Dungeness crab, *Cancer magister.*

Stierhoff, K. L., Renfree, J. S., Rojas-González, R. I., Vallarta-Zárate, J. R. F., Zwolinski, J. P., and Demer, D. A. 2023a. Distribution, biomass, and demography of coastal pelagic fishes in the California Current Ecosystem during summer 2021 based on acoustic-trawl sampling. U.S. Dep. Commer., NOAA Tech. Memo., NOAA-TM-NMFS-SWFSC-676: 85.

Stierhoff KL, Zwolinski JP, Renfree JS, Demer DA (2023b) Distribution, biomass, and demography of coastal pelagic fishes in the California Current Ecosystem during summer 2022 based on acoustic-trawl sampling. U.S. Dep. Commer., NOAA Tech. Memo., NOAA-TM-NMFS-SWFSC-683:84.

Stierhoff KL, Zwolinski JP, Renfree JS, Demer DA (in prep) Distribution, biomass, and demography of coastal pelagic fishes in the California Current Ecosystem during summer 2023 based on acoustic-trawl sampling. NOAA Tech. Memo.

Strange JS (2012) Migration strategies of adult Chinook salmon runs in response to diverse environmental conditions in the Klamath River basin. Transactions of the American Fisheries Society. 141(6):1622-36.

Sturrock AM, Satterthwaite WH, Cervantes-Yoshida KM, Huber ER, Sturrock HJ, Nusslé S, Carlson SM (2019) Eight decades of hatchery salmon releases in the California Central Valley: Factors influencing straying and resilience. Fisheries 44:433-44.

Sykes GE, Johnson CJ, Shrimpton JM (2009) Temperature and flow effects on migration timing of Chinook salmon smolts. Transactions of the American Fisheries Society. 138(6):1252-65.

Szoboszlai AI, Thayer JA, Wood SA, et al (2015) Forage species in predator diets: Synthesis of data from the California Current. Ecological Informatics 29:45–56

Theil H (1967) Economics and information theory. Rand McNally and Co.; North-Holland Publishing Company, Chicago and Amsterdam

TNC & WWF (2008) Freshwater Ecoregions of the World. The Nature Conservancy and World Wildlife Fund, Inc., Washington, DC USA. URL https://www.feow.org/files/downloads/GIS_hs_snapped.zip Accessed: 10 Jan 2023.

Thompson AR, Harvey CJ, Sydeman WJ, Barceló C, et al (2019a) Indicators of pelagic forage community shifts in the California Current Large Marine Ecosystem, 1998–2016. Ecological Indicators 105:215-228.

Thompson AR, Schroeder ID, Bograd SJ, Hazen EL, et al (2019b) State of the California Current 2018–19: a novel anchovy regime and a new marine heatwave? California Cooperative Oceanic Fisheries Investigations Reports 60:1-65.

Thorson JT (2018) Three problems with the conventional delta-model for biomass sampling data, and a computationally efficient alternative. Canadian Journal of Fisheries and Aquatic Sciences, 75(9), 1369-1382. doi:10.1139/cjfas-2017-0266

Thorson JT (2019) Guidance for decisions using the vector autoregressive spatio-temporal (VAST) package in stock, ecosystem, habitat and climate assessments. Fisheries Research 210:143–161

Tolimieri N, Wallace J, Haltuch M (2020) Spatio-temporal patterns in juvenile habitat for 13 groundfishes in the California Current ecosystem. PLoS One 15:e0237996

Trainer VL, Moore SK, Hallegraeff G, et al (2020) Pelagic harmful algal blooms and climate change: Lessons from nature's experiments with extremes. Harmful algae 91:101591

Treakle AT, Holland DS (2023) Not by fishing alone: Non-fishing employment and income for US West Coast fishers. Ocean & Coastal Management 243:106763

Wells BK, Grimes CB, Sneva JG, McPherson S, Waldvogel JB (2008). Relationships between oceanic conditions and growth of Chinook salmon (*Oncorhynchus tshawytscha*) from California, Washington, and Alaska, USA. Fisheries Oceanography 17:101-25.

Zwolinski JP, Demer DA, Cutter Jr GR, et al (2014) Building on fisheries acoustics for marine ecosystem surveys. Oceanography 27:68–79

Zwolinski JP, Demer, DA (2023). An updated model of potential habitat for northern stock Pacific Sardine (*Sardinops sagax*) and its use for attributing survey observations and fishery landings. Fisheries Oceanography, 1–14, https://doi.org/10.1111/fog.12664

SUPPLEMENTAL MATERIALS TO THE 2023-2024 CALIFORNIA CURRENT ECOSYSTEM STATUS REPORT

Appendix A: LIST OF CONTRIBUTORS BY AFFILIATION

NWFSC, NOAA Fisheries Mr. Kelly Andrews, Dr. Brian Burke, Dr. Jason Cope, Mr. Jeff Cowen, Dr. Blake Feist, Ms. Jennifer Fisher, Dr. Correigh Greene, Dr. Thomas Good, Dr. Chris Harvey, Dr. Daniel Holland, Dr. Mary Hunsicker (co-editor), Dr. Kym Jacobson, Ms. Su Kim, Dr. Stephanie Moore, Dr. Stuart Munsch, Dr. Karma Norman, Dr. Jameal Samhouri, Dr. Kayleigh Somers, Dr. Nick Tolimieri (co-editor), Dr. John Wallace, Mr. Curt Whitmire, Dr. Jen Zamon

AFSC, NOAA Fisheries Dr. Stephen Kasperski, Dr. Sharon Melin

SWFSC, NOAA Fisheries Dr. Eric Bjorkstedt, Dr. Steven Bograd, Dr. David Demer, Dr. Heidi Dewar, Ms. Lynn deWitt, Dr. John Field, Dr. Elliott Hazen, Dr. Michael Jacox, Dr. Andrew Leising (co-editor), Dr. Nate Mantua, Dr. Barbara Muhling, Dr. Tanya Rogers, Mr. Keith Sakuma, Dr. Jarrod Santora, Dr. Kevin Stierhoff, Dr. Andrew Thompson, Dr. Brian Wells

NOAA Fisheries West Coast Region Ms. Abigail Harley (co-editor), Ms. Jennifer (Lilah) Isé, Mr. Dan Lawson, Ms. Lauren Saez

Pacific States Marine Fishery Commission Mr. Toby Auth, Mr. Connor Lewis-Smith, Mr. Gregory Williams (co-editor)

California State Polytechnic University, Humboldt Ms. Roxanne Robertson

Oregon State University Dr. Jack Barth, Ms. Anna Bolm, Ms. Elizabeth Daly, Mr. William Kennerly, Ms. Cheryl Morgan, Dr. Rachael Orben, Dr. Stephen Pierce, Ms. Samantha Zeman

University of California-San Diego Dr. Dan Rudnick

University of California-Santa Barbara Dr. Chris Free

University of California-Santa Cruz Dr. Megan Cimino, Dr. Jerome Fiechter, Ms. Rebecca Miller, Dr. Catherine Nickels, Dr. Antonella Preti, Dr. Travis Richards, Dr. Isaac Schroeder, Dr. Juan Zwolinski

University of Oregon Dr. Alan Shanks

California Department of Public Health Ms. Christina Grant, Ms. Ali Hossain, Mr. Duy Trong, Ms. Vanessa Zubkousky-White

California Department of Fish and Wildlife Ms. Christy Juhasz

CA Office of Env. Health Hazard Assessment Ms. Shannon Murphy, Dr. Beckye Stanton

Oregon Department of Fish and Wildlife Ms. Kelly Corbett, Mr. Matthew Hunter, Dr. Leif Rasmusson

Washington Department of Fish and Wildlife Mr. Zachary Forster, Dr. Matt George, Dr. Scott Pearson

Washington Department of Health Ms. Tracie Barry, Mr. Jerry Borchert

Beach Watch (Greater Farallones Association) Ms. Kirsten Lindquist, Ms. Jan Roletto

Coastal Observation and Seabird Survey Team Dr. Tim Jones, Dr. Julia Parrish

Farallon Institute Dr. William Sydeman, Ms. Sarah Ann Thompson

Monterey Bay Aquarium Research Institute Dr. Monique Messie

Oikonos Ecosystem Knowledge Ms. Jessie Beck, Ms. Danielle Devincenzi

Point Blue Conservation Science Ms. Meredith Elliott, Dr. Jaime Jahncke, Dr. Mike Johns, Mr. Peter Warzybok

Appendix B: FIGURES AND DATA SOURCES FOR THE MAIN BODY

Figure 1.1: Map of the California Current Ecosystem (CCE) and U.S. west coast Exclusive Economic Zone (EEZ) created by B. Feist, NMFS/NWFSC. GIS layers of freshwater ecoregions derived from TNC & WWF (2008), based on Abell et al. (2008).

Figure 2.1: Oceanic Niño Index data are from the NOAA Climate Prediction Center (https://origin.cpc.ncep.noaa.gov/products/analysis_monitoring/ensostuff/ONI_v5.php). PDO data are from N. Mantua, NMFS/SWFSC, and are served on the CCIEA ERDDAP server (https://oceanview.pfeg.noaa.gov/erddap/tabledap/cciea_OC_PDO.html). North Pacific Gyre Oscillation data are from E. Di Lorenzo, Georgia Institute of Technology (http://www.o3d.org/npgo/).

Figure 2.2: Standardized sea surface temperature anomaly plots were created by A. Leising, NMFS/SWFSC, using SST data from NOAA's optimum interpolation sea surface temperature analysis (OISST; https://www.ncei.noaa.gov/products/optimum-interpolation-sst); SST anomaly calculated using climatology from NOAA's AVHRR-only OISST dataset. MHW conditions are delineated by values of the normalized SST + 1.29 SD from normal. Methods for tracking and classifying heatwaves are described in Thompson et al. 2019b and at the CCIEA blocktracker website project page.

Figure 2.3: Newport Hydrographic (NH) line temperature data from J. Fisher, NMFS/NWFSC. Glider data along CalCOFI lines are from D. Rudnick and obtained from https://spraydata.ucsd.edu/projects/CUGN/.

Figure 2.4: Daily 2023 values of BEUTI and CUTI are provided by M. Jacox, NMFS/SWFSC; detailed information about these indices can be found at https://go.usa.gov/xG6Jp.

Figure 2.5: Habitat compression index estimates developed and provided by J. Santora, NMFS/SWFSC, and I. Schroeder, NMFS/SWFSC, UCSC.

Figure 2.6: Dissolved oxygen data from bottom mooring CE07 (https://oceanobservatories.org/site/ce07shsm/) obtained from NSF Ocean Observatories Initiative (2024). Newport Hydrographic (NH) line dissolved oxygen data are from J. Fisher, NMFS/NWFSC.

Figure 2.7: Newport Hydrographic (NH) line aragonite saturation state data provided by J. Fisher, NMFS/NWFSC.

Figure 2.8: Snow-water equivalent data were derived from the California Department of Water Resources snow survey (http://cdec.water.ca.gov/) and the Natural Resources Conservation Service's SNOTEL sites in WA, OR, CA and ID (http://www.wcc.nrcs.usda.gov/snow/). Data compilation and summary calculations by S. Munsch, NMFS/NWFSC, Ocean Associates, Inc.

Figure 2.9: Minimum and maximum streamflow data were provided by the US Geological Survey (http://waterdata.usgs.gov/nwis/sw). Data compilation and summary calculations by S. Munsch, NMFS/NWFSC, Ocean Associates, Inc.

Figure 3.1: Copepod biomass anomaly data were provided by J. Fisher, NMFS/NWFSC.

Figure 3.2. Krill data were provided by E. Bjorkstedt, NMFS/SWFSC SWFSC, Cal Poly, Humboldt and R. Robertson, Cooperative Institute for Marine Ecosystems and Climate (CIMEC) at Cal Poly, Humboldt.

Figure 3.3: Krill biomass estimates derived from 2023 Joint U.S.-Canada Pacific Hake Ecosystem and Acoustic Trawl (PHEAT) survey hydroacoustic data; provided by E. Phillips, NMFS/NWFSC.

Figure 3.4: Cumulative estimated CPS biomass data from the 2023 summer CPS survey. Surveys typically span the area between Cape Flattery and San Diego, but in some years also include Vancouver Island, Canada (2015-2019) and portions of Baja CA (2021-2022). Data and figure provided by K. Stierhoff, NMFS/SWFSC and J. Zwolinski, UCSC and NMFS/SWFSC.

Figure 3.5: Pelagic forage data from the Northern CCE from B. Burke, NMFS/NWFSC and C. Morgan, OSU/CIMRS. Data are derived from surface trawls taken during the NWFSC Juvenile Salmon & Ocean Ecosystem Survey (JSOES; https://www.fisheries.noaa.gov/west-coast/science-data/ocean-ecosystem-indicators-pacific-salmon-marine-survival-northern). Similarity analysis and cluster plot by A. Thompson, NMFS/SWFSC.

Figure 3.6: Pelagic forage data from the Central CCE were provided by J. Field, T. Rogers, K. Sakuma, and J. Santora, NMFS/SWFSC, from the SWFSC Rockfish Recruitment and Ecosystem Assessment Survey (https://go.usa.gov/xGMfR). Similarity analysis and cluster plot by A. Thompson, NMFS/SWFSC.

Figure 3.7: Pelagic forage larvae data from the Southern CCE were provided by A. Thompson, NMFS/SWFSC, from spring CalCOFI surveys (https://calcofi.org/); data were not collected in 2020 due to survey cancellations associated with the COVID pandemic. Similarity analysis and cluster plot by A. Thompson, NMFS/SWFSC.

Figure 3.8: Data for at sea juvenile salmon provided by B. Burke, NMFS/NWFSC and C. Morgan, OSU/CIMRS, from surface trawls taken during the NWFSC Juvenile Salmon and Ocean Ecosystem Survey (JSOES).

Figure 3.9: Estimates of juvenile abundance for West Coast groundfish were provided by N. Tolimieri, NMFS/NWFSC, based on data from the NOAA West Coast bottom trawl survey (https://www.fisheries.noaa.gov/west-coast/science-data/us-west-coast-groundfish-bottom-trawl-survey).

Figure 3.10: Center of gravity biomass estimates of West Coast groundfish were provided by N. Tolimieri, NMFS/NWFSC, based on data from the NOAA West Coast bottom trawl survey. Data available via API download from: https://www.webapps.nwfsc.noaa.gov/data/map

Figure 3.11: Albacore, swordfish, and bluefish tuna diet data provided by H. Dewar and C. Nickels, NMFS/SWFSC; A. Preti and T. Richards, UCSC.

Figure 3.12: California sea lion data provided by S. Melin, NMFS/AFSC.

Figure 3.13: Whale entanglement data provided by D. Lawson and L. Saez, NMFS/WCR.

Figure 3.14: Seabird fledgling production data at nesting colonies on Southeast Farallon Island provided by J. Jahncke and P. Warzybok, Point Blue Conservation Science.

Figure 3.15: WA domoic acid data are provided by the Washington State Department of Health, OR data from the Oregon Department of Agriculture, and CA data from the California Department of Public Health.

Figure 4.1: Data for commercial landings are from PacFIN (http://pacfin.psmfc.org) and NORPAC (North Pacific Groundfish Observer Program).

Figure 4.2: Data for recreational landings are from RecFIN (http://www.recfin.org/) and the CDFW Pelagic Fisheries and Ecosystem Data Sharing index).

Figure 4.3: Relative suitability scores were calculated by NMFS/NWFSC based on ecosystem indicator data sources outlined in report text. Boundaries of proposed Wind Energy and Lease Areas from BOEM (https://www.boem.gov/renewable-energy/state-activities/Oregon; https://www.boem.gov/renewable-energy/state-activities/California). Figure created by K. Andrews, NMFS/NWFSC.

Figure 5.1: Community social vulnerability index (CSVI), commercial fishery reliance, and recreational fishing reliance data provided by C. Weng (NEFSC), L. Colburn (NMFS/OST), K. Norman, NMFS/NWFSC, and C. Lewis-Smith, NMFS/NWFSC, PSMFC, based on data derived from the US Census Bureau's American Community Survey (ACS; https://www.census.gov/programs-surveys/acs/), PacFIN (http://pacfin.psmfc.org), ESRI business analyst, and guide and charter license data from Oregon and Washington state.

Figure 5.2: Fishery revenue diversification estimates were provided by D. Holland, NMFS/NWFSC, and S. Kasperski, NMFS/AFSC, utilizing data provided by PacFIN (http://pacfin.psmfc.org) and AKFIN (https://akfin.psmfc.org).

Figure 5.3: Fishery Participation Network data and analyses provided by J. Samhouri, M. Fisher, UW, and C. Lewis-Smith, PSMFC, with data derived from PacFIN (http://pacfin.psmfc.org) and the US Census Bureau's American Community Survey (ACS; https://www.census.gov/programs-surveys/acs/).

Table 3.1: Stoplight table of indicators related to salmon in the northern CCE courtesy of B. Burke, J. Fisher, and K. Jacobson, NMFS/NWFSC, and C. Morgan, and S. Zeman, OSU/CIMRS (https://www.fisheries.noaa.gov/west-coast/science-data/ocean-ecosystem-indicators-pacific-salmon-marine-survival-northern).

Table 3.2: Table of indicators and qualitative outlook for 2024 Central Valley fall Chinook salmon returns courtesy of N. Mantua and B. Wells, NMFS/SWFSC.

Appendix C: CHANGES IN THIS YEAR'S REPORT

Below we summarize major changes in the 2023-2024 Ecosystem Status Report. As in past reports, many of these changes are in response to requests and suggestions received from the Council and advisory bodies (including those related to FEP Initiative 2, "Coordinated Ecosystem Indicator Review" (March 2015, Agenda Item E.2.b), or in response to annual reviews of indicators and analyses by the SSC-Ecosystem Subcommittee (SSC-ES). We also note items we have added and information gaps that we have filled since last year's report (Harvey et al. 2023).

Table C.1: Changes to this year's Ecosystem Status Report

Request/Need/Issue	Response/Location in Document
The ESR is labor-intensive to produce, and efficiencies such as automation are needed to sustain the report and build it out to meet evolving needs of the Council and other partners. (March 2022, Agenda Item H.2.b, Supplemental EWG Report 1)	The ESR team continued to improve automation of the report in 2023 and brought on a new team member to help with the transition to a more automated, efficient, user-friendly process for updating the report annually. This year's report was produced in Bookdown, an open-source package in the R programming language. Howeverin the upcoming year we are changing to Quarto, the next generation version of Rmarkdown with enhanced functionality. A data uploader was also implemented to streamline data intake and management. Lastly, this year's report follows on criteria established in agreement with the council in 2022, that the length of the current ESR would be by word count (~8000) rather than page number (20), in order to allow for improved formatting and larger figures. Total word count this year is 7787 with 31 figures.
General improvements to figures and analyses for climate and ocean drivers	The ESR team made multiple changes to climate and ocean drivers this year, including: 1. Added plots of cumulative upwelling back into the report (Appendix F) 2. Included new climatology for marine heatwave analysis; 1982-2022 rather than 1982-2010 (Appendix F). 3. Introduced a new possible regional indicator of El Niño for the southern California region - the SCTI (Southern California Temperature Index) (Appendix E).
New sources of dissolved oxygen data from the CCE	This year we included near-bottom DO levels collected from CTD casts during the June JSOES survey (2007-2023) that extend from Newport,

(*Response to HC interest in learning more about hypoxia trend at larger spatial scale*)	OR to La Push, WA. We also present oxygen data collected via a moored instrument package off the Washington coast (46.9859°N, 124.566°W), which has been developed and maintained from 2015-2023 through the NSF Ocean Observatories Initiative (2024). See Appendix F. We are continuing to explore and summarize additional sources of DO data collected via NOAA surveys and partnerships to better describe DO levels throughout the CCE, and particularly in areas north of Coos Bay, OR that are most vulnerable to low levels of dissolved oxygen
Expanded information on forage species in the CCE *(Response to feedback from the SSC to incorporate more coastwide surveys of prey)*	Krill are an important prey source for managed and protected species in the CCE and time series of their abundance in the ESR have been limited to northern CA (Trinidad Head line). This year we also provide estimates of relative krill abundance (2007-2023) from the biennial Joint U.S.- Canada Pacific Hake Ecosystem and Acoustic Trawl survey, which is conducted in June-September and spans from Point Conception to British Columbia. (Section 3.1 and Appendix H). In addition, we present preliminary data on Dungeness crab megalopae abundance in southern OR, as a possible new indicator of lipid-rich prey availability in that region (Appendix H). For the first time, the main report also includes estimates of CPS biomass from the annual coastwide CPS survey, including preliminary estimates from 2023 (Fig. 3.4), complemented by additional CPS information in Appendix I.
Refinements to salmon stoplight tables and suite of indicators *(Partial response to feedback from SSC-ES from ESR topic review in September 2022)*	This year the ESR team removed the seabird predation indicator from the Central Valley Fall Chinook (CVFC) stoplight table as these data are no longer being updated (Table 3.2). We will, however, continue to report on the diet composition of seabirds in the central CCE as it pertains to juvenile salmon and other forage species. In addition, we are now including egg thiamine concentration as an indicator in the CVFC table. Thiamine deficiency is an important stressor in Central Valley Chinook salmon that is linked to the dominance of anchovy in the marine food web supporting these salmon. Further, we introduce a new

	salmon stock-specific metric, CMISST (Covariance Map Index of Sea Surface Temperature), that is still in development but shows high prediction skill for spring Chinook salmon and steelhead returns (Appendix J).
Improvements to groundfish indicators and analyses (*Response to EAS recommendation for indicators that detect or confirm changes in species distribution, and how such changes could affect fishing communities*)	The CCIEA team updated and expanded groundfish analyses that have been included in past reports and well-received by Council advisory bodies. These include: 1. Time series of groundfish spatial distributions (center-of-gravity) through 2023. 2. Times series of groundfish availability indices to West Coast fishing ports through 2023. 3. Juvenile groundfish recruitment indices for four species through 2023. See Section 3.4 and Appendix K.
Delays in marine mammal sample processing	In 2023, sea lion pups were counted using uncrewed aerial systems for the first time. Due to delays in image processing, sea lion pup counts were not available in time for this year's report, only preliminary counts were reported. Thus, Figure 3.12 includes only pup weights and not pup counts.

Expanded analyses and figures on human well-being components of the ESR	The ESR has regularly reported on diversification of fishing revenue, and this year we present trends in non-fishery income (NFI) diversification for the first time as well (Appendix S). We have not presented this information in prior reports due to a lack of regularly collected data on NFI until recently. After initial inclusion in 2016, the recreational fishing reliance and engagement measures for the West Coast have been reestablished and included in this year's ESR. Input variables were refined to ensure reproducibility annually across WA, OR, and CA (see Section 5.1 in main document and Appendix S). Further, we included a new, easily interpretable figure on the spatial-temporal history of closures and management restrictions in the West Coast Dungeness crab fishery from 2015 to 2023 (Fig. O.1) that was adapted from Free et al. (2022).
Changes in fishery participation network (FPN) analysis (*Aligns with SSC-ES and EAS interest to better understand the vulnerability of communities to negative changes in salmon fishing opportunity)*	In last year's ESR, we conducted a FPN analysis focused on salmon and examined the vulnerability of West Coast port groups to future changes in salmon fishing. We built on that work in this year's report by including a new analysis that compared the number of active salmon vessels and the revenue of commercial salmon vessels between two periods (2017-2022 and 2022-2023) for 17 ports. This subsequent analysis demonstrated that the outcomes of the FPN vulnerability analysis from last year offered predictive insights into port-level impacts of salmon fisheries closures in California in 2023. Section 5.3 and Appendix U.
Changes to offshore wind energy (OWE) analysis and figures (*Aligns with CPSAS interest on understanding impacts of offshore wind development on spawning habitat, ocean transport, and nutrition.)*	Last year, the ESR featured seven fisheries indicators that describe variation in groundfish bottom trawling activity in regions under consideration for OWE development. This year we introduce 6 ecosystem indicators of spatial variation in oceanography and productivity in the CCE. We also present a spatial suitability analysis, based on the six indicators, for areas

	off of northern California being considered for OWE development in 2024 (Section 4.2 in main document and Appendix Q). Together, the fisheries and ecosystem indicators can be used to identify potential interactions across the CCE social-ecological system.
New topics in the Climate Change Appendix (*Response to EWG 2023 recommendation on including information on the congruence between basin- and local-scale indices, as well as the decoupling of these indices with ecological observations*) *(Partial response to feedback from SSC-ES from ESR topic review in September 2022)* (*Response to the EAS recommendation to include indicators for projecting, detecting, or confirming changes or shifts in species distribution, and how such changes could affect fishery diversification and fishing communities*)	We note that the full Climate Change Appendix (Appendix E) will be included in the supplemental briefing materials for the March 2024 Council meeting (Agenda Item H.1.a, Supplemental CCIEA Report 2: 2023-2024 California Current Ecosystem Status Report Appendices). The ESR team updated the appendix this year to include three overarching themes. 1. Discussion of sources of uncertainty in climate predictions and projections, including how climate is related to biological responses, and how those relationships may change over time in the CCE. 2. Discussion about anticipated impacts of the ongoing El Niño of 2023-24, and the indices that might be used to forecast and track the impacts of El Niño. 3. New long-term climate projections of shifts in the distribution of managed species alongside the social-ecological vulnerability and climate risk for West Coast fishing fleets.

Appendix D: SUMMARY INFOGRAPHICS FOR THE 2023-2024 ECOSYSTEM STATUS REPORT

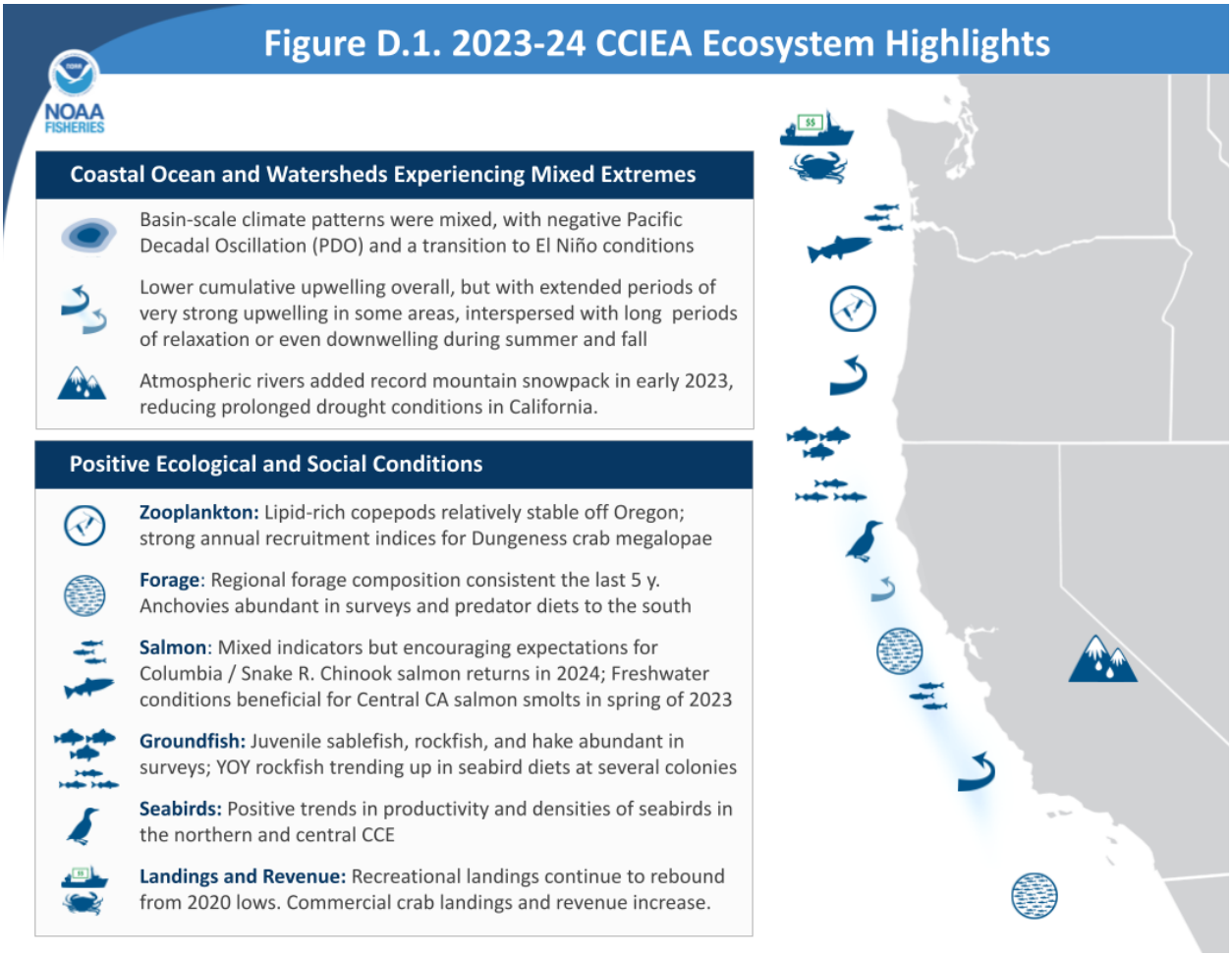

Figure D.2. 2023-24 CCIEA Ecosystem Highlights

NOAA FISHERIES

Unfavorable Conditions/Risk Factors

Ocean Temperatures & Marine Heatwave: Overall ocean warming in the NE Pacific and transition to El Niño conditions. 4th largest marine heatwave with episodic intrusions into US EEZ

Terrestrial Disturbances: Atmospheric rivers and rapid snow melt-off bring flooding in early 2023; low mountain snowpack through west by late 2023. Warmer streams in the north

Krill: 2nd lowest coastwide acoustic biomass estimates on record

California Chinook Salmon: Relatively poor habitat conditions for all California stocks the last three years; potential thiamine deficiency impacts in Central Valley natural-area fish.

Seabirds: Lowest recorded densities of sooty shearwaters in the north; Avian flu decimates nesting tern colonies in Lower Columbia

Sea lions: First decline in average pup weight in 5 years

Whale Entanglement: Remained above-average in 2023

HABs: HAB activity continued through 2024, leading to shellfish fishery closures & delays; wildlife mortalities in the south

Mixed Ocean Uses: Impacts of wind lease area locations continue to come into focus with new ecosystem indicator portfolios

Fishery Landings & Revenue: Declining catches and revenue for most sectors; uptick in geographic concentration of revenue; salmon fishery closures in CA impact salmon-dependent ports

Appendix E: DEVELOPING INDICATORS OF CLIMATE VARIABILITY AND CHANGE

This appendix is intended to (1) update the Council on research advances that support climate-informed decision-making for managed and protected species in the CCE, and (2) continue the ongoing "conversation" between the CCIEA team and the PFMC on how best to present climate considerations in the CCIEA-ESR. This effort stems from an EAS recommendation to incorporate climate change information into the ESR for Council management considerations (Supplemental EAS Report 1, March 2021, Agenda item I.2.b), echoed by the Climate and Communities Initiative Core Team (CCCT Report 1, September 2021, Agenda Item H.2.a), and has been improved based on recommendations from the SSC-ES (Agenda Item H.1.a SSC-ES Report 1 March 2023). We are eager to expand the provision of forward-looking climate information as Council needs, CCIEA team workload, and page limits allow.

The 2023-2024 ESR climate variability and change appendix is designed to provide context for the use of forward-looking climate information and then offer examples of our capabilities on two timescales: short term forecasts (i.e., what will happen in the next year), and long-term projections (i.e., what trends can be expected over multi-decadal timescales). It is divided into three sections:

1. Discussion of sources of uncertainty in climate predictions and projections, to contextualize the use of this information in decision making. There are a number of sources of uncertainty, including how the climate will evolve, how climate is related to biological responses, and how those relationships may change over time. Nevertheless, this imperfect information can support improved outcomes over time.
2. Discussion of the potential impacts of the ongoing El Niño of 2023-24, predicted ocean conditions in the coming months, and the relevant indices that might be used to forecast and track the impacts of El Niño on the CCE.
3. Projections of long-term shifts in the distribution and abundance of managed species under climate change scenarios, as well as associated vulnerability and risk for West Coast fishing fleets. This section highlights recent work stemming from the Groundfish, Climate Change, and Communities in the California Current (GC5) and Future Seas projects.

The main body of this appendix will be available in the supplemental briefing materials for the March 2024 Council meeting under Agenda Item H.1.a, Supplemental CCIEA Report 2: 2023-2024 California Current Ecosystem Status Report Appendices.

Appendix F: CLIMATE AND OCEAN INDICATORS

Link to main section: Climate and Ocean Drivers

F.1 Basin-scale Climate/Ocean Indicators at Seasonal Time Scales

Figure F.1 shows seasonal averages and trends of the three basin-scale climate forcing indicators shown in the main report in Figure 2.1. The sharp increase in Summer ONI in 2023 (Fig. F.1, top right) reflects the onset of El Niño conditions, as detailed elsewhere in this report.

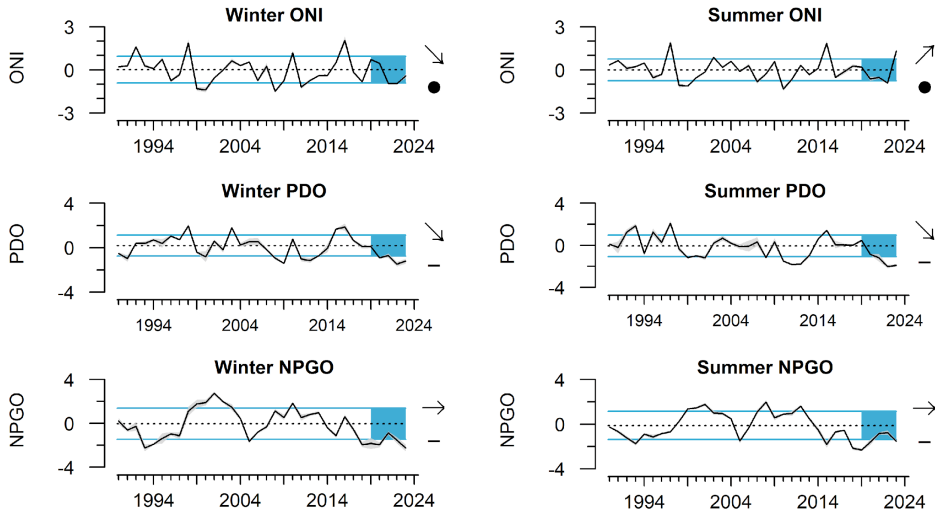

Figure F.1: Winter (Jan-Mar) and Summer (July-Sep) values for the basin-scale climate indicators: Ocean Niño Index (ONI), Pacific Decadal Oscillation (PDO), and North Pacific Gyre Oscillation (NPGO) through 2023. Mean and s.d. for 1991-2020. Lines, colors, and symbols are as in Fig. 2.1.

Satellite data, which has been collected in a similar fashion since 1982, allows for a basin-scale view of sea surface temperature (SST) at up to daily and sub-degree (spatial) resolution. Here we show seasonal averages of SST anomalies (the difference from climatology) across the NE Pacific (Fig. F.2). Winter saw anomalously high SST to the west of the region, which was an expression of the large marine heatwave that had continued from 2022. This trend in warming continued during spring, with the warm waters expanding throughout the region, coming closer to the US west coast, particularly off WA. During spring, OR and northern CA saw cooler than normal conditions, due to strong upwelling. During summer 2023, average temperatures throughout the NE Pacific were warmer than normal, and for the entire US west coast. Fall saw the largest warm anomaly in basin-scale SST, with temperatures often > 3°C warmer than normal for much of the region. This coincides with the maximum real extension of the marine heatwave of 2023, which penetrated to almost the entire coastline during August and into September.

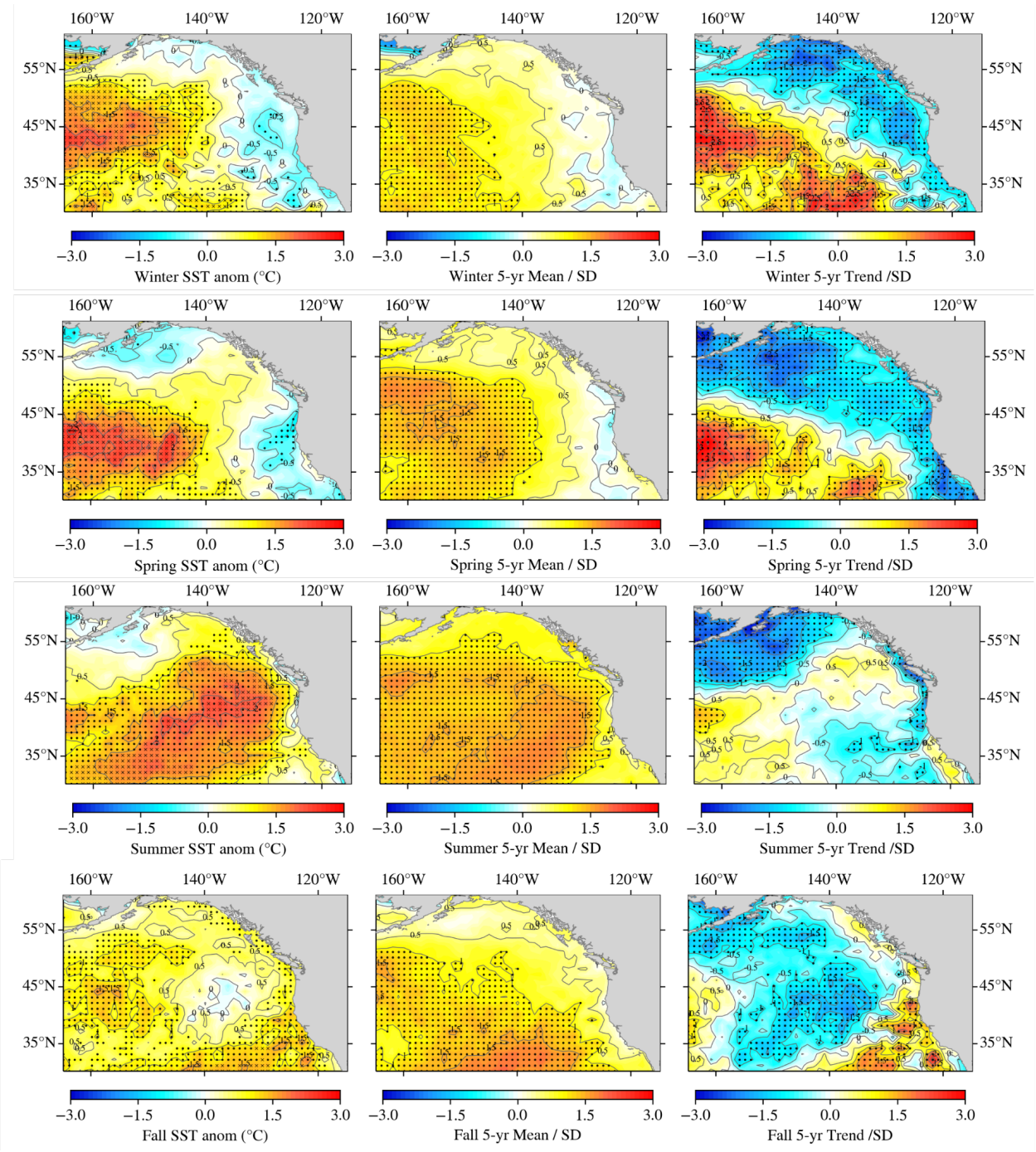

Figure F.2: Left: Sea surface temperature (SST) anomalies in 2023, based on 1982-present satellite time series in winter (Jan-Mar; top), spring (Apr-Jun), summer (Jul-Sep), and fall (Oct-Dec; bottom). Center: Mean SST anomalies for 2019-2023. Right: trends in SST anomalies from 2019-2023. Black dots mark cells where the anomaly was >1 s.d. above the long-term mean (left, middle) or where the trend was significant (right). Black x's mark cells where the anomaly was the highest in the time series.

Glider data has become an increasingly useful tool for analyzing trends in subsurface water temperatures over time. The following series of plots represents data from subsurface gliders, which generally sample in onshore-offshore transects on a weekly to monthly basis, and have been in service long enough for the development of climatologies, which are then used to compute temperature anomalies. Examination of these subsurface anomalies over time suggests that during 2023 subsurface temperatures off Newport, OR were generally cooler than previous years during the winter and spring, but warmer than normal during summer and into fall (Fig. F.3). Off Northern CA, subsurface temperatures were also generally cool in the winter and spring, although during the summer, the intrusion of the marine heatwave can be seen in the upper 50m during the later summer and fall (Fig. F.4). Off Monterey, 2023 saw average surface and subsurface temperatures (Fig. F.5) in winter and spring, with warmer waters dominating from summer through fall. From Pt. Conception south (Figs. F.6 and F.7), there has been an increase in stratification, due to a return of deeper waters (>50m) to a more "normal" temperature (e.g. anomalies close to zero), while surface waters remained anomalously warm, as in previous years.

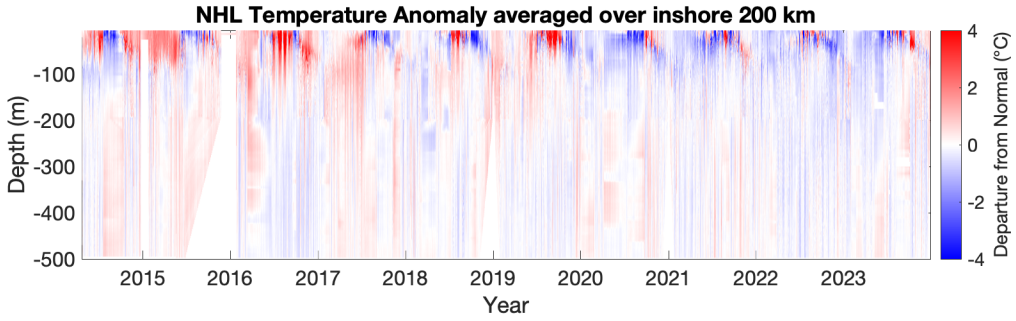

Figure F.3: Time-depth plot of average subsurface temperature anomalies from the shore to 200 km offshore along the Newport Hydrographic Line, based on OSU-OOI coastal endurance array gliders (https://ceoas.oregonstate.edu/ocean-observatories-initiative-ooi). Climatology based on monthly averages created over 2014-2022

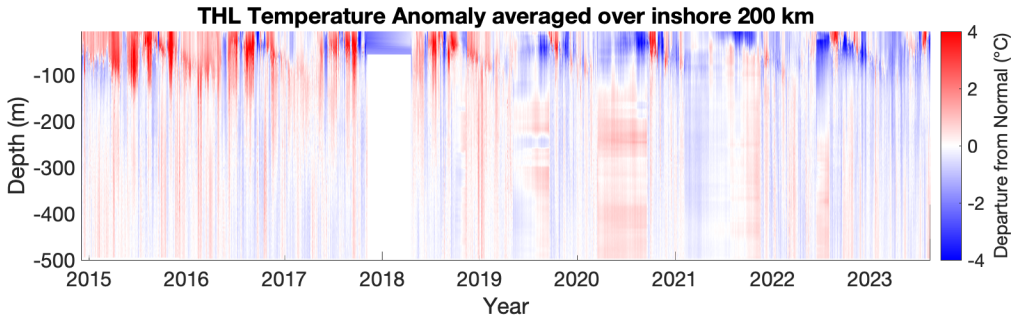

Figure F.4: Time-depth plot of average subsurface temperature anomalies from the shore to 200 km offshore along the Trinidad Head Line. Data courtesy of CeNCOOS and NANOOS.

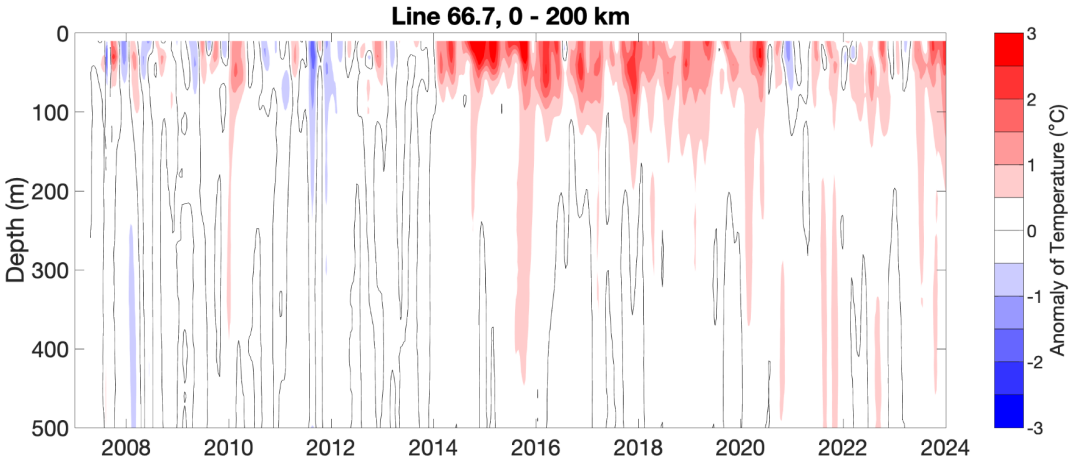

Figure F.5: Time-depth plot of average subsurface temperature anomalies from the shore to 200 km offshore along CalCOFI line 66.7, based on SPRAY gilder data and climatology. Data from the California Underwater Glider Network are provided by D. Rudnick, Scripps Institute of Oceanography Instrument Development Group (doi: 10.21238/S8SPRAY1618).

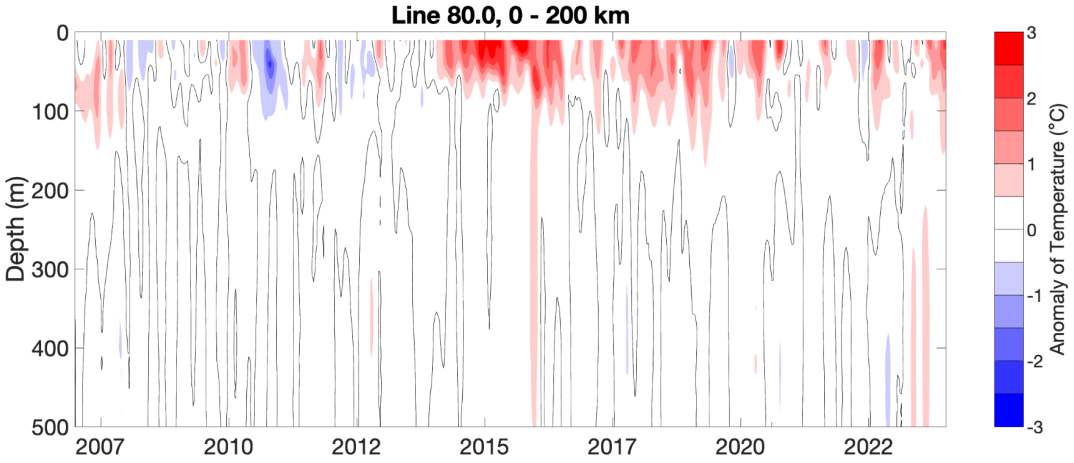

Figure F.6: Time-depth plot of average subsurface temperature anomalies from the shore to 200 km offshore along CalCOFI line 80, based on SPRAY gilder data and climatology. Data from the California Underwater Glider Network are provided by D. Rudnick, Scripps Institute of Oceanography Instrument Development Group (doi: 10.21238/S8SPRAY1618).

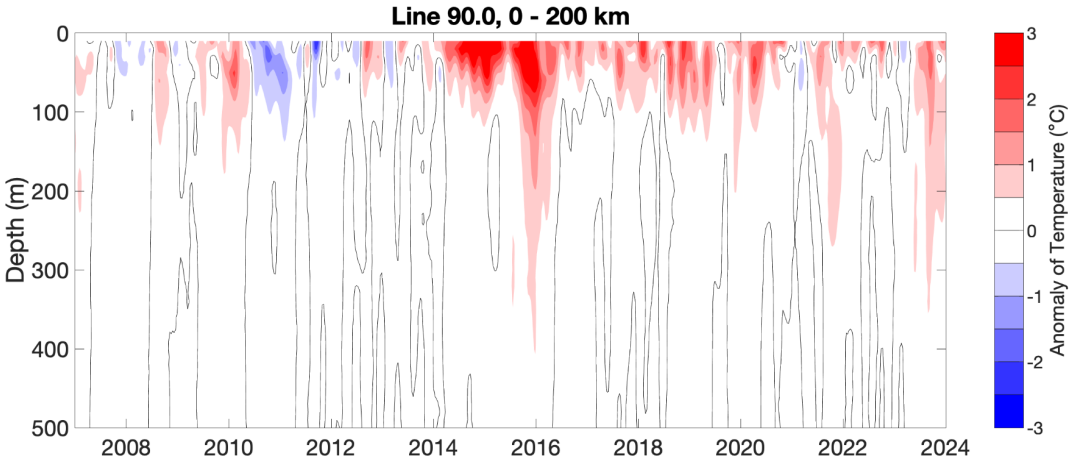

Figure F.7: Time-depth plot of average subsurface temperature anomalies from the shore to 200 km offshore along CalCOFI line 90, based on SPRAY gilder data and climatology. Data from the California Underwater Glider Network are provided by D. Rudnick, Scripps Institute of Oceanography Instrument Development Group (doi: 10.21238/S8SPRAY1618).

The CCE is an upwelling dominated system, with the interaction between upwelling, stratification, and source water properties controlling much of coastal temperatures, nutrient input, and overall productivity. Time series of upwelling indices (CUTI and BUTI, Fig. 2.4) provide information on upwelling strength at sub-seasonal frequency and upwelling phenology, and allow interannual comparisons of seasonal upwelling timing and frequency. Additionally, the calculation of cumulative upwelling allows for a comparison of the total amount of upwelling a region receives during the entire course of the year (Fig. F.8). Cumulative upwelling is calculated as the daily summation of upwelling values (additive for positive upwelling, and subtractive for negative upwelling - aka downwelling) starting on Jan 1 and ending on Dec 31st. These plots demonstrate that cumulative upwelling in 2023 (red lines) was below the climatological average (black lines) for most of the year, including during the spring-summer season of peak productivity. This was the case at all latitudes except for 33°N, where cumulative upwelling was above normal.

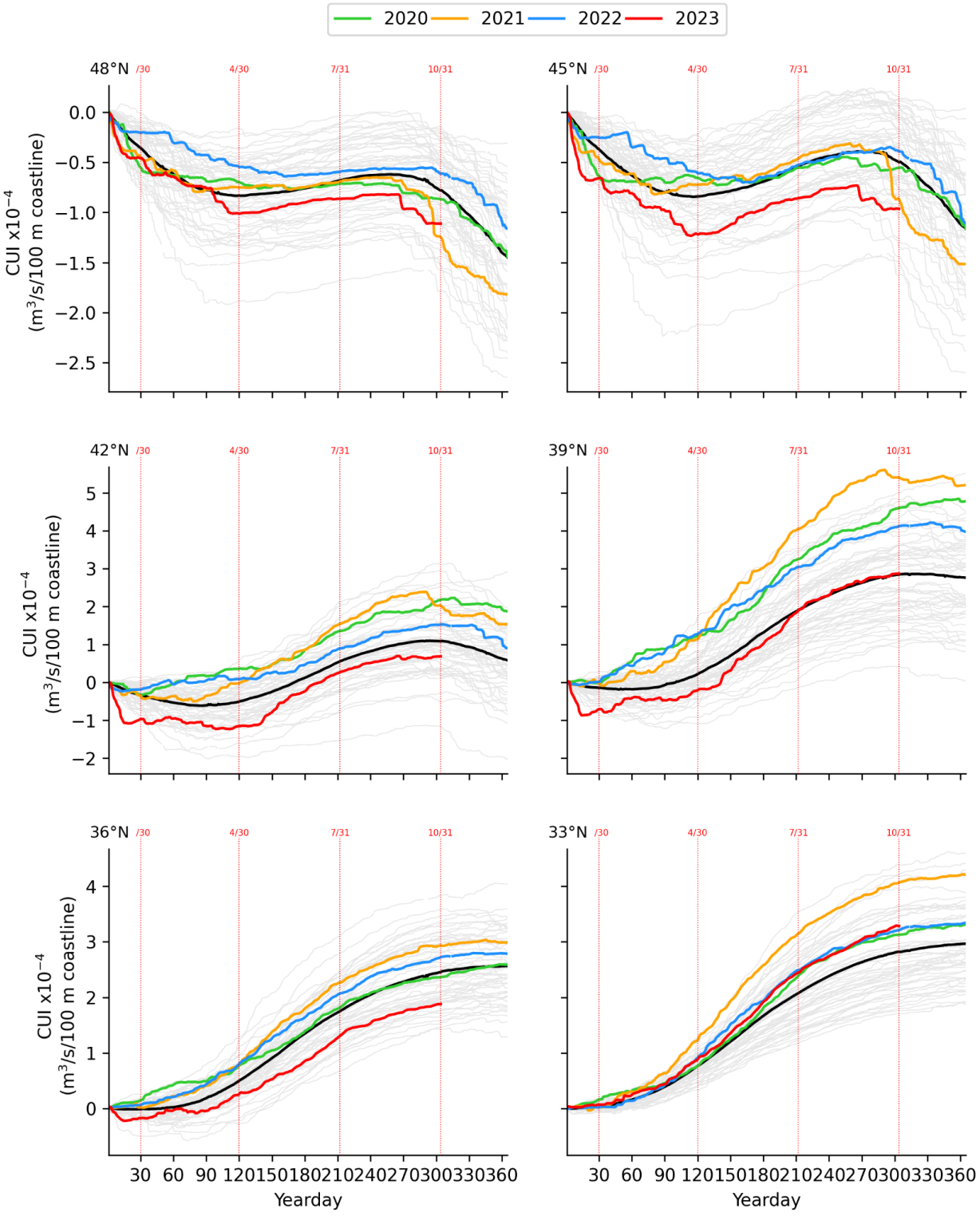

Figure F.8: Cumulative upwelling index (CUI) calculated for respective locations throughout the CCE for 2023 and select years for comparison. CUI based on the Bakun upwelling index.

F.2 Assessing Marine Heatwaves in 2023

There is growing recognition that marine heatwaves can have strongly disruptive impacts on the CCE (e.g., Morgan et al. 2019). Based on an analysis of sea surface temperature anomalies (SSTa) obtained from satellite measurements (OISST; we define marine heatwaves as 1) times when normalized SSTa >1.29 s.d. (90th percentile) of the long-term SSTa time series at a location, and 2) lasts for >5 days; which are analogous to the thresholds suggested in Hobday et al. (2016). Here, we further report on statistics concerning large heatwaves (LHW) which were tracked through space and time, with LHW defined as those heatwaves with an area > 400,000 km^2 (these denote the top 20% of all heatwaves by area as measured since 1982 when satellite data became available for tracking; Leising, in revision). 2023 saw extensive coverage of the US West Coast EEZ by marine heatwaves from August through September, and then again for much of November (Fig. F.9), due to the LHW that occurred during 2023. The 2023 heatwave was the 4th largest by area, and 5th longest (Fig. F.10) recorded since monitoring began in 1982.

Note: the underlying climatology used for SST anomaly analysis has changed from 1982-2010, to now encompass 1982-2020; hence small changes in the retrospective analysis of tracked heatwaves reported in Figure F.10 as compared to last year's report (fewer total tracked heatwaves N, and a downgrading of maximum area for the 2022 event).

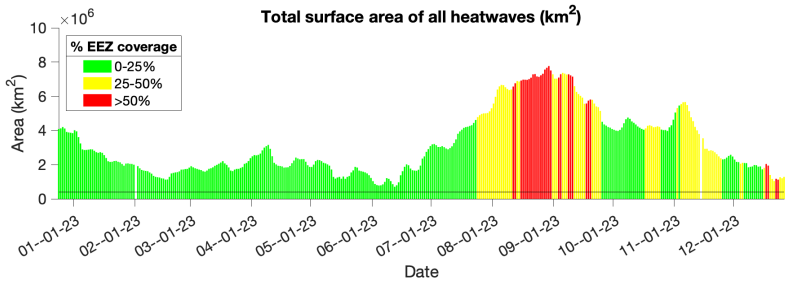

Figure F.9: Areas of North Pacific marine heatwaves during 2023. The horizontal line represents 400,000 km^2, the area threshold that we use for tracking individual events over time (top 20% of heatwaves by area; Leising, in revision). Color indicates the percentage of the US West Coast EEZ that was in heatwave state.

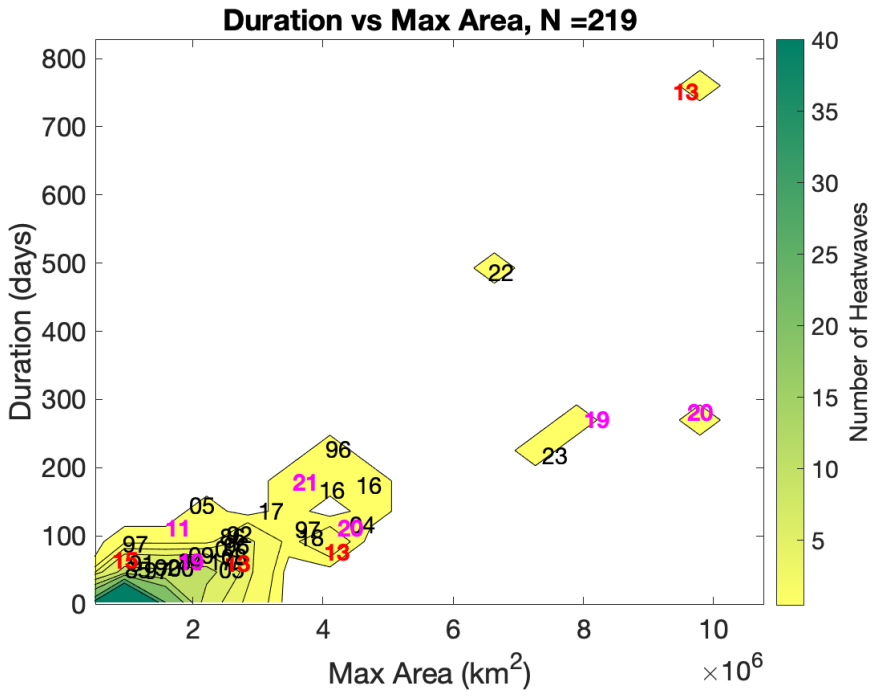

Figure F.10: Duration and maximum areas of NE Pacific large marine heatwaves, 1982-2023. Shading indicates the number of heatwaves (out of 219). Outliers are marked with numbers indicating the year the heatwave formed.

F.3 Habitat Compression Index

Spatial variability in patterns of upwelling, including the distribution of upwelled water and associated development of hydrographic fronts, is important for ecosystem monitoring and assessment of marine heatwaves and ecosystem shifts that can impact coastal fishing communities. Coastal upwelling creates a band of relatively cool coastal water, which is suitable habitat for a diverse and productive portion of the CCE food web. Monitoring the area and variability of upwelling habitat provides regional measures of habitat compression—an indicator to monitor the incursion of offshore warming (e.g., from heatwaves or reduced upwelling conditions) over shelf waters, which relates to shifts in the pelagic forage species community in space and time. Santora et al. (2020) applied principles of ecosystem oceanography and integration of fisheries surveys to develop the Habitat Compression Index (HCI) to quantify how offshore warming during the 2013–2016 marine heatwave and previous warming events restricted the cool upwelling habitat to a narrower-than-normal band along the coast. This compression of habitat consequently altered prey community composition and distribution, spatial aggregation patterns of top predators, and contributed to increased rates of whale entanglements in fixed fishing gear.

HCI is derived from the CCE configuration of the Regional Ocean Modeling System (ROMS) model with data assimilation (Neveu et al. 2016), and is estimated in four biogeographic provinces within the CCE: 30°-35.5°N, 35.5°-40°N, 40°-43.5°N, and 43.5°-48°N. HCI is defined as the area of monthly averaged ROMS model temperatures at a depth of 2 m that fall below a temperature threshold. Each region/month has a unique temperature

threshold, based on its distinct historic climatology. Seasonal means for central California are shown in the main body of the report (Fig. 2.5). Winter and spring means for all four regions are shown here in Figure F.11, and indicate above-average availability of cool surface habitats in all regions during winter and spring of 2023, continuing recent positive trends.

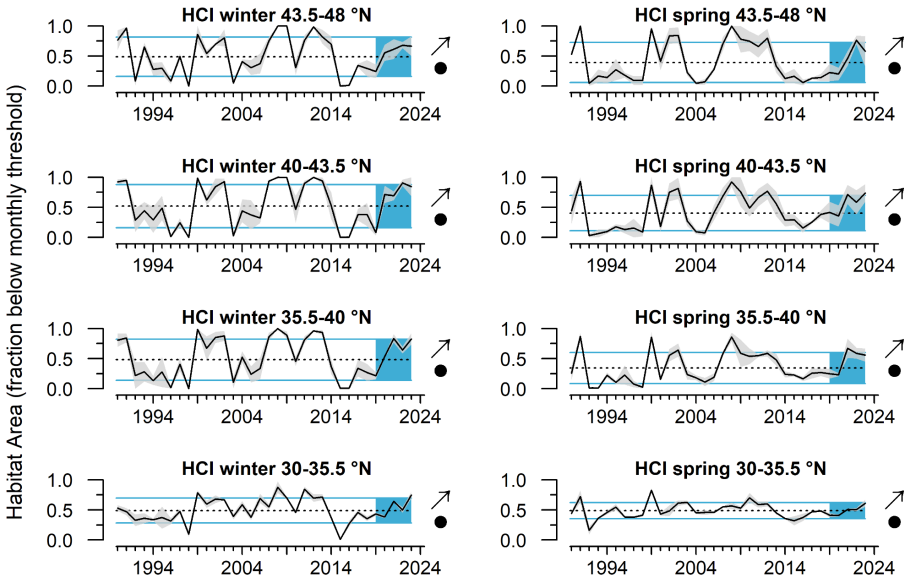

Figure F.11: Mean winter (January - March) and spring (April - June) habitat compression index by region, 1990 - 2023. Gray envelope indicates ±1 s.e. Data provided by J. Santora, NMFS/SWFSC, and I. Schroeder, NMFS/SWFSC, UCSC. Lines, colors, and symbols are as in Fig. 2.1.

F.4 Seasonal Dissolved Oxygen and Ocean Acidification Indicators

Nearshore dissolved oxygen (DO) depends on many processes, including currents, upwelling, air–sea exchange, and community-level production and respiration in the water column and benthos. DO is required for organismal respiration; low DO can compress habitat and cause stress or die-offs for sensitive species. Waters with DO levels <1.4 mL/L (~ 2 mg/L, note unit change) are considered to be hypoxic; such conditions may occur on the shelf following the onset of spring upwelling, and continue into the summer and early fall months until the fall transition vertically mixes shelf waters. Upwelling-driven hypoxia occurs because upwelled water from deeper ocean sources tends to be low in DO, and microbial decomposition of organic matter in the summer and fall increases overall system respiration and oxygen consumption, particularly closer to the seafloor (Chan et al. 2008). Except for summer 2023 off the coast of northern WA, oxygen levels were above hypoxic levels at most locations (Fig. F.12). Spring and summer oxygen levels were generally higher in 2023 than spring 2022 at the different stations and depths sampled, with fall oxygen levels close to time series averages (Fig. F.12).

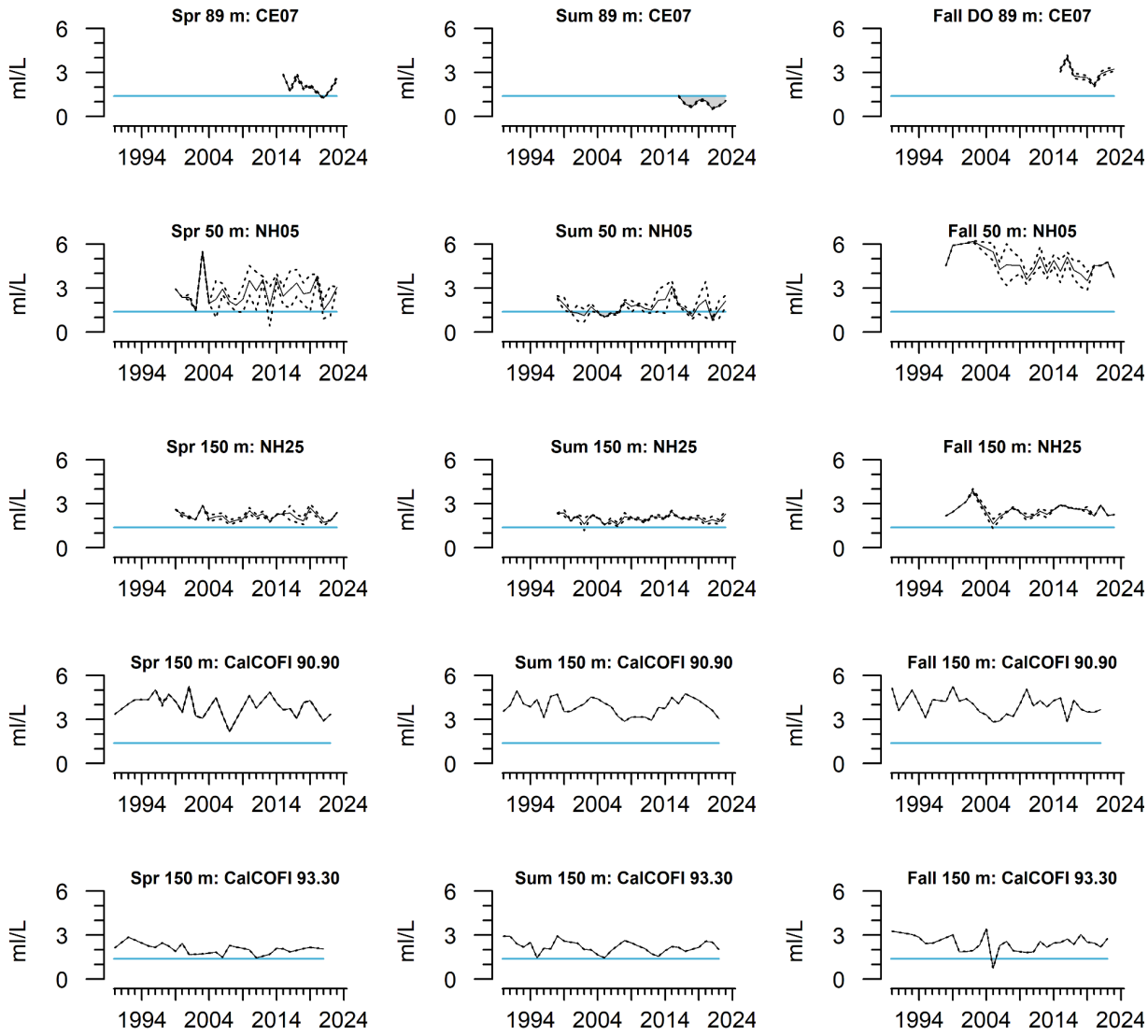

Figure F.12: Dissolved oxygen in spring (April-June), summer (July-September), and fall (Oct-Dec) off of Washington (CEO7, 2016-2023), Oregon (NH, 1998/1999-2023), and California (CalCOFI, 1990 - 2023).

Annually, on the JSOES surveys conducted mid-summer, CTD casts are taken which include measurements of oxygen levels (Fig. F.12). Figure F.13 shows the June map of oxygen compiled from this survey. This year's oxygen distribution in June supports the higher frequency measurements reported above; most waters off Oregon remained just above hypoxic levels during the summer, whereas waters off the southern Washington coast had decreased oxygen and occasional hypoxia.

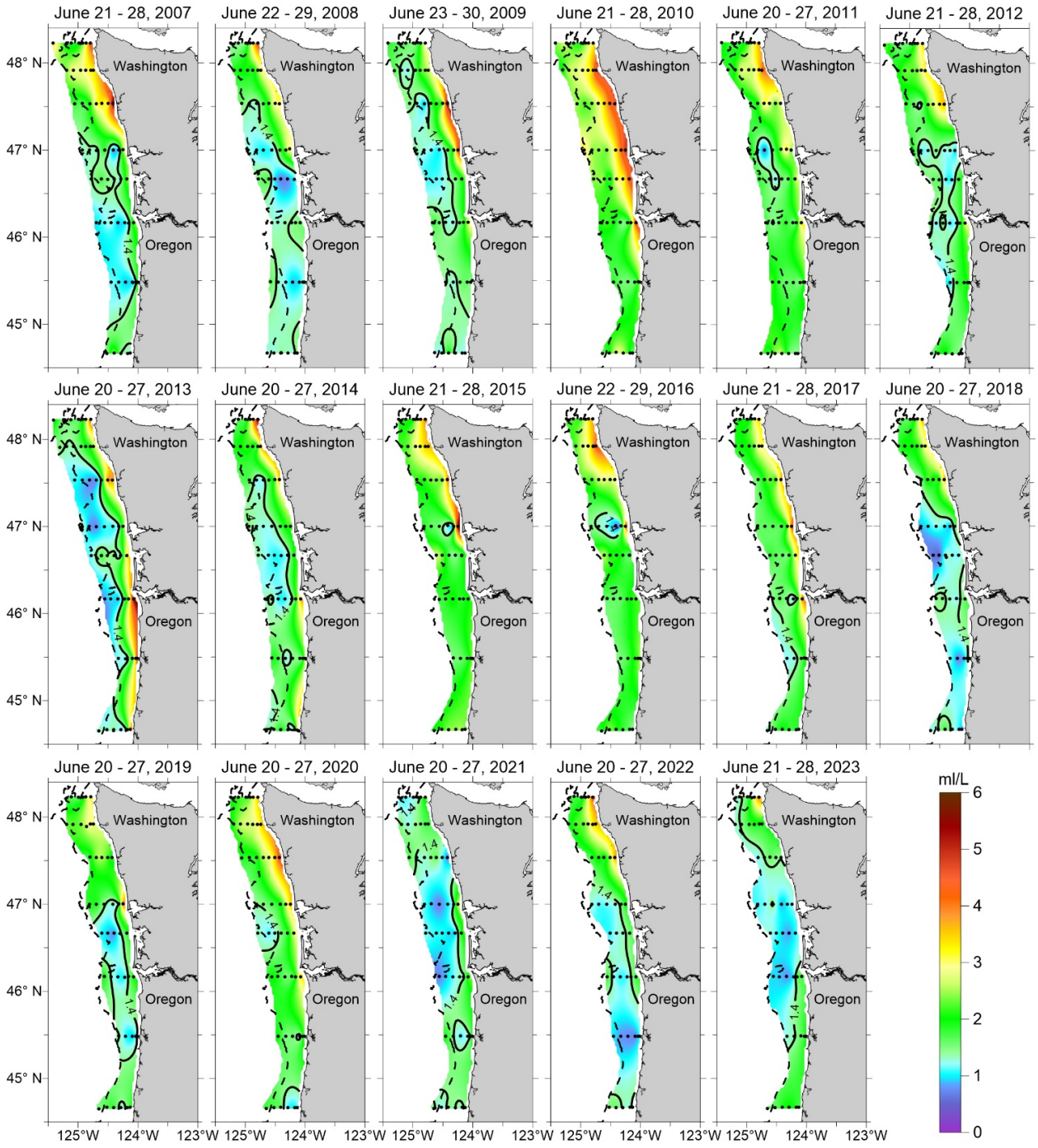

Figure F.13: Near-bottom dissolved oxygen levels (ml/L) collected from CTD casts during the June JSOES survey, 2007-2023. Solid contour represents the 1.4 mL/L hypoxia threshold; dashed contour is the 200 m isobath (shelf break); dots represent data collection locations (stations). Data provided by C. Morgan, OSU/CIMRS.

Ocean acidification (OA), which occurs when atmospheric CO_2 dissolves into seawater, reduces seawater pH and carbonate ion levels. Upwelling transports hypoxic, acidified waters from deeper offshore onto the continental shelf, where increased community-level metabolic activity can further exacerbate OA (Feely et al. 2008). A key indicator of OA is aragonite saturation state, a measure of the availability of aragonite (a form of calcium carbonate). Aragonite saturation <1.0 indicates relatively acidified, corrosive conditions that are stressful for many CCE species, particularly shell-forming invertebrates. OA impacts on these species can propagate through marine food webs and potentially affect fisheries (Marshall et al. 2017). Aragonite saturation states tend to be lowest during spring and summer upwelling, and highest in winter.

Figure F.14 shows the time-series of winter and summer aragonite saturation from near-bottom at stations NH05 and NH25.

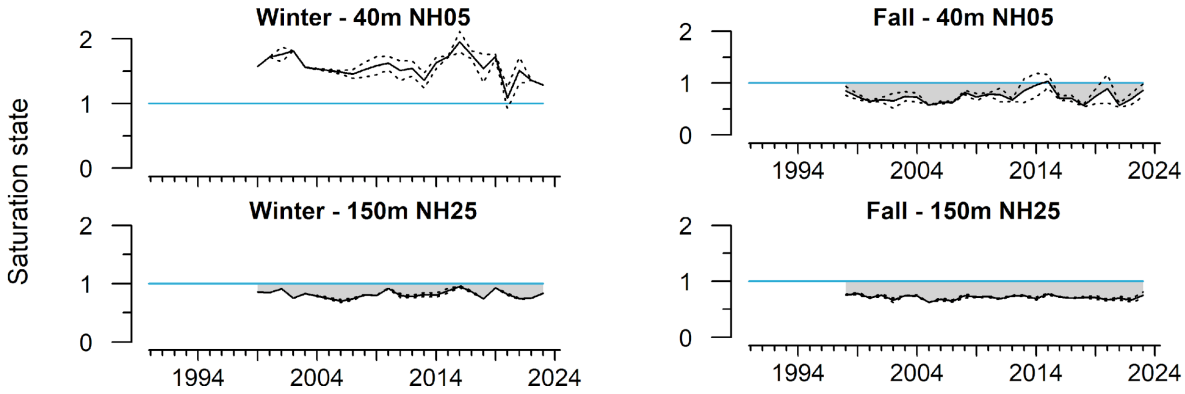

Figure F.14: Winter (Jan-Mar) and summer (Jul-Sep) mean aragonite saturation states at stations NH05 and NH25 off Newport, OR, 1998 - 2023. The blue line indicates aragonite saturation state = 1.0, below which are corrosive conditions for many shell-forming species. Dotted lines indicate ± 1.0 s.e. Data provided by J. Fisher, NMFS/NWFSC.

The corrosive water on the shelf at NH05 is largely driven by seasonal upwelling, where upwards of 80% of the water column becomes corrosive each summer (Fig. F.15).

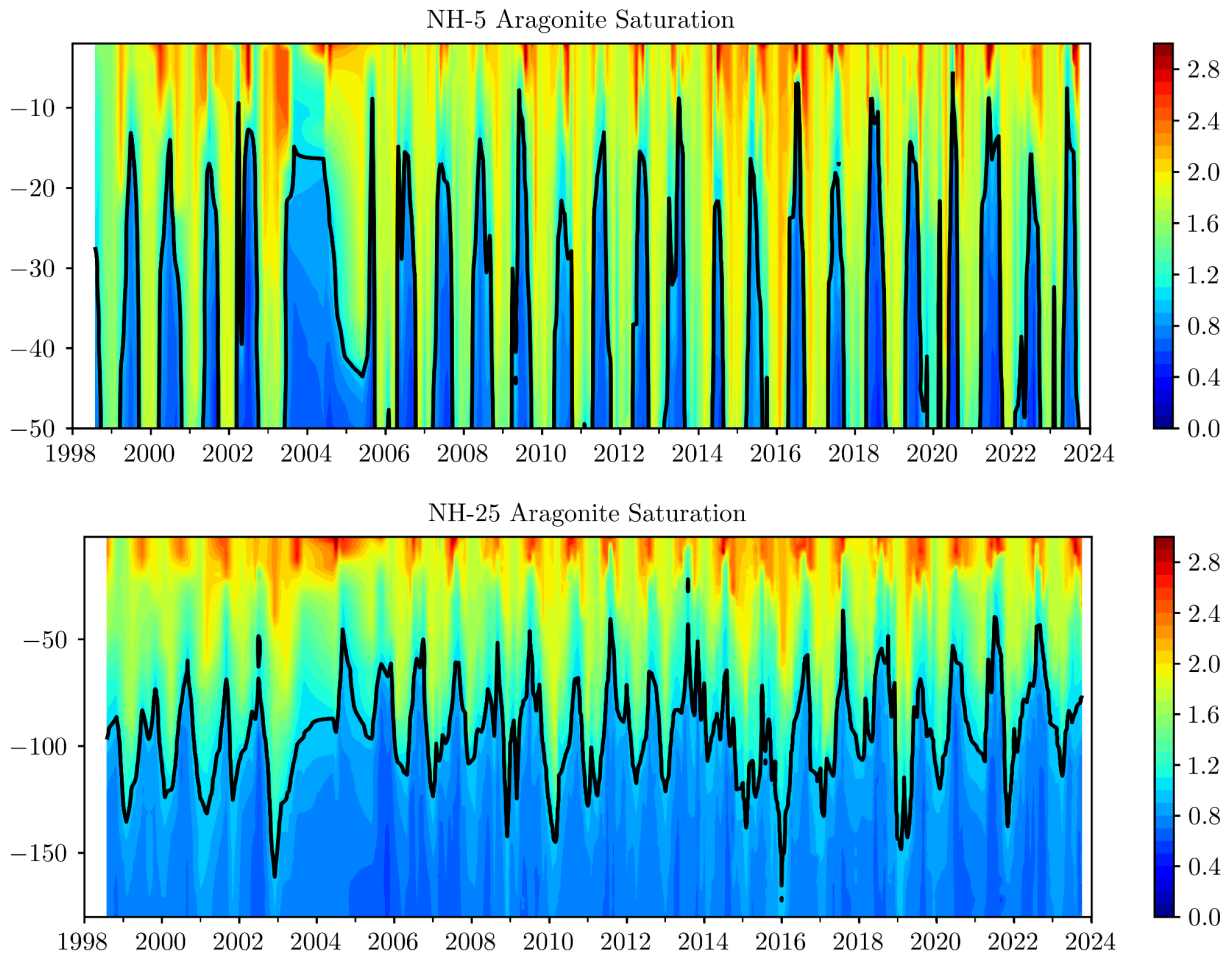

Figure F.15: Aragonite saturation state profiles for stations NH05 and NH25 off Newport, OR. Depths (y-axis) are in m. Black line indicates the depth at which aragonite saturation state = 1.0. Data provided by J. Fisher, NMFS/NWFSC.

Appendix G: SNOWPACK, STREAMFLOW, AND STREAM TEMPERATURE

Link to main section: Snowpack and Hydrology

Freshwater habitat indicators are reported based on a hierarchical spatial framework. The framework facilitates comparisons of data at the right spatial scale for particular users, whether this be the entire California Current, ecoregions within the CCE, or smaller spatial units. The framework we use divides the region encompassed by the CCE into ecoregions (Fig. 1.1), and ecoregions into smaller physiographic units. Freshwater ecoregions are based on the biogeographic delineations in Abell et al. (2008), see also www.feow.org, who define six ecoregions for watersheds entering the California Current, three of which comprise the two largest watersheds directly entering the California Current (the Columbia and the Sacramento-San Joaquin Rivers). Within ecoregions, we summarized data at scales of evolutionary significant units (ESUs) and 8-field hydrologic unit classifications (HUC-8). Status and trends for all freshwater indicators are estimated using space-time models that account for spatial and temporal autocorrelation (Lindgren and Rue 2015).

Snow-water equivalent. Snow-water equivalent (SWE) is measured using data from the California Department of Water Resources snow survey program (California Data Exchange Center, cdec.water.ca.gov) and The Natural Resources Conservation Service's SNOTEL sites across Washington, Oregon, California and Idaho. Snow data are converted into SWEs based on the weight of samples collected at regular intervals using a standardized protocol. Measurements on April 1 are considered the best indicator of maximum extent of SWE; thereafter snow tends to melt rather than accumulate.

Anomalies of SWE in 2023 were mixed across the Pacific's mountain ranges, with northerly ecoregions receiving near average snowpack, but with most Oregon Cascades and Sierra Nevada areas at much higher levels (Fig. 2.8). This situation helped Oregon and California recover from drought conditions, but also resulted in extensive flooding in California.

The outlook for snowpack in 2024 is limited to cumulative snowpack through February 1, an imperfect predictor of SWE in April. Thus far, SWE in the mountain west has been well below median levels (Fig. G.1), despite winter storms that are generating median levels of precipitation along much of the Pacific Coast except the Sierra Nevada. It remains too soon to say whether patterns will change by the end of this winter, although atmospheric conditions associated with the El Niño suggest a relatively warm and wet outlook for California and a drier outlook for the northernmost portions of the CCE.

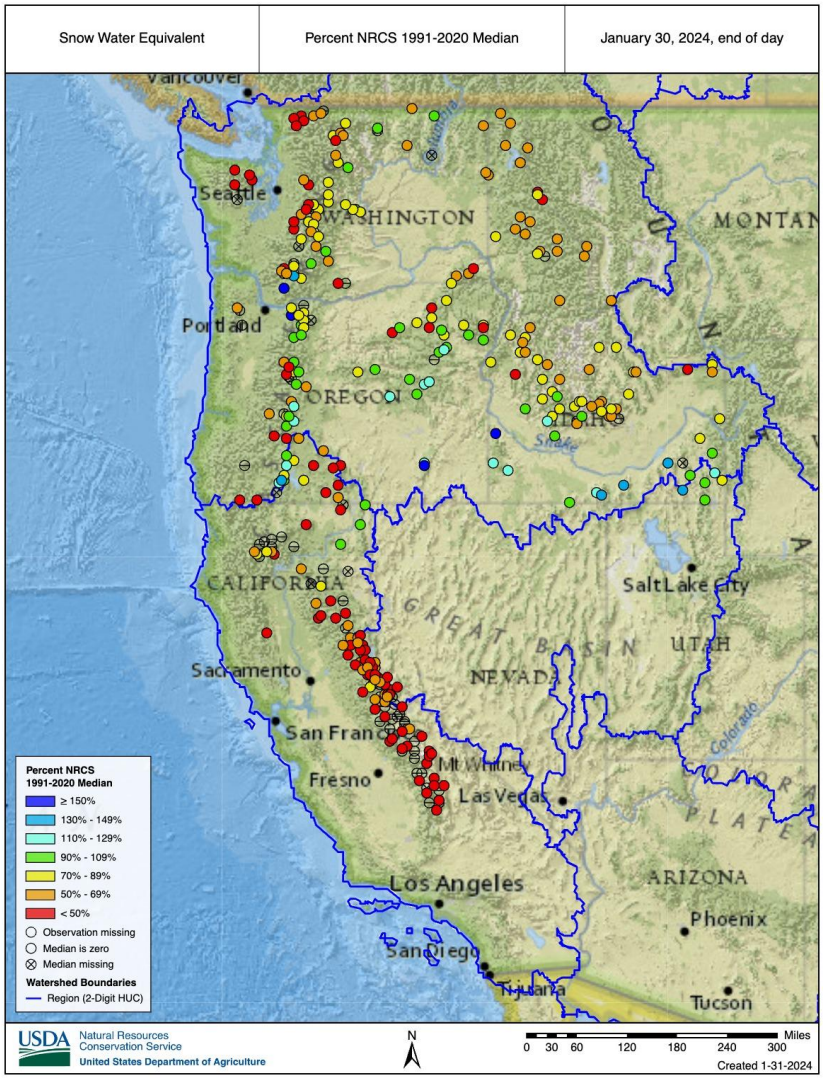

Figure G.1: Snow water equivalent (left panel) and total precipitation (right panel) as of January 30, 2024, relative to the 1991-2020 median. Data are from the California Data Exchange Center and the USDA Natural Resource Conservation Service SNOTEL database. Open circles indicate stations that either lack current data or long-term median data.

Stream temperature. Mean maximum stream temperatures in August (Fig. G.2) were determined from 446 USGS gauges with temperature monitoring capability. While these gauges did not necessarily operate simultaneously throughout the period of record, at least two gauges provided data each year in all ecoregions. Stream temperature records are limited in California, so two ecoregions (Sacramento/San Joaquin and Southern California Bight-Baja) were combined. Maximum temperatures exhibit strong ecoregional differences in absolute temperature (for example, Salish Sea and Washington Coast streams are much cooler on average than California streams).

The most recent five years have been marked by stream temperatures that primarily increased within and across regions (Fig. G.2) since the early 2010s. August stream temperatures in 2023 were within the five worst years on record (since 1981) for 3 of the 5 ecoregions. The Columbia Unglaciated Sacramento/San Joaquin ecoregions differ from this pattern, although even the former ecoregion continues to follow the recent trend of rising temperatures.

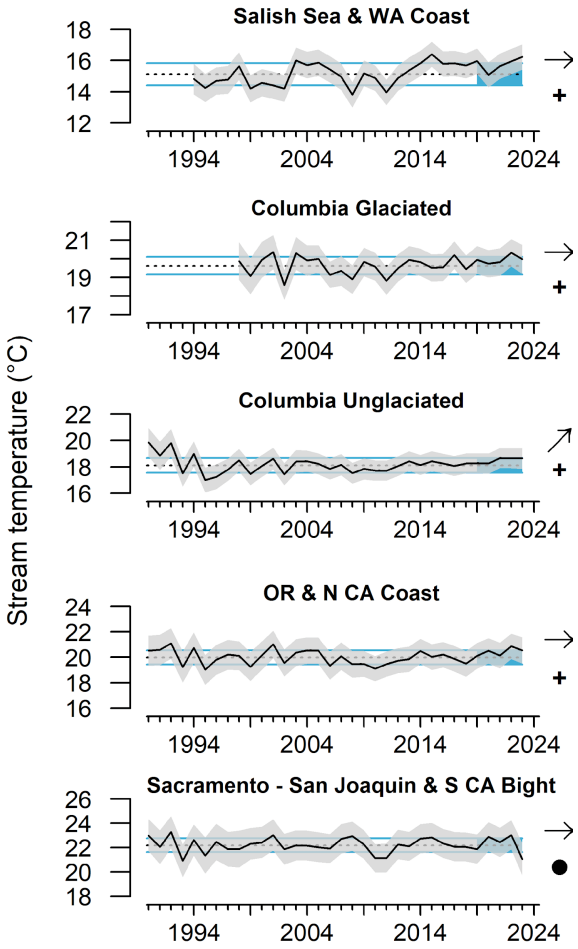

Figure G.2: Mean maximum stream temperatures in August measured at 466 USGS gages from 1990 - 2023. Gages include both regulated (subject to hydropower operations) and unregulated systems, although trends are similar when these systems are examined separately. Error envelopes represent 95% credible intervals (CI). Lines, colors and symbols are as in Fig. 2.1.

Minimum and maximum streamflow. Flow is derived from active USGS gages with records that are of at least 30 years' duration (waterdata.usgs.gov/nwis/sw). Daily means from 213 gauges were used to calculate annual 1-day maximum and 7-day minimum flows. These indicators correspond to flow parameters to which salmon populations are most sensitive. We use standardized anomalies of streamflow time series from individual gages (Fig. G.3).

Ecoregional patterns in snowpack (Fig. 2.8) translated to similar differences in stream flow. Minimum stream flows (Fig. G.3) continued a downward trend for many ecoregions, despite rebounds in California and Oregon. Since 1981, minimum flow in water year 2023 was the third lowest for the Salish Sea and within the lowest quartile for the Southern California Bight. These patterns were not reflected in maximum flows in 2023, which were average or above average across the Pacific Coast, except the Salish Sea and WA coast (Fig. G.4). This contrast emphasizes the increasing importance of summer extremes in limiting salmon and other species with freshwater life stages.

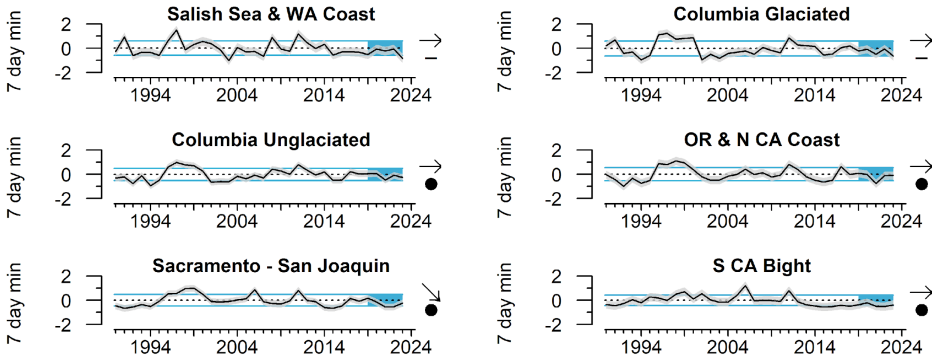

Figure G.3: Anomalies of 7-day minimum streamflow measured at 213 gages in six ecoregions from 1990 - 2023. Gages include regulated (subject to hydropower operations) and unregulated systems, though trends are similar when these systems are examined separately. Gray envelopes represent 95% credible intervals. Lines, colors and symbols are as in Fig. 2.1.

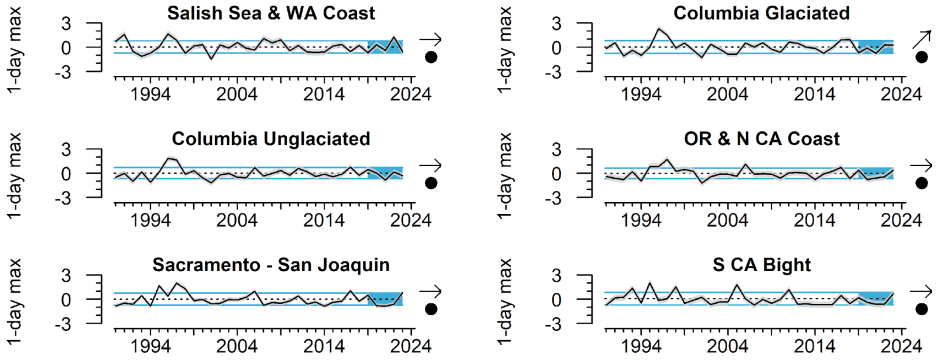

Figure G.4: Anomalies of 1-day maximum streamflow measured at 213 gages in six ecoregions from 1990 - 2023. Gages include both regulated (subject to hydropower operations) and unregulated systems, although trends are similar when these systems are examined separately. Gray envelopes represent 95% credible intervals. Lines, colors and symbols are as in Fig. 2.1.

Appendix H: REGIONAL FORAGE AVAILABILITY

Link to main section: Regional Forage Availability

H.1 Northern California Current Forage

The Northern CCE survey (known as the Juvenile Salmon Ocean Ecology Survey, JSOES) occurs in June and targets juvenile salmon in surface waters off Oregon and Washington (Fig. 1.1). It also collects adult and juvenile (age 1+) pelagic forage fishes, market squid, and gelatinous zooplankton with regularity. A Nordic 264 rope trawl is towed for 15-30 min at approximately 6.5 km/hr. The gear is fished during daylight hours in near-surface (upper 20 m) waters, which is appropriate for targeting juvenile salmon.

In 2023, catches of juvenile chum salmon were over 1 s.d. above the long-term survey mean, while juvenile sockeye catches were just below the long-term mean (Fig. H.1, top). Catches of juvenile subyearling and yearling Chinook salmon and juvenile coho salmon were close to average in 2023 (Fig. 3.7).

Among non-salmonids, catches of many species have been dynamic since the 2013–2016 marine heatwave (Fig. H.1). Catches of age-0 sablefish were above average in 2023, but below the sharp peak in 2020. Pacific pompano (butterfish), a warmer-water fish whose catches peaked in 2016, were close to the time series average in 2023. Catches of market squid in 2023 were average as well. Among the gelatinous zooplankton off Washington and Oregon, beginning in 2015 community composition transitioned from dominance of the large, cool-water sea nettle jellyfish (*Chrysaora fuscescens*) to the more offshore-oriented water jellyfish (*Aequorea* spp.). By 2019, both returned to roughly average densities. In 2022, catches of both sea nettles and water jellies were low relative to the time series averages, and in 2023 catches were higher than average (Fig. H.1). Catches of egg yolk and moon jellies returned to average levels after being above average in recent years. These two jellyfish species tend to be associated with warmer or offshore water masses.

Several other taxa collected by the June JSOES surface trawl are noted in terms of their relative prevalence (proportion of stations where they were caught), but are not considered to be sampled quantitatively due to their behavior and mesh size of sampling gear. Taxa with above average prevalence in 2023 included YOY rockfish, larval smelts, and adult whitebait and surf smelts. Pyrosomes were not caught in the 2023 survey.

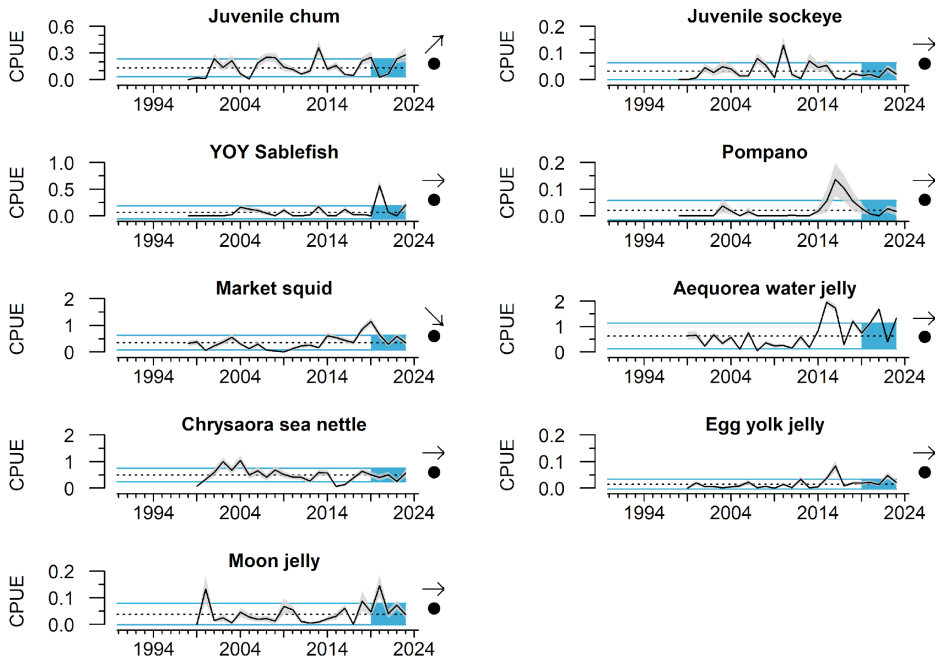

Figure H.1: CPUE (log_{10}(number/km+1)) of pelagic species in the Northern CCE from the JSOES survey, 1998-2023. Lines, colors, and symbols are as in Fig. 2.1.

H.2 Central California Current Forage

The Central CCE forage survey (known as the Rockfish Recruitment and Ecosystem Assessment Survey, RREAS) samples much of the West Coast each May to mid-June, using midwater trawls sampling between 30 and 45 m depths during nighttime hours. The survey targets young-of-the-year (YOY) rockfish species and a variety of other YOY and adult forage species, market squid, adult krill, and gelatinous zooplankton. Juvenile rockfish, anchovy, krill, and market squid are among the most important prey for CCE predators (Szoboszlai et al. 2015). Time series presented here are from the "Core Area" of that survey, centered off Monterey Bay (Fig. 1.1). Catch data were standardized by using a delta-GLM to estimate year effects while accounting for spatial and temporal covariates to yield relative abundance indices, shown with their approximate 95% confidence limits (Santora et al. 2021). The 2023 survey effort in the "Core Area" was comparable to previous years apart from 2020.

Standardized anomalies of log-transformed catch indices of key forage taxa in 2023 suggest continued high abundance of adult northern anchovies, while YOY anchovy continued to decline below the time series average (Fig. H.2). Catches of Pacific sardine showed a modest increase in the central region to slightly above average level. The anchovy and sardine results in this region are consistent with findings from a coastwide acoustic-trawl CPS survey in 2023 (see Appendix I).

The survey observed high abundances of YOY rockfish and YOY Pacific hake in 2023 (Fig. H.2). YOY rockfish catches were at the highest level since the 2015-16 marine heatwave, and there was a notable increase in juvenile groundfish diversity as well. Krill abundance

declined after several years of increasing; coastwide RREAS data indicate that krill abundance has been generally higher in northern areas relative to southern areas in recent years. Myctophids (lanternfishes) also declined to the below long-term average levels observed in recent years. Catches of market squid were slightly less abundant in 2023 and near the long-term average, while octopus abundance remained at below-average levels. Similar to 2022, the cumulative results of these trends indicate a fairly productive ecosystem, with anchovy continuing to dominate the forage community but with a greater abundance of alternative forage, and with very few taxa being at low abundance levels.

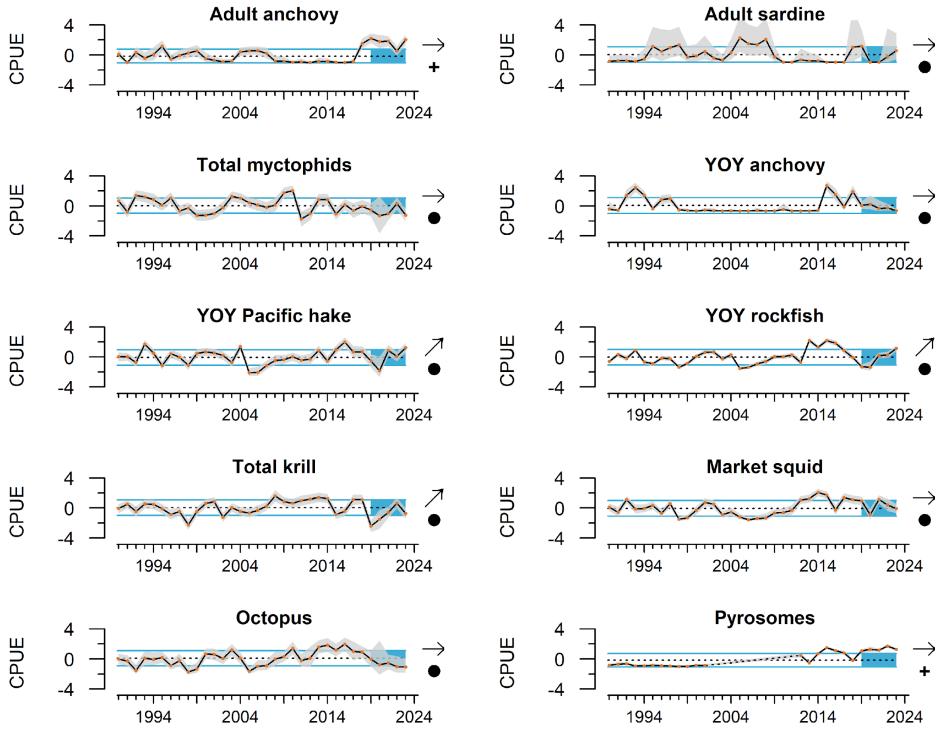

Figure H.2: CPUE (delta-GLM index and 95% CL) anomalies of a subset of key forage groups in the core area of the RREAS survey in the Central CCE, 1990 - 2023. Lines, colors, and symbols are as in Fig. 2.1.

H.3 Southern California Current Forage

Abundance indicators for forage in the Southern CCE come from fish and squid larvae collected in the spring (May-June) across all core stations of the CalCOFI survey (Fig. 1.1). Larval data are indicators of the relative regional abundances of adult forage fish, such as sardines and anchovy, and other species, including certain groundfish, market squid, and mesopelagic fishes. The survey samples a variety of fish and invertebrate larvae (<5 d old) from several taxonomic and functional groups, collected via oblique vertical tows of fine mesh Bongo nets to 212 m depth. In 2020, the spring larval survey was canceled due to COVID-19, and thus no data are available for that year, but survey operations resumed in 2021.

Catches of larval anchovy in spring 2023 were down from 2022 but still at a historically high level (Fig. H.3). Larval California smoothtongue (a mesopelagic species) also continued a strongly increasing trend and have been historically high since 2019. Market squid paralarvae, which were absent from 2013-2017, increased steadily and significantly since 2017, had the second highest abundance in 2022, but were absent in 2023. Catches of larval sardines have been low since 2012 and remained low in 2023. Southern mesopelagic species increased dramatically in 2015 and remained relatively abundant in 2023. Recent trends for most species or species groups were non-significant.

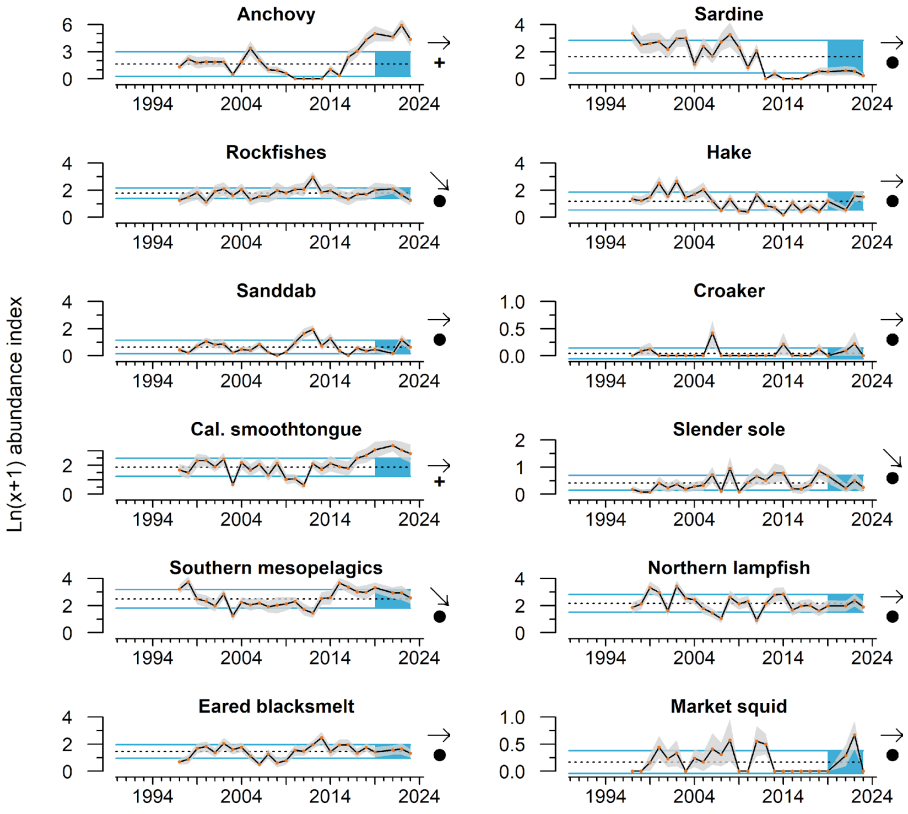

Figure H.3: Mean abundance (ln(x+1)) index of the larvae of key forage species in the Southern CCE, from spring CalCOFI surveys during 1997 - 2023 (no data from 2020). Lines, colors, and symbols are as in Fig. 2.1.

H.4 Coastwide Krill Abundance

Krill were detected acoustically during the 2023 Joint U.S.-Canada Pacific Hake Ecosystem and Acoustic Trawl (PHEAT) Survey, conducted between June-September 2023 from Point Conception, California to Dixon Entrance, British Columbia. The coastwide nautical-area-backscattering coefficient (NASC), which represents relative krill abundance observed between 50-300 m water depth, indicated krill abundance was highest near the 200 m shelf break in northern California and Oregon waters, and lowest south of Cape Mendocino (Fig. H.4, see Phillips et al. 2022 for methodology). Overall krill abundance was lower this year than most past years (Fig. 3.3 from main body), although most of that overall reduction was due to lower numbers to the northern and southern portions of the sampled area.

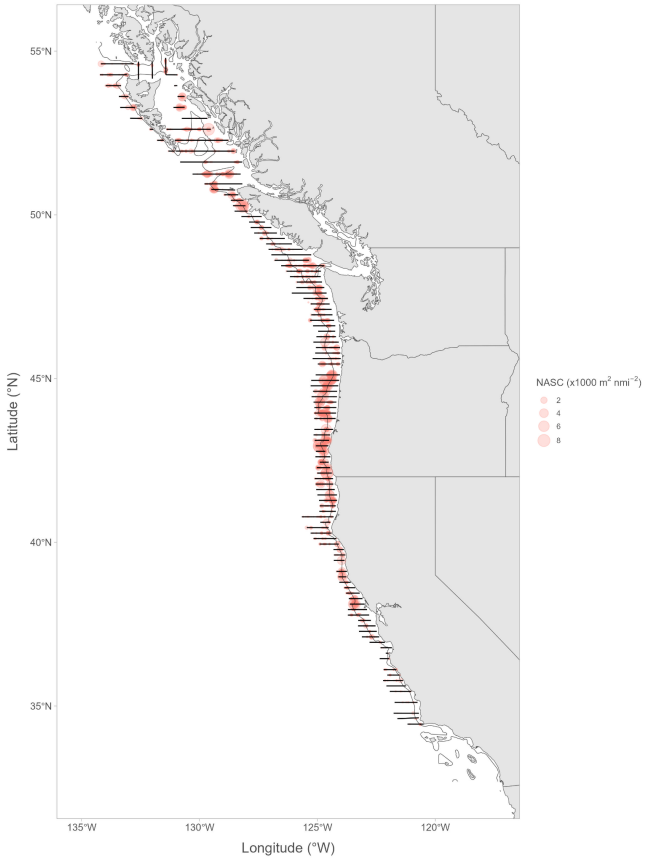

Figure H.4: The relative abundance, or NASC (red dots, x1000 m^2 nmi^{-2}), of krill detected acoustically during the 2023 Pacific Hake Ecosystem and Acoustic Trawl Survey, conducted between June-September 2023. Black lines represent survey transects.

H.5 Pyrosomes and Salps

Catches of pyrosomes (warm-water pelagic tunicates) remained high in 2023 research surveys off central California (Fig. H.2; RREAS core area, see Fig. 1.1) and in stations throughout the Southern CCE (data not shown). Pyrosome catches in the Northern CCE were considered low, from Trinidad Head (pers. obs., R. Robertson, Cal Poly Humboldt) through the northern CCE; however, salps were notably abundant in this region (pers. obs., J. Fisher, NMFS/NWFSC, B. Wells, NMFS/SWFSC). Salps were highly abundant in the central CCE as well.

H.6 Dungeness crab megalopae abundance

Dungeness crab megalopae were highly abundant throughout central CCE sampling stations in 2023, but were not enumerated (pers. obs, J. Field). These observations corroborate similar findings near Coos Bay, Oregon, where a long-term monitoring program of Dungeness crab megalopae yielded almost 2.5 million megalopae in 2023, a notable peak from recent years (Fig. H.5).

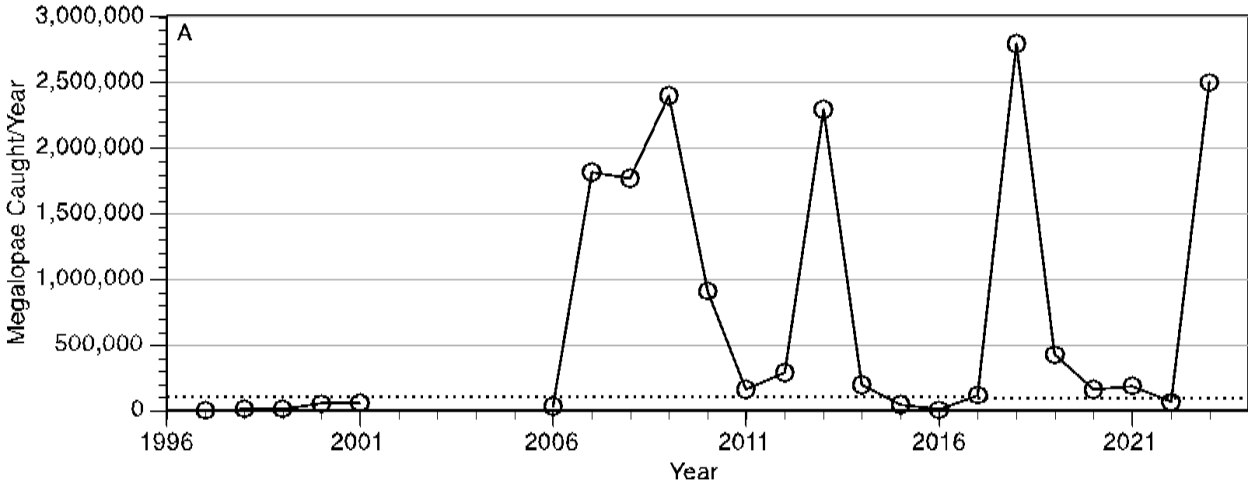

Fig. H.5: A 23-year time series of total annual catch of megalopae to a light trap fished in Coos Bay, Oregon (43° 20' 41" N, 124° 19' 15" W). The trap was fished from Apr-Sept annually. Samples were collected daily and then summed for the annual catch. Strong El Nino events occurred in 1997 and 2016 when catch was lowest, 1,094 and 3,040, respectively. A gap in sampling occurred between 2001 and 2006.

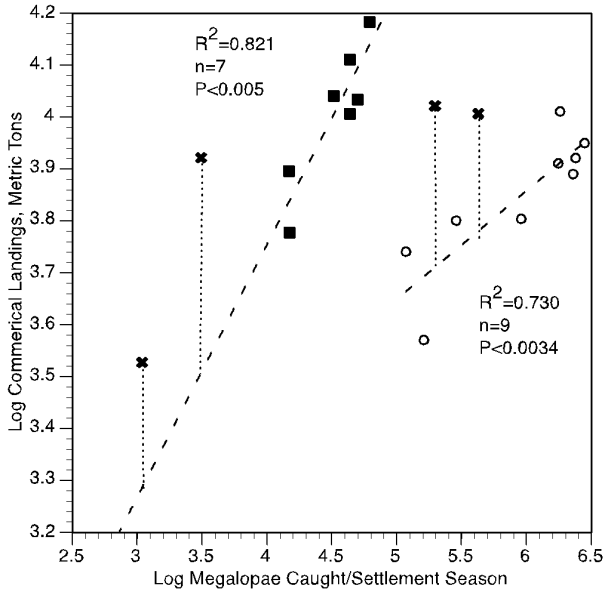

Fig H.6. Log of the megalopae catch in Coos Bay per settlement season plotted with the log of the commercial landings of Dungeness crabs in Oregon. The distribution of data points suggests that there are two curves, one associated with data from annual catches <100,000 (left) and a second associated with years with catches >100,000 (right).

In addition to being a lipid-rich prey source, preliminary analyses suggest the megalopae index from Oregon light traps is strongly correlated with commercial landings of Dungeness crab four years later (Fig. H.6, Shanks et al., in prep). Note that commercial catches are limited to males that are roughly 4 years old, so landings can also be interpreted as the 4-year-old year class of the population. There was also a noted difference in the relationship between heatwave and non-heatwave years. Within this time series, there were three years (2015, 2016, and 2019) when marine heat waves occurred over the continental shelf off Oregon. Data from these years are plotted with X's in Fig. H.6, and they fall well above the regression lines, which were calculated without these points. These results suggest that the size of the Dungeness crab population is strongly influenced by the annual larval success, as indicated by the number of megalopae caught; and in years with marine heat waves, recruitment from megalopae to 4-year-old crabs is higher. While only Oregon data are shown, the light trap data is positively correlated with commercial catch in California, but is not correlated with catches in Washington. This index stems from a collaborative effort between the Oregon Institute of Marine Biology (OIMB, University of Oregon) and ODFW and warrants further attention in the future as an additional index of prey availability in this region.

Appendix I: COASTAL PELAGIC SPECIES DATA FROM SUMMER 2023

Link to main section: Coastal Pelagic Species

Acoustic-trawl method (ATM) surveys have been used by the NOAA Southwest Fisheries Science Center in most years since 2006 to map the distributions and estimate the abundances of coastal pelagic fish species (CPS) in the coastal region from Vancouver Island, Canada, to San Diego, California (e.g., Zwolinski et al. 2014). In 2021 and 2022, the surveys were expanded to include portions of Baja California, Mexico (Stierhoff et al. 2023a, Stierhoff et al. 2023b). The surveys cover waters to at least the 1,000-fathom (1829-m) isobath, or 65 km from shore. The five most abundant CPS in this domain are Northern Anchovy, Pacific Herring, Pacific Sardine, Jack Mackerel, and Pacific Mackerel (Fig. I.1). The ATM combines data from echosounders, which record CPS echoes, and trawls, which produce information about the composition, sizes, and ages of the fishes. This survey also samples the densities of CPS eggs at 3-m depth using a continuous underway fish egg sampler (CUFES) mounted on the ship's hull.

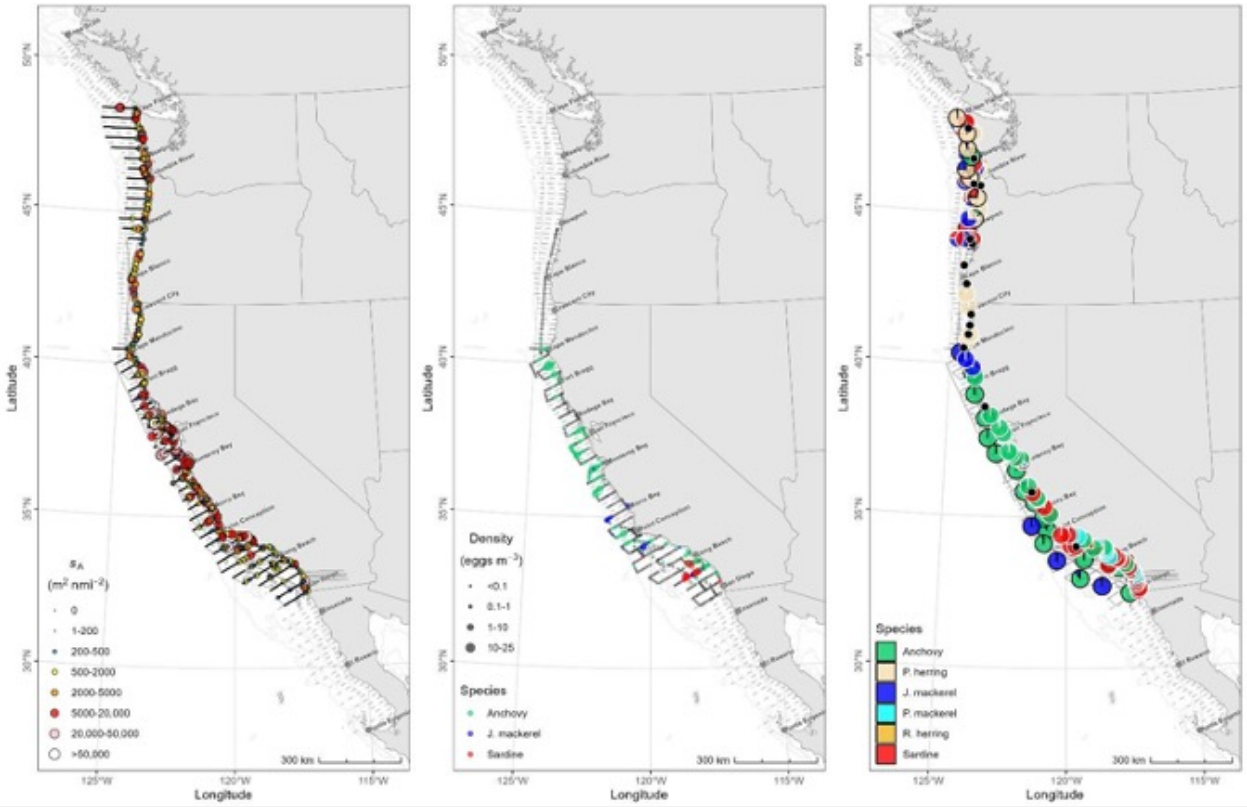

Figure I.1: Data from the 2023 summer CPS survey including: a) integrated 38-kHz volume backscatter coefficients attributed to CPS; b) CPS eggs collected with a Continuous Underway Fish Egg Sampler; c) proportions of CPS in NOAA Ship

Lasker *and* Shimada*'s nighttime trawl catches (black outlines) and F/V* Lisa Marie *and* Long Beach Carnage*'s daytime purse seine sets.*

The summer 2023 survey was to sample from Cape Flattery, WA to Punta Eugenia, Baja California from 5 July to 30 September (Renfree et al., In prep.). However, due to insufficient crew, mechanical issues, or both, nearly 60% of the allocated sea days aboard NOAA Ship *Reuben Lasker* were lost, and the ship sampled only from San Diego to Cape Mendocino. To mitigate, NOAA Ship *Bell M. Shimada* sampled the area between Cape Blanco and Cape Flattery from 12-26 October. Additionally, two charter fishing vessels, *Lisa Marie* and *Long Beach Carnage*, sampled within 5 NM from shore between Cape Flattery and San Diego, and around the northern Channel Islands (Fig. I.1).

Acoustic backscatter from CPS was mapped throughout the survey area (Fig. I.1). Egg samples, collected between San Diego and Cape Mendocino only, were mostly comprised of Northern Anchovy eggs, with some Jack Mackerel eggs around Pt. Conception and the northern Channel Islands, and Pacific Sardine eggs between Long Beach and San Diego (Fig. I.1). Trawl samples were mostly comprised of Northern Anchovy south of Fort Bragg, and Pacific Herring north of Cape Mendocino (Fig. I.1). Pacific Sardine from the northern stock were caught from Cape Flattery to Cape Blanco (Fig. I.1), and those from the southern stock were caught nearshore south of Morro Bay (Fig. I.1). Jack Mackerel were collected north of Cape Blanco, around Cape Mendocino, and offshore in the Southern California Bight (Fig. I.1). The few Pacific Mackerel collected throughout the survey area were mostly nearshore in the Southern California Bight (Fig. I.1).

The survey-estimated CPS biomasses from summer 2008 to 2023 (Fig. 3.4) was dominated by northern stock Pacific Sardine until 2013, Jack Mackerel in 2014 and 2015, and then central stock of Northern Anchovy since 2015, when it began to resurge. The latter stock grew to ~2.75 million t by 2021, and has hovered around ~2.5 million t since (Fig. 3.4; Stierhoff et al. 2023a, Stierhoff et al., in prep). Meanwhile, the biomass of Pacific Mackerel remained the lowest in the assemblage, and the biomass of Jack Mackerel trended up from 2017 through 2022. In 2023, the timing of the survey in the north area and its reduced footprint created uncertainty about the representativity of the 2023 decrease observed in Jack Mackerel (Fig. 3.4).

The biomass of Pacific Sardine is calculated separately for the northern and southern stocks based on oceanographic habitat, spatial separation, and demographic structure (Zwolinski and Demer 2023). The southern stock has been present in U.S. waters since at least 2015, located mostly nearshore, south of Monterey Bay (Zwolinski and Demer 2023, Stierhoff et al., in prep.). The biomass of the northern stock has been fluctuating at below 100 kt, whereas the southern stock has surpassed that value yearly since 2021 (Fig. 3.4).

Appendix J SALMON

Link to main section: Salmon Indicators

J.1 Salmon Stoplight Table Format

For the stoplight tables presented in Section 3.1 and below in Appendix J.3, we use color to represent anomalous years. As described in last year's report (Harvey et al. 2023), we have addressed past feedback from the SSC and others by developing a more statistically based stoplight table format, which produces five bins that are determined relative to a fixed baseline reference period. In this new format, we assumed a normal distribution for each of the indicators and estimated a mean and standard deviation for the base period. For each cell within a given indicator, we determined how many standard deviations the values were from their respective base period mean and used a five-color set to indicate whether a value was >2 s.d. below the mean, 1 to 2 s.d. below the mean, within 1 s.d. of the mean in either direction, 1 to 2 s.d. above the mean, or >2 s.d. above the mean. This approach overcomes many of the issues that had been previously identified (e.g., better highlighting values that represent truly exceptional years; past values are now static and do not suddenly change colors; etc.).

J.2 Ecosystem Indicator-based Outlooks for Chinook Salmon Escapement in the Columbia River Basin

Table 3.1 in the main body of the report is a stoplight table that provides a qualitative, ecosystem-based outlook of returns of adult Columbia Basin Chinook salmon in 2024, based on indicators of conditions affecting marine growth and survival of outmigrating smolts. A related quantitative analysis, which is still being refined in response to feedback from the SSC-ES and other partners (see Appendix C), uses a summary metric of the stoplight table, a new stock-specific metric (B. Burke, unpublished), and mark-recapture data to estimate smolt-to-adult survival of Chinook salmon from the Upper Columbia and Snake River basins.

In this analysis, models are fit to past smolt-to-adult return (SAR) data, and use the most recent ecosystem indicator data to predict what smolt-to-adult survival will be for cohorts that have gone to sea but not yet returned. Separate models have been developed for spring and fall Chinook salmon and steelhead from the Snake River basins and spring Chinook salmon from the Upper Columbia basin. The specific approach uses a Dynamic Linear Model, founded on linear regressions of single ecosystem indicators vs. survival rates of PIT-tagged fish that left Bonneville Dam as smolts and returned as adults (Fig. J.1, white points). The model labeled "Stoplight PC1" uses the first principal component (PC1) from a Principal Component Analysis of the stoplight chart as a covariate. The second model, labeled "CMISST" uses a Covariance Map Index of Sea Surface Temperature (B. Burke, unpublished), which is a metric derived by calculating the similarity of sea surface temperature (SST) spatial patterns in the North Pacific Ocean to a stock-specific optimal pattern. The CMISST metric is still in development, but analyzes to date indicate that the

CMISST model has better prediction skill for spring Chinook salmon and steelhead SAR, while the PC1 model has better prediction skill for fall Chinook salmon SAR.

For smolts that went to sea in 2022 (which should dominate adult returns in 2024), the survival estimates are slightly above the averages for the past ten years (Fig. J.1). Each stock is estimated to have survival range from about 1.0 to about 1.8%, though the PC1 model for Snake River steelhead estimated survival closer to 2.3%. For smolts that went to sea in 2023 (most of which will return in 2025), the models suggested almost identical survival as those that went to sea in 2022 (Fig. J.1). This is not too surprising as both years were somewhat average in terms of the stoplight indicators and had very similar mean ranks (Table 3.1). Survival estimates from the PC1 and CMISST models were similar, though the CMISST model suggested slightly higher survival for Upper Columbia River spring Chinook salmon than did the PC1 model. Uncertainty in the estimates (95% prediction intervals, colored vertical lines in (Fig. J.1) is relatively high, particularly for Snake River fall Chinook and Upper Columbia River spring Chinook salmon.

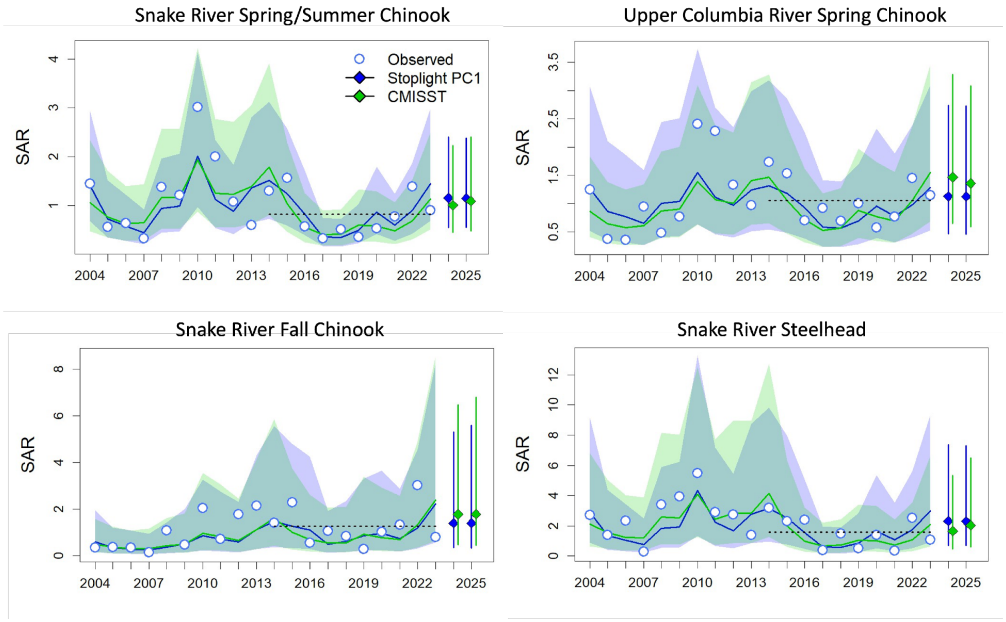

Figure J.1: Observed and modeled smolt-to-adult returns (SAR) of Chinook salmon and steelhead from the Snake River and Chinook salmon from the Upper Columbia River. Years on the x-axes are smolt migration years. Dark lines are different model fits; shaded areas are 95% confidence intervals; open circles are estimated SAR values based on PIT tag data; dashed lines are recent 10-year averages; and colored points are model outlooks with 95% prediction intervals for smolt years 2022 and 2023 (dominant return classes in 2024 and 2025, respectively). Blue points are from models that use the original stoplight chart (Table 3.1) summary metric and green points are from a new unpublished stock-specific metric.

Although Table 3.1 represents a general description of ocean conditions related to multiple populations, we acknowledge that the importance of any particular indicator will vary among salmon species and runs. These analyses represent progress toward greater distinction among different ESUs than some results shared in previous ecosystem status reports. NOAA scientists and partners continue to work toward stock-specific salmon outlooks by using both correlative and mechanistic methods that can optimally weight the indicators for each response variable in which we are interested. We will continue to work with the Council and advisory bodies to identify data sets for Council-relevant stocks for which analysis like these could be possible.

J.3 Ecosystem Conditions for Fall Chinook Salmon in California

Central Valley Fall Chinook salmon stoplight table: In our 2019-2020 ecosystem status report, we introduced a relatively simple "stoplight" table of ecosystem indicators that were shown by Friedman et al. (2019) to be correlated with returns of naturally produced Central Valley Fall Chinook salmon. An updated stoplight chart for adult Fall Chinook salmon returning to the Central Valley in 2024 is in Table 3.2. The focal ecosystem indicators are: spawning escapement of parent generations; egg incubation temperature between October and December at Red Bluff Diversion Dam (Sacramento River); egg thiamine concentrations based on averages of samples collected from Central Valley fall run hatchery programs; median flow in the Sacramento River in the February after fry emergence; and a marine predation index based on the abundance of common murres at Southeast Farallon Island and the proportion of juvenile salmon in their diets. Reflecting discussions with the SSC-ES in September 2020, we emphasize that the stoplight chart in Table 3.2 is strictly qualitative and contextual decision-support information. Qualitative descriptors (color-coded terms like "very poor" in Table 3.2) are based on recent time series and on expert opinion of how a given indicator relates to quantitative analysis of the relationship between the indicator and life-stage specific survival (Figure 5 in Friedman et al. 2019). For example, in Table 3.2, Flows rated "very low" (<7,000 cfs) are consistent with <25% rearing/outmigration survival rates, while the flows rated "low" (7,000 to 20,000 cfs) were consistent with 25-50% outmigrant survival (see Fig. 5 in, Friedman et al. 2019). Egg incubation temperatures in Table 3.2 were consistent with egg-to-fry survival ranging from ~50% (which we rated as "suboptimal") to 0% at > 13 C ("very poor/cohort failure"). We will work to refine these qualitative categories for future reports so that their basis is more explicit.

The escapement descriptor is a qualitative evaluation of how natural-area escapement of a parent generation relates to the natural area + hatchery escapement goal of 122,000–180,000 fish, with 122,000 spawners as the SMSY target (PFMC 2022d). Natural area escapement is relevant to Table 3.2 as an indicator of total natural area egg production (e.g., Munsch et al. 2020). However, the qualification of this indicator requires future research. Obviously, our using a natural+hatchery target as the qualifier for natural-only escapement is problematic. Perhaps more importantly, the SSC and STT have both recommended research and reconsideration of the Sacramento River fall Chinook SMSY objective (PFMC 2022e,f), and Satterthwaite (2022) has concluded that an escapement of

122,000 adults is insufficient to maximize natural production. We have not been able to fully address the SSC and SST comments yet.

The qualitative nature of this stoplight table is in part due to the fact that some of the parameters used by Friedman et al. (2019) were estimated using information from both natural-origin and hatchery-origin fish, and while it is reasonable to assume that true parameter values would be similar, given correlations between natural and hatchery escapements, additional data specific to natural-origin fish are likely necessary in order to improve model fits, evaluate other potential covariates, and support adequate testing of model predictive skill.

Stoplight tables for Sacramento River and Klamath River Fall and Central Valley Spring-run Chinook salmon: Rebuilding plans in 2019 for Sacramento River and Klamath River fall Chinook salmon runs prompted annual updates of habitat indicators for these two stocks (see Harvey et al. 2020), which have been expanded to include Central Valley Spring-run Chinook salmon (CVSC) to inform risk assessment for this poorly assessed stock. Currently, the indicator suite includes 22, 18, and 24 indicators for Sacramento River Fall (SRFC), Klamath River Fall (KRFC), and Central Valley Spring-run Chinook salmon (CVSC), respectively, spanning the full life history of natural area fish and also including indicators related to hatchery-origin stocks (Table J.1, methodology and indicator descriptions below).

Updates to indicators for the most recent brood year and for previous years suggest that across California, Chinook salmon stocks encountered relatively poor conditions during spawning in 2022, but much better outmigration conditions in 2023. Marine indicators for 2023 were mixed but below average. Hence, in the parlance of the Ecosystem Workgroup's risk classification rubric (EWG 2023), 2022-2023 demonstrated "substantially increased concerns" for ecosystem considerations for the current cohort. In addition, habitat conditions in multiple life stages have been relatively poor for the last three years in all three stocks, a situation that could lead to poor productivity across multiple cohorts. From a population dynamics standpoint, this situation could reduce resilience of stocks to future ecosystem variability (Munsch et al. 2022).

Table J.1: Klamath River Fall (KF), Sacramento Fall (SF), and Central Valley Spring-run (CS) Chinook salmon habitat indicators, definitions, and key references. Months indicates the time period for which indicators were summarized, Effect is the predicted direction of the indicator's effect on productivity, and Stock indicates the runs for which indicators were produced. With the addition of Central Valley Spring-run indicators, abbreviations of indicator names have changed slightly compared to the previous Ecosystem Status Report.

Life-stage	Abbreviation	Time period	Expected effect	Reference	Stock
Adult spawners					
Spawner counts	Spawners		+	Friedman et al. 2019	KF, SF, CS
Fall closures of Delta Cross Channel	CChannel.F	Se-Oc	+	Rebuilding plan	SF
Low flows during upstream migration	Flows.U	Se-Oc*	+	Strange et al. 2012	KF, SF, CS
Temperatures during upstream mainstem	Temp.U	Se-Oc*	-	Fitzgerald et al. 2021	KF, SF
Holding period flows in Butte Creek	Flows.H	Jn-Se	+	USFWS, 1995	CS
Holding temperature in Butte Creek	Temp.H	Jn-Se	-	USFWS, 1995	CS
Prespawn mortality rate	PrespawnM		-	USFWS, 1995	CS
Incubation and emergence					
Fall-winter low flows in tributaries (7Q10)	Flows.I	Oc-De*	+	Jager et al. 1997	KF, SF, CS
Egg-fry temperatures (avg of max daily)	Temp.I	Oc-De*	-	Friedman et al. 2019	KF, SF, CS
Egg-fry productivity	FW.surv		+	Hall et al. 2018	KF, SF, CS
Freshwater/delta residence					
Winter-spring tributary flows	Flows.T	Fe-My	+		CS
Winter-spring mainstem outmigration flows	Flows.O	De-My	+	Friedman et al. 2019	KF, SF, CS
Delta outflow index	Delta	Ap-Jl	+	Reis et al. 2019	SF, CS
7-day flow variation (SD)	SDFlow.O	De-My	-	Munsch et al. 2020	KF, SF, CS
Maximum flushing flows	Max.flow	No-Mr	+	Jordan et al. 2012	KF
Total annual precipitation	Precip	Annual	+	Munsch et al. 2022	KF, SF, CS
Spring outmigration temperatures	Temp.O	My-Jn	-	Munsch et al. 2022	KF, SF, CS
Spring closures of Delta Cross Channel	CChannel.S	Fe-Jl	+	Perry et al. 2013	SF, CS
Days floodplain bypasses were accessible	Floodpln	Annual	+	Limm and Marchetti 2009	SF, CS
Marine residence					
Coastal sea surface temperature	CSTarc	Mr-My	-	Wells et al. 2008	KF, SF, CS
North Pacific Index	NPI	Mr-My	+	Wells et al. 2008	KF, SF, CS

Life-stage	Abbreviation	Time period	Expected effect	Reference	Stock
North Pacific Gyre Oscillation	NPGO	Mr-My	+	Wells et al. 2008	KF, SF, CS
Marine predation index	Predation		-	Friedman et al. 2019	SF, CS
Krill length**	Prey	Mr-Se	+	Robertson & Bjorkstedt 2020, Robertson et al. in prep.	KF
Hatchery releases					
Release number	Releases		+	Sturrock et al. 2019	KF, SF, CS
Prop net pen releases	Net.pen		+	Sturrock et al. 2019	SF, CS
Release timing relative to spring transition	FW.Timing	Ja-Au	+	Satterthwaite et al. 2014	KF, SF, CS
Release timing relative to peak spring flow	M.Timing	Ja-Au	+	Sykes et al. 2009	KF, SF, CS

*For CS, adult upstream migration time period and incubation period is Fe-My and Se-De, respectively.

**Update from previous indicator (krill biomass) to reflect a metric with a demonstrable positive influence on KRFC.

Klamath River Fall Run Chinook salmon: For brood year 2022, habitat indicators improved slightly from the previous year but were still mixed. 11 of 18 habitat indicators were within 1 s.d. of the long-term average (Table J.2A). Six of those 12 were below average, in addition to four indicators that were >1 s.d. below normal. These patterns resulted in a rebound in 2022-23 to a near-average cumulative freshwater score and marine conditions (Table J.2B). Indicators for adult spawning were uniformly below average and spawning temperatures were the second worst on record. However, most incubation and outmigration conditions greatly improved due to better snowpack and corresponding flows and temperatures. A majority of indicators for hatchery stocks and early marine conditions likewise showed improvements compared to 2022. NPGO was a notable exception to this pattern, as it was the third worst year in the indicator time series.

Long-term changes in some of the habitat indicators track KRFC's life cycle attributes, which exhibit evidence of nonstationarity (Shaftel 2022). In particular, evaluation of the changing correlations between indicators and recruits per spawner using a running 15-year time series has revealed that indicators such as outmigration temperature and flow are much more strongly correlated with productivity in recent years. This pattern may be an outcome of the apparent rise of infections by *Ceratomyxa shasta*, a parasitic polychaete sensitive to both flow and temperature conditions and which can cause high mortality in juvenile migrants (Jordan 2012).

Table J.2: (A) Habitat indicators for five life stages of Klamath River Fall Chinook salmon. Each row is an indicator (grouped by life stage at left) and each column is a brood year. Colors represent a given year's indicator relative to the full time series. Blue: >2 s.d. above the mean (= highly favorable); green: >1 s.d. above the mean; yellow: ±1 s.d. of the mean; orange: >1 s.d. below the mean; red: >2 s.d. below the mean (= highly unfavorable). (B) Trend over brood years in the average of freshwater indicators (black line; adult migration and spawning, incubation, freshwater and delta residence, and all hatchery indicators except marine timing) and marine indicators (blue line; marine timing, early marine residence suite). Brood years on x-axis match years of the indicator suite in (A).

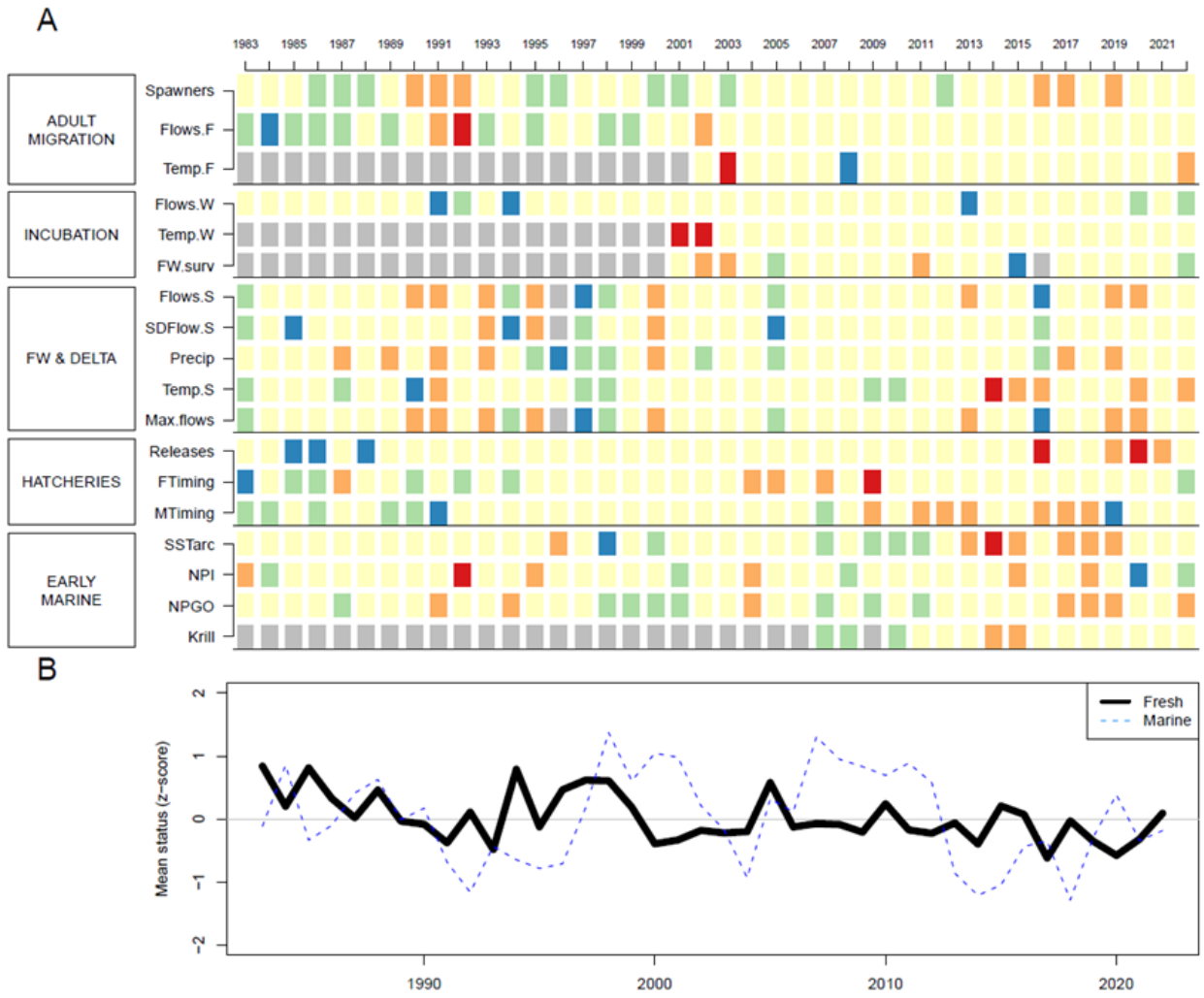

Sacramento River Fall Chinook salmon: Like KRFC, many of the indicators for the SRFC 2022 brood year fell within 1 s.d. of average (Table J.3A), although 7 of the 17 freshwater indicators with data were below-average or worse. SRFC faced poor conditions during the spawning run, and three of the four indicators were >1 s.d. below average and worse than the previous year. Incubation and outmigration indicators were the opposite pattern: all except one were above average (two were > 1 s.d. better) and much improved compared to the previous year. Marine conditions in 2023 were mixed: while NPI was > 1 s.d. above average, SSTarc was below average and NPGO experienced its third worst year. The

cumulative effects of multiple indicators resulted in a return to slightly above-average freshwater and slightly below-average marine conditions (Table J.3B).

Table J.3: Habitat indicators for five life history components of Sacramento River Fall Chinook. Each row is an indicator (grouped by life stage at left) and each column is a brood year. Colors are as in Table J.2A. (B) Trend over brood years in the average of habitat indicators for freshwater life stages (black line, as in Table J.2B) and marine habitat indicators (blue line, as in Table J.2B). Brood years on x-axis match years of the indicator suite in (A).

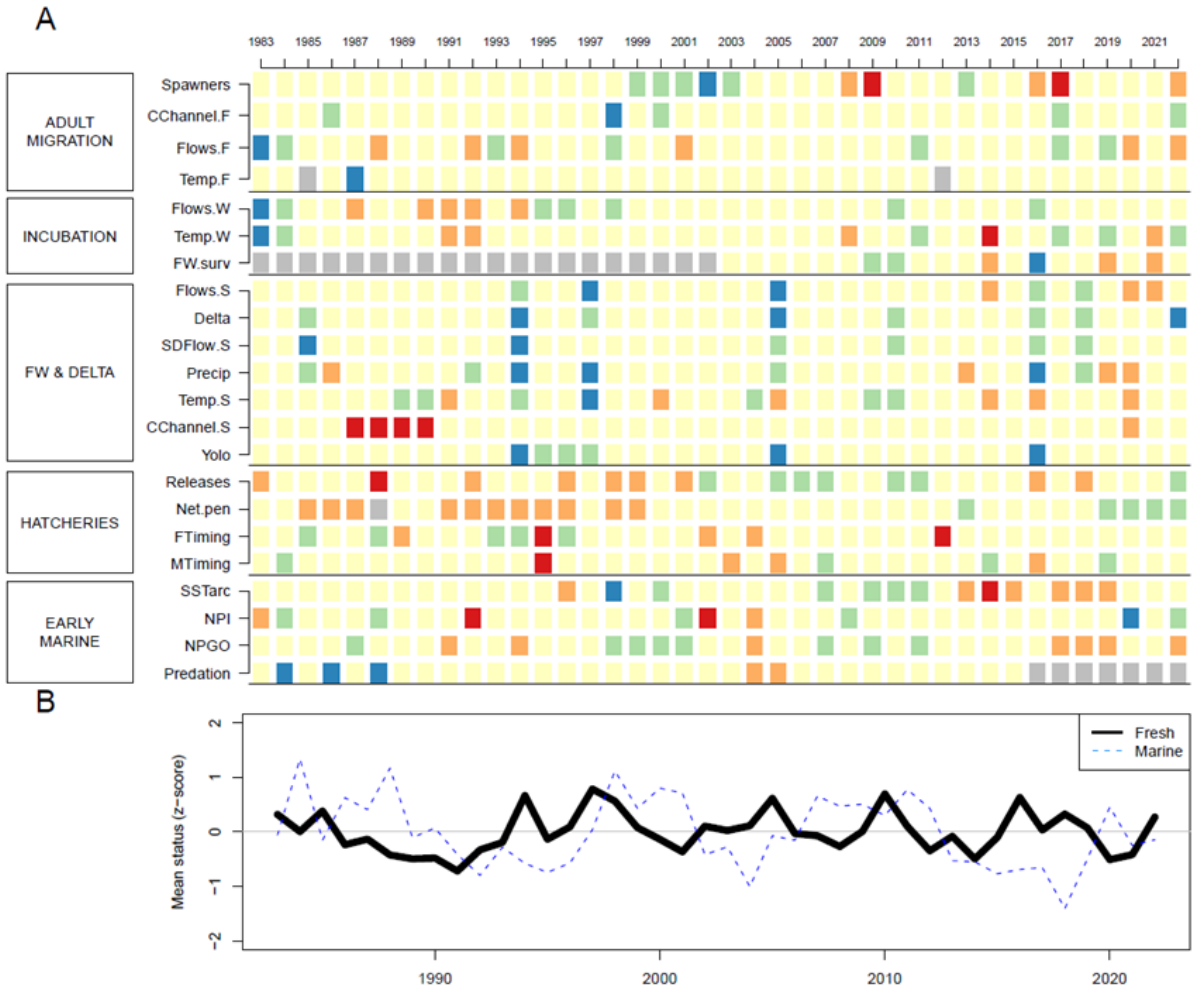

Central Valley Spring-run Chinook salmon: CVSC shares 11 indicators with SRFC, so it should come as no surprise that habitat conditions for CVSC were also mixed. While most indicators for the 2022 cohort were within 1 s.d. of their time series averages (Table J.4A), spawning and incubation conditions were uniformly below average while outmigration conditions were uniformly above average (and two indicators exceeded 2 s.d.). Almost all freshwater indicators showed improvements in 2022-23 compared to the previous year. One exception (freshwater productivity) was likely poorly measured: trap placement was delayed because of extended high river flows. In contrast, hatchery and marine indicators were mixed. Overall, cumulative freshwater conditions increased from the previous year

and were slightly above average, while cumulative marine conditions slightly improved but remained below average (Table J.4B).

Table J.4: (A) Habitat indicators for five life stages of Central Valley Spring Chinook salmon. Each row is an indicator (grouped by life stage at left) and each column is a brood year. Colors are as in Table J.2A. (B) Trend over brood years in the average of habitat indicators for freshwater life stages (black line, as in J.2B) and marine habitat indicators (blue line, as in Table J.2B). Brood years on x-axis match years of the indicator suite in A.

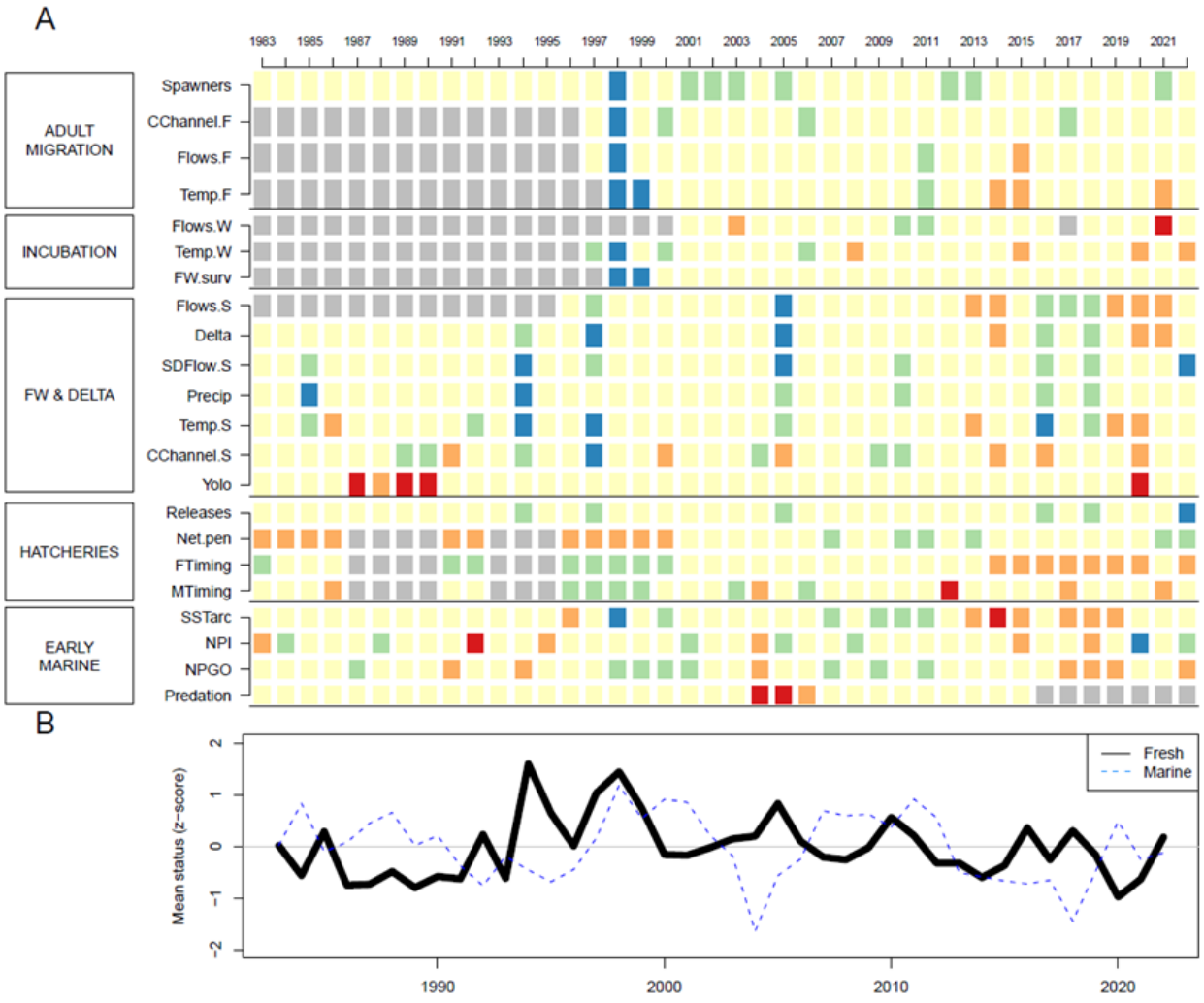

J.3.1 Methodology

The indicators in Table J.1 have been shown in previous studies or were proposed in rebuilding plans to be strongly related with life-stage specific Chinook salmon productivity, and these studies helped determine expected directionality of indicators with stock productivity (see below and Harvey et al. 2020 for additional justification). Four of the five broad categories of indicators in the stoplight charts align with the simpler stoplight chart for Central Valley fall Chinook salmon presented in the main body of this report (Table 3.2): Adult Spawners, Incubation conditions, Freshwater/Estuarine Residence conditions, and Marine Residence conditions (for the first year of marine residence). The fifth category of

indicators, Hatchery Releases, expands the scope of these tables relative Table 3.2, which focuses only on natural-area fish. The habitat indicator charts also share qualities with the stoplight chart developed for Columbia Basin Chinook salmon and Oregon coast coho salmon (Table 3.1) by including regional and basin-scale oceanographic indicators as part of early marine residence conditions. Data on krill off northern California are also presented within the table for KRFC.

The indicators in Table J.1 and in the stoplight tables above have undergone several important adjustments from previous reports:

1. Updates to SRFC and KRFC include changes in some indicators to ensure more reliable and timely data capture. However, updates of many indicators in 2023 remain challenging due to delays in posting of online datasets, resulting in several indicators that could not be updated for this year's report and preliminary estimates for several others. These challenges underscore the importance of including multiple indicators, highlight the potential fragility of these annual summaries, and point to the importance of many individuals for maintaining the databases required for summarizing habitat indicators.

2. Recent analysis of krill off northern California have revealed that krill length is a much better indicator than krill biomass for predicting productivity of Klamath Fall run (see Section 3.1), so we have substituted length for this indicator.

3. CVSC differs from SRFC not only in migration timing but also in their behavior and spatial distribution. Habitat indicators reflect these differences, by characterizing early upstream migration starting in February, holding in pools through the summer, and spawning in a small number of creeks in the late summer and fall. Adult numbers focused on spawner counts in Butte, Mill, and Deer Creeks. Butte Creek spawners migrate from the Sacramento River through Sutter Bypass to Butte Creek, and outmigrants may rear within Sutter Bypass during outmigration. Hence, flow and temperature metrics relied on gages from these systems in addition to the Sacramento mainstem, and Sutter Bypass inundation instead of Yolo Bypass. Finally, the sole hatchery for CVSC is from Feather River, so releases and timing metrics focused on data from just this hatchery.

4. The stoplight tables are categorized from favorable to poor conditions using the same approach as described for the Northern California Current salmon indicator stoplight table (see Appendix J.1). Specifically, after indicator datasets were collected, all indicators were "directionalized" to account for their expected relationships with stock productivity (based on the "Effect" column in (Table J.1) and converted into standardized values. These values are reported in the stoplight tables above, with colors delineating statistically meaningful departures (>2 s.d.) toward poorer (warm shades) or more productive (cool shades) conditions compared to near-average years (within ±1 s.d., yellow). The main difference for the tables shown here relative to (Table 3.1) is that we have not yet determined a fixed historic reference period for the SRFC, KRFC and CVSC tables, due in part to missing data from one or more indicators in large portions of the time series.

J.3.2 Habitat Indicator descriptions

Adults returning and migrating to spawning grounds: Spawning adults set the cohort size (Friedman et al. 2019) and potential for density-dependent habitat limitations at future life stages (Munsch et al. 2020), so we incorporated estimated escapements from PFMC preseason forecasts. Adults must navigate multiple potential barriers to reach spawning grounds, including low river flows and high temperatures at the end of summer. We used flow and temperature measurements from the lower portions of the Sacramento and Klamath Rivers in September and October. In the Sacramento River, adults must also navigate the channel network of the delta, and the rebuilding plan proposed examining potential effects of the Delta Cross Channel as a migration barrier. We used the proportion of time the Cross Channel was closed in September and October as the indicator.

Indicators for adult migrations differ for CVSC due to their early migration timing (February to May), spring-summer holding in pools, and spawning in a small number of Sacramento tributaries. We restricted the enumerated spawner abundance to Deer, Mill, and Butte Creeks, for which records were consistently maintained throughout the 1983-present period of record. To fill in data gaps of spawner counts for Butte Creek (the largest spawning population) to complete the retrospective time series to the 1983 brood year, we used predictions from regressions of Butte Creek spawner counts and snorkel surveys. Flows and temperatures during holding were restricted to the river with the greatest spawner abundance (Butte Creek). In addition, CDFW conducts estimates of pre-spawn mortality which we added as an indicator due to CVSC's exposure to warm in-river conditions.

Incubation to emergence: After spawning, incubating eggs may be subject to dewatering in the river (Jager et al. 1997) and are sensitive to high temperatures (Friedman et al. 2019). For SRFC, the river flow indicator was derived from the seven-day 10th percentile of flow for the Sacramento River from October to December at Bend Bridge near Red Bluff. For CVSC, we used similar flow conditions for Butte Creek. For KRFC, dewatering previously was observed in various tributaries of the Klamath. Hence, minimum flows from four gages (Klamath at Iron Gate, Scott River, Shasta River, and Trinity River at Lewiston Dam) were used, and the index was calculated from the average of standardized flow values. Incubation temperature records were obtained for all three river systems, albeit for a much shorter time series in the Klamath. SRFC incubation temperature estimates are from Red Bluff Diversion Dam (data in Friedman et al. 2019), CVSC records are from Butte Creek, and Klamath records are from Seiad Valley. Egg-fry productivity as measured by migrants per spawner were initiated in the early 2000s for all stocks.

Freshwater and estuary residence: During migration to the ocean, fall Chinook salmon stocks take advantage of temporary residence in riverine and estuary habitats before transitioning to marine environments. We used a variety of indicators of habitat conditions during this stage. Freshwater conditions are set by precipitation and spring air temperatures, both of which influence snowpack salmon runs and river flow (Munsch et al. 2019) in both tributaries (important for CVSC in particular) and mainstem. In turn, flows from December to May (and their temporal variation) set conditions for rearing in river and estuary systems as fish move downstream, and have been linked to freshwater

(Munsch et al. 2019) and life-cycle productivity (Michel 2019, Friedman et al. 2019). Higher flows also determine access to floodplain rearing in reaches such as the Yolo Bypass for SRFC (Limm and Marchetti 2009) and Sutter Bypass for CVSC, as well as the potential to flush polychaete hosts of the parasite *Ceratomyxa shasta* that infects juvenile salmon during outmigration (Jordan 2012). Flows also determine the outflow through the Sacramento delta (Reis et al. 2019), which can influence estuarine rearing opportunities (Munsch et al. 2020). To shift freshwater flows to pumping facilities, the Bureau of Reclamation opens the Delta Cross Channel, and this pathway can entrain salmon in pumps or otherwise expose them to higher mortality (Perry et al. 2013).

Magnitude and timing of hatchery releases: While much of the habitat indicators focus on natural-area fish, hatchery releases make up a significant contribution of each run and may also contribute to density dependence. We therefore included the annual total of hatchery releases, using data from up to four SRFC hatcheries on the Sacramento (San Joaquin hatcheries were not included), the Feather River hatchery for CVSC, and Trinity and Iron Gate hatcheries in the Klamath. While hatchery-origin juveniles are also sensitive to the conditions natural-origin juveniles face, they are generally raised until they are primed for rapid migration. Following concepts of match-mismatch theory (Cushing 1990), we compared release date with the date of peak spring flow in freshwater and the spring transition in the ocean, as Satterthwaite et al. (2014) showed that both timing of release relative to the spring transition and overall later release timing were positively correlated with survival rates. Fates of hatchery fish may be a consequence of release location (Sturrock et al. 2019), including locations external to the Sacramento River system, so we also included the proportion of releases that were seaward of Sherman Island in the lower delta.

Marine residence: Marine residence of 1 to 5 years completes the life cycle for fall run Chinook salmon populations. While a broad number of marine habitat indicators have been examined (Wells et al. 2008), we focused on a limited subset of possible indicators representing initial set-up of ocean entry conditions (March-May), including sea surface temperature, the North Pacific Index, and North Pacific Gyre Oscillation. We also included an index of predation by common murres nesting at Southeast Farallon Island, which was a strong predictor in Friedman et al. (2019). Unfortunately, this indicator currently cannot be updated quantitatively. On the positive side, we have updated the krill prey indicator for Klamath River fall Chinook salmon from biomass to average length to better reflect stronger correlations with recruits per spawner. Where indicators were averaged to obtain a marine habitat conditions score, hatchery release timing relative to the spring transition was also included as a marine habitat condition.

Appendix K: GROUNDFISH

Link to main section: Groundfish

K.1 Stock Abundance and Fishing Intensity

The CCIEA Team regularly presents the status of groundfish biomass and fishing pressure based on the most recent stock assessments. This year's report includes updated information for seven stocks (black rockfish, canary rockfish, copper rockfish, Pacific hake, petrale sole, Rex sole, sablefish, shortspine thornyhead) from the 2023 assessment cycle.

Most groundfish stock biomasses are above biomass limit reference points (LRPs; Fig. K.1), though two substocks since 2021 have been estimated to be below the LRP: copper rockfish in southern California and quillback rockfish in California. For management purposes, the southern California substock of Copper rockfish was combined with the northern California substock, and the California substock is not considered overfished. None of the new stock assessments present any stocks as overfished. Yelloweye rockfish continues rebuilding toward its target reference point (TRP; dashed vertical line in Fig. K.1), but is above the overfished level (i.e., its biomass is greater than the LRP), meaning that it remains under a protective rebuilding plan from PFMC. China rockfish in California is also notably lower in biomass, but above limit levels.

"Overfishing" occurs when catches exceed overfishing limits (OFLs), but not all stocks are managed by OFLs. For summary purposes, our best alternative is to compare fishing rates to proxy rates that are based on a stock's spawner potential ratio (SPR; Fig. K.1, y-axis). Black rockfish in Oregon is above F_{MSY} proxy fishing rates, so there are now six stocks exceeding the fishing rate at the proxy MSY: Copper (SCA), Quillback (CA and OR), Black (OR), and Rougheye rockfishes, and Petrale sole. Two other rockfish stocks— the southern stock of China rockfish and northern California stock of Vermilion/ Sunset rockfishes— were near the proxy for overfishing (dashed horizontal line in Fig. K.1) in their most recent assessments.

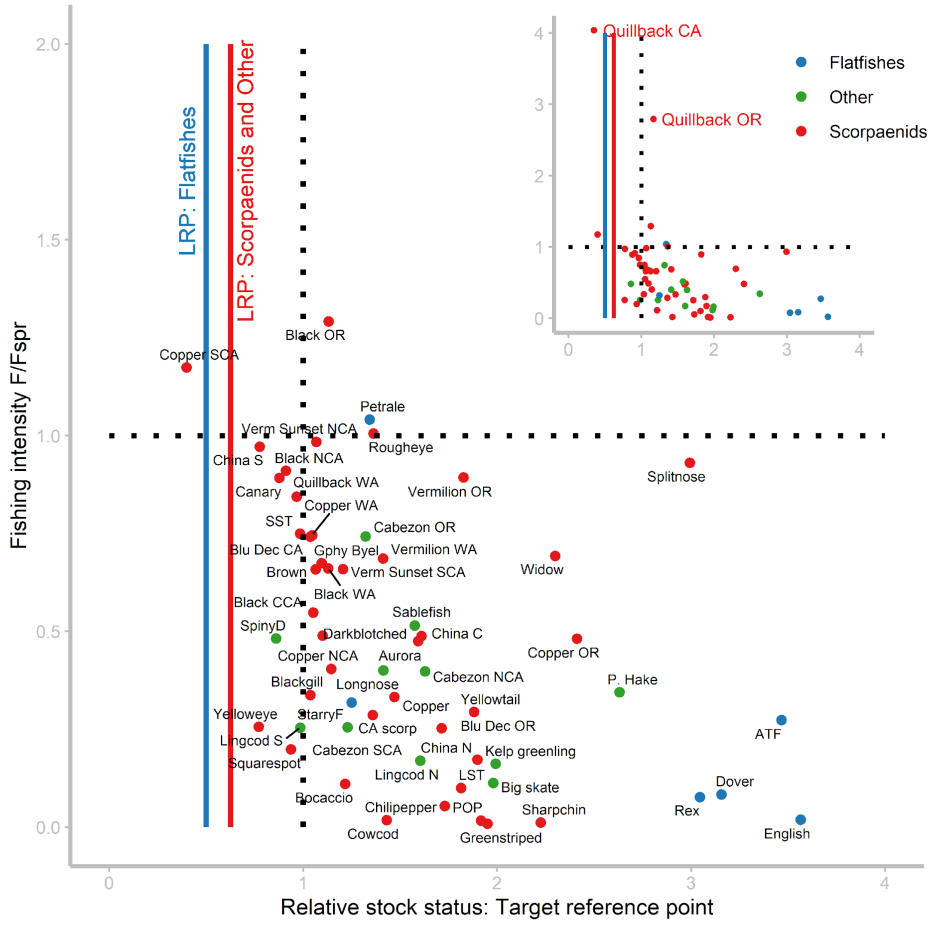

Figure K.1: Stock status of CCE groundfish. Relative Stock Status is the ratio of the current year spawning biomass (in mt) or output (typically in billions of eggs) to unfished relative to the target reference point (as a percentage of unfished biomass; 0.4 for scopaenids and other fishes; 0.25 for flatfishes). Fishing Intensity uses the fishing rate to achieve a specific spawner potential ratio (SPR), defined as F/F_{SPR}, where SPR is the maximum sustainable yield (MSY) proxy. The horizontal line is the fishing intensity rate reference; above the line is above the reference level and indicates overfishing. Vertical lines are the biomass target reference points (TRP=1; dashed line) and limit reference points (LRPs; red lines); left of the LRP indicates an overfished status. Symbols indicate taxonomic groups. All points represent values from the most recent PFMC-adopted full stock assessments. Groundfish stock status data provided by J. Cope, NMFS/NWFSC, derived from NOAA Fisheries stock assessments.

K.2 Juvenile groundfish abundance

Indices of abundance for juvenile groundfish were calculated using species distribution models (SDM). Data come from the West Coast Groundfish Bottom Trawl Survey (WCGBTS; Keller et al. 2017) for 2003-2023. There is no data for 2020 as COVID restrictions

prevented the survey from being completed. Details of the modeling approach can be found in Appendix K in Harvey et al. 2023.

The juvenile recruitment indices for the four groundfish species from the DTS assemblage are shown in the main document (Section 3.4.1). In most years, the sablefish index (age-0, ≤ 29 cm) can be considered an estimate of annual abundance because the analysis is limited to one age class (age-0 fishes), although 2022 appears to be an exception (see Section K.2 below). For Dover sole (age-1 & age-2, ≤ 17 cm), longspine thornyhead (≤ 7 cm), and shortspine thornyhead (≤ 8 cm), the indices represent an estimate of juvenile abundance since the data span multiple age classes (multiple age classes were necessary to produce enough positive observations for model convergence). Estimated juvenile biomass (instead of an index ranging from 0-1) from the SDM analysis is shown in Fig. K.3 for reference.

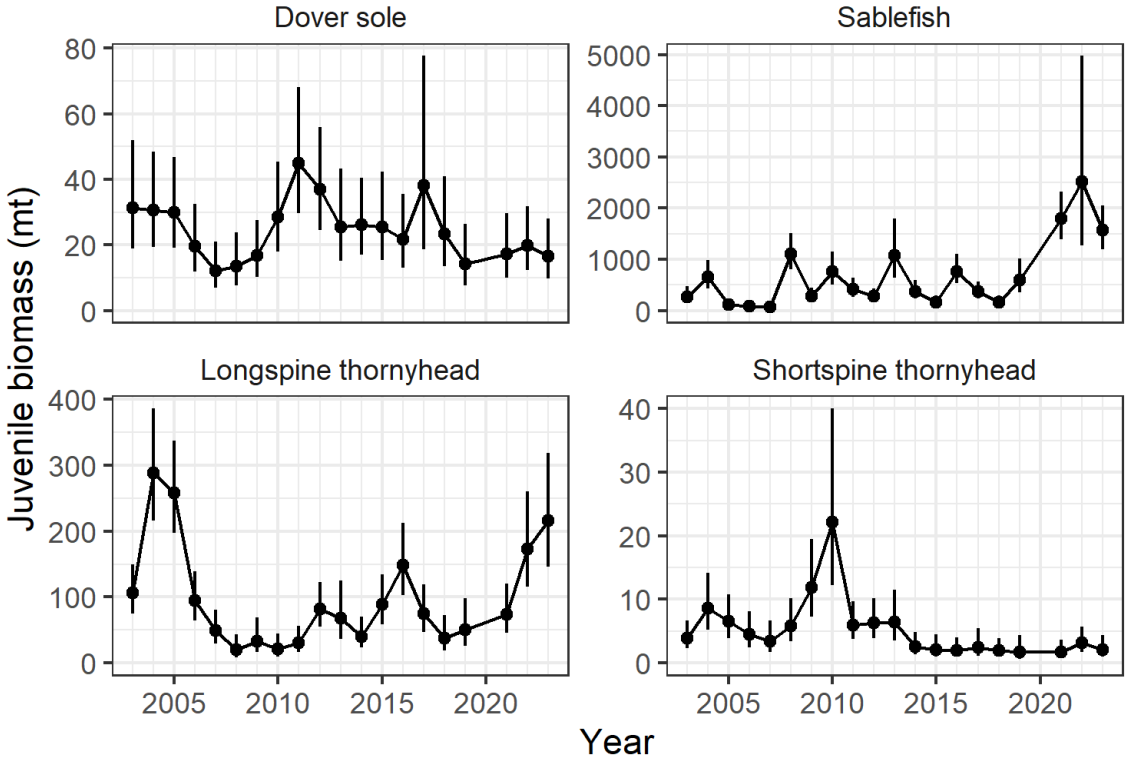

Figure K.3: Simple catch per unit effort (CPUE) for four juvenile groundfishes calculated as the mean kg per square km for all trawls within a year.

K.3 Sablefish size distributions

High abundances of sablefish can impact both the sablefish fishery and other fisheries in which sablefish can be caught as bycatch, such as the at-sea and the shoreside hake fisheries (see Appendix A in Haltuch and Castillo-Jordán 2019). Sablefish are also caught as part of the DTS assemblage and catch of sablefish can constrain catch of Dover sole and thornyhead. The sablefish recruitment index captured large increases in juvenile abundance in 2021, 2022, and 2023 (Fig. 3.9). However, examination of the size structure

suggests that the high biomass of sablefish ≤ 29 cm fork length in 2022 does not represent high recruitment of age-0 fishes but slow growth of the 2021 age class. In earlier years, the size-at-age data are clearly bi-modal with a mode of individuals below around 25 cm representing age-0 recruits. However, in 2022, there is no mode less than 29 cm, and the high abundance in the recruitment index appears to be related to large numbers of 28 and 29 cm fishes that are likely slow growing individuals from 2021. The strong recruitment in 2021 appears to have led to density-dependent reductions in growth leaving some age-1 fishes below the 29 cm cut off used here and in Tolimieri et al. (2020). In 2023, there were large numbers of individuals around 25 cm suggesting a strong year class as in 2021. Thus, while Tolimieri et al. (2020) refer to these sablefish as age-0 recruits, here they are better thought of as simply juvenile sablefish, and not an index of recruitment, at least for 2022. Nevertheless, these smaller sablefish may present bycatch issues to other fisheries, like the at-sea hake fishery, regardless of their actual age.

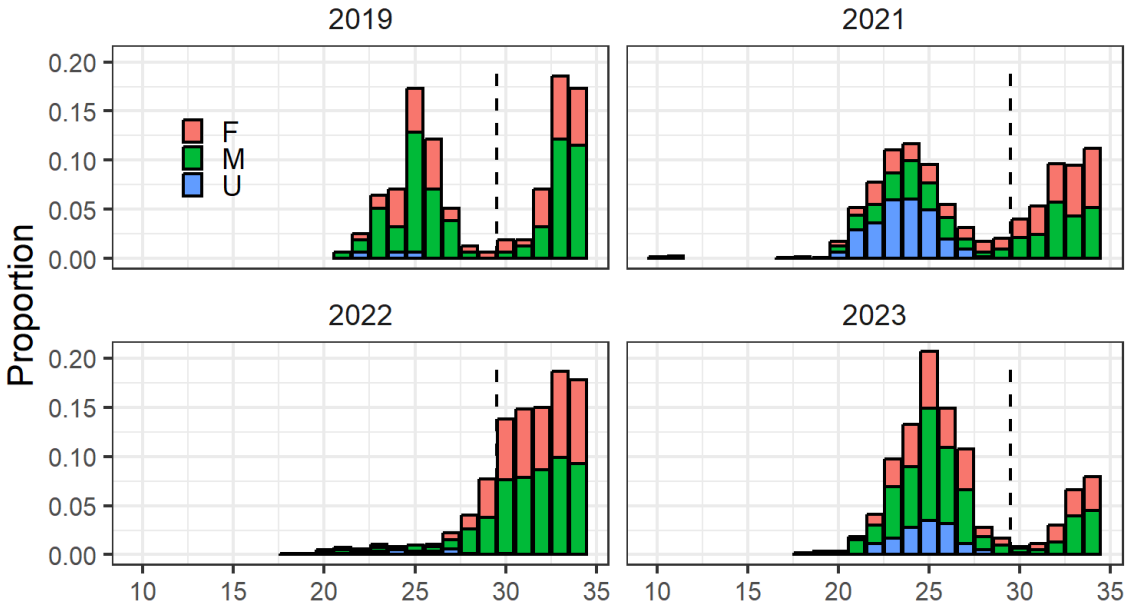

Figure K.4: Size distributions of juvenile sablefish (≤35 cm) captured in the NOAA West Coast Groundfish Bottom Trawl Survey from 2019, and 2021-2023.

K.4 Availability of juvenile sablefish to ports that fish for hake and salmon

Bycatch of juvenile sablefish can impact other fisheries, especially the hake (Pacific whiting) and salmon fisheries. The relative availability of juvenile sablefish (≤ 29 cm) was calculated for selected ports along the West Coast that have high shoreside hake or salmon landings. Biomass estimates from the SDM analysis used for juvenile sablefish in Figure 3.9 was summed within 232 km of a port for hake ports and within 65 km of a port for salmon ports. Total biomass was converted to an index ranging from 0-1 by dividing the time series by its maximum value.

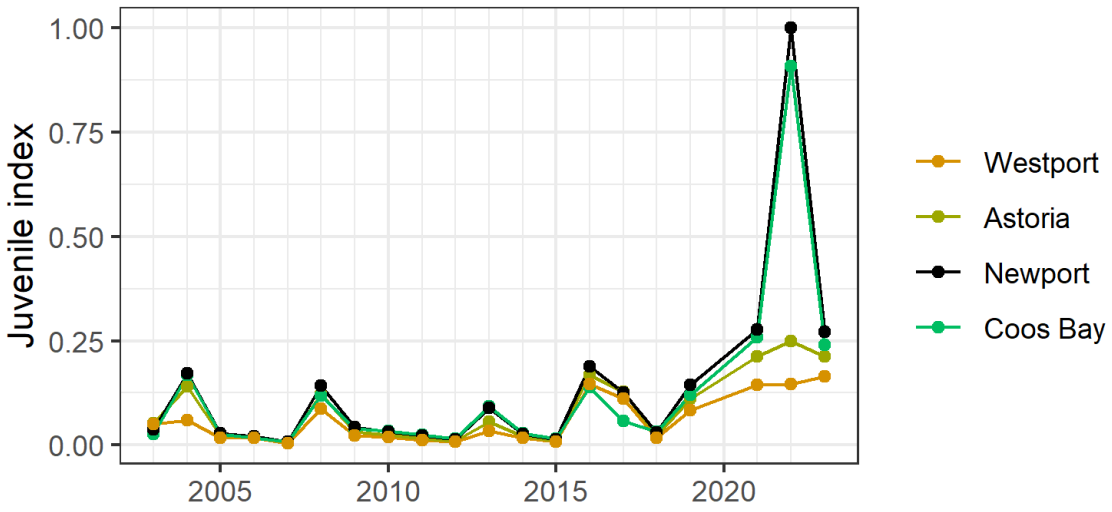

Figure K.5: Index of availability of juvenile sablefish (≤29 cm) to selected ports along the West Coast for Pacific hake for 2003-2023. Annual values were scaled to 0-1 by dividing by the maximum observed biomass.

Relative abundance of juvenile sablefish around ports that support shoreside hake landings was high in 2021 and extremely high in 2022 (Fig. K.5). As noted above, the high relative abundance in 2022 appears to be due to a large number of age-1 28 and 29-cm fish, not high recruitment of age-0 fish in 2022. In 2023, availability was similar to 2021. Newport and Coos Bay had the highest relative abundances of juvenile sablefish within the 232-km fishing radius. Shoreside hake ports farther to the north (Westport, Astoria) had high exposure to sablefish juveniles relative to previous years, but much lower relative density when compared to ports farther south.

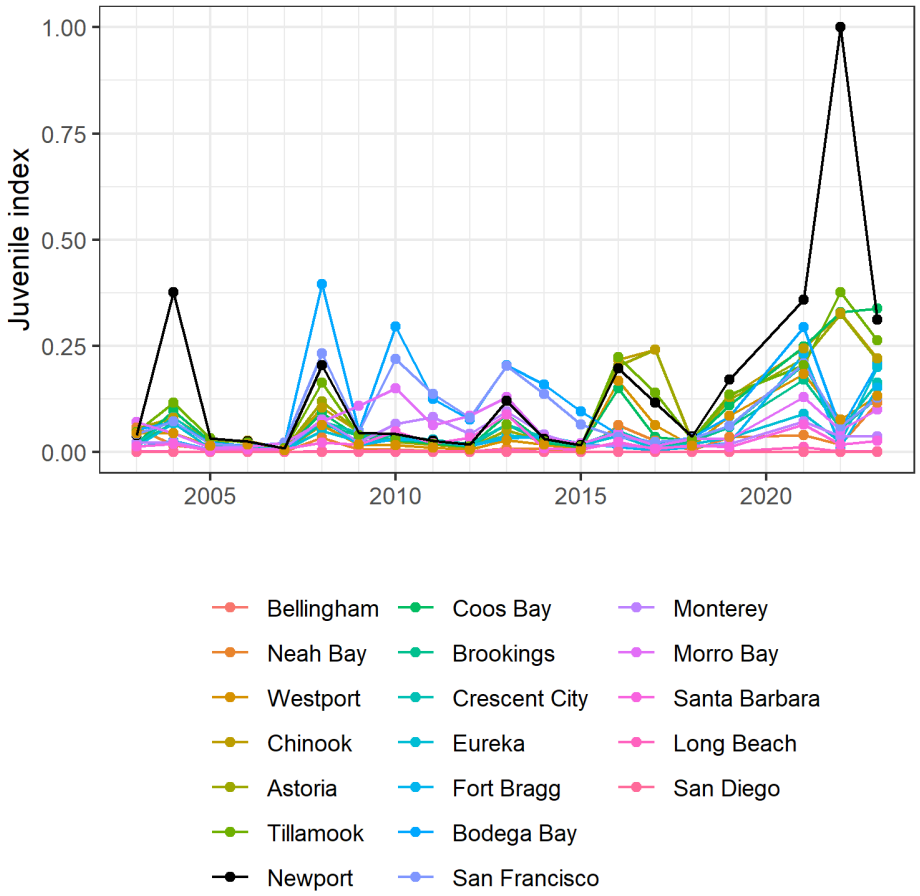

Figure K.6: Index of availability of juvenile sablefish (≤29 cm) to selected ports along the West Coast that fish for salmon for 2003-2023. Annual values were scaled to 0-1 by dividing by the maximum observed biomass.

For salmon ports, Newport had the highest relative exposure to juvenile sablefish (Fig. K.6) in 2021 and 2022 with very high exposure in 2022. Chinook, Astoria, and Coos Bay also had high relative exposure to juvenile sablefish in 2022, while other more southerly ports had low relative abundance of juvenile sablefish, as did ports farther north. Thus for both hake ports and salmon ports, exposure to potential bycatch of sablefish juveniles (age-0 and age-1 fishes) was highest in the central coast of Oregon and southern Washington. In 2023, availability was similar to 2021.

K.5 Availability of groundfish species to ports

We estimated the relative availability of groundfish biomass to individual ports from 2002-2023. Methodology for calculating the relative availability of groundfish biomass to individual ports follows that of Selden et al. (2020), with some exceptions. In brief, we used data from the Northwest Fisheries Science Center's West Coast Groundfish Bottom Trawl Survey (Keller et al. 2017) to estimate spatial distribution of species-specific biomass (Location Biomass), and the Center of Gravity (CoG) of the Location Biomass. We then calculate the Availability Index for each port by summing the Location Biomass within a

radius from that port based on the 75th quantile of the distance traveled from port to harvest of species of interest, weighted by catch, as measured from trawl logbooks (Fig. K.7). We analyzed 12 species that make up a large component of landings for vessels using bottom trawl gear along the West Coast, or that have broader management interest (e.g., shortbelly rockfish).

The present analysis differs from Selden et al. (2020) in three ways:

1- We estimated the spatial distribution of species using the R package sdmTMB (Anderson et al. 2022; R Core Team 2023) instead of VAST (Thorson 2019). The sdmTMB models included Pass and scaled depth as fixed parameters. Year was a time variable and models included both spatial and spatiotemporal (iid) autocorrelation, and a delta-poisson-link-gamma error distribution (Thorson 2018) error distribution.

2- We used the Location Biomass directly instead of scaling it by spawning stock biomass from the assessment. Thus, the Availability Index is a relative biomass index and not actual available biomass. Biomass was then scaled to 0-1 for presentation by dividing by the highest value in any year.

3- We used only the WCGBTS, and did not combine the Triennial survey (1980-2004) with the WCGBTS. This approach shortens the analysis period but allows us to expand the depth range to 55-1250 m.

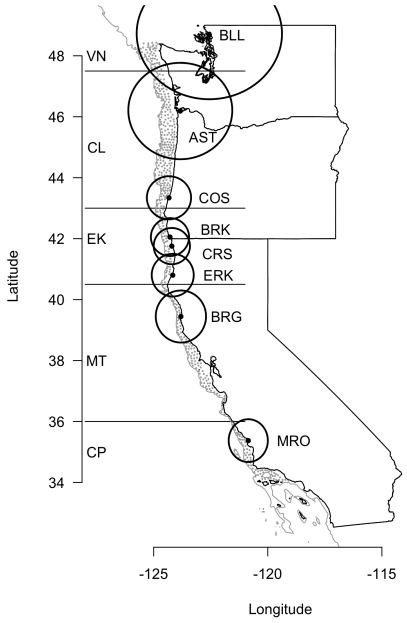

Figure K.7: Ports used in the Availability Analysis. The radii of the black circles centered on each port represent the areas within which groundfish availability is estimated (see text). Ports are Bellingham (BLL), Astoria (AST), Charleston (Coos Bay, COS), Brookings (BRK), Crescent City (CRS), Eureka (ERK), Fort Bragg (BRG) and Morro Bay (MRO). Gray line is the 1200-m contour.

The CoG of species biomass shifted to the north over the time series for big skate, petrale sole, sablefish, shortbelly rockfish, and shortspine thornyhead (Fig. K.8), while arrowtooth CoG shifted south through about 2015 when it began to drift northward. For sablefish, the northern shift returned the CoG to approximately 41.5°N in 2022–similar to its 2003 distribution, but the CoG then shifted slightly north in 2023 to about 42°N. The CoG for lingcod varied through time but showed a northern shift of almost 2.0°N since 2018. For shortbelly rockfish the change in CoG was almost 5.0°N through 2022 with a slight shift back south in 2023. Canary rockfish, darkblotched rockfish, Dover sole and yellowtail rockfish all had variable CoG but no obvious latitudinal trend.

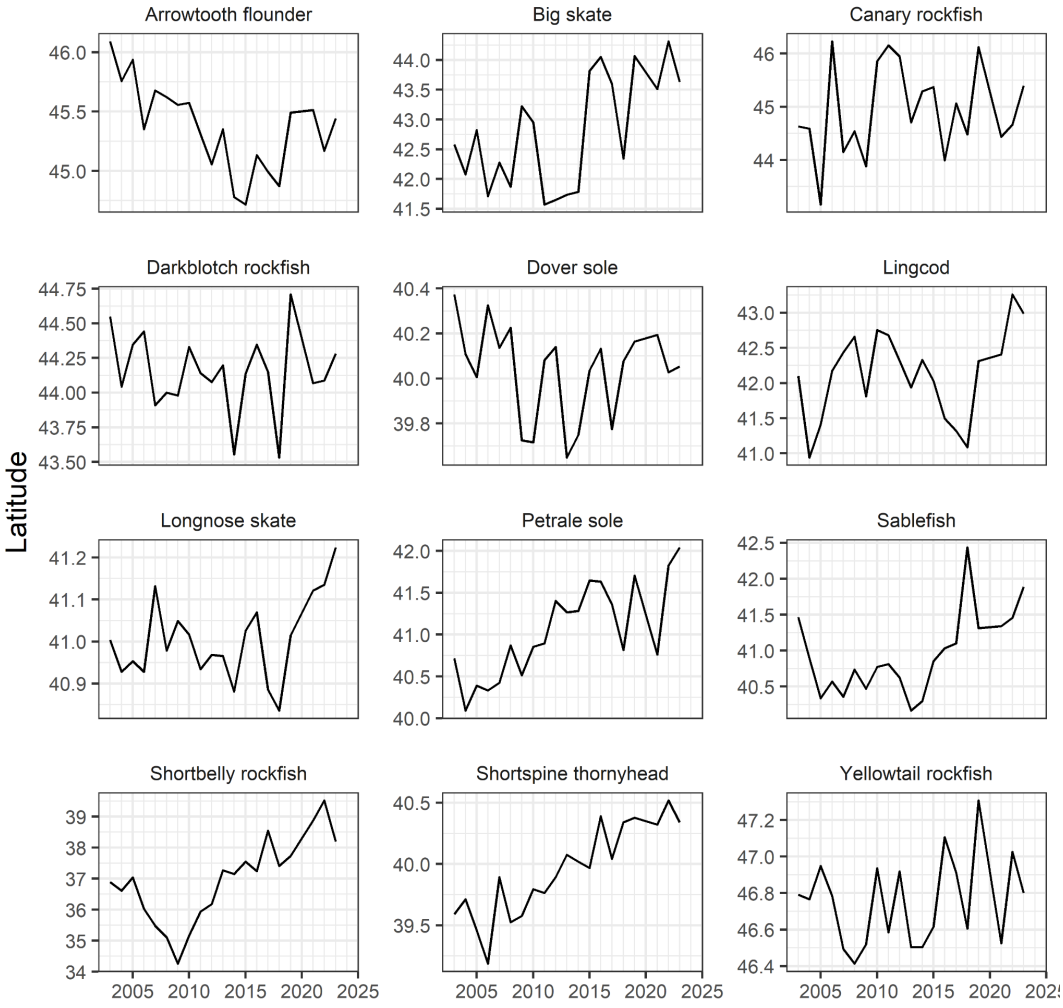

Figure K.8: Center of gravity of biomass of 12 groundfish species along the West Coast.

The availability indices show that sablefish, shortspine thornyhead, arrowtooth flounder, big skate, longnose skate, canary rockfish, darkblotched rockfish, and yellowtail rockfish were all generally more available to fishers operating from Astoria than from other ports, although Bellingham saw similar availability in some cases (Fig. K.9). Availability of Dover sole was more broadly distributed while shortbelly rockfish were more available to more

southerly ports. For lingcod, the pattern varied through time with those more available to southern ports early in the time series becoming more available in the north over time.

Petrale sole, big skate, and yellowtail rockfish all increased in availability to northern ports over time, as did sablefish, which had the highest availability to Astoria compared to the other ports and high availability in 2022 and 2023 compared to the rest of the time series (Fig. K.9). The same was true for big skate in 2022.

Figure K.9: Indices of availability of biomass of 12 groundfish species to selected ports along the West Coast for 2003-2023. Ports are Bellingham (BLL), Astoria (AST), Charleston (Coos Bay, COS), Brookings (BRK), Crescent City (CRS), Eureka (ERK), Fort Bragg (BRG) and Morro Bay (MRO).

Appendix L: HIGHLY MIGRATORY SPECIES (HMS)

Link to main section: Highly Migratory Species

L.1 HMS Stock Assessment Information

Biomass and recruitment estimates for many HMS stocks that occupy the California Current are available from stock assessments conducted by collaborators under the International Scientific Committee (ISC) for Tuna and Tuna-like Species in the North Pacific Ocean or the Inter-American Tropical Tuna Commission (IATTC). The only assessment updates since last year's report are for North Pacific albacore (ISC 2023) and North Pacific swordfish. The swordfish assessment underwent major changes because the spatial definitions of the stock have changed. Therefore, the time series for biomass and recruitment are different than in previous reports. We should emphasize that the status and trends symbols shown below in Figures L.1 and L.2 reflect short-term patterns relative to time series averages (with a period of reference of 1991-2020), and do not necessarily reflect reference points based on, e.g., unfished stock biomass. For example, bluefin tuna is considered to be overfished relative to potential biomass-based reference points adopted for other tuna species (ISC 2022) even though it falls >1 s.d. above the biomass time series average in our Figure L.1.

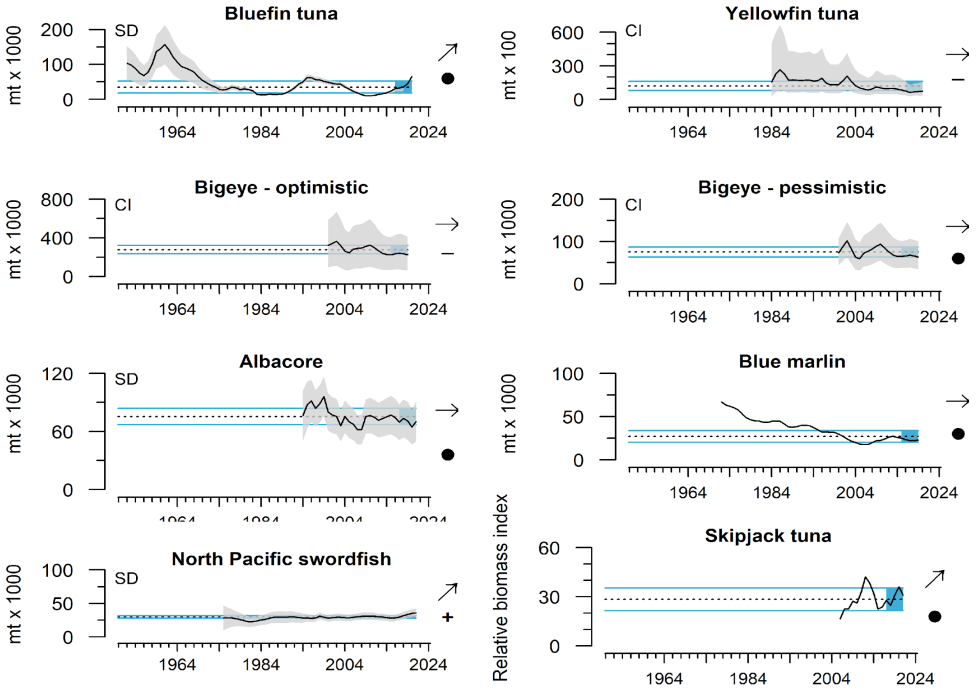

Figure L.1: Spawning stock biomass for highly migratory species in the north Pacific. The type of error envelope is indicated in the upper left of each panel: SD = ±1 s.d.; SE = ±1 s.e.; CL = ±95% C.L. Assessment dates were: Albacore (2023), Bigeye tuna (2019), Blue marlin (2021), Bluefin tuna (2022), Eastern Pacific swordfish (2012), Skipjack tuna (2022), North Pacific swordfish (2023), and Yellowfin tuna (2020). Lines, colors, and symbols are as in Fig. 2.1.

The most recent spawning stock biomass (SSB) estimates range from above the time series average (bluefin tuna, swordfish) to ~1 s.d. below average (yellowfin tuna, bigeye tuna), with generally wide error estimates (Fig. L.1). Estimated SSBs of bluefin tuna, swordfish, and skipjack tuna have positive five-year trends. HMS recruitment trends from the most recent assessments are generally trending either neutrally or positively, typically with high uncertainty (Fig. L.2).

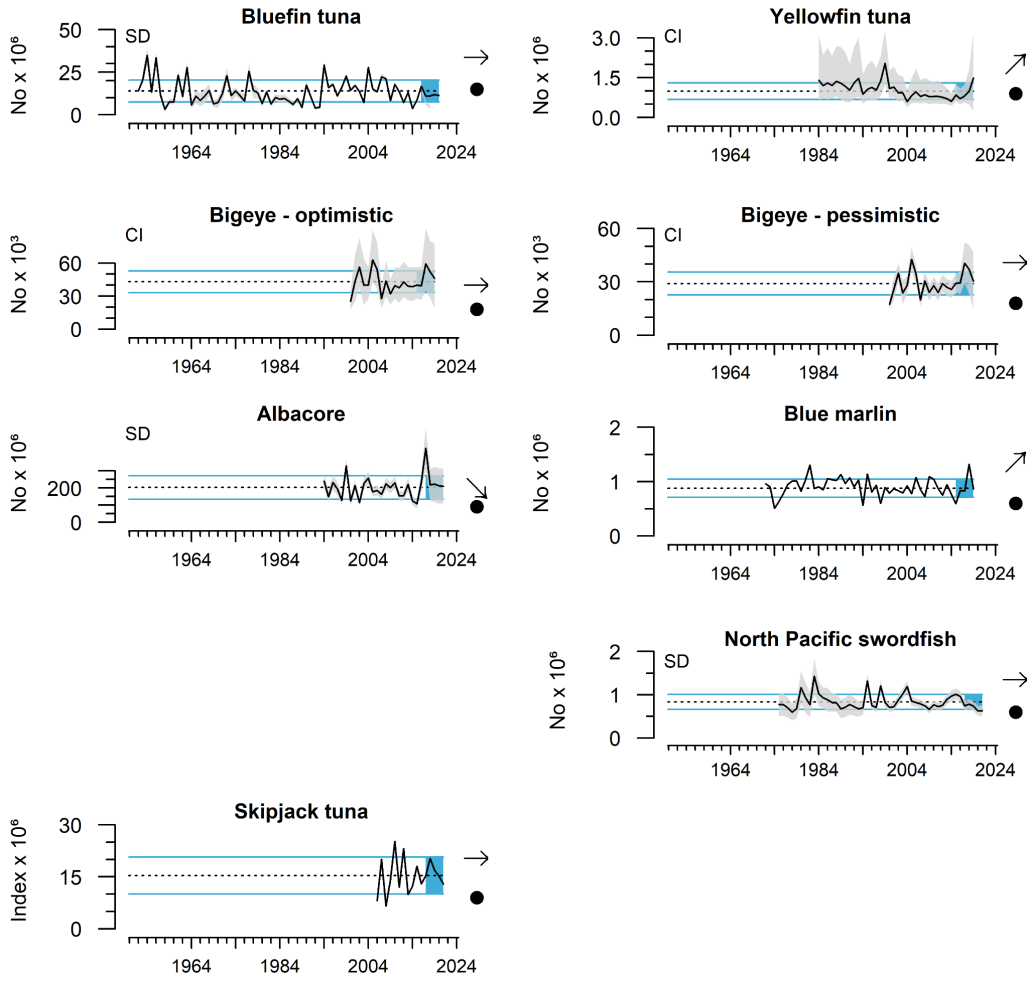

Figure L.2: Recruitment for highly migratory species in the North Pacific. The type of error envelope is indicated in the upper left of each panel: SD = ±1 s.d.; SE = ±1 s.e.; CL = ±95% C.L. Assessment dates were: Albacore (2023), Bigeye tuna (2019), Blue marlin (2021), Bluefin tuna (2022), Skipjack tuna (2022), North Pacific swordfish (2023), and Yellowfin tuna (2020). Lines, colors, and symbols are as in Fig. 2.1.

L.2 HMS Diet Information

Quantifying the diets of highly migratory fishes in the CCE can complement existing trawl-based assessments of the available forage, provide insight into how forage varies over time

and space, as well as provide a direct metric of forage utilization. Albacore Tuna, Bluefin Tuna, and Broadbill Swordfish are opportunistic predators that consume a wide variety of prey taxa across a range of depths and habitats. Albacore, Bluefin, and Swordfish stomachs were provided by commercial and recreational fishers, and prey were identified from whole or hard part remains and are reported as a mean percent abundance. A subset of prey species are presented here focusing on prey that are either themselves under a management plan, or considered ecosystem component species, to highlight their links to highly migratory species. Juvenile Albacore Tuna were collected off Northern California, Oregon, and Washington during the summer and fall fishing season. Bluefin Tuna were collected by recreational fishers in the Southern California Bight from spring until early fall. Swordfish were collected off Southern and Central California during the commercial drift gillnet season (August 15th through January 31st). Swordfish stomachs are classified by the year the fishing season began (stomachs from January are assigned to the previous year's fishing season). Data are available through 2023 for Bluefin Tuna (Fig. L.3) and through 2022 for Albacore Tuna (Fig. L.4) and Swordfish (Fig. L.5). A subset of the data are shown in Figure 3.12 in the main document.

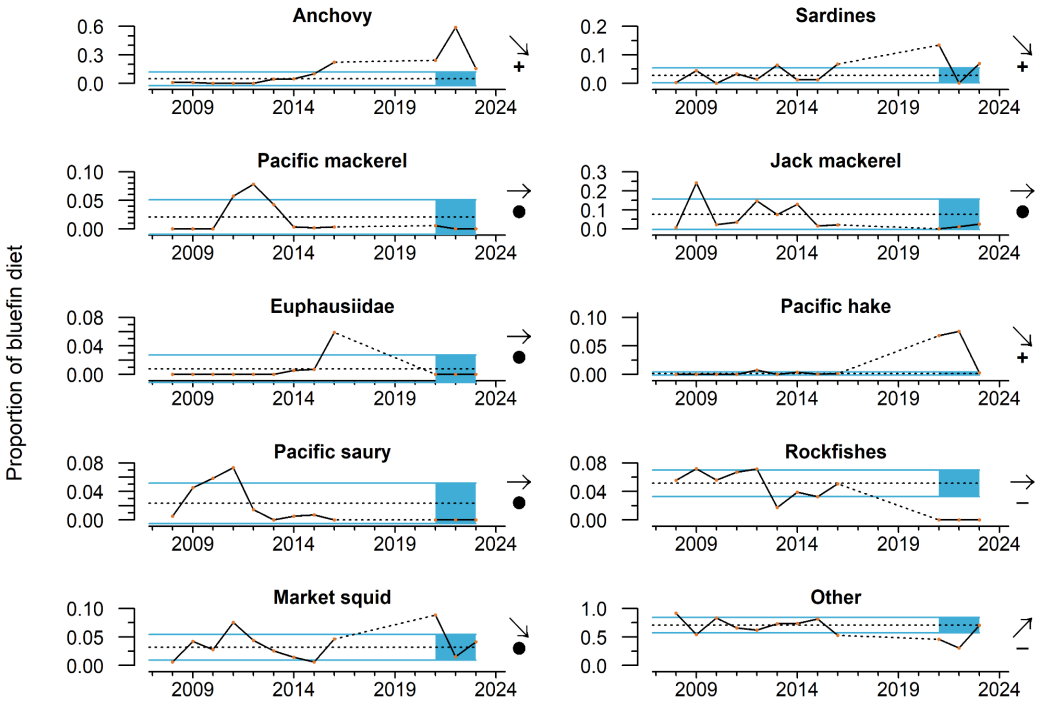

Figure L.3: The proportion of prey items in bluefin tuna diets. Lines, colors, and symbols are as in Fig. 2.1.

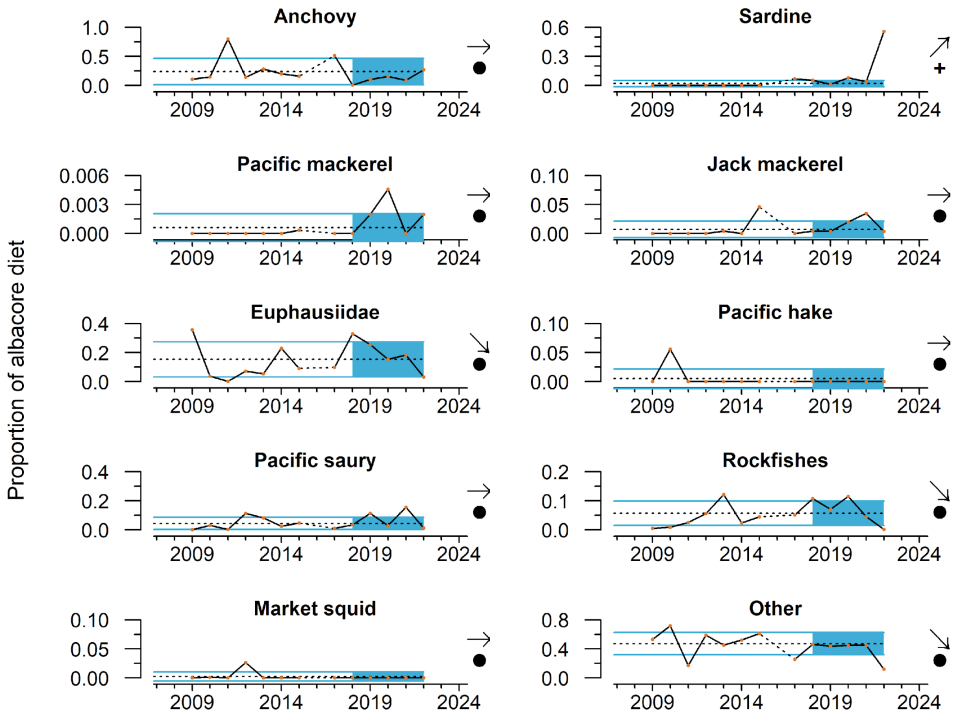

Figure L.4: The proportion of prey items in albacore tuna diets. Lines, colors, and symbols are as in Fig. 2.1.

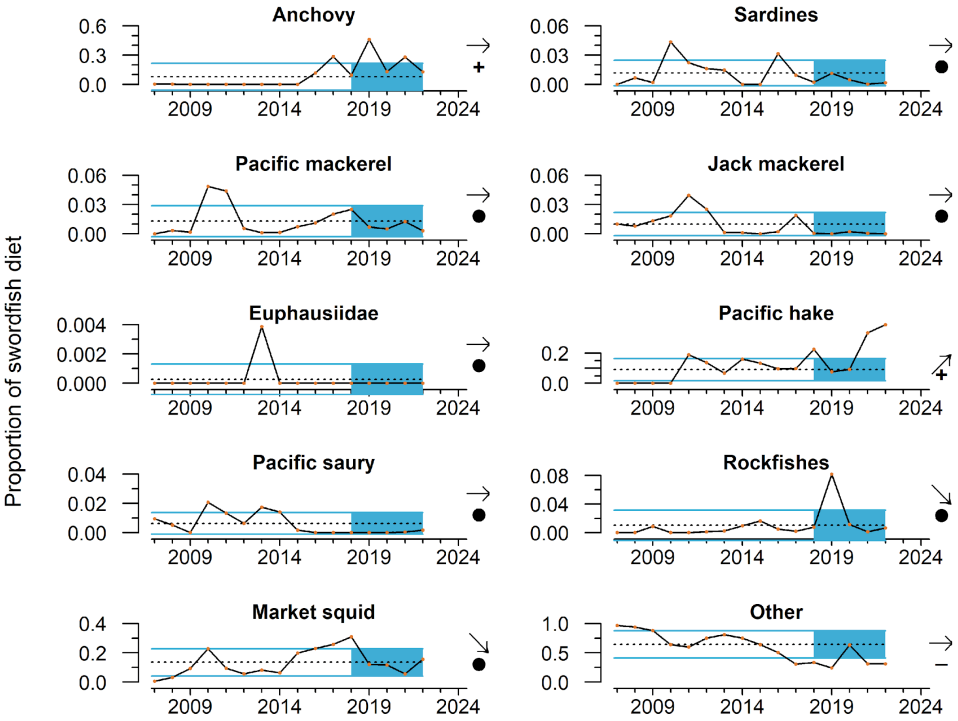

Figure L.5: The proportion of prey items in swordfish diets. Lines, colors, and symbols are as in Fig. 2.1.

Appendix M: MARINE MAMMALS

Link to main section: Marine Mammals

M.1 Sea Lion Productivity

California sea lion pup count and condition are robust indicators of prey quality and abundance even when the sea lion population is at or near carrying capacity (see Appendix L in Harvey et al. 2022). Pup count relates to prey availability and nutritional status for gestating females from October to June. Pup growth from birth to age 7 months is related to prey availability to lactating females from June to February. Data on the overwinter growth rate of sea lion pups were not available at the time of submission of this document. Nursing female diet information was also not available in time for this report but the lower number of births and moderate condition of pups for the 2023 cohort indicates that foraging conditions may have declined for nursing females in the past year.

M.2 Whale Entanglements

Total confirmed whale entanglements have remained fairly consistent for the last five years after declining from a high in 2015-2016 (Fig. M.1). The trend in total confirmed entanglements is driven largely by incidents with humpback whales, which are the most frequently entangled species in absolute numbers. Confirmed entanglements of killer whales increased after 2020 and have remained at 1-2 whales per year.

Multiple actions were taken in 2023 to reduce entanglement risk (see also Appendix O). California delayed commercial and recreational Dungeness crab season openers in 2022/23 and implemented early season closures of the central California 2022/23 commercial and recreational Dungeness crab fisheries. Washington and Oregon implemented late-season restrictions in the deployment of gear in 2022/23 commercial Dungeness crab fisheries. The 2022/23 season openers for commercial Dungeness crab fisheries in Washington and Oregon were also delayed due to crab meat quality and domoic acid concerns. High numbers of humpback whales on California crab fishing grounds and low Dungeness crab meat yields in Washington and Oregon resulted in delayed openings for the 2023/24 commercial Dungeness crab fishery in all three states.

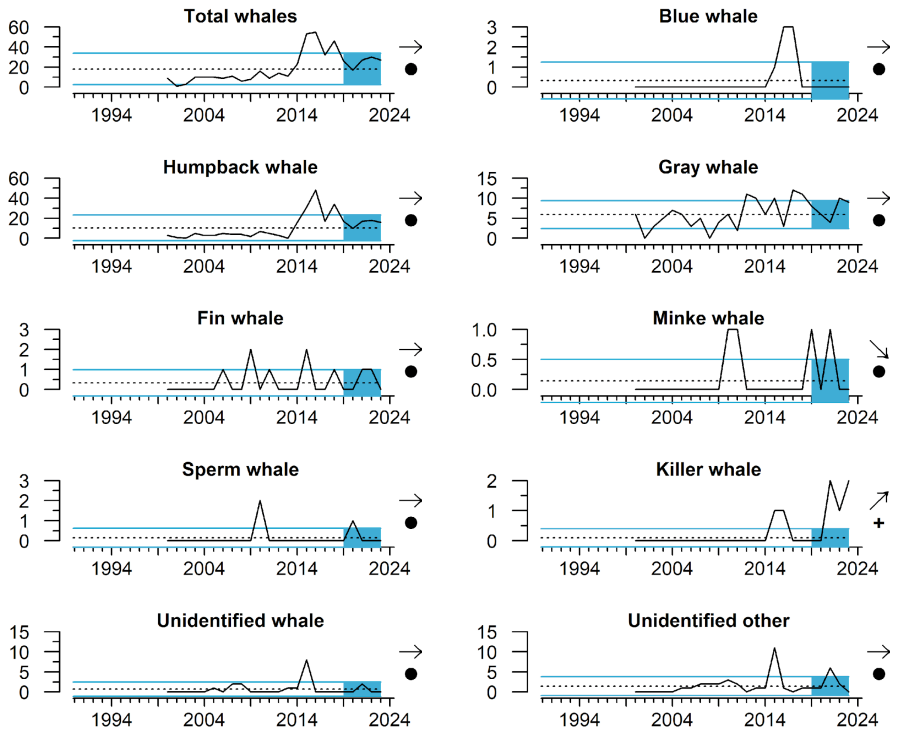

Figure M.1: Numbers of whales confirmed as entangled in fishing gear along the West Coast from 2000-2023. 2023 data are preliminary. Lines, colors, and symbols are as in Fig. 2.1.

Appendix N: SEABIRD PRODUCTIVITY, DIET, AT-SEA DENSITY, AND MORTALITY

N.1 Seabird Productivity

Seabird population productivity, measured through indicators of reproductive success, tracks marine environmental conditions and often reflects forage production near breeding colonies. We report on standardized anomalies of fledgling production per pair of breeding adults for the Northern CCE (one species at Destruction Island, Washington and three species at Yaquina Head, Oregon) and the Central CCE (five species on Southeast Farallon Island and two species on Año Nuevo Island). These focal species span a range of feeding habits and ways of provisioning their chicks, and thus provide a broad picture of the status of foraging conditions (Table N.1).

Table N.1. Preferred forage type and location by colonial seabird species in the CCE.

Species	Forage items/period	Foraging location
Brandt's cormorants	pelagic and benthic fishes/daytime	Continental shelf, within 20 km of colonies
Cassin's auklet	zooplankton/daytime, nighttime	Continental shelf break, within 30 km of colonies
Common murres	pelagic fishes/daytime	Deeper continental shelf and shelf break, within 80 km of colonies
Pelagic cormorants	pelagic and benthic fishes/daytime	Continental shelf, within 20 km from colonies
Pigeon guillemots	small benthic and pelagic fishes/daytime	Continental shelf, within 10 km of colonies
Rhinoceros auklets	pelagic fishes/daytime, into early evening	Shallow continental shelf, within 50 km of colonies

In the Northern CCE, productivity of rhinoceros auklets is monitored on Destruction Island, located 6 km off the outer coast of Washington. In 2023, chick production of rhinoceros auklets was above average, rebounding after at least two years of below-average chick production (Fig. N.1).

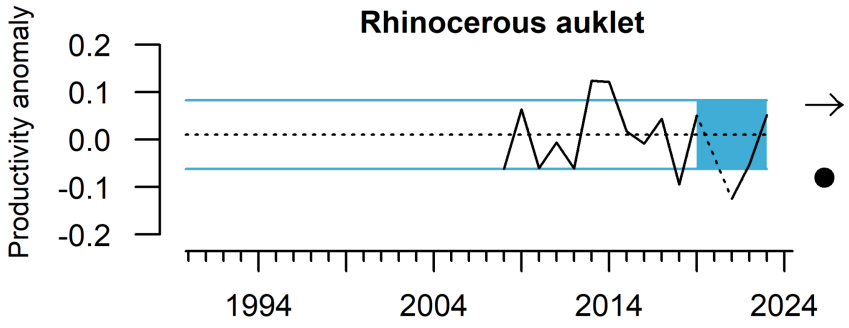

Figure N.1: Standardized productivity anomalies for rhinoceros auklets breeding on Destruction Island, WA through 2023. Data courtesy of S. Pearson, WDFW. Lines, colors, and symbols are as in Fig. 2.1.

Also in the Northern CCE, productivity of common murres and Brandt's and pelagic cormorants is monitored at Yaquina Head on the central Oregon coast. Brandt's cormorant fledgling production in 2023 was well above average, and mean production over the past five years was significantly greater than the long-term mean (Fig. N.2). Common murres bounced back to average fledgling production in 2023 after breeding failure in 2022 (Fig. N.2). Bald eagle disturbance often contributes to seabird reproductive failure at this location and was substantial early in the 2023 season (June and early July). Disturbances led to western gulls and turkey vultures consuming most of the common murre eggs when adults were flushed off the colony. Later egg-laying efforts experienced fewer disturbances and resulted in better hatching and fledging success and produced the latest median hatch date recorded at this location. Pelagic cormorants, which were not observed to attempt nesting at all at Yaquina Head in 2022, fledged more chicks per nest in 2023 than during any other season since cormorant monitoring at Yaquina Head began in 2008 (Fig. N.2).

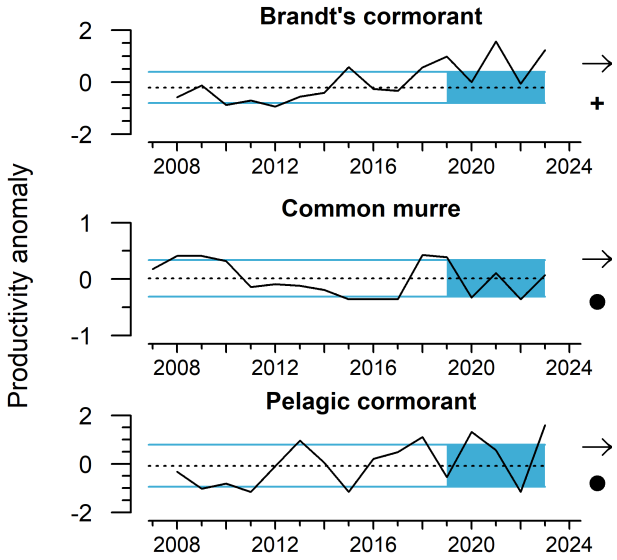

Figure N.2: Standardized productivity anomalies for three seabird species breeding at Yaquina Head, OR through 2023. Data courtesy of R. Orben, Oregon State University. Lines, colors, and symbols are as in Fig. 2.1.

In the Central CCE, productivity of several seabird species is monitored on Southeast Farallon Island, located 48 km west of San Francisco Bay. In 2023, productivity was generally good, as four of the five indicator species had above average fledgling production (see Fig. 3.15 in the main report). Brandt's cormorants had above average chick production, while pigeon guillemots had below average chick production. For Cassin's auklets, rhinoceros auklets, and common murres, chick production was close to time series averages, with all three species showing a significant positive trend since low chick production values in 2019.

Also in the Central CCE, productivity of several seabird species is monitored on Año Nuevo Island, located southeast of the Farallon Islands between San Francisco and Santa Cruz, CA. In 2023, chick production was mixed at this location (Fig. N.3). Brandt's cormorant productivity was above average, while rhinoceros auklets experienced below-average productivity; contrasting productivity for these two species has persisted at this location for the last five years. Brandt's cormorant numbers breeding on Año Nuevo have increased dramatically in recent years (Devincenzi et al. 2023); this is likely related to the recent local dominance of northern anchovy, an essential prey species that is correlated with surges in Brandt's cormorant population (Ainley et al. 2018).

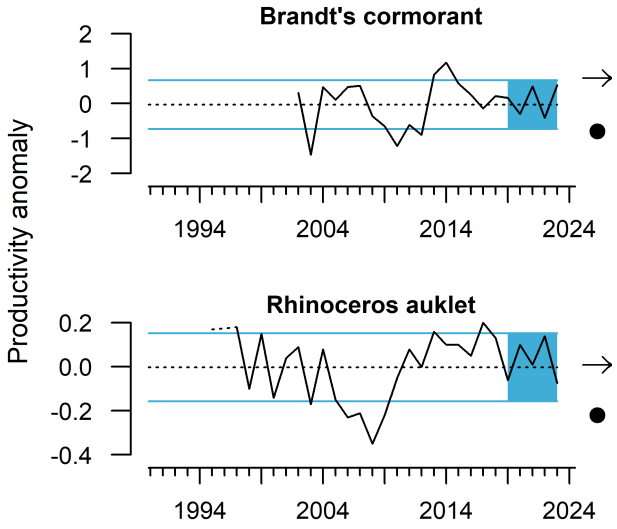

Figure N.3: Standardized productivity anomalies for two seabird species breeding at Año Nuevo Island, CA through 2023. Data courtesy of Oikonos. Lines, colors, and symbols are as in Fig. 2.1.

N.2 Seabird Diet

Seabird diet composition during the breeding season often tracks marine environmental conditions and reflects production and availability of forage within regions. Here, we present seabird diet data from the Northern and Central CCE that may shed light on forage conditions in 2023.

In the Northern CCE, rhinoceros auklet chick diet data are collected at Destruction Island, WA. Northern anchovy were nearly absent from diet samples in 2023, as they have been since 2018, and the anchovy proportion of the diet over the past five years was significantly lower than the long-term mean (Fig. N.4). This is consistent with forage and Coastal Pelagic Species (CPS) surveys that show the bulk of the current anchovy population to be in the Central and Southern CCE (Section 3.2, and Appendices H and I). The proportion of Pacific herring in the rhinoceros auklet diet was close to average in 2023, while the proportion of Pacific sandlance was above average and significantly greater in the last five years than the long-term mean (Fig. N.4). The proportion of smelts in the rhinoceros auklet diet in 2023 was well above average (more than 50%) and was significantly greater in the last five years than the long-term mean (Fig. N.4). While rockfish juveniles formed a relatively small part (9%) of the rhinoceros auklet chick diet in 2023, rockfish proportion of the diet was above average and has increased significantly over the last five years (Fig. N.4).

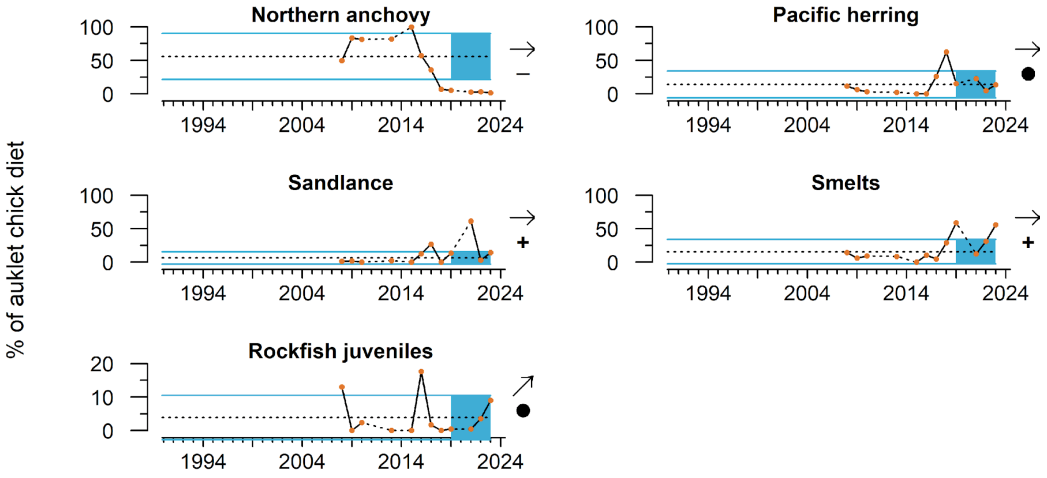

Figure N.4: Percentages of key prey items delivered to Rhinoceros auklet chicks at Destruction Island, WA through 2023. Data courtesy of S. Pearson, WDFW. Lines, colors, and symbols are as in Fig. 2.1.

Also in the Northern CCE, common murre chick diet data are collected at Yaquina Head, OR. While smelts have dominated the diet of common murre chicks at Yaquina Head since 2010, the proportion of smelts, herring and sardines, and Pacific sandlance was around average in 2023 (Fig. N.5). Flatfishes dropped out of the common murre chick diet in 2023 for the second year in a row and showed a significant negative trend over the last five years. The proportion of rockfish juveniles in the common murre chick diet was above average in 2023 and showed a significant positive trend over the last five years. The proportion of Pacific salmon juveniles in the diet was near average in 2023, and the recent 5-year mean is significantly greater than the long-term mean due to anomalously high consumption in 2021.

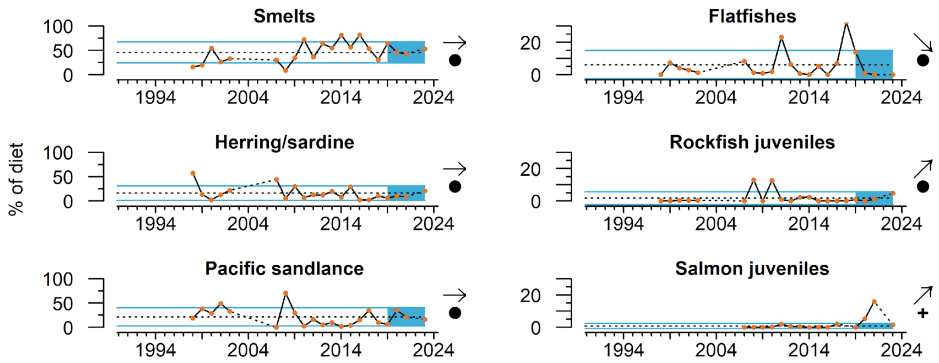

Figure N.5: Percentages of key prey items delivered to common murre chick diets at Yaquina Head, OR through 2023. Data courtesy of R. Orben, Oregon State University. Lines, colors, and symbols are as in Fig. 2.1.

In the Central CCE, diet data have been collected for seabirds at breeding colonies on Southeast Farallon Island for more than 30 years. These colonies are close to the most intense upwelling region in the California Current and are thus a valuable source of information about system productivity and prey availability to higher trophic levels. In 2023, most piscivorous birds at this colony continued to rely on northern anchovy. For Brandt's cormorants, the proportion of northern anchovy in their diet was average in 2023; despite a drop from the last few years, the mean of the last five years was significantly greater than the long-term mean (Fig. N.6). By contrast, the proportion of rockfish juveniles in their diet was well above average in 2023 and showed a significant positive trend over the last five years (Fig. N.6). These patterns are consistent with catches of adult anchovy and YOY rockfish in forage sampling off central California over the same time period (see Fig. H.2).

For rhinoceros auklet chicks, the proportion of northern anchovy in their diet was well above average in 2023, and the recent average was significantly greater than the long-term mean. The proportion of rockfish juveniles in their diet was below average (Fig. N.6). Similar trends were observed for anchovy/sardine and rockfish in common murre chick diets (Fig. N.6). While low relative to other prey, the proportion of Pacific salmon in common murre chick diets in 2023 was nearly triple the average value and showed a significant positive trend over the last five years (Fig. N.6). For Cassin's auklets, which feed primarily on zooplankton, the proportion of the two focal krill species *Euphausia pacifica* and *Thysanoessa spinifera* were below average in 2023 (Fig. N.6), and the bulk of their remaining diet was made up of other krill species. Not all Cassin's auklet diet samples from 2023 have been processed, however, so values could change. High prevalence of *T. spinifera* in the Cassin's auklet chick diet, as was observed in 2020 and 2021, is linked to increased late-winter upwelling and decreased habitat compression, which enhances productivity in the species' cooler nearshore coastal habitats.

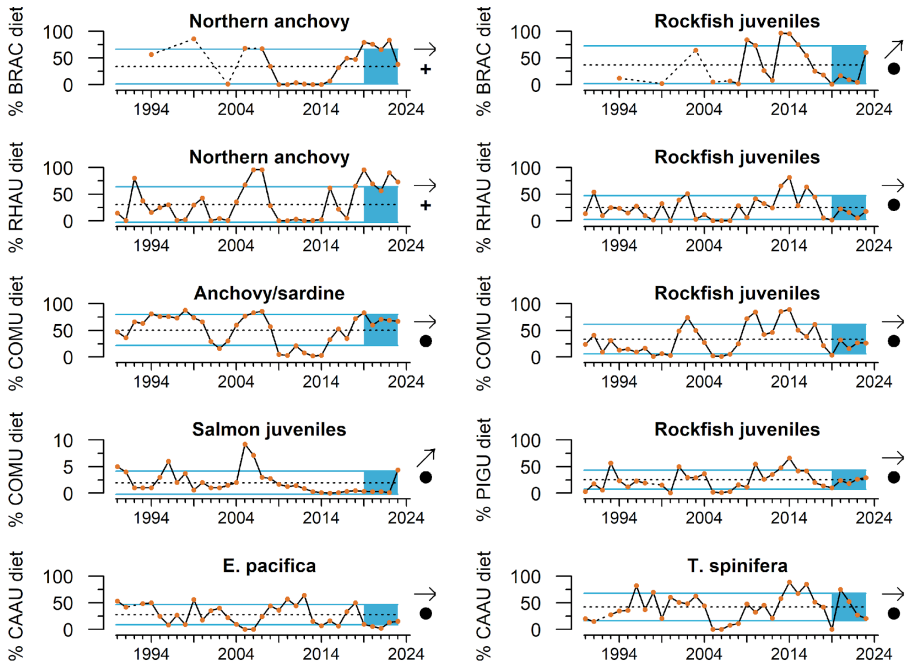

Figure N.6: Percentages of key prey items delivered to seabird chicks at Southeast Farallon Island, CA through 2023. BRAC = Brandt's cormorant; RHAU = rhinoceros auklet; COMU = common murre; PIGU = pigeon guillemot; CAAU = Cassin's auklet. Data provided by J. Jahncke, Point Blue Conservation Science. Lines, colors, and symbols are as in Fig. 2.1.

Also in the Central CCE, long-term diet data have been collected for rhinoceros auklets breeding on Año Nuevo Island, CA. For rhinoceros auklet chicks, the proportion of northern anchovy in their diet in 2023 continued a recent string of mostly above-average years, while the proportion of juvenile rockfish in their diet was below average in 2023 and continued a string of below-average years (Fig. N.7). The proportion of market squid in their diet in 2023 was around average, while the proportion of Pacific salmon in their diet in 2023 was at a 20-year high (11%), surpassed only by the highest value (24%) observed in 2003 (Fig. N.7).

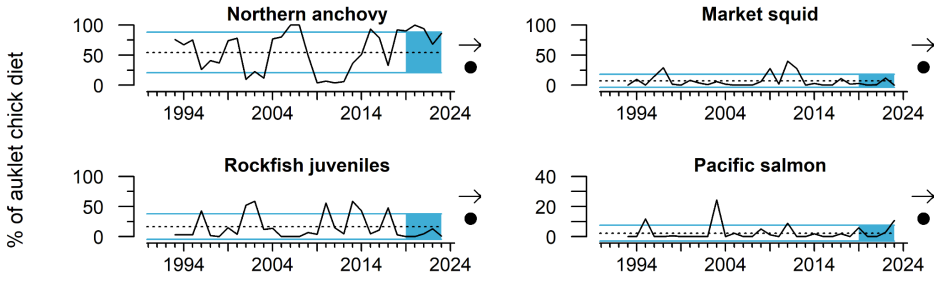

Figure N.7: Percentages of key prey items delivered to rhinoceros auklet chicks at Año Nuevo Island, CA through 2023. Data provided by Oikonos/Point Blue Conservation Science. Lines, colors, and symbols are as in Fig. 2.1.

The length of anchovy provided to rhinoceros auklet chicks at Año Nuevo Island was around average in 2023 (Fig. N.8), rebounding from a significant negative recent trend through 2022. In recent years, researchers have expressed concern that anchovy, while abundant, may have been too large to be ingested by rhinoceros auklet and other colonial seabird chicks. Fledgling production for rhinoceros auklets at this colony was below average in 2023, in contrast to the above average production in 2022 when anchovy were below average in size (see Fig. N.3).

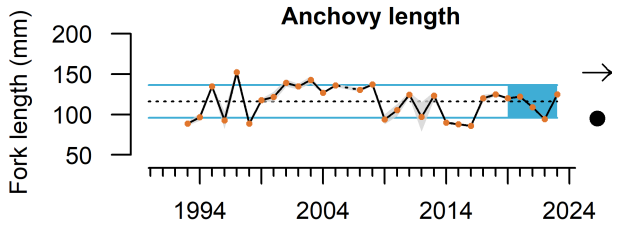

Figure N.8: Fork length of anchovy brought to rhinoceros auklet chicks at Año Nuevo Island from 1993-2023. Data provided by Oikonos/Point Blue Conservation Science. Lines, colors, and symbols are as in Fig. 2.1.

N.3 Seabird At-Sea Density

Seabird densities on the water during the breeding season can track marine environmental conditions and may reflect regional production and availability of forage. Data from this indicator type can establish habitat use and may be used to detect and track seabird population movements or increases/declines as they relate to ecosystem change. We monitor and report on at-sea densities of three focal seabird species in the Northern, Central, and Southern CCE.

Sooty shearwaters migrate to the CCE from the Southern Hemisphere in spring and summer to forage on the shelf and near the shelf break on small fish, including northern anchovy, as well as squid and zooplankton. Common murres and Cassin's auklets are resident species in the CCE that feed primarily over the shelf (Table N.1). Common murres target a variety of pelagic fish, while Cassin's auklets prey mainly on zooplankton and small fish.

At-sea density patterns varied among CCE regions and focal species in 2023. In the Northern CCE, the sooty shearwater density anomaly for 2023 was the lowest of the time series for the second year running (Fig. N.9, top row). The recent average was significantly lower than the long-term mean, and there was a significant negative trend over the last five years. Peak densities of sooty shearwaters in 2023 were again found in their usual location north of the Columbia River; in 2022, sightings were confined to the survey's southernmost transect off Newport, OR (44.7°N). The Cassin's auklet density anomaly for 2023 was the highest recorded in the time series; the recent average was significantly greater than the long-term mean, and there was a significant positive trend over the last five years (Fig N.9, top row). Peak densities in 2023 were seen near known breeding colonies within 30 km of La Push, WA (47.5°N) and on the Queets River, WA survey lines (47.9°N). Cassin's auklet were present on less than half of survey transects early in the time series (2003-2010) but

present on almost all transects in recent years (2018-2023), indicating an increase in habitat occupancy. The common murre density anomaly in 2023 was almost 1 s.d. below average (Fig. N.9, top row). Peak densities of common murres in 2023 were in typical locations offshore of large breeding colonies south of the Columbia River, as opposed to being distributed farther to the north as they were in 2022. No data were collected during 2020 and 2021 due to COVID-19 restrictions on at-sea surveys, so recent trends should be interpreted with caution.

In the Central CCE, the sooty shearwater density anomaly for 2023 was the highest of the time series for the third year running (Fig. N.9, middle row). The mean over the last five years was significantly greater than the long-term mean, and there was a significant positive trend over the last five years. It is notable that sooty shearwater density anomaly metrics in the Central CCE (record high, greater recent mean, positive recent trend) mirror those in the Northern CCE (record low, lower recent mean, negative recent trend). The Cassin's auklet density anomaly was below average in 2023 and has been since 2014 (Fig. N.9, middle row). While this pattern does reflect Cassin's auklet status at Southeast Farallon Island, where the population appears to be low but stable, recent negative anomalies do not match the increasing trend in krill abundance in the central CCE (Fig. H.2) but do align with lower krill abundances observed in the north and south in 2023 (Fig. H3). Krill densities in the central CCE do match the increase in humpback whales, an abundant year-round krill consumer whose abundance increased during the 2010s, with exponential growth (~8%) over the past couple of decades (Calambokidis and Barlow 2020). Thus, Cassin's auklets may be competing for krill resources with a "recovered competitor." The common murre density anomaly in 2023 dropped from above average values from 2019 to 2022, but the mean over the last five years was still significantly greater than the long-term mean (Fig. N.9, middle row). No data were collected during 2020 due to COVID-19 restrictions. Surveys were truncated in 2023 due to staffing issues; this resulted in lower than normal effort and relatively high overall densities (potentially from undersampling low-density areas), so recent trends should be interpreted with caution.

In the Southern CCE, the sooty shearwater density anomaly was average in 2023, down in recent years from relatively large, positive values from 2013-2016 and in 2018 (Fig. N.9, bottom row). Cassin's auklet density anomalies were average in 2023 and have been consistently low throughout the time series except for peaks in 1990 and 2005 (Fig. N.9, bottom row). Common murre density anomalies mostly have been small and negative, except for large and positive values from 2015-2018 (Fig. N.9, bottom row). No data were collected during 2020 and 2021 due to COVID-19 restrictions.

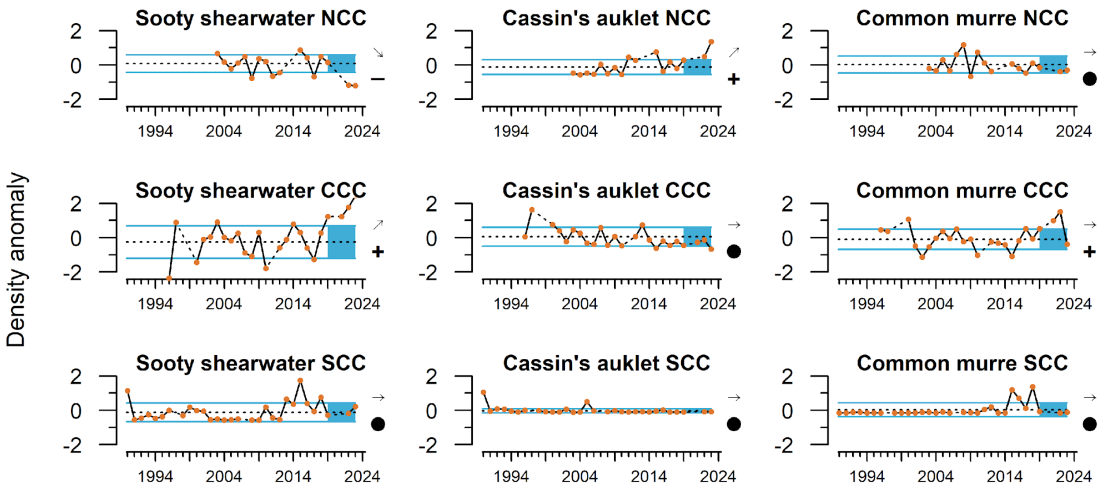

Figure N.9: Anomalies in the summer at-sea densities of sooty shearwaters, Cassin's auklets and common murres in the Northern, Central, and Southern CCE. Data are shipboard counts, transformed as ln(bird density/km² +1) and expressed as an anomaly relative to the long-term mean. Seabird abundance data from the Northern CCE were collected and provided by Dr. Jeannette Zamon (NOAA). Seabird abundance data from the Central and Southern CCE are collected on SWFSC RREAS and CalCOFI surveys, respectively, and are provided by W. Sydeman. Lines, colors, and symbols are as in Fig. 2.1.

N.4 Seabird Mortality

Monitoring of dead beached birds provides information on the health of seabird populations, ecosystem health, and unusual mortality events, and previous ESRs from the anomalously warm and unproductive years of 2014–2016 noted major seabird mortality events in each year. In 2023, no unusual mortality events were reported for the focal species by the beach monitoring programs. In the Northern CCE, the Coastal Observation And Seabird Survey Team (COASST) at the University of Washington monitors beaches in Washington, Oregon, and northern California. In 2023, COASST documented average encounter rates of beachcast Cassin's auklets, northern fulmars, and sooty shearwaters (Fig. N.10). The common murre encounter rate was above average in 2023, although 64% of common murre carcasses were juveniles, which is above the range (15-40%) that COASST typically documents. Years where a high percentage of beachcast common murres are juveniles are often correlated with years of good colony productivity. The recent positive trend in common murre encounter rate is driven by the 2023 data.

While no unusual mortality events were reported for the focal indicator species, COASST documented an above average number of Caspian tern carcasses were encountered from June to August 2023 on beaches immediately adjacent to the mouth of the Columbia River. Another 350 Caspian tern carcasses were independently reported from throughout the Columbia River estuary (J. Lawonn, OR; Oregon Department of Fish & Wildlife). These encounters likely resulted from an outbreak of highly-pathogenic H5N1 avian flu (HPAI) that was documented at the East Sand Island colony in the Columbia River estuary. In 2023,

avian flu also decimated a Caspian tern colony located in Puget Sound, killing 56% of the almost 2,000 birds nesting there; between these two locations, an estimated 10-14% of the Pacific Flyway Caspian tern population may have died (S. Pearson, WA Dept. Fish & Wildlife). As has occurred in South America, HPAI avian flu also spread to harbor seals, some of which stranded on nearby Marrowstone Island in the first highly-pathogenic avian flu detection in marine mammals along the U.S. West Coast.

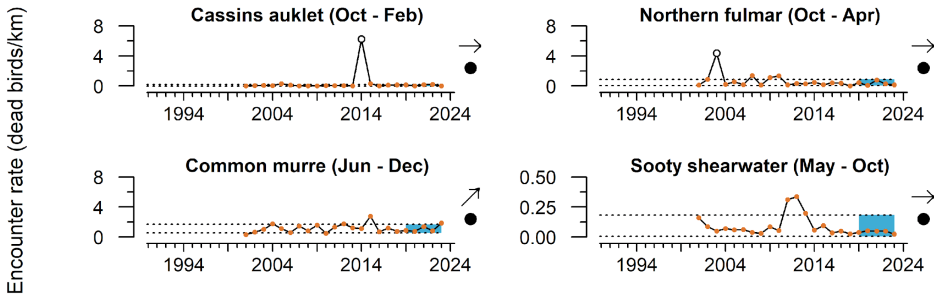

Figure N.10: Encounter rates of dead beachcast birds in Washington, Oregon and northern California. The mean and trend of the last five years (blue shaded area) are evaluated relative to the mean and s.d. (dotted lines) of the full time series with the outliers (open circles) removed. Outliers were identified as encounter rates > 5 times the average of all other years. Data provided by the Coastal Observation and Seabird Survey Team (https://depts.washington.edu/coasst/). Symbols at right are as in Fig. 2.1.

In the Central CCE, the Beach Watch program monitors beaches from Point Arena to Point Año Nuevo, California. In 2023, Beach Watch documented average encounter rates for Brandt's cormorants (Fig. N.11). For Cassin's auklets, the most recent data (which includes data from October 2022 through February 2023) documented a number of large but isolated wrecks; almost 70 birds came from one January 2023 survey at the northernmost beach (Manchester Beach). During the previous five years, there was a significantly negative trend in Cassin's auklet encounter rates (2022 was an outlier, so it is excluded from calculations). For common murres, encounter rates were average in 2023; rates were relatively low during the typical post breeding season uptick (July- September) but higher than usual and climbing through October and November (December data are not processed yet). For northern fulmars, the most recent encounter rate (which includes data from October 2022 through April 2023) was above average and shows a significantly positive trend over the last five years. For sooty shearwaters, the 2023 encounter rate was average but still shows a significant negative trend over the last five years.

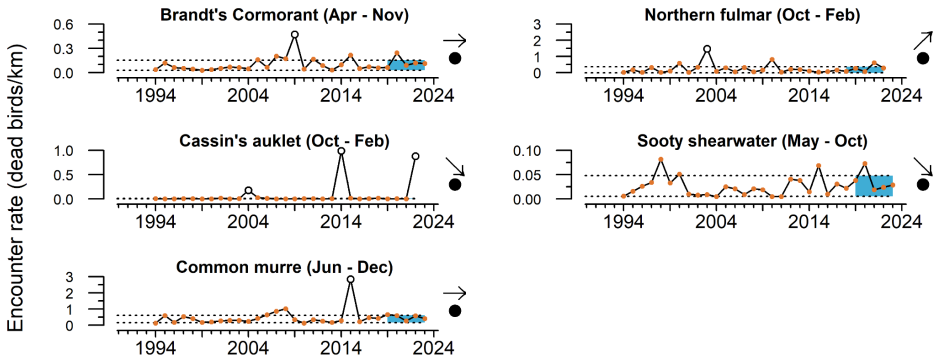

Figure N.11: Encounter rate of dead beachcast birds in north-central California through 2023. The mean and trend of the last five years (shaded blue area) are evaluated relative to the mean and s.d. (dotted lines) of the full time series with the outliers (open circles) removed. Outliers were identified as encounter rates > 5 times the average of all other years. Data provided by Beach Watch (https://farallones.noaa.gov/science/beachwatch.html). Symbols at right are as in Fig. 2.1.

Appendix O: HARMFUL ALGAL BLOOMS

Link to main section: Harmful Algal Blooms

Harmful algal blooms (HABs) of diatoms in the genus *Pseudo-nitzschia* have been a recurring concern along the West Coast. Certain species of *Pseudo-nitzschia* produce the toxin domoic acid, which can accumulate in filter feeders and extend through food webs to cause harmful or lethal effects on people, marine mammals, and seabirds (Lefebvre et al. 2002; McCabe et al. 2016). Because domoic acid can cause amnesic shellfish poisoning in humans, fisheries that target shellfish (including razor clam, Dungeness crab, rock crab, and spiny lobster) are delayed, closed, or operate under special orders or health advisories when domoic acid concentrations exceed regulatory thresholds for human consumption. Fishery closures can cost tens of millions of dollars in lost revenue, and cause a range of sociocultural impacts in fishing communities (Dyson and Huppert 2010; Ritzman et al. 2018; Holland and Leonard 2020; Moore et al. 2020), including a "spillover" of fishing effort into other fisheries.

Ocean conditions associated with marine heatwaves, El Niño events, or positive PDO regimes may further exacerbate domoic acid toxicity and fishery impacts, and domoic acid toxicity tracks anomalies of southern copepod biomass (Fig. 3.1) (McCabe et al. 2016; McKibben et al. 2017). The largest and most toxic HAB of *Pseudo-nitzschia* on the West Coast occurred in 2015, coincident with the 2013-2016 marine heatwave, and caused the longest-lasting and most widespread HAB-related fisheries closures on record (McCabe et al. 2016; Moore et al. 2019; Trainer et al. 2020). Closures and delays in the opening of West Coast crab fisheries resulted in the appropriation of >$25M in federal disaster relief funds (McCabe et al. 2016).

According to thresholds set by the U.S. Food and Drug Administration, domoic acid levels ≥20 parts per million (ppm) trigger actions for all seafood and tissues except Dungeness crab viscera, for which the level is >30 ppm (California applies this to rock crab viscera as well) (FDA 2011). Under evisceration orders, Dungeness crab can be landed when the viscera exceeds the threshold but the meat does not, provided that crab are eviscerated by a licensed processor. Oregon was the first West Coast state to pass legislation allowing evisceration, in November 2017, followed by California in October 2021. Washington adopted an emergency evisceration rule in February 2021, and is considering legislation to grant long-term authority for issuing evisceration orders.

A summary of management actions in the Dungeness crab fishery in response to domoic acid and other issues, such as poor body condition and marine life entanglement risk, is shown in Figure O.1. Since the massive 2015-16 domoic acid event, the majority of management actions impacting the fishery in California were related to marine life entanglement risk; in contrast, domoic acid contamination requiring evisceration or delay of the opening of the season as well as poor body condition has mostly impacted the fishery in Oregon and Washington. To date, evisceration orders have primarily been used in Oregon and usually midseason. In general, there has been a preference to delay the season opener rather than open under an evisceration order when domoic acid levels have been

high at the start of the season (although the fishery did open under an emergency evisceration order in southern Washington in 2021).

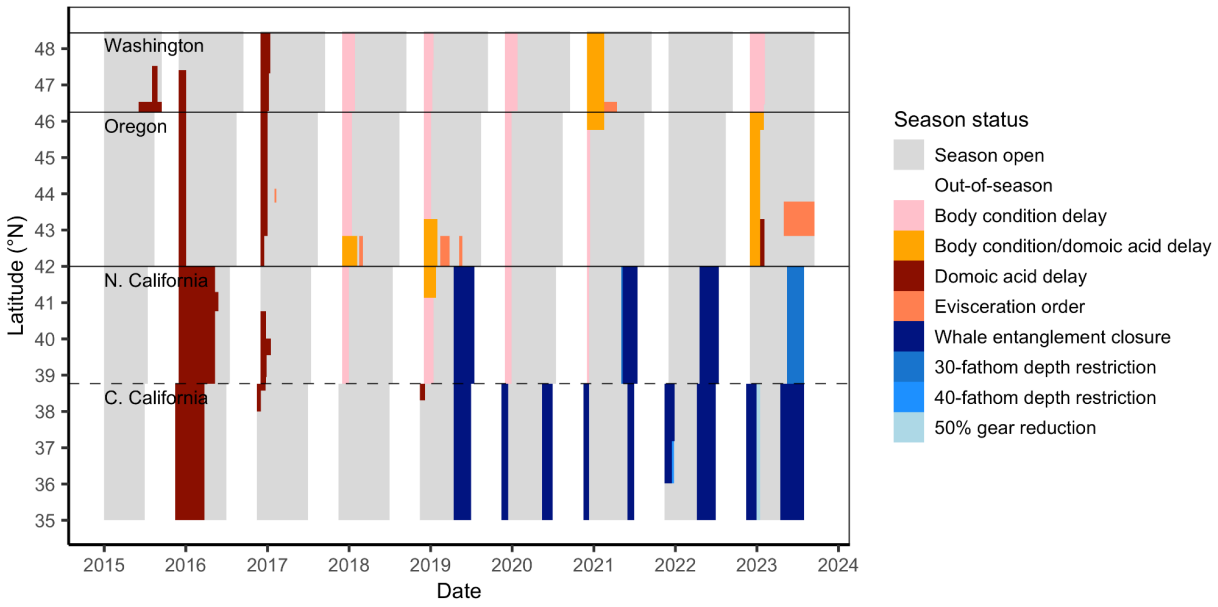

Figure O.1: The spatial-temporal history of closures and management restrictions in the U.S. West Coast Dungeness crab fishery from 2015 to 2023, both HAB and non-HAB related. Solid black lines indicate state borders and the dashed line indicates the border between the Northern and Central California management zones. Gray shading indicates the commercial Dungeness crab fishing season in each region. Figure adapted from Free et al. (2022) using news releases from the California, Oregon, and Washington Departments of Fish and Wildlife.

O.1 Domoic Acid in Washington

High domoic acid levels resulted in closures of the state and tribal razor clam fisheries in Washington State starting in the fall of 2022 that extended into 2023 (Fig. O.2). Limited tribal and recreational razor clam harvests resumed in February, 2023 on select northern beaches (Kalaloch, Copalis, and Point Grenville). The recreational razor clam fishery was opened coast-wide on March 23, 2023 with the commercial fishery on Willapa Spits proceeding on April 1. *Pseudo-nitzschia spp.* levels remained relatively low in the spring of 2023 until the development of a toxic bloom in late July that delayed the fall opening of beaches for razor clam harvesting coastwide. Long Beach, Twin Harbors, and Copalis opened in late September, however, Mocrocks and Quinault beaches did not open until late October due to persistent elevated levels of domoic acid in razor clams harvest. Low levels of domoic acid that do not meet the action level continue to be observed in Washington razor clams and, less frequently, in Dungeness crab. The Washington commercial Dungeness crab fishery opening was delayed until at least January 1, 2024 per the Tri-State protocols due to low meat yields.

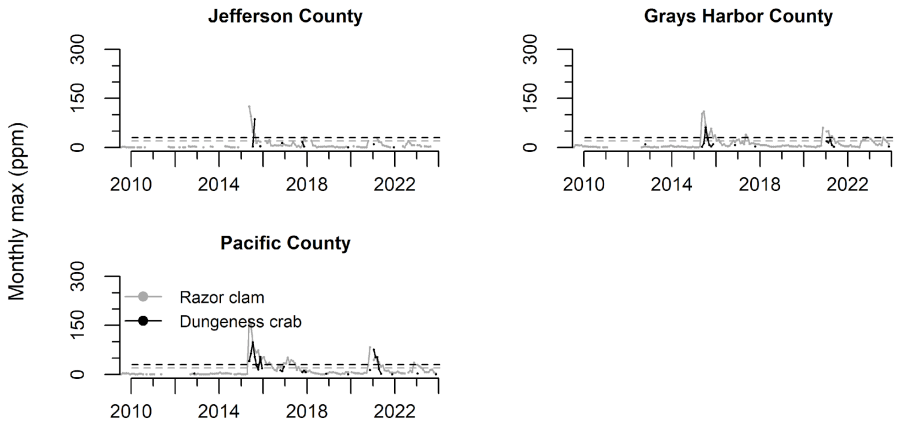

Figure O.2: Monthly maximum domoic acid concentration in razor clams and Dungeness crab viscera through 2023 by coastal counties in Washington (north to south). Horizontal dashed lines are the management thresholds of 20 ppm (clams, gray) and 30 ppm (crab viscera, black). Data compiled by the Washington Department of Health, from samples collected and analyzed by a variety of local, tribal, and state partners.

O.2 Domoic Acid in Oregon

Domoic acid exceedances resulted in multiple closures of Oregon shellfish fisheries in 2023. At the beginning of 2023, domoic acid levels were still elevated in shellfish along the entire Oregon coast in response to a particularly toxic bloom of *Pseudo-nitzschia* spp. in the fall of 2022 (Fig. O.3). In addition, lengthy exceedances of domoic acid in shellfish were again observed in southern Oregon, the result of a continued pattern of persistent toxic blooms of *Pseudo-nitzschia* spp. associated with a northern California "hot spot" that emerged in 2015 (Trainer et al. 2020). Thus, the razor clam fishery was closed along the entire Oregon coast until levels depurated below the closure threshold to allow an opening on the northern coast on May 6, 2023. Another section in the central portion of the coast, from Seal Rock State Park to the Siuslaw River opened to razor clam harvesting on August 4, 2023.

Beginning August 4, 2023, the northern Oregon coast experienced another *Pseudo-nitzschia* spp. bloom that produced enough domoic acid to close razor clam harvesting from Seal Rock State Park to the OR/WA border (Fig. O.3). While this closure was occurring, the southern coast razor clam fishery, from Cape Blanco to the OR/CA border, opened as domoic acid levels fell well below the closure threshold. On October 4, 2023, the northern coast of Oregon opened to razor clam fishery as levels of domoic acid decreased below the closure threshold. Abundances of toxic *Pseudo-nitzschia* spp. in nearshore waters increased in mid to late October on the southern Oregon coast, and by the beginning of November domoic acid accumulation was seen in shellfish and the razor clam fishery from Cape Blanco to the OR/CA border closed.

The opening of the commercial crab fishery was delayed until February 4, 2023 in the southern portion of the state from Cape Arago to the OR/CA border due to elevated domoic acid in crab viscera (Fig. O.3). There were two smaller area in-season evisceration requirements that went into effect due to elevated domoic acid in crab viscera. They included Charleston to Bandon from January 19 to February 1, 2023 and from just north of Winchester Bay to Cape Blanco from April 27 through May 10, 2023.

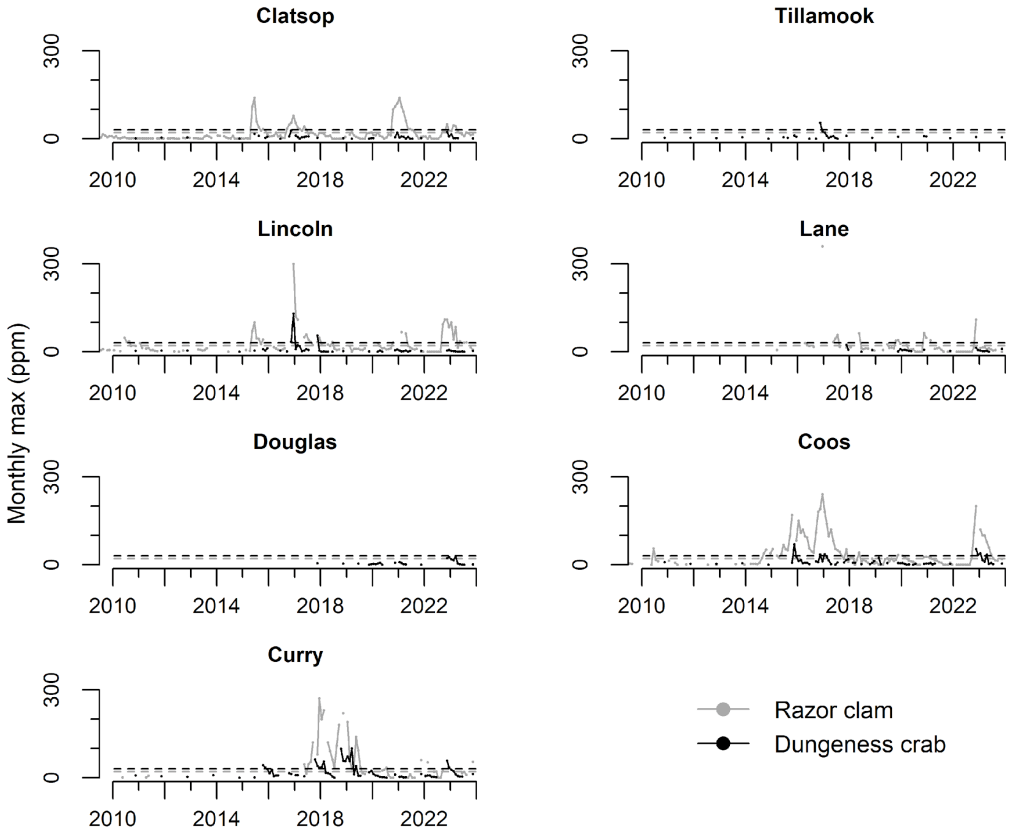

Figure O.3: Monthly maximum domoic acid concentration in razor clams and Dungeness crab viscera through 2023 by coastal counties in Oregon (north to south). Horizontal dashed lines are the management thresholds of 20 ppm (clams, gray) and 30 ppm (crab viscera, black). Razor clam tissue sampling is conducted twice monthly from multiple sites across the Oregon coast. Data compiled and reported by Oregon Department of Fish and Wildlife from analyses conducted by the Oregon Department of Agriculture.

O.3 Domoic Acid in California

Similar to 2022, domoic acid continued to be problematic for the recreational razor clam fishery in northern California. The razor clam fishery closure in Del Norte County was issued on November 3, 2022 and lasted until July 6, 2023 (Fig. O.4). The fishery closed again on November 9, 2023, due to elevated levels of domoic acid. The razor clam fishery in Humboldt County closed on April 21, 2023 and the area opened on August 7, 2023.

A "red tide" of *Tripos* and *Prorocentrum* spp. in southern California in April 2023 garnered a lot of public attention due to prolonged discoloration of the water and bioluminescence at night. This was followed by a major domoic acid event in central and southern California that developed towards the end of May and lasted about 3 months. The *Pseudo-nitzschia* spp. bloom, which seemed largely offshore in nature, resulted in the strandings of >1,000 California sea lions and seal species and >100 long-beaked common dolphins. A domoic acid-related health advisory against the consumption of sport-harvested bivalve shellfish from Santa Barbara County was instituted on June 16 through August 3, 2023.

Because domoic acid can persist in sediments and benthic food webs, this event resulted in a domoic acid delay to the start of some recreational and commercial spiny lobster fisheries off the mainland coast of Los Angeles County in late September through early October. The northern rock crab fishery remained closed in two areas due to domoic acid concerns (see CDFW 2023); these areas have not been open since November 2015. Even though only low levels of domoic acid (≤ 30 ppm) were detected in the viscera of Dungeness crab during the fall and winter of 2023, the 2023-24 commercial Dungeness crab fishery was delayed in California due to low meat yields in northern California and the presence of high numbers of whales, particularly humpbacks. This is the fifth consecutive year that the Dungeness crab fishery has been delayed in California because of insufficient meat quality and/or marine mammal entanglement risk concerns.

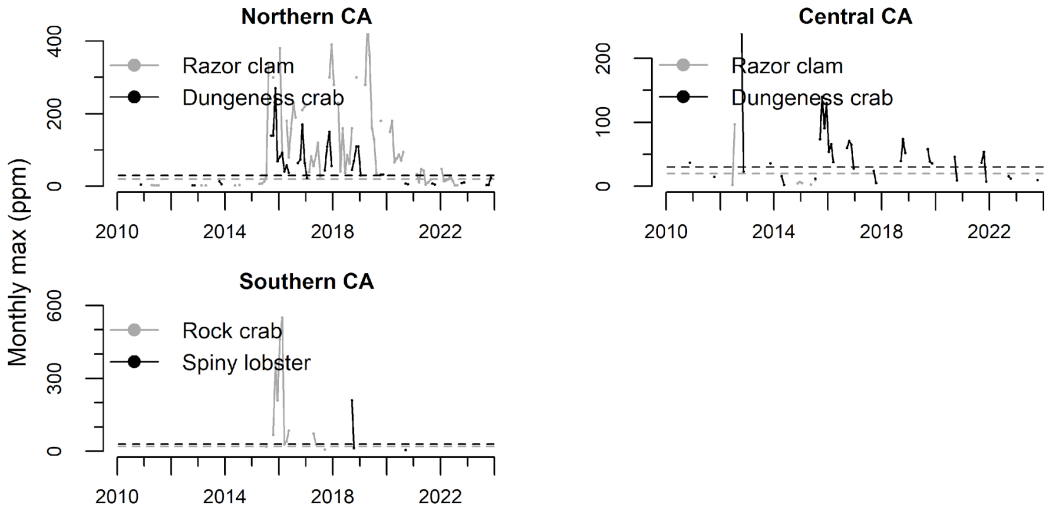

Figure 0.4: Monthly maximum domoic acid concentration in razor clams, Dungeness crab, rock crab, and spiny lobster through 0 - 3033in California (Northern CA: Del Norte to Mendocino counties; Central CA: Sonoma to San Luis Obispo counties; Southern CA: Santa Barbara to San Diego counties). Horizontal dashed lines are the management thresholds of 20 ppm (clams and lobsters, gray) and 30 ppm (crab viscera, black). Data compiled by the California Department of Public Health from samples collected by a variety of local, tribal, and state partners.

Appendix P: STATE-BY-STATE FISHERY LANDINGS AND REVENUES

Link to main section: Coastwide Landings and Revenue

The Council and EWG have requested information on state-by-state fisheries landings and revenues; these values are presented here. Commercial landings and revenue data are best summarized by the Pacific Fisheries Information Network (PacFIN; pacfin.psmfc.org), and recreational landings are best summarized by the Recreational Fisheries Information Network (RecFIN; www.recfin.org). Data from 1981 to 2023 were downloaded from PacFIN and RecFIN on January 16, 2024. Landings provide the best long-term indicator of fisheries removals. Revenues are calculated based on consumer price indices in 2023 dollars. Status and trends are estimated relative to a frame of reference of 1991-2020.

P.1 State-by-State Landings

Total fisheries landings in Washington decreased and were >1 s.d. below the long-term average from 2019 to 2023, with the lowest total landings in the time series observed in 2023 and a 14% decrease from 2022 (Fig. P.1). These patterns were driven primarily by a steep decrease in Pacific whiting landings over the last five years, including a 9% decrease in 2023 from 2022. Commercial crab was the only fishery in Washington with a significantly increasing 5-year trend. Commercial salmon landings remained >1 s.d. below the long-term average. All other major commercial fisheries showed no trends and were within 1 s.d. of the long-term average from 2019 to 2023.

Total recreational landings data (excluding salmon and halibut) in Washington were complete through October 2023 and were within long-term averages from 2019 to 2023 (Fig. P.1). Recreational landings during COVID-impacted years of 2020-2021 were near the lowest range of long-term averages, but have recovered in 2022-2023. This pattern is driven primarily by landings of albacore tuna. Recreational landings of Chinook and coho salmon were within 1 s.d. of the long-term average from 2018 to 2022 (2023 data were not available at time of report).

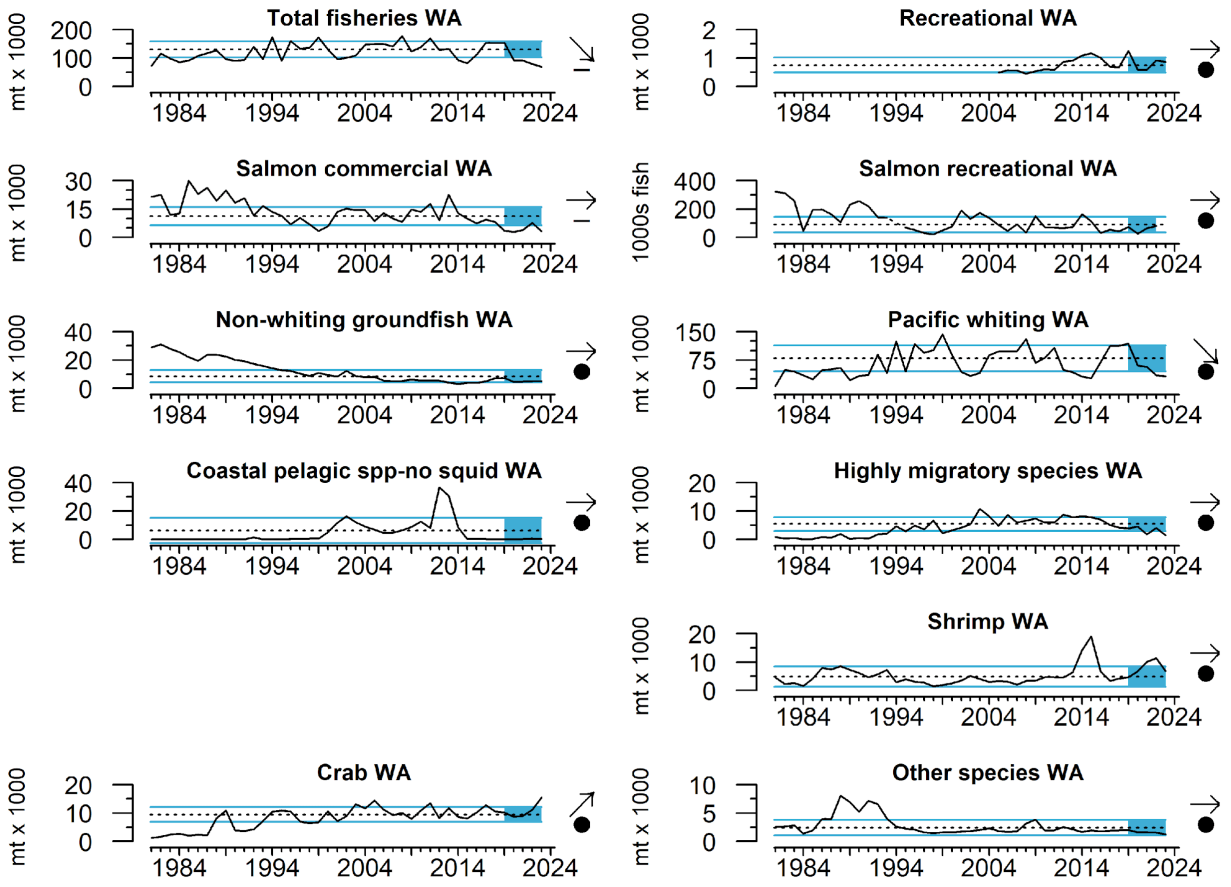

Figure P.1: Annual Washington landings from West Coast commercial (data from PacFIN) and recreational (data from RecFin) fisheries, including total landings across all fisheries from 1981 - 2023. Lines, colors, and symbols are as in Fig. 2.1. There are no landings of market squid in Washington State.

Total fisheries landings in Oregon were consistently >1 s.d. above the long-term average from 2019 to 2023, even with a 14% decrease from 2022 (Fig. P.2). Similar to Washington, these patterns were driven primarily by landings of Pacific whiting, which were also consistently >1 s.d. above the long-term average for the most recent five years. Commercial landings of crab increased by 84% from 2022 to 2023, leading to an overall increasing trend over the last five years. HMS landings were >1 s.d. below the long-term average from 2019-2023. Landings of market squid to Oregon ports were nearly zero in 2023 after relatively new and promising levels of landings from 2018-2022. Commercial landings of all other commercial fisheries showed no significant recent trends and had short-term averages within 1 s.d. of long-term averages.

Recreational fisheries landings data (excluding salmon and Pacific halibut) in Oregon were complete through November 2023 and have reached 1 s.d. above the long-term average (Fig. P.2). Similar to Washington, variation in landings of albacore have been primarily responsible for the overall trends in recreational landings in Oregon, with relatively consistent landings of black rockfish and lingcod over the last decade. Recreational

landings of Chinook and coho salmon showed no significant recent trend, and have been within 1 s.d. of the long-term average since 2018 (2023 data were not available at time of report).

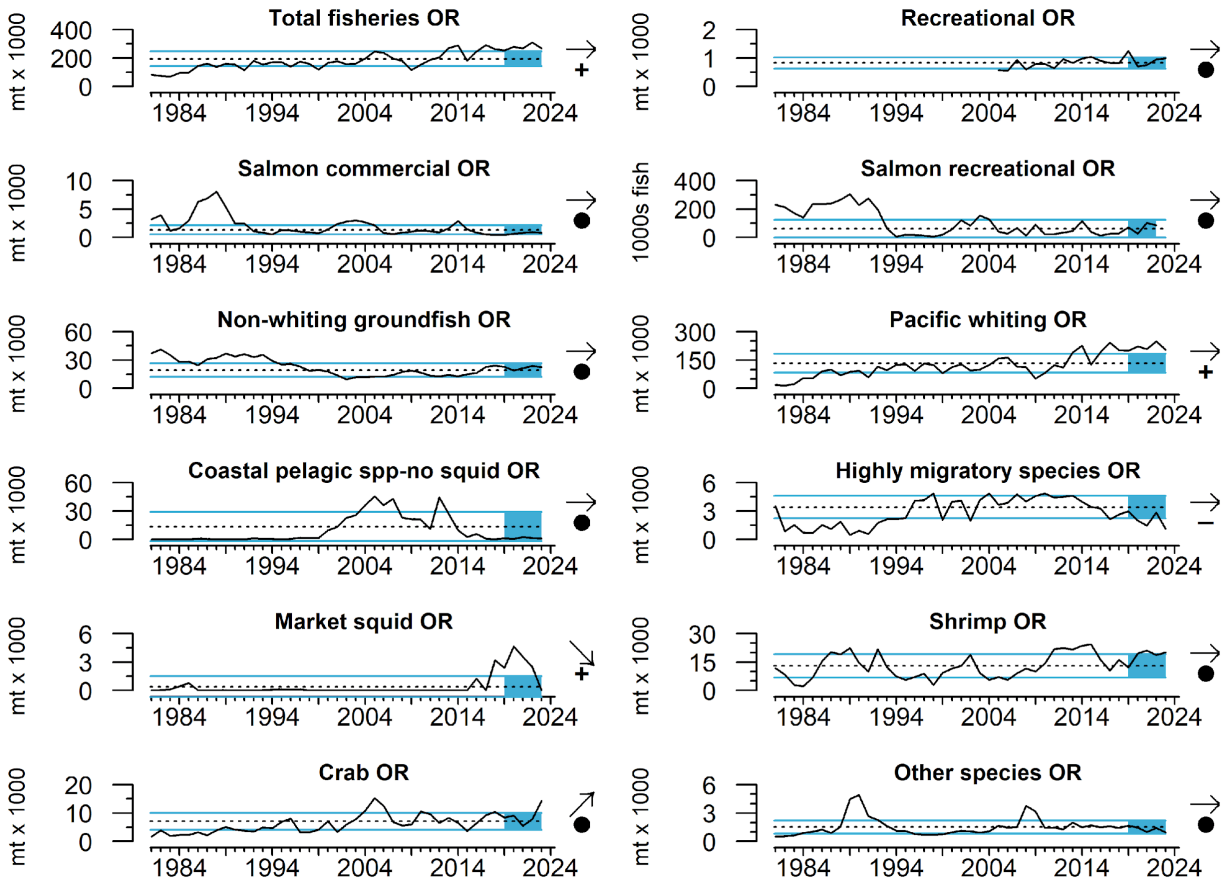

Figure P.2: Annual Oregon landings from West Coast commercial (data from PacFIN) and recreational (data from RecFin) fisheries, including total landings across all fisheries from 1981 - 2023. Lines, colors, and symbols are as in Fig. 2.1.

Total fisheries landings in California decreased 42% in 2023 and were >1 s.d. below the long-term average, primarily due to large decreases in market squid (-63%) and salmon (-99%; due to fishery closure) from 2022-2023 (Fig. P.3). Commercial landings of CPS finfish, shrimp and Other species were also >1 s.d. below the long-term average from 2019-2023. All other major fisheries showed no significant trends and were within 1 s.d. of long-term averages over the last five years, although crab landings have been increasing since 2021.

Recreational landings data (excluding salmon, Pacific halibut and HMS) in California were complete through October 2023. Recreational landings were >1 s.d. below the long-term average over the past five years (Fig. P.3). The decreasing trend was the result of interactions between relatively large decreases in landings of lingcod, vermilion rockfish and yellowtail, and relatively large increases in landings of California halibut and bocaccio over the last five years. These landings exclude HMS, whose recreational catch data were incomplete at the time of this writing. Recreational salmon landings in California were

within 1 s.d. of the long-term average over the last 5 years, and have increased slightly since COVID-impacted years of 2020 and 2021.

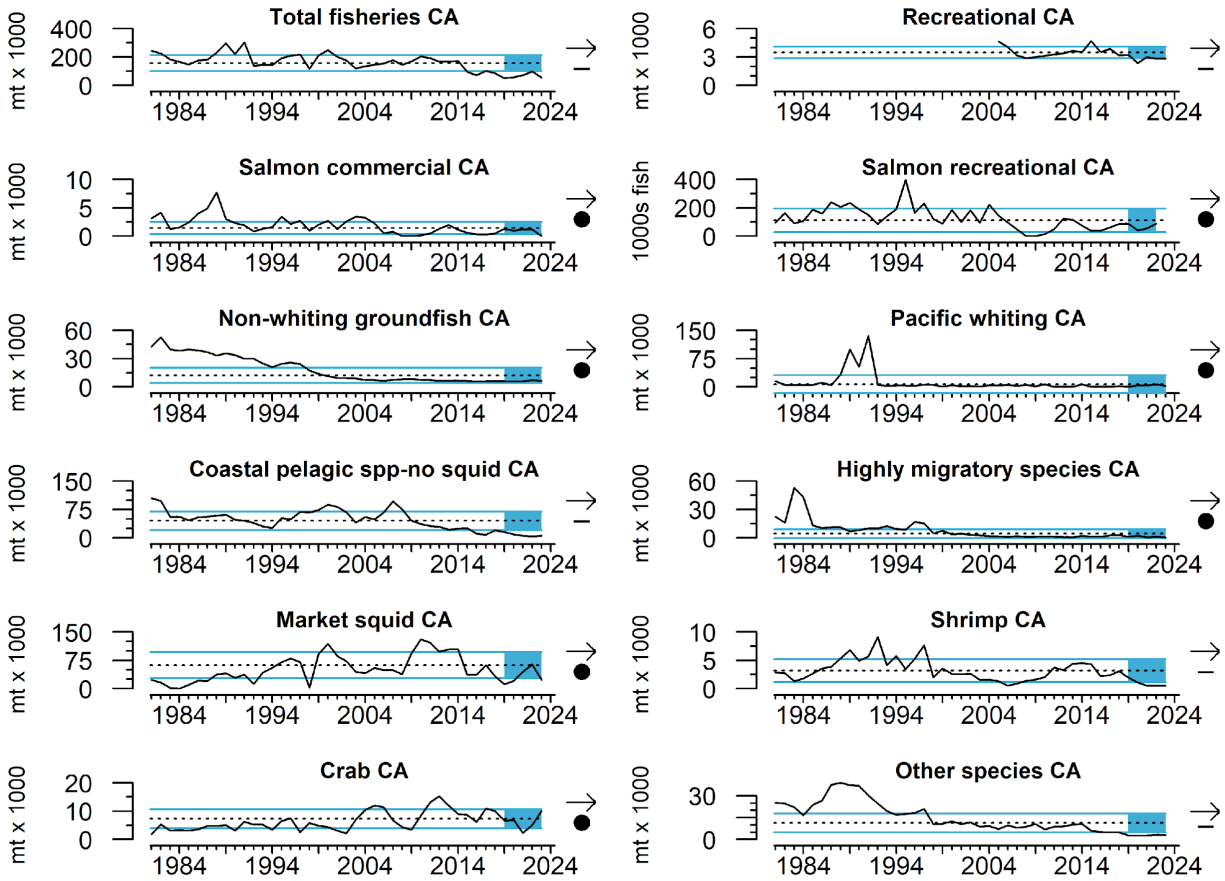

Figure P.3: Annual California landings from West Coast commercial (data from PacFIN) and recreational (data from RecFin) fisheries, including total landings across all fisheries from 1981 - 2023. Lines, colors, and symbols are as in Fig. 2.1.

P.2 Commercial Fisheries Revenue

Total revenue across U.S. West Coast commercial fisheries in 2023 decreased by 32% from 2022, based on data currently available (Fig. P.4). Over the most recent five years, total revenue was highly variable, but remained within 1 s.d. of the long-term average. This variation has been driven by revenue for market squid, crab and Pacific whiting fisheries over the last five years, with particularly higher revenue levels in 2022 followed by lower revenue in 2023 for these three fisheries. Revenue for all 9 commercial fisheries decreased from 2022 to 2023: HMS (-72%), market squid (-68%), salmon (-68%), Pacific whiting (-36%), CPS finfish (-29%), crab (-19%), shrimp (-19%), non-whiting groundfish (-18%), and Other species (-11%). Revenue from non-whiting groundfish, CPS finfish and HMS remain >1 s.d. below the long-term average over the last five years. In addition to below-average landings, HMS fisheries have been decreasing >1 s.d. from 2019-2023. All other fisheries' revenues showed no trends and were within 1 s.d. of long-term averages. Comparing landings (Fig. 4.1 in the main report) and revenue among fisheries reveals the importance

of variation in price-per-pound to the resiliency of particular fisheries and the communities they support: crab landings increased over the past five years, and increased significantly from 2022 to 2023, even as revenue remained relatively unchanged over the last five years and actually decreased from 2022 to 2023.

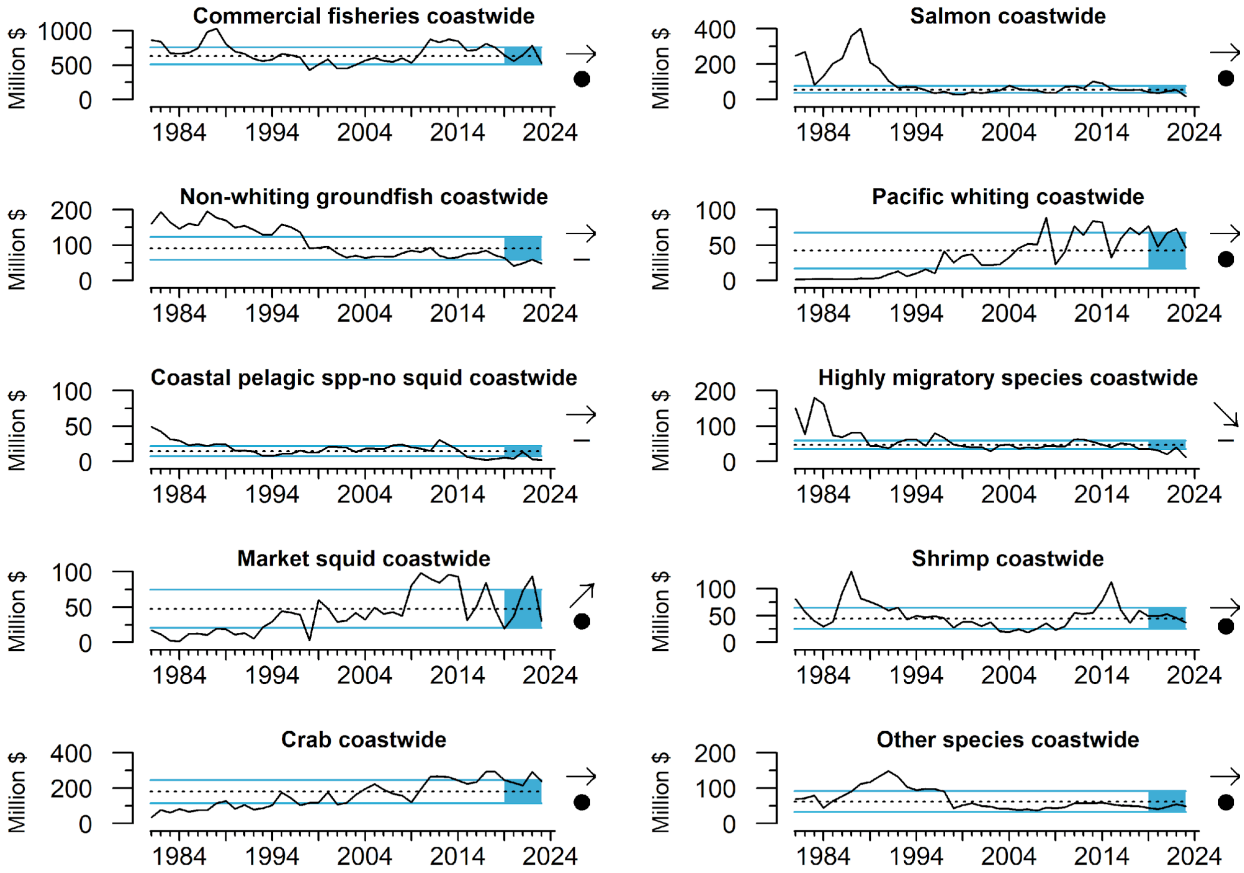

Figure P.4: Annual coastwide revenue (ex-vessel value in 2023 dollars) from West Coast commercial fisheries (data from PacFin) from 1981 - 2023. Whiting revenue includes shoreside and at-sea values from PacFIN, NORPAC (North Pacific Groundfish Observer Program) and NMFS Office of Science & Technology. Lines, colors, and symbols are as in Fig. 2.1.

Total revenue across commercial fisheries in Washington was highly variable from 2019 to 2023, with a 35% decrease in 2023 from 2022 levels (Fig. P.5). These patterns are largely driven by variability in revenue from crab landings, coupled with decreasing trends in Pacific whiting and HMS revenue over the last five years. Overall, all 8 major fisheries in Washington decreased in revenue in 2023 from 2022 levels: HMS (-81%), salmon (-57%), CPS finfish (-53%), shrimp (-39%), non-whiting groundfish (-34%), Other species (-33%), crab (-30%) and Pacific whiting (-22%). Crab fisheries' revenue was >1 s.d. above long-term averages while non-whiting groundfish and salmon revenue was >1 s.d. below long-term averages. All other fisheries showed no trends and were within long-term averages over the last five years.

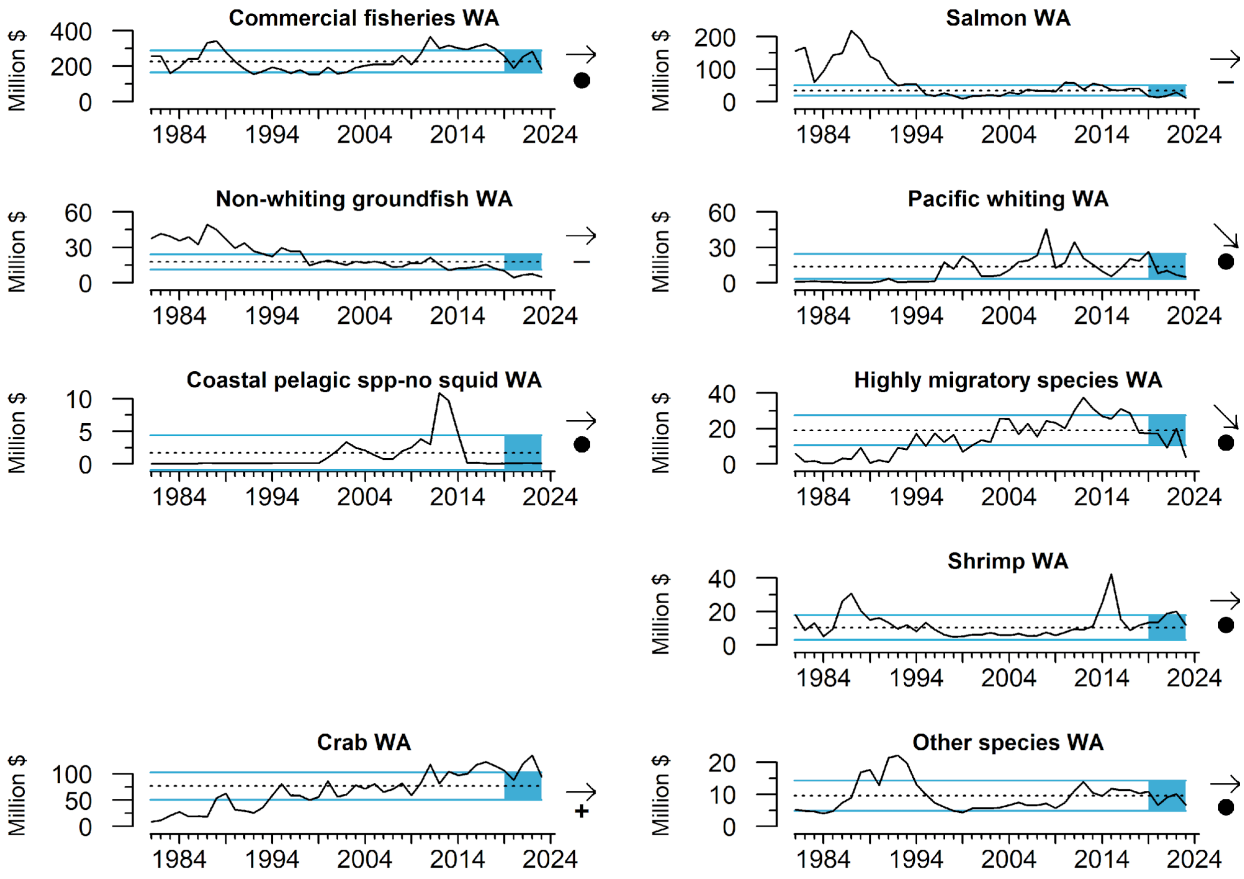

Figure P.5: Annual Washington revenue (ex-vessel value in 2023 dollars) from West Coast commercial fisheries (data from PacFin) from 1981 - 2023. Whiting revenue includes shoreside and at-sea values from PacFIN, NORPAC (North Pacific Groundfish Observer Program) and NMFS Office of Science & Technology. Lines, colors, and symbols are as in Fig. 2.1. There are no landings of market squid in Washington State.

Total revenue across commercial fisheries in Oregon was near 1 s.d. above the long-term average from 2019 to 2023, despite a 26% decrease in 2023 from 2022 levels (Fig. P.6). These patterns are largely driven by changes in revenue from crab and Pacific whiting fisheries over the last five years. Overall, all 9 major fisheries decreased in revenue in 2023 from 2022 levels: market squid (-100%), CPS finfish (-84%), HMS (-77%), Pacific whiting (-37%), salmon (-36%), Other species (-20%), non-whiting groundfish (-18%), crab (-13%) and shrimp (-6%). Revenue from landings of market squid into Oregon ports has been highly variable with a steep decreasing trend over the last five years, while all other fisheries showed no significant trends from 2019 to 2023. Pacific whiting and crab fisheries' revenues were >1 s.d. above long-term averages, while all other fisheries were within long-term averages over the last five years.

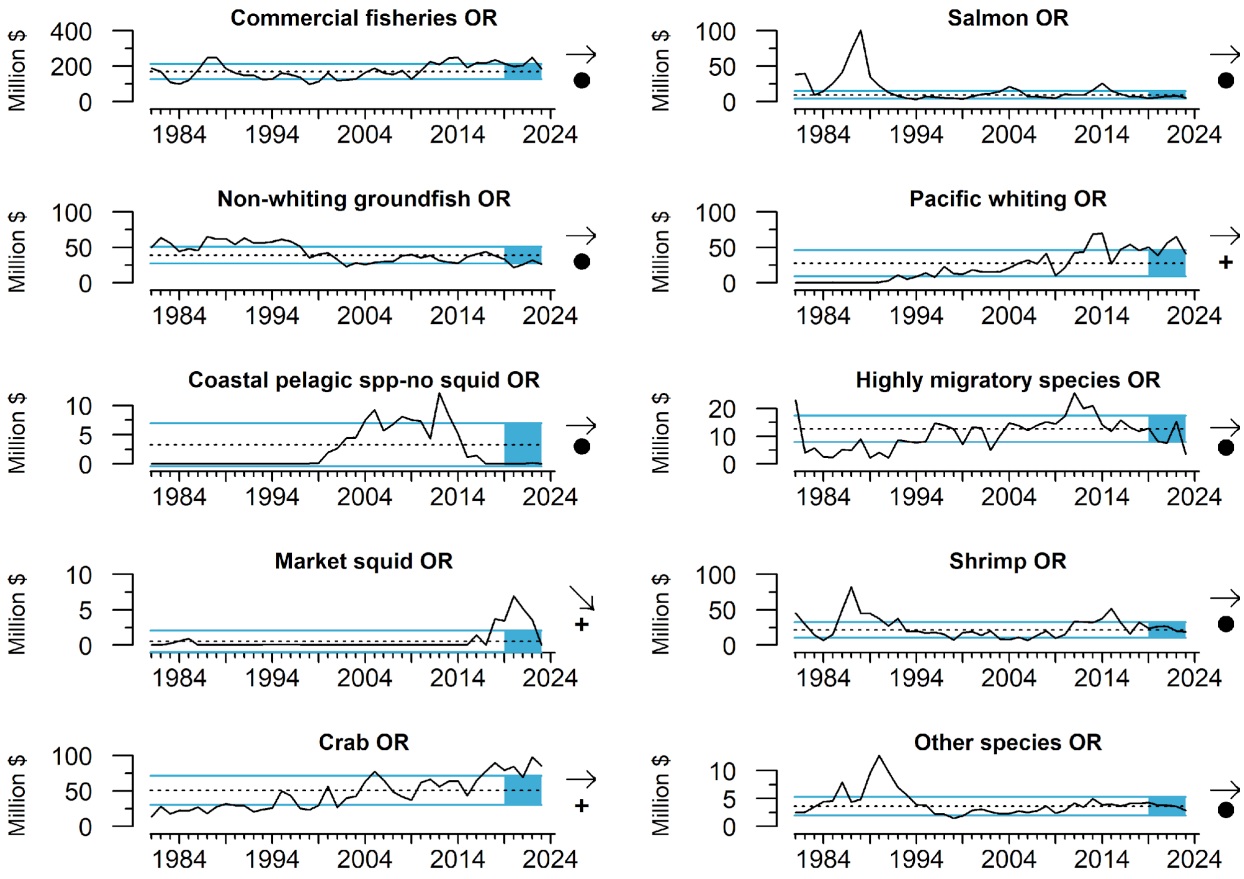

Figure P.6: Annual Oregon revenue (ex-vessel value in 2023 dollars) from West Coast commercial fisheries (data from PacFin) from 1981 - 2023. Whiting revenue includes shoreside and at-sea values from PacFIN, NORPAC (North Pacific Groundfish Observer Program) and NMFS Office of Science & Technology. Lines, colors, and symbols are as in Fig. 2.1.

Total revenue across commercial fisheries in California had increased in 2021 & 2022, but a 35% decrease in 2023 from 2022 levels has revenue nearly 1 s.d. below its long-term average (Fig. P.7). These patterns are largely driven by variation in revenue from market squid from 2019 to 2023, but the closure of commercial salmon in 2023 contributed greatly to lower revenue in 2023. Overall, 8 of 9 major fisheries decreased in revenue in 2023 from 2022 levels: salmon (-100%), Pacific whiting (-67%), market squid (-66%), CPS finfish (-25%), HMS (-23%), non-whiting groundfish (-12%), crab (-5%) and Other species (-4%). In contrast, revenue from shrimp (6%) fisheries was higher in 2023 compared to 2022. Even though there was an increasing trend in revenue observed in the Pacific whiting fishery, revenue levels are still at very low values, and this revenue comes from fishing events that occur in CA waters but processed at sea and landed outside of California. Revenue from market squid increased and revenue from shrimp and salmon fisheries decreased, while all others showed no trends from 2019 to 2023. Revenue from non-whiting groundfish was >1 s.d. below the long-term average, while all other fisheries were within 1 s.d. of their respective long-term average over the last five years in California.

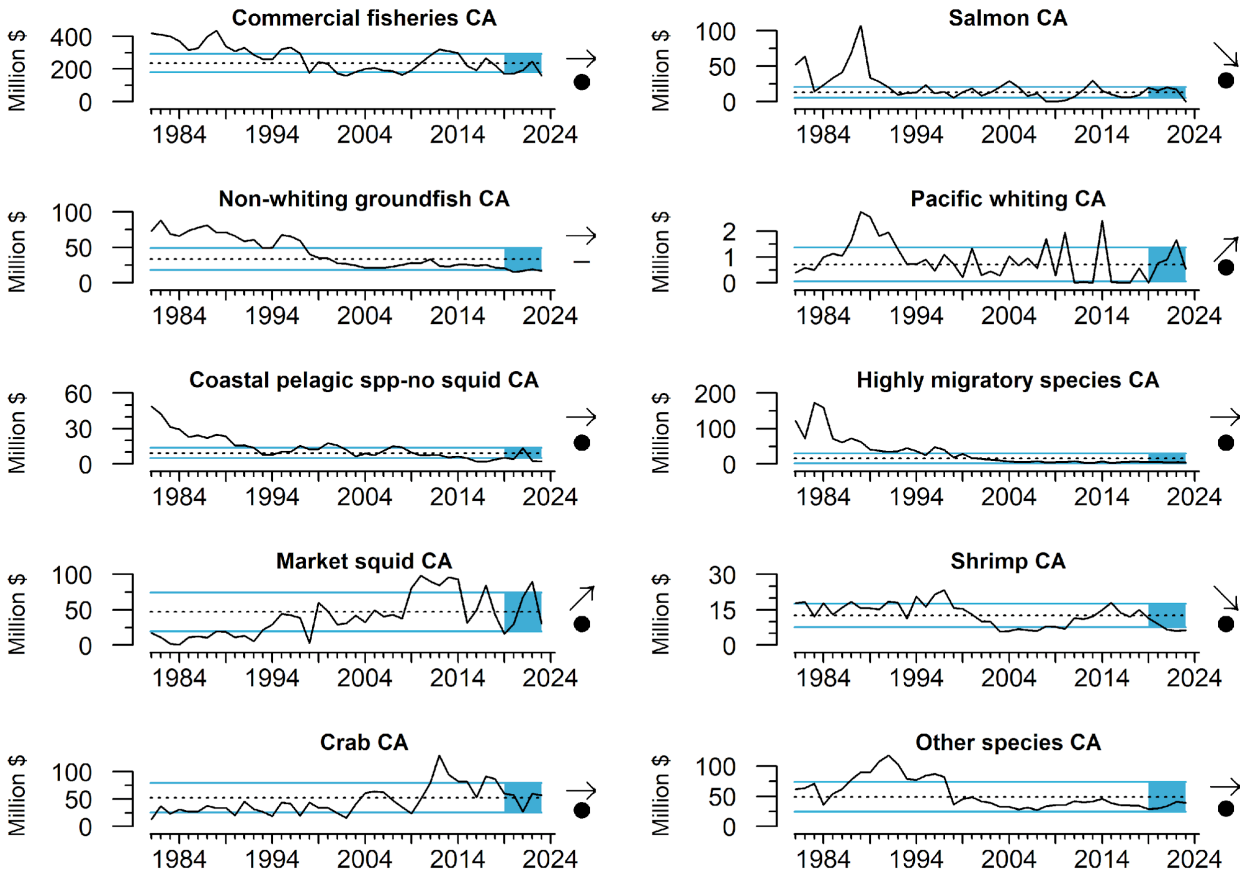

Figure P.7: Annual California revenue (ex-vessel value in 2023 dollars) from West Coast commercial fisheries (data from PacFin) from 1981 - 2023. Whiting revenue includes shoreside and at-sea values from PacFIN, NORPAC (North Pacific Groundfish Observer Program) and NMFS Office of Science & Technology. Lines, colors, and symbols are as in Fig. 2.1.

Appendix Q: POTENTIAL FOR SPATIAL INTERACTIONS AMONG ECOSYSTEM INDICATORS & OCEAN-USE SECTORS

Link to the main section: Potential Interactions Between Offshore Wind and Ecosystem Indicators

New ocean-use sectors of the economy (e.g., renewable energy and aquaculture) are becoming a reality off the West Coast, particularly with the Bureau of Ocean Energy Management's (BOEM) two proposed offshore draft wind energy areas (WEAs) off the southern coast of Oregon and five existing lease areas off the northern and central California coast. Understanding how oceanic and atmospheric processes, protected species and their habitats, fisheries and fisheries stocks' habitat, fishing communities, and NMFS scientific surveys will be affected by new ocean-use sectors, such as offshore wind energy (OWE), is needed to ensure effective marine spatial planning and adaptive management, and to minimize conflicts across the West Coast into the future. Below, we describe two portfolios of indicators for i) oceanographic and lower-trophic level productivity and ii) fisheries activity that can help identify ocean areas important to the overall structure and function of the CCE, and that can track potential social-ecological impacts across all stages of OWE development.

Q.1 Ecosystem Indicators

Here we introduce six broad-scale indicators of long-term, spatial variation in oceanography and lower-trophic level productivity that could be used to inform spatial suitability analyses in areas off northern California being considered for OWE development in 2024. The ecosystem indicators include:

1. Average wind-driven upwelling during March-July (Fig. Q.1a), calculated at 40m depth from 1988-2012 using the Regional Ocean Modeling System (Raghukumar et al. 2023).
2. Long-term, spatial variability and hotspots in primary productivity (Fig. Q.1b), calculated from a biogeochemistry model as the average concentration of surface phytoplankton in May-July, 1995-2020 (Fiechter et al. 2018).
3. Long-term, spatial variability and hotspots in secondary productivity from May-August (Fig. Q.1c), calculated as an ensemble of four different estimates of krill abundance/biomass across the West Coast (Cimino et al. 2020; Fiechter et al. 2020; Messié et al. 2022; Phillips et al. 2022).
4. Long-term, spatial variability and hotspots for young-of-year (YOY) rockfishes during their pelagic juvenile life stage in May-June from 2001-2022 (Fig. Q.1d; Field et al. 2021).
5. Long-term, spatial variability and hotspots for YOY Pacific hake in May-June from 2001-2022 (Fig. Q.1e; Field et al. 2021).
6. Long-term, spatial variability and hotspots of groundfish nursery habitat on the seafloor (Fig. Q.1f), based on summed average densities of juveniles from 13 groundfish species in May-October from 2003-2018 (Tolimieri et al. 2020).

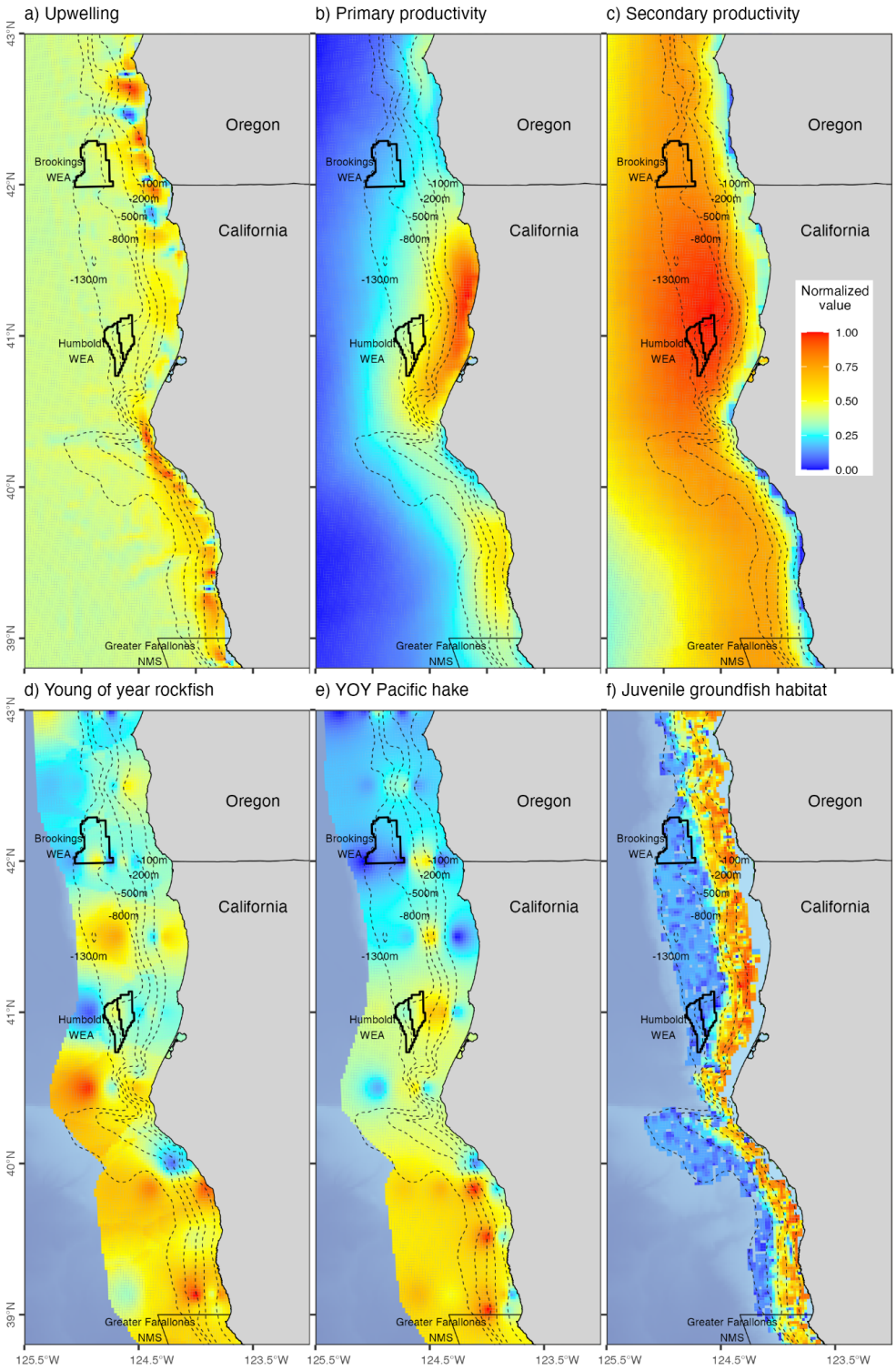

Figure Q.1: Ecosystem indicators to be considered for offshore wind energy development planning. Values for each indicator have been cropped and normalized across the area of interest and represent long-term, spatial variation during peak seasonal production. The draft WEA off the coast of Brookings, OR and the two lease areas off the coast of Humboldt Bay, CA are outlined in black.

Data compiled by NMFS/NWFSC from sources summarized in report text. Boundaries of proposed Wind Energy and Lease Areas from BOEM (https://www.boem.gov/renewable-energy/state-activities/Oregon; https://www.boem.gov/renewable-energy/state-activities/California). Figure created by K. Andrews, NMFS/NWFSC.

The Bureau of Ocean Energy Management (BOEM) has been using a spatial suitability analysis developed by NOAA's National Centers for Coastal and Ocean Science (NCCOS) to identify areas BOEM may consider for OWE development. In order to inform an analysis of new areas along the northern California coast, we used BOEM's methods to calculate an overall suitability score across the six ecosystem indicators for each grid cell (Fig. Q.2; Riley et al. (2021)). Briefly, the raw data for each indicator was cropped to the area-of-interest, interpolated across a 2x2-km spatial grid, transformed using a z-membership function, and then geometrically averaged across all indicators for each grid cell. This geometric mean represents the suitability score of a grid cell for OWE development relative to the importance of these areas to the processes represented by each indicator; thus, a suitability score of '1' is most suitable for OWE, while suitability scores closer to 0 are less suitable. In addition to being applicable to siting of new areas, these indicators could be used to establish baseline conditions that can be used to identify potential effects resulting from OWE development and to identify relevant mitigation strategies.

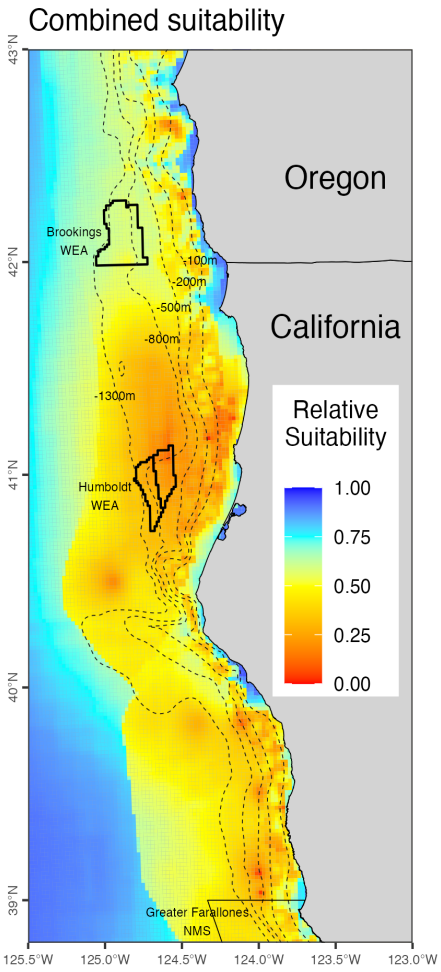

Figure Q.2: Relative suitability scores of 2x2-km grid cells offshore of northern CA based on six broad-scale ecosystem indicators. Scores near 1.00 (blue cells) are most suitable for offshore wind energy development relative to the six ecosystem indicators, while scores near zero (red cells) are less suitable due to overlap with important areas for ecosystem structure and function.

Q.2 Fisheries Indicators

We developed seven indicators that describe spatial and temporal variation in groundfish bottom trawling activity from 2002-2021 in the same region being considered for OWE development off the coast of northern California. These indicators were presented in the 2022 ESR and are meant to capture the spatial and temporal variation in fishing effort for the groundfish bottom trawl fishery and to be used in tandem with the ecosystem indicators to identify potential interactions across the entire social-ecological system.

For the groundfish indicators herein, we used logbook set and retrieval coordinates from the limited-entry/catch shares groundfish bottom trawl fisheries to estimate total duration trawled on a 2x2-km grid. These durations were then used to calculate (1) total duration

trawled in the most recent year (2021), (2) the anomaly of the most recent year relative to the entire time series, (3) the most recent 5-year mean (2017-2021), (4) the most recent 5-year trend (2017-2021), (5) the sum of duration trawled across all years, (6) the proportion of years trawled, and (7) the number of years since trawling occurred within each grid cell. To maintain confidentiality, grid cells with <3 vessels operating within the grid cell across the years associated with the indicator have been removed. The first four indicators are consistent with measuring the 'status' and 'trends' of other ecosystem indicators presented in this report, while the last three have been developed as indicators to use within a risk analysis framework. These indicators account for only federal limited-entry/catch shares groundfish bottom trawl fisheries from 2002-2021, but provide a useful framework for identifying the potential for overlap and conflict between day-to-day fisheries operations and OWE areas. Other fisheries were included in a similar framework presented in last year's ESR and will be added here as analyses are completed.

Across this region (Fig. Q.3), recent groundfish bottom trawl activity occurred along depth contours just inshore of the current draft WEAs (Coos Bay and Brookings) and the lease areas within the Humboldt WEA (Fig. Q.3a), with above-average activity (red cells in Fig. Q.3b), higher mean-activity (red cells in Fig. Q.3c), and an increasing trend over the last five years (red cells in Fig. Q.3d) along the 200-m contour in 2021. Decreasing trends of bottom trawl fishing activity occurred in two particular areas along the central Oregon coast and near the Oregon/California border (blue cells in Fig. Q.3d). Across the entire time series, bottom trawl activity occurs broadly between the 200-m and 1300-m depth contours, with the highest levels of activity concentrated along specific depth contours (Fig. Q.3e), but nearly all grid cells had bottom trawling activity in >60% of all years (Fig. Q.3f) and had activity within the last decade (Fig. Q.3g). There are several areas within this region that are heavily used year-after-year and other areas showing changes in bottom trawl fishing activity (Fig. Q.3). Indicators such as these for fisheries activity and the broad-scale ecosystem indicators presented in the main body of the ESR (Section 4.2) can help identify potential interactions and conflicts with new ocean-use sectors and contribute to efforts to avoid and/or minimize these conflicts across the CCE.

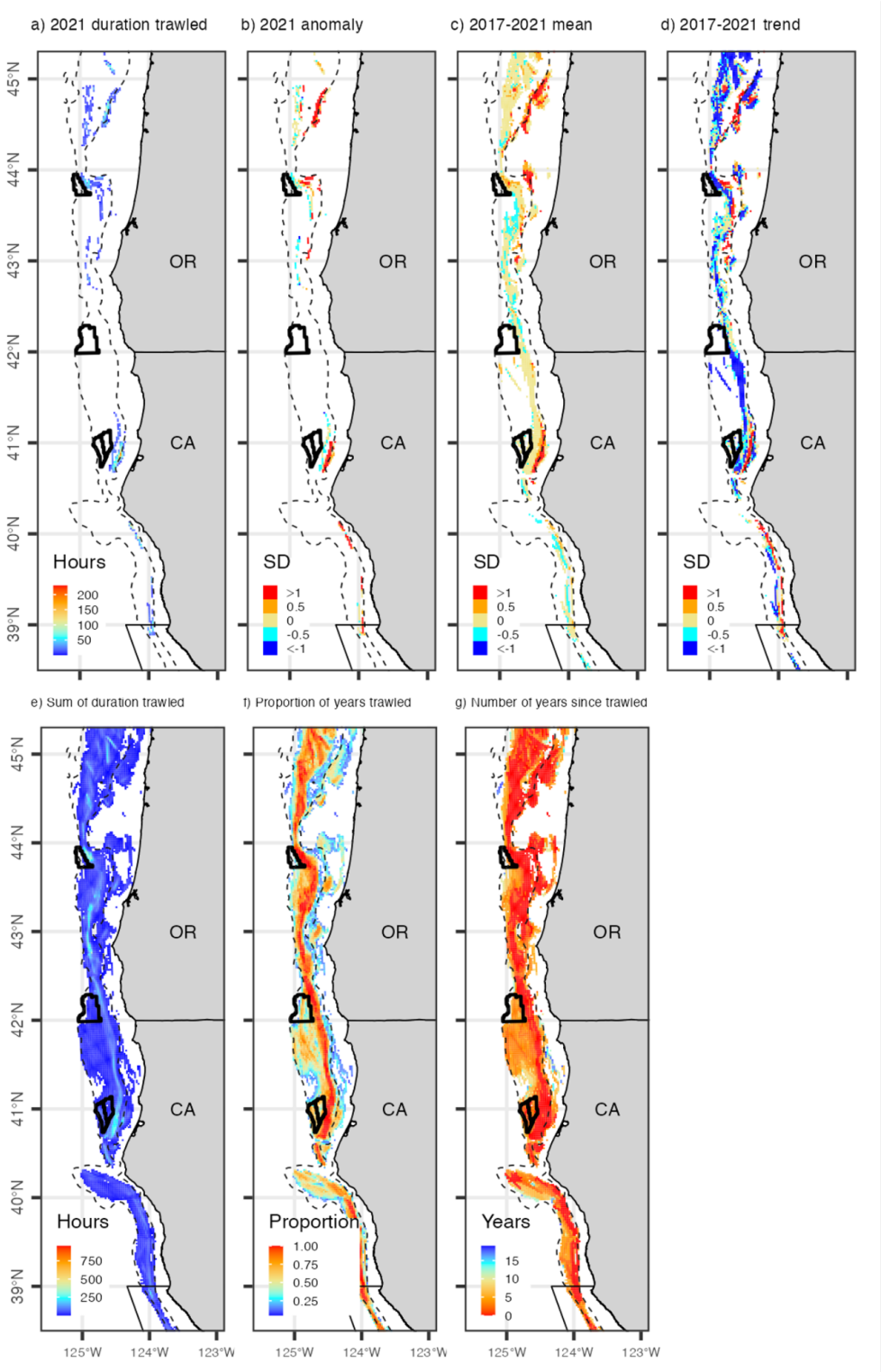

Figure Q.3: Indicators of groundfish bottom trawl fisheries activity in areas under consideration for new offshore wind energy areas. Panels show (a) total duration trawled in 2021, (b) anomaly of distance trawled relative to the entire time series, (c) the most recent 5-year mean, (d) the most recent 5-year trend,

(e) the sum of duration trawled across all years, (f) the proportion of years trawled (2002-2021), and (g) the number of years since trawling last occurred within each 2x2-km grid cell. Coos Bay and Brookings draft Wind Energy Areas and the Humboldt Wind Energy Area shown in heavy black lines from north to south, respectively. Grid cell values in (b-d) > 1 (red) or < -1 (blue) represent a cell in which the annual anomaly or 5-year mean was at least 1 s.d. from the long-term mean or where the 5-year trend increased or decreased by >1 s.d. of the long-term mean of that cell. The dashed lines are the 200-m and 1300-m depth contours. Figure created by K. Andrews, NMFS/NWFSC.

Appendix R: SOCIAL VULNERABILITY OF FISHING-DEPENDENT COMMUNITIES

Link to main section: Social Vulnerability

In Section 5.1 of the main report, we present information on the Community Social Vulnerability Index (CSVI) as an indicator of social vulnerability in coastal communities that are dependent upon commercial fishing. To gain further insight into community vulnerability in relation to commercial fishing, fishing dependence, which can be expressed in terms of engagement, reliance, or by a composite of both, can be considered in relation to CSVI. Engagement refers to the total extent of fishing activity in a community; it can be expressed in terms of commercial activity (e.g., landings, revenues, permits, processing, etc). Reliance is the per capita engagement of a community; thus, in two communities with equal engagement, the community with the smaller population would have a higher reliance on its fisheries activities.

Similar to the commercial fishing reliance and engagement measures produced as a part of the Community Social Vulnerability Index (CSVI), we have developed index measures for recreational fishing engagement and reliance, absent in prior versions of this report as consistent annual data had not been identified. As with the commercial fishing Index construction, following the method proposed by Jepson and Colburn (2013), data directly linking place-based communities to the economic aspects of recreational fishing, which could be attributed to specific calendar years, were compiled from six distinct sources as inputs for the measures. Charter and guide permit data collected by state managers were obtained and linked to Census-Designated Place (CDP) based communities. Additionally, historic fishing tackle business location data was compiled from Data Axel, the provider of business location data to Environmental Systems Research Institute's (ESRI) business analyst application. Marina business location data was also obtained from ESRI and ESRI's provider. These data enable interannual comparisons and allow for future replicable iterations.

Communities that score highly in either commercial or recreational reliance in addition to higher social vulnerability scores may be especially socially vulnerable to downturns in fishing. Fishing reliance can be volatile: communities can move left on the x-axis in years with reduced landings, and may thus appear to be less dependent on commercial fishing when in fact they have actually just experienced a difficult year; therefore, these results should be interpreted with care. These same qualifications apply to recreational fishing reliance measures, and several communities are among the most reliant in their respective regions for both commercial and recreational fishing. These data are difficult to groundtruth and interpreting trends requires further study.

In the main body of the report, Figure 5.1 plots CSVI against commercial and recreational reliance for the five most reliant communities respectively for 2021 from each of the five regions of the CCE. With a similar plot, here we show CSVI relative to fishing engagement scores from 2021 instead of relative to fishing reliance. Figure R.1 shows highly engaged West Coast commercial and recreational fishing communities and their corresponding social vulnerabilities. Of note are the groupings of communities above and to the right of

the dashed lines, which mark at least 1 s.d. above the mean of both indices as averaged across all fishing communities.

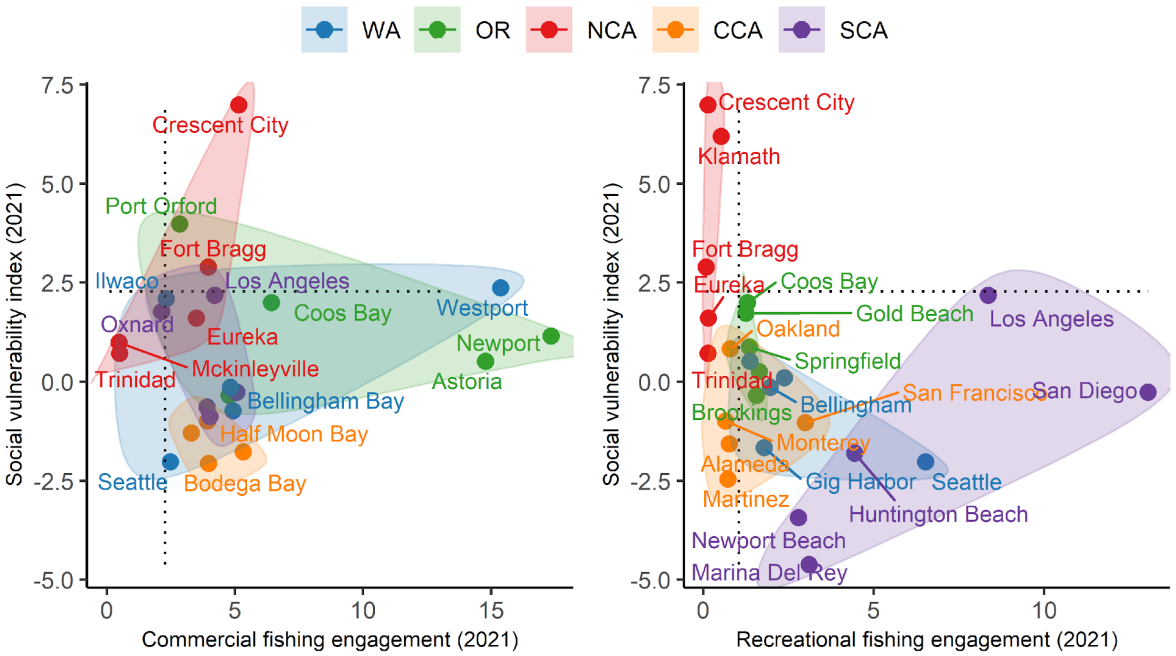

Figure R.1: Commercial (left) and recreational (right) fishing engagement with social vulnerability scores in 2020 for communities in Washington, Oregon, and northern, central and southern California. The five highest-scoring communities for fishing engagement are shown for each region. Dotted lines indicate 1 s.d. above the means for all communities. Data from the Pacific Fisheries Information Network (PacFIN), U.S. Census' American Community Survey (ACS), and ESRI Business Analyst as analyzed by K. Norman (NMFS/NWFSC), C. Lewis-Smith (PSMFC/NWSFSC), C. Weng (NEFSC) and L. Colburn (NMFS OST), and figure by C. Lewis-Smith (PSMFC) and N. Tolimieri (NWFSC).

To provide further insight into the social vulnerability of both top commercial and recreational engaged and reliant coastal communities, Figure R.2 displays the social vulnerability categorically with annual scores provided as categorical rankings. Dark red reflects a high representing scores at or above 1 standard deviation above the mean, light red is medium high as between 0.5 and 0.99 standard deviations above the mean, light blue is medium as 0 to 0.49 standard deviations above the mean, and dark blue is low as equal to the mean or below.

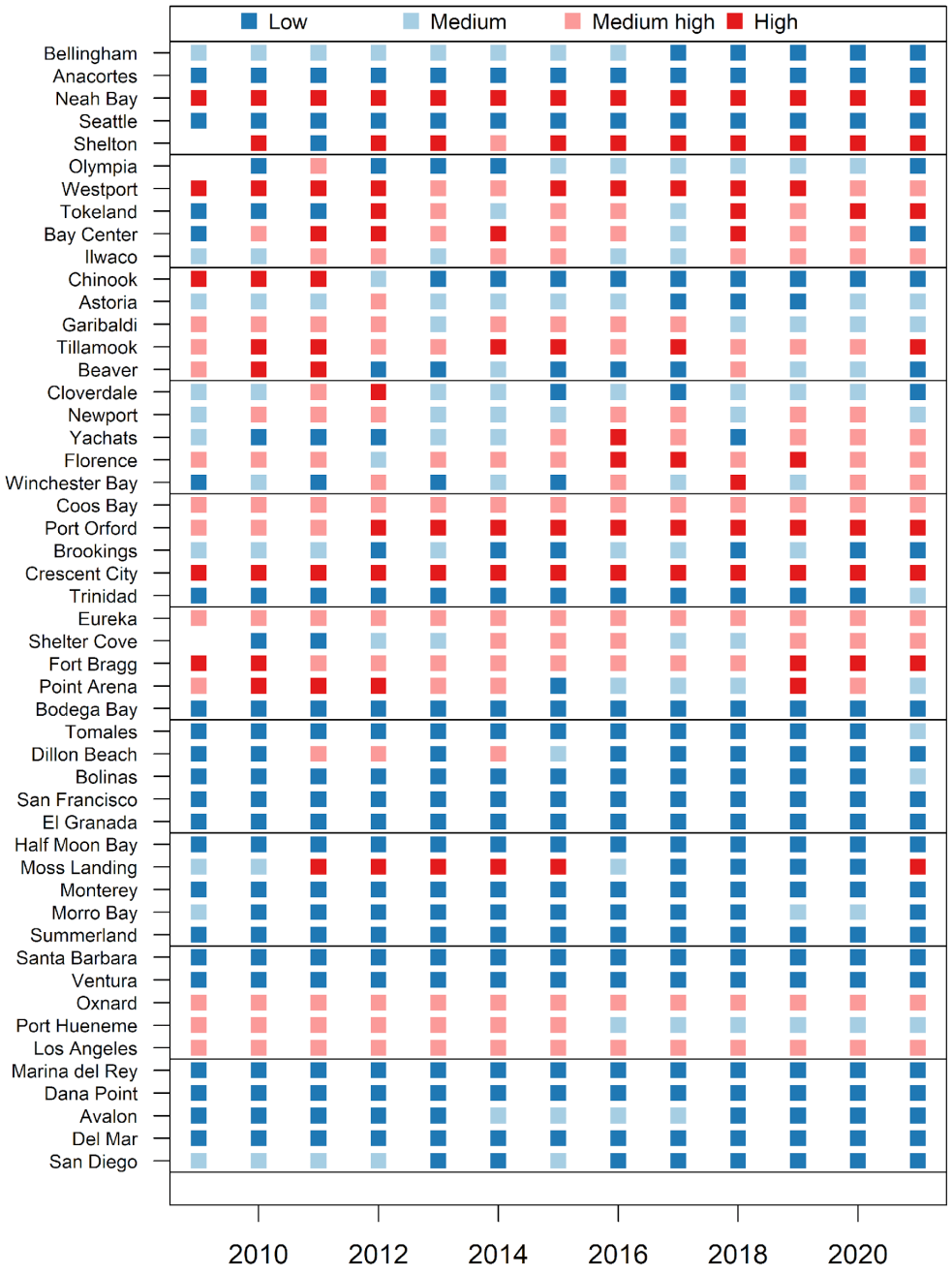

Figure R.2: Top commercial and recreational fishing communities concerning engagement and reliance with categorical social vulnerability scores from 2009 to 2021. Data from the Pacific Fisheries Information Network (PacFIN) and U.S. Census' American Community Survey (ACS) as analyzed by K. Norman (NMFS/NWFSC), C. Lewis-Smith (PSMFC/NWSFSC), C. Weng (NEFSC) and L. Colburn (NMFS OST) and figure by N. Tolimieri (NMFS/NWFSC).

Appendix S: FLEET DIVERSIFICATION INDICATORS

Link to main section: Diversification of Fisheries Revenue

S.1 Fishery Income Diversification of West Coast Vessel Owners

Catches and prices from many fisheries exhibit high interannual variability, leading to high variability in fisher's revenue, but variability can be reduced by diversifying activities across multiple fisheries or regions (Kasperski and Holland 2013). Individuals may have good reasons to specialize, including reduced costs or greater efficiency; thus while diversification may reduce income variation, it does not necessarily promote higher average profitability. We use the Effective Shannon Index (ESI) to examine diversification of fishing revenue for more than 28,000 vessels fishing off the West Coast and Alaska over the last 40 years. In the main body of the report (Fig. 5.2), ESI increases as revenues are spread across more fisheries, and as revenues are spread more evenly across fisheries; ESI = 1 when a vessel's revenues are from a single species group and region; ESI = 2 if revenues are spread evenly across 2 fisheries; ESI = 3 if revenues are spread evenly across 3 fisheries; and so on. If revenue is not evenly distributed across fisheries, then the ESI value is lower than the number of fisheries a vessel enters.

Coastwide, average fishery diversification by species group has been trending down for decades across virtually all vessel classifications (see main report, Fig. 5.2). Changes in diversification are due both to entry and exit of vessels and changes for individual vessels. Although vessels remaining in the fishery have become less diverse on average, less-diversified vessels have been more likely to exit, and newer entrants generally have been more diversified than those who left (Abbott et al. 2023). Within the average trends are wide ranges of diversification levels and strategies, and some vessels remain highly diversified.

As with individual vessels, the variability of landed value at the port level is reduced with greater diversification of landings. Revenue diversification scores are highly variable year-to-year for some ports, making it difficult to discern trends, but some ports have seen declines since the early 1990s. Bellingham, WA is one of the few ports that increased over the long term but it has seen declines since a peak in 2004. Increases in revenue diversification from 2021 to 2022 were seen for major West Coast ports in Washington, Oregon and Northern California but diversification of major ports in Southern California declined for all but Moss Landing (Fig. S.1).

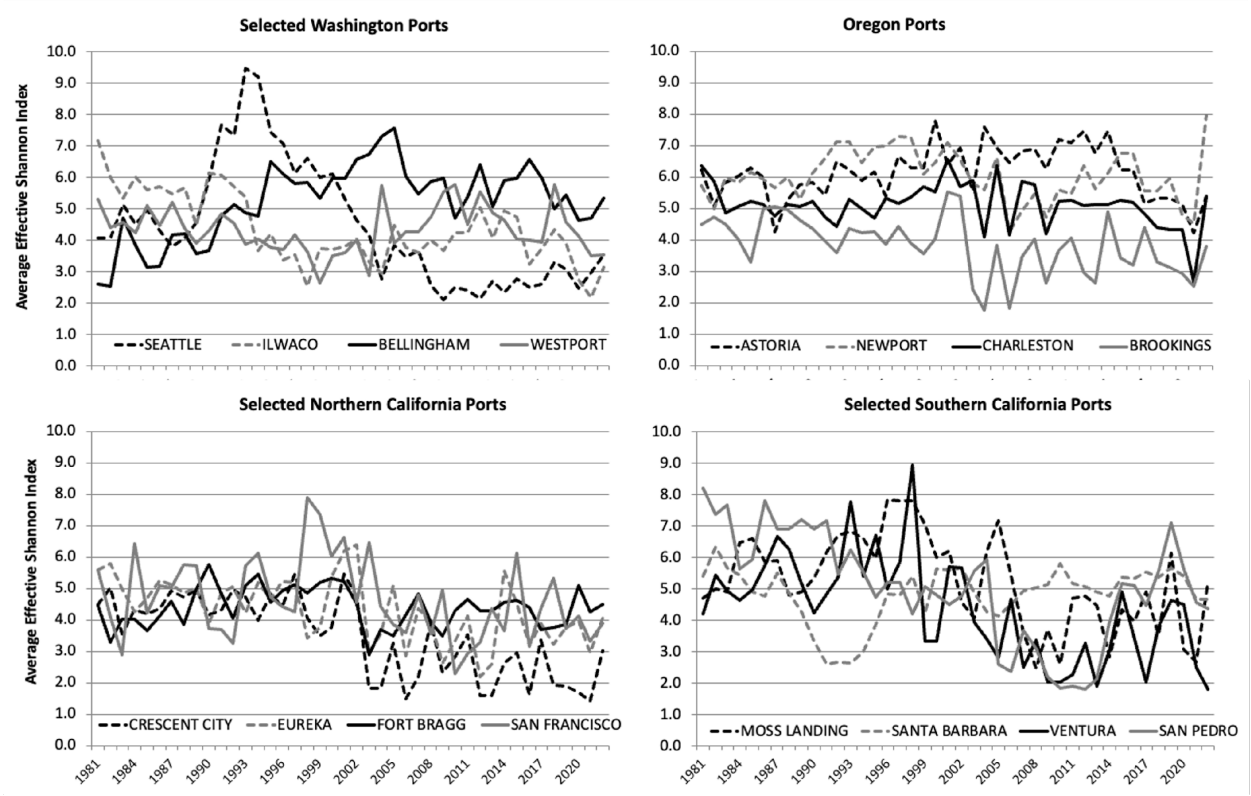

Figure S.1: Trends in fishery revenue diversification in major U.S. West Coast ports, grouped by state. Data from D. Holland (NMFS/NWFSC) and S. Kasperski (NMFS/AFSC).

Diversification can take other forms. Spreading effort and catch over the year, or simply fishing more weeks of the year, can both increase revenue and decrease interannual variation of revenue just as species diversification does. In fact, Abbot et al. (2023) showed that reductions in revenue variation associated with species diversification can be explained mainly by increased temporal diversification, which can be achieved by fishing in multiple fisheries but also by fishing for more weeks of the year in a single fishery. Below, Figure S.1 shows temporal diversification for the same vessel groups and classes shown in the main body (Fig. 5.2). Here we use an Effective Shannon Index that reflects how widely and evenly vessel revenues are spread across weeks of the year as an indicator or temporal diversification. Like the species diversification metric, this index increases the more weeks of the year a vessel has revenue and the more evenly that revenue is distributed across weeks. A vessel fishing 15 weeks of the year with the same revenue each of those weeks would have a temporal ESI of 15, and that number would decline as revenue is spread less evenly over the 15 weeks.

Unlike species diversification, which has been trending down since the early 1990s for most vessel groups (main report, Fig. 5.2), temporal diversification generally trended up though the early 2000s and oscillated without a clear trend through 2014 (Fig. S.2). However, since 2014, temporal diversification has declined for most vessel groups other than West Coast vessels with average revenue under $25K (Fig. S.2A-D). This mainly

reflects individual vessels fishing fewer weeks of the year on average. Much of the decline since 2014 can be attributed to reduced effort and compression of fishing seasons for salmon and Dungeness crab, as well as impacts of COVID-19 in 2020 and 2021. There was a small increase in 2022 for some vessel groups, but the average remains well below the 2014 high.

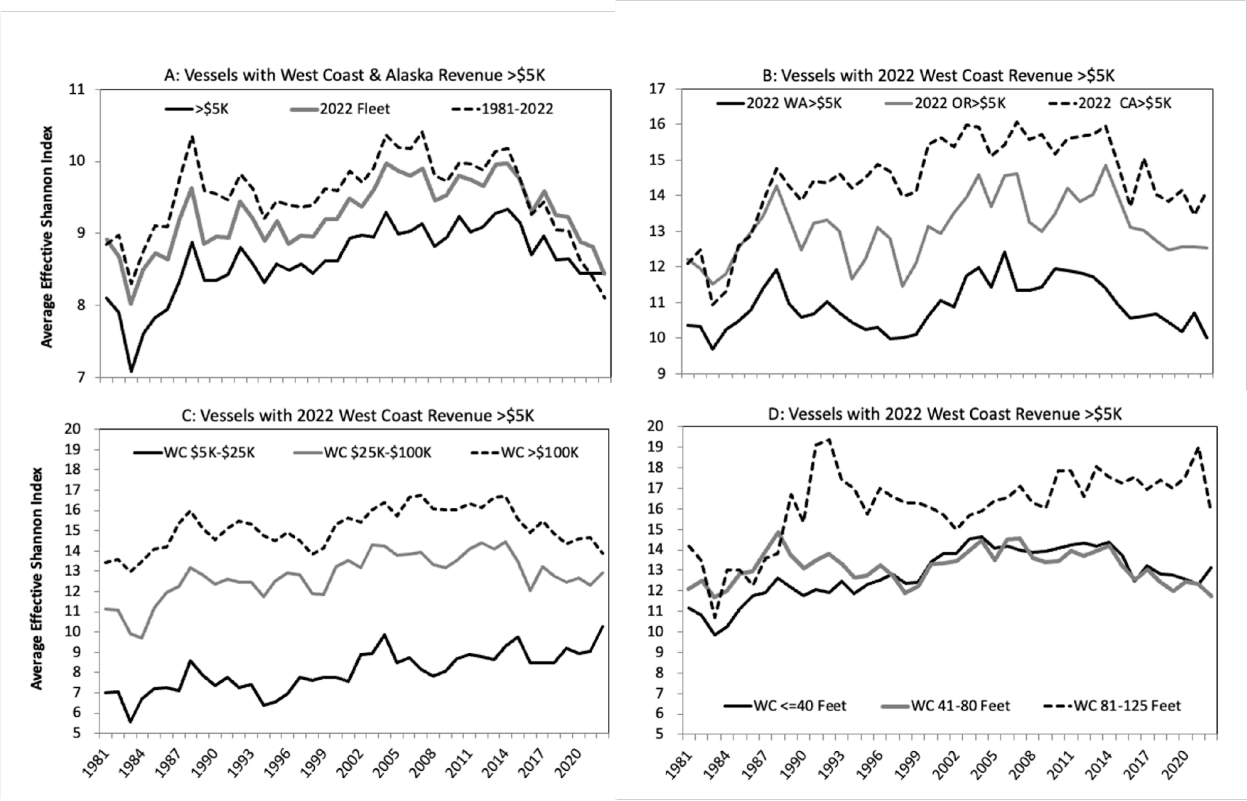

Figure S.2: Trends in average temporal diversification for U.S. West Coast and Alaskan fishing vessels with over $5K in average revenues (top left) and for vessels in the 2021 West Coast Fleet with revenues over $5K, grouped by state (top right), by average gross revenue class (bottom left) and by vessel length class (bottom right). Data from D. Holland (NMFS/NWFSC).

S.2 Non-Fishery Income Diversification of West Coast Vessel Owners

Compared to many other professions, fishers face unusually high year-to-year variability in their income levels (Fig. S.3). Diversifying fishing income can help reduce income variability and reduce financial risk, but focusing solely on diversification opportunities within the fishery misses a potentially important form of financial risk reduction - income diversification from non-fishing occupations (i.e., livelihood diversification). Livelihood diversification may actually be a more effective form of financial risk reduction for fishing households if their non-fishing income streams are unaffected by changes in fishery productivity or profitability or if they can be actively increased when fishing income is low.

While the ESR has regularly reported on diversification of fishing income, levels and trends in non-fishery income diversification have not been presented in prior ESRs due to a lack of

regularly collected data on non-fishery income (NFI). To address this and other informational gaps, the NWFSC began periodically surveying West Coast fishing vessel owners on a triennial basis with surveys carried out in 2017, 2020, and 2023. Surveys were sent to all vessel owners with commercial revenue from West Coast fisheries (federal and state) the prior year. Response rates were around 50% in 2017 and 2020 with over 1400 surveys returned each year. The response rate in 2023 fell to 40% with 1163 surveys returned.

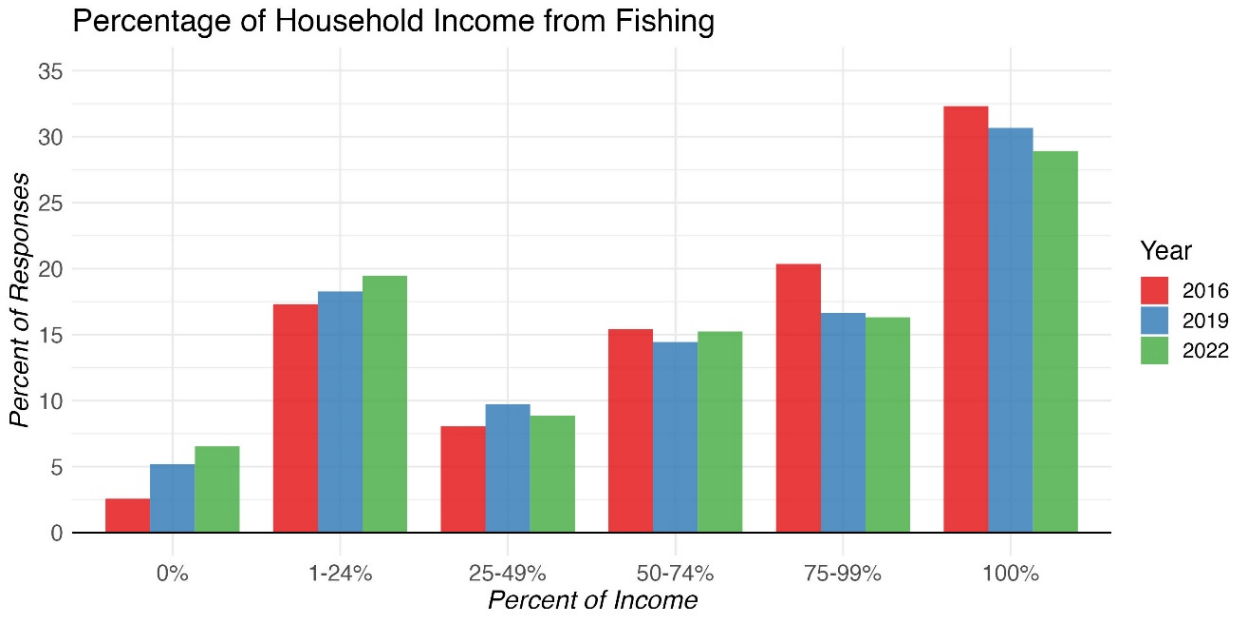

Figure S.3: Frequency distribution of responses on the percentage of household income vessel owners' households derived from fishing in 2016, 2019 and 2022. Data from the West Coast Fisheries Participation Survey as analyzed by D. Holland (NMFS/NWFSC) and C. Lewis-Smith (PSMFC/NWSFSC), with the figure by C. Lewis-Smith (PSMFC/NWFSC).

Among other questions, the surveys ask fishing vessel owners what percentage of their household income came from fishing versus non-fishing sources in the prior calendar year (e.g. 2022 for the 2023 survey; Fig. S.3) and also what percentage of the income they personally contribute to the household is from non-fishery sources. The survey also asks vessel owners that personally contributed NFI to their household what type of non-fishing work they did. Treakle et al. (2023) provides a detailed analysis of the survey data on non-fishing income from the 2017 and 2020 surveys showing that NFI levels and sources vary geographically and by the respondents' primary fishery. The analysis also shows that households with higher diversification of fishing income tend to derive lower proportion of household income from non-fishing sources. This suggests that a broader metric of livelihood diversification that includes fishing and non-fishing income diversification may be a better indicator of overall financial vulnerability of fishing households than fishing income diversification alone.

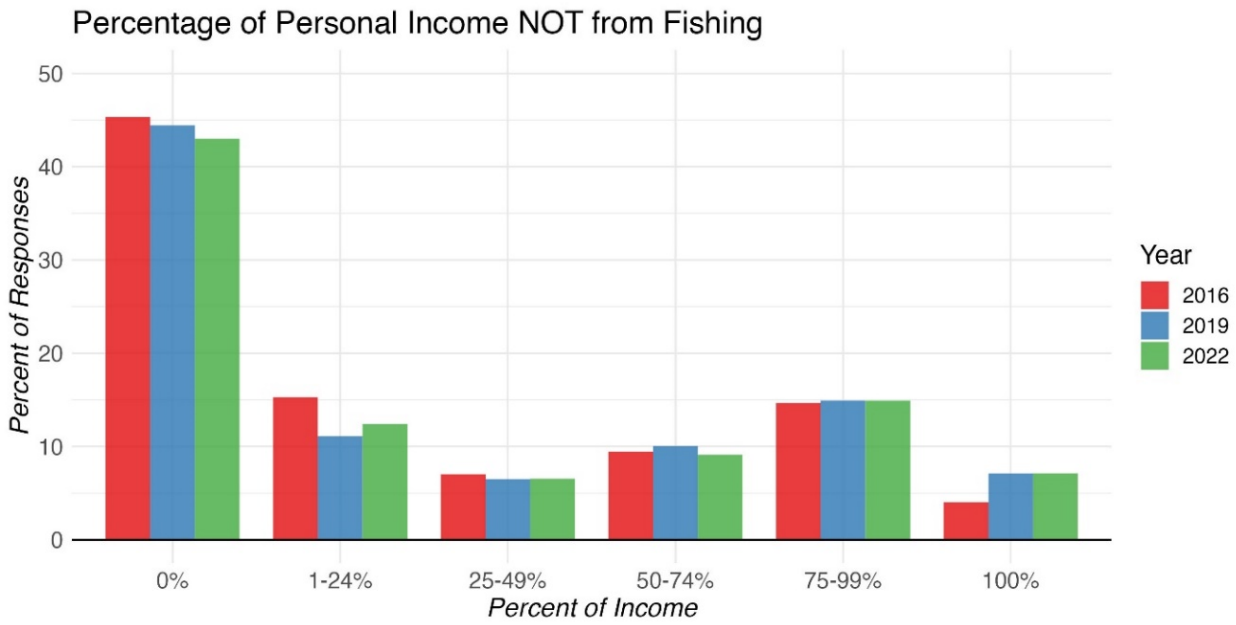

Figure S.4: Frequency distribution of responses on the percentage of vessel owners' personal contribution to household income that was not from fishing in 2016, 2019 and 2022. Data from the West Coast Fisheries Participation Survey as analyzed by D. Holland (NMFS/NWFSC) and C. Lewis-Smith (PSMFC/NWSFSC), with the figure by C. Lewis-Smith (PSMFC/NWFSC).

Figures S.4 and S.5 show the distribution of responses across the three years covered by the survey (2016, 2019 and 2022) as well as the distribution of responses by state for 2022 income. The results indicate that in 2016 about one-third of responding West Coast vessel owners derived 100% of their household income from fishing while about 30% of households derived less than 50% of household income from fishing. There has been a small shift over the six-year period with the percentage of fishing vessel owner households 100% dependent on fishing income falling below 30% and the percentage deriving less than 50% of income from fishing rising to above one-third of respondents. Considering the percent of income the vessel owner personally contributes to the household that comes from NFI, we see that more than half of vessel owners personally contribute some NFI to their household (Fig. S.4), and the proportion of respondents that do so has increased slightly between 2016 and 2022.

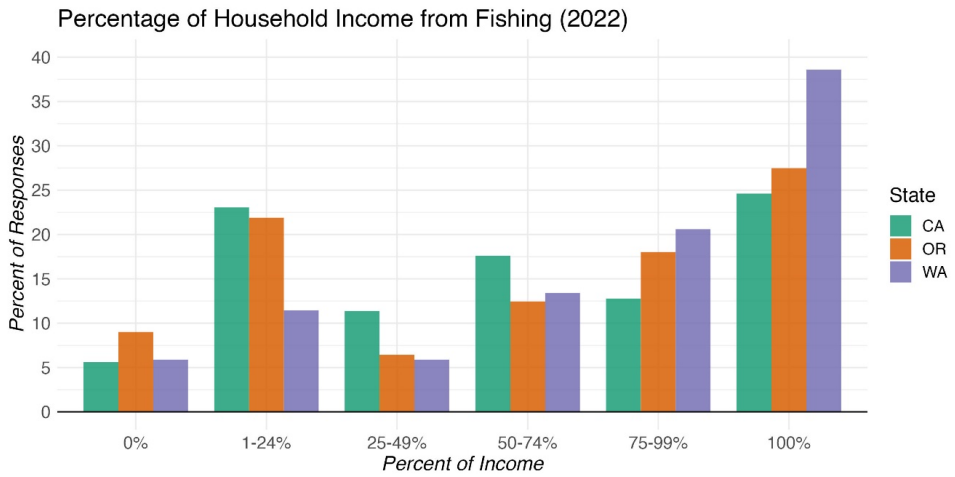

Figure S.5: Frequency distribution of responses on the percentage of household income vessel owners' households derived from fishing in 2022 for Washington, Oregon and California vessel owners. Data from the West Coast Fisheries Participation Survey as analyzed by D. Holland (NMFS/NWFSC) and C. Lewis-Smith (PSMFC/NWSFSC), with the figure by C. Lewis-Smith (PSMFC/NWFSC).

The share of household income and personal income from non-fishing sources varies by state as well (Figs. S.5, S.6). In 2022, vessel owners from Washington tended to derive a higher percentage of household income from fishing than Oregon and California vessel owners, and they also tended to have a higher share of their personal contribution to household income coming from fishing.

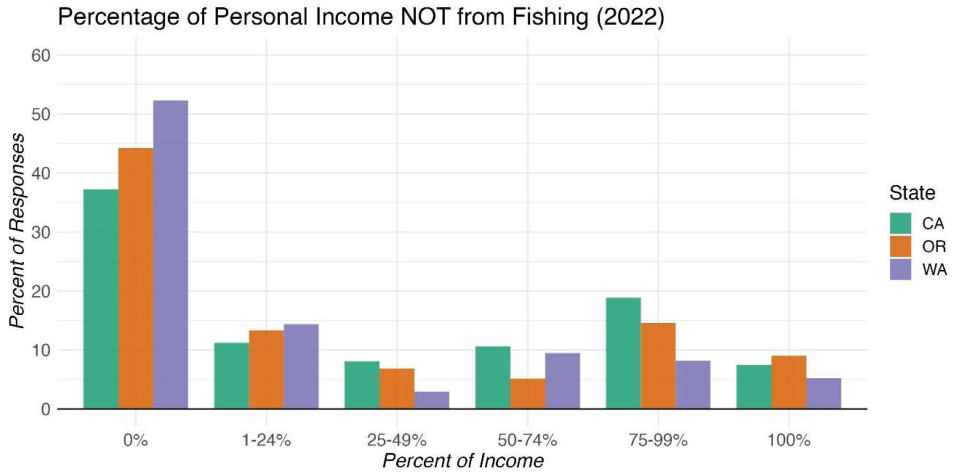

Figure S.6: Frequency distribution of responses on the percentage of vessel owners' personal contribution to household income that was not from fishing in 2022 for Washington, Oregon and California vessel owners. Data from the West Coast Fisheries Participation Survey as analyzed by D. Holland (NMFS/NWFSC) and C. Lewis-Smith (PSMFC/NWSFSC), with the figure by C. Lewis-Smith (PSMFC/NWFSC).

Appendix T: FISHERY REVENUE CONCENTRATION

Link to main section: Port-level revenue concentration

Variability in individual fishing effort from year-to-year in Section 5.2 and Appendix T compounds at the port level. Along with factors like processor availability and local infrastructure influence, variability in port-level landings can impact the overall distribution of fishing revenue along the coast. The Theil Index metric assesses the geographic concentration of fishing revenues, and is used to track progress toward meeting NS-8. The index estimates the difference between observed revenue concentrations and what they would be if they were perfectly equally distributed across ports; higher values indicate greater concentration in a subset of ports. Annually, we calculate the Theil Index for all fisheries and for specific management groups, at the scale of the 21 port groups previously established for the economic Input-Output model for Pacific Coast fisheries (Leonard and Watson 2011).

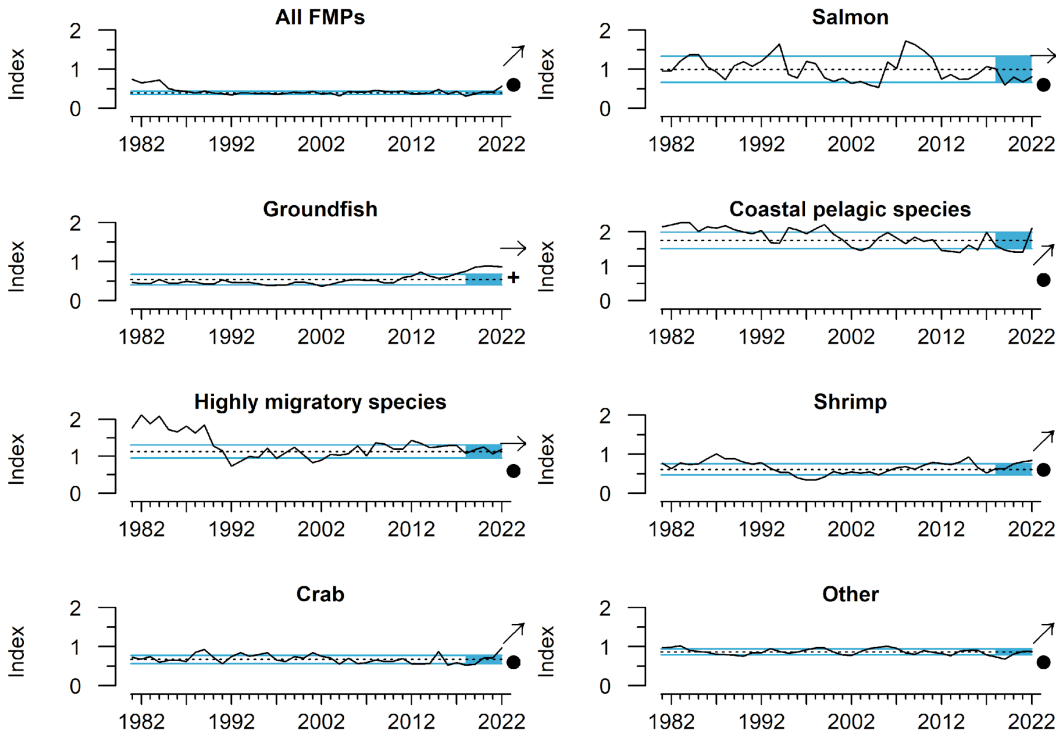

Figure T.1: Theil Index estimation of commercial fishery revenue concentration in West Coast IO-PAC port groups, 1981 - 2022. Increasing values indicate greater concentration of revenue in a smaller number of port groups. Data from the Pacific Fisheries Information Network (PacFIN) as analyzed by K. Norman (NMFS/NWFSC) and C. Lewis-Smith (PSMFC/NWSFSC), with the figure by N. Tolimieri (NMFS/NWFSC).

The annual Theil Index values for total commercial fishing revenue (upper left) and six management groups, as well as an 'other' category, are displayed in Figure T.1. The total revenue trend is relatively flat with low values in each year for the over 40-year time

period, suggesting total fishery revenue has not experienced dramatic changes in geographic concentration. Between 2021 and 2022 (the most recent year of data analyzed), there was an increase in the overall Theil Index value for all fisheries.

When considering individual management groups, there are distinctions in the overall degree of geographic concentration. CPS and HMS fisheries continue to have the highest Theil Index values, as they have for the last decade, indicating those groups' relatively high concentration of revenue in a smaller number of port groups (Fig. T.1). Following the removal of Humboldt squid, Pacific bonito, Pacific herring and round herring from the CPS FMP as requested from the CPSMT during the summer of 2022, we now see some decline in CPS consolidation over the last 40 years. Without the influence of Pacific herring on revenue, marked squid has become less consolidated in southern ports, shifting north, and has driven the CPS Theil Index value lower over the last 40 years. However, the 2022 increase in the Theil Index reflects an increase in CPS revenue in Santa Barbara with less CPS revenue in other Port groups (Fig. T.2).

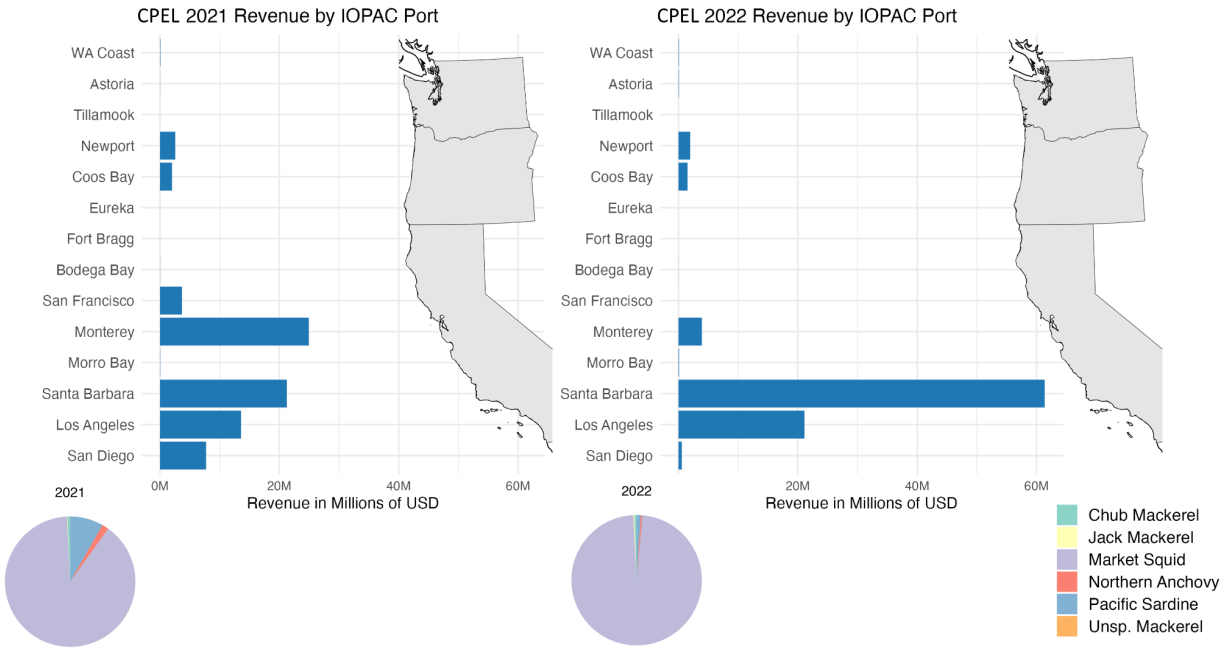

Figure T.2: Coastal Pelagic FMP revenue for 2021 (left) and 2022 (right) across IOPAC port groups. Pie-charts reflect individual species contributions to the overall FMP revenues of the given years. Data from the Pacific Fisheries Information Network (PacFIN) as analyzed by K. Norman (NMFS/NWFSC) and C. Lewis-Smith (PSMFC/NWSFSC), with the figure by C. Lewis-Smith (PSMFC/NWSFSC).

Theil values for groundfish have increased gradually for decades as groundfish revenue became concentrated in northern port groups. HMS revenues follow a more U-shaped trend, from high revenue concentration in southern ports in the early 1980s, to more equal distribution in the middle of the time period, and back to high values in the 2000s and

2010s as HMS revenues became more concentrated in northern port groups. Crab revenues exhibit short-term variability in geographic concentration, but overall have become more equally distributed coastwide since the 1990s, yet experienced an uptick in northern concentration in 2021 and 2022. The Theil Index also captures an increase in revenue consolidation for the Crab FMP that extends beyond the average interannual variability. This is likely due to the revenue in southern ports being lower in 2022 compared with 2021, thus driving the Theil Index higher than normal (Fig. T.3). Salmon also shows relatively high short-term variability, while shrimp revenue concentration has varied at decadal scales. This index may provide the Council with relevant information on particular fisheries and port groups where revenue concentrations are changing, as a basis for evaluating trade-offs related to NS-8 considerations.

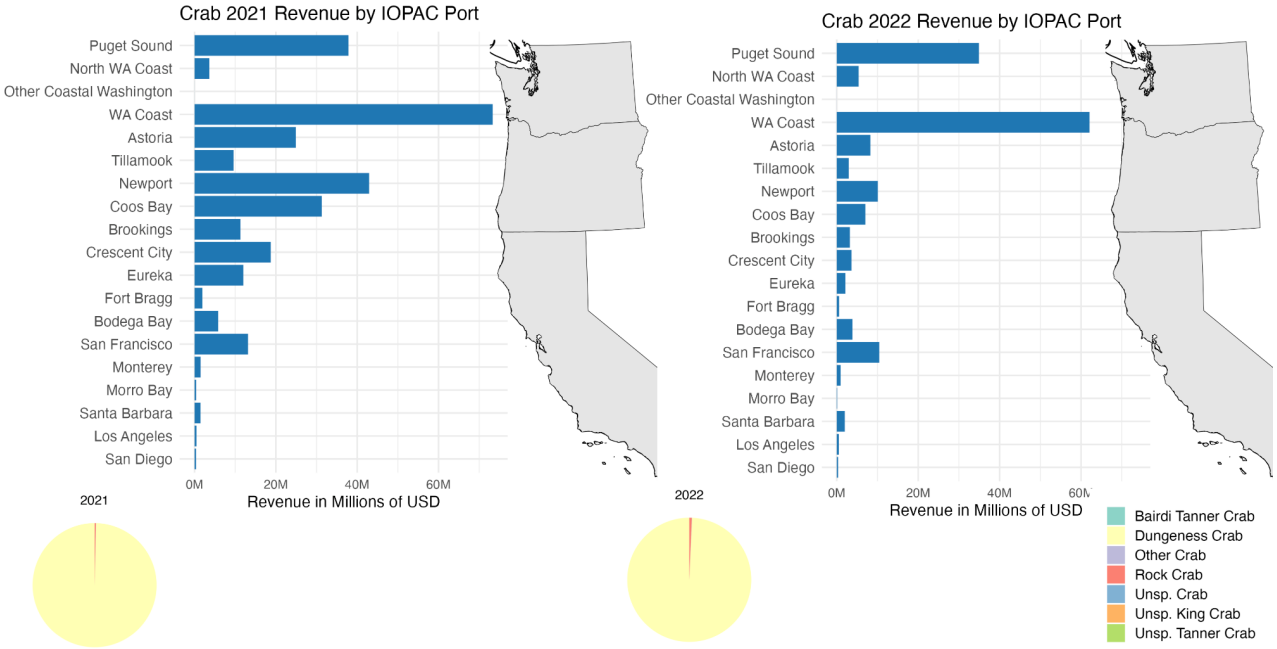

Figure T.3: Crab FMP revenue for 2021 (left) and 2022 (right) across IOPAC port groups. Pie-charts reflect individual species contributions to the overall FMP revenues of the given years. Data from the Pacific Fisheries Information Network (PacFIN) as analyzed by K. Norman (NMFS/NWFSC) and C. Lewis-Smith (PSMFC/NWSFSC), with the figure by C. Lewis-Smith (PSMFC/NWSFSC).

To date, only rudimentary effort has been spent exploring how changes in revenue concentration might be attributed to management actions, environmental drivers, food web changes, or changes within coastal communities. Thus, it is too early to conclude the effectiveness of this indicator in the context of NS-8, or what changes in the index mean for Council considerations. Community-scale estimation of the Theil Index is possible, and we would anticipate different qualitative and quantitative outcomes than those presented here if the scale is refined to the community level, in keeping with the CDP scale used for the social vulnerability and fishing reliance and engagement measures.

Appendix U: FISHERIES PARTICIPATION NETWORKS

Link to main section: Fisheries Participation Networks

Fisheries participation networks (FPNs) represent how diversified harvest portfolios create connections between fisheries (Fuller et al 2017, Fisher et al 2021). In past reports we have shown how West Coast networks change over time, and how groundfish fisheries are connected to other fisheries in different IO-PAC port groups (Harvey et al. 2022). Last year, we conducted a FPN analysis focused on salmon and examined the vulnerability of West Coast port groups to future shocks to salmon fishing, based on economic dependence (a measure of sensitivity) and a resilience index based on fisheries connectivity (a measure of adaptive capacity) (Harvey et al. 2023). In this year's report, we compare the number of active salmon vessels and the revenue of commercial salmon vessels between two periods (2017-2022 and 2022-2023) for West Coast port groups. Figure 5.3 in Section 5 of the main document highlights results for four California fishing ports (Monterey, Bodega Bay, Morro Bay and Santa Barbara) and results for 13 additional ports are shown below (Fig. U.1).

Participation in commercial fisheries by salmon vessels that were active from 2017-2022 declined across almost all of the fishing ports included in the analysis (Fig. 5.3, Fig. U.1). Among the California ports shown in Figure U.1, participation fell by >50% for San Francisco and Fort Bragg, 30% for Eureka, and 10% for Crescent City (Fig. U.1a, top panel). The total revenue from commercial fishing in 2022-2023 for salmon vessels in California increased for Crescent City (23%) but declined for the other three ports by as much as 55% (San Francisco) (Fig. U.1b, top panel).

Unlike most of the West Coast ports, salmon vessel participation in commercial fisheries increased for the Columbia River (14%) and Astoria (1%) in 2022-2023 compared to 2017-2022 (Fig. U.1a, middle panel). Other Oregon ports showed declines in participation, with the highest declines for Coos Bay (40%), followed by Newport (32%), Tillamook (24%) and Brookings (22%). Total revenue from commercial fishing increased for multiple Oregon ports in 2022-2023, with a 50% increase for Columbia River (Fig. U.1b, middle panel), but revenue declined for Coos Bay, Newport and Tillamook (13-25%). In Washington, participation declined for all three ports in 2022-2023, ranging from 12% for the Washington Coast to 32% for both North Washington Coast and Puget Sound ports (Fig. U.1a, bottom panel). Total revenue increased for salmon vessels on the Washington Coast (16%) but declined for ports in the north (20%) and Puget Sound (57%) (Fig. U.1b, bottom panel).

In future iterations of this work, we plan to only include commercial vessels that generate greater than $5,000 in total fisheries revenue each year and greater than $500 in revenue from individual fisheries. See Harvey et al. (2023) for previous work using FPNs.

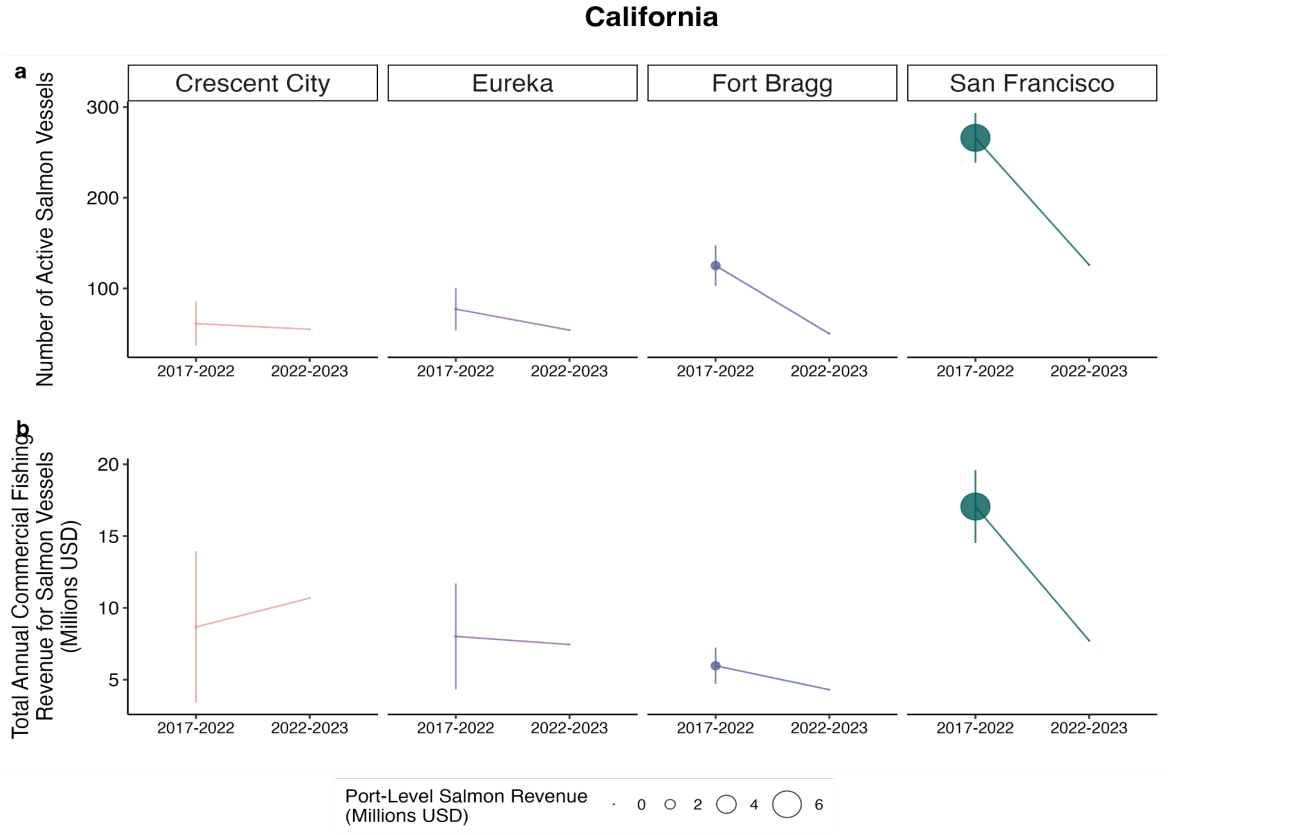
California
a
Crescent City
Eureka
Fort Bragg
San Francisco
Number of Active Salmon Vessels
300
200
100
2017-2022
2022-2023
b
Total Annual Commercial Fishing Revenue for Salmon Vessels (Millions USD)
20
15
10
5
Port-Level Salmon Revenue (Millions USD)
0
2
4
6

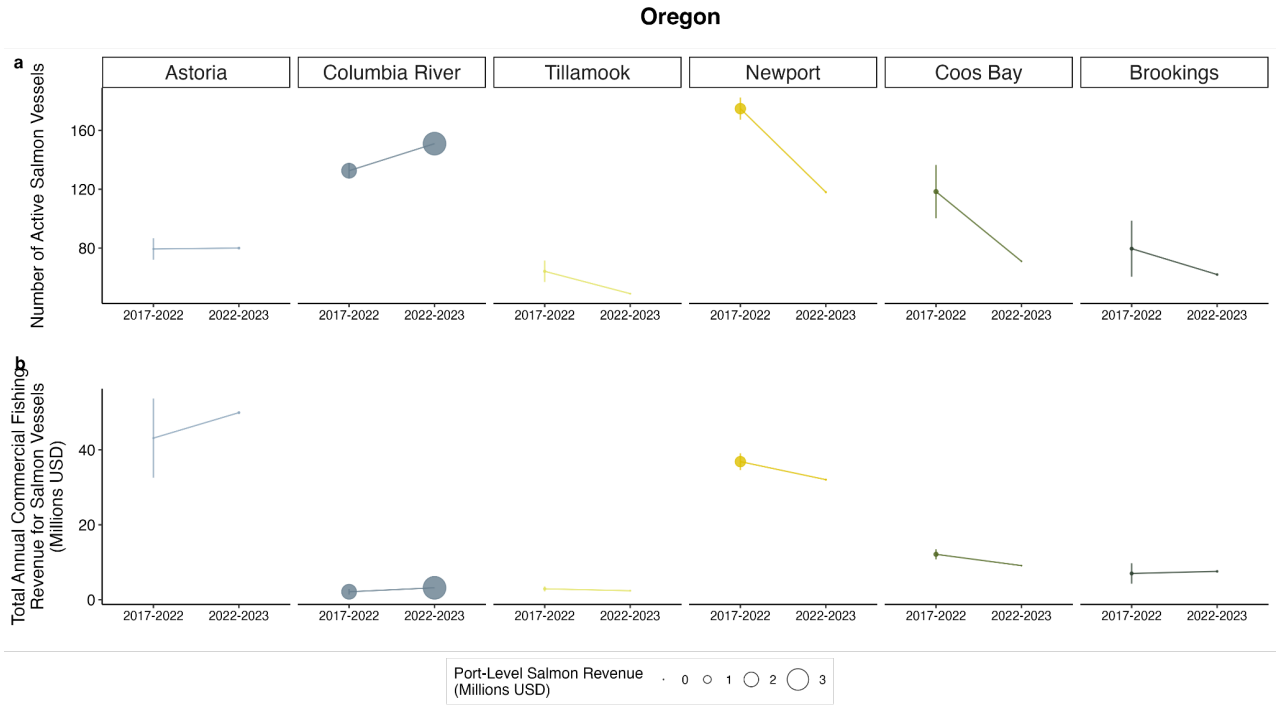
Oregon
a
Astoria
Columbia River
Tillamook
Newport
Coos Bay
Brookings
Number of Active Salmon Vessels
160
120
80
2017-2022
2022-2023
b
Total Annual Commercial Fishing Revenue for Salmon Vessels (Millions USD)
40
20
0
Port-Level Salmon Revenue (Millions USD)
0
1
2
3

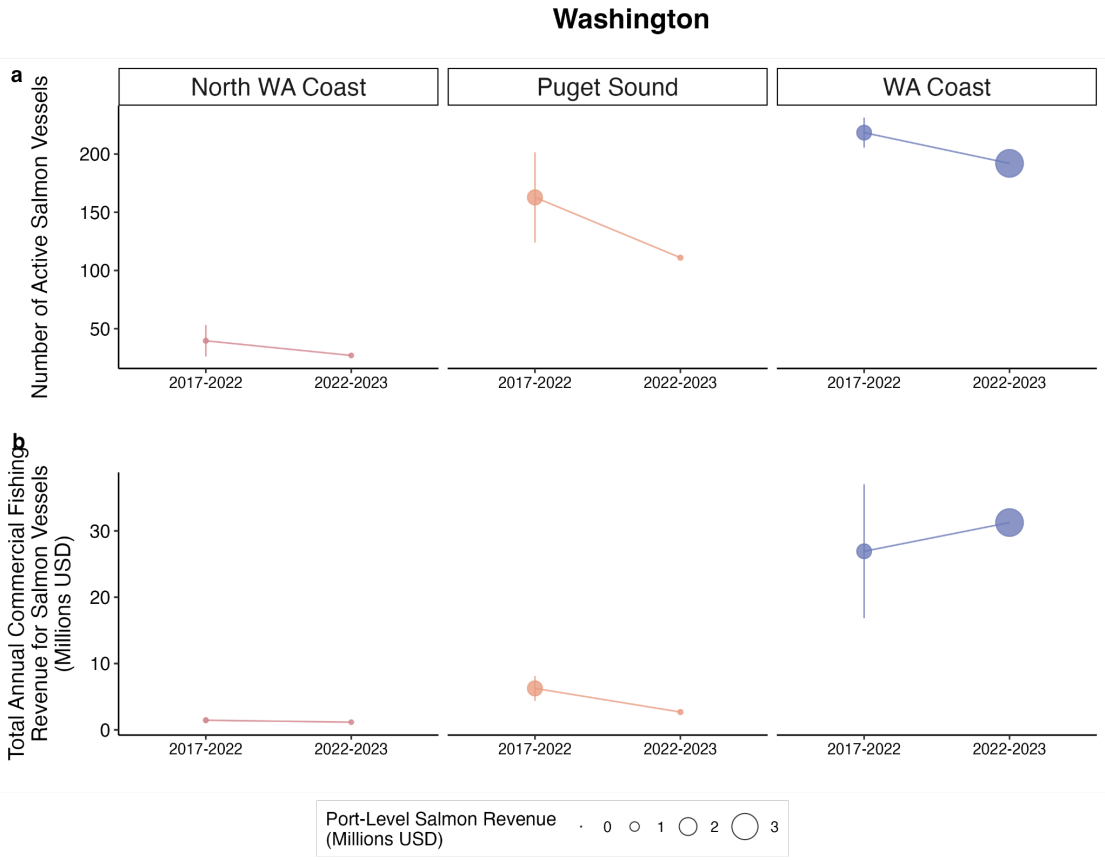

Figure U.1: California, Oregon and Washington port groups with salmon fishing participation (a) Mean number of active salmon vessels (±2 SD) during the 5 fishing seasons from November 2017 through November 2022 compared to the total number of active salmon vessels during the 2022-2023 for the 13 West Coast fishing ports (excludes ports shown in Figure 5.3 in main document). Active vessels are those that had commercial salmon landings anytime between November 2016 and October 2023, and participated in the fishery or any other commercial fishery during the two time periods. (b) Total annual revenue (adjusted for inflation to 2022) of commercial fishing vessels for salmon vessels (includes revenue from any fishery) for the same time periods and ports described in (a). In both panels, point size scales with the mean (2017-2022) or total (2022-2023) salmon revenue generated in each port. A fishing season is defined from November of year y through November of year (y+1), specifically week 46 of year y through week 45 of year (y+1), to capture the strong influence of the Dungeness crab fishery on commercial fishing patterns. Results for four additional California port groups are shown in Fig. 5.3 and not included here.

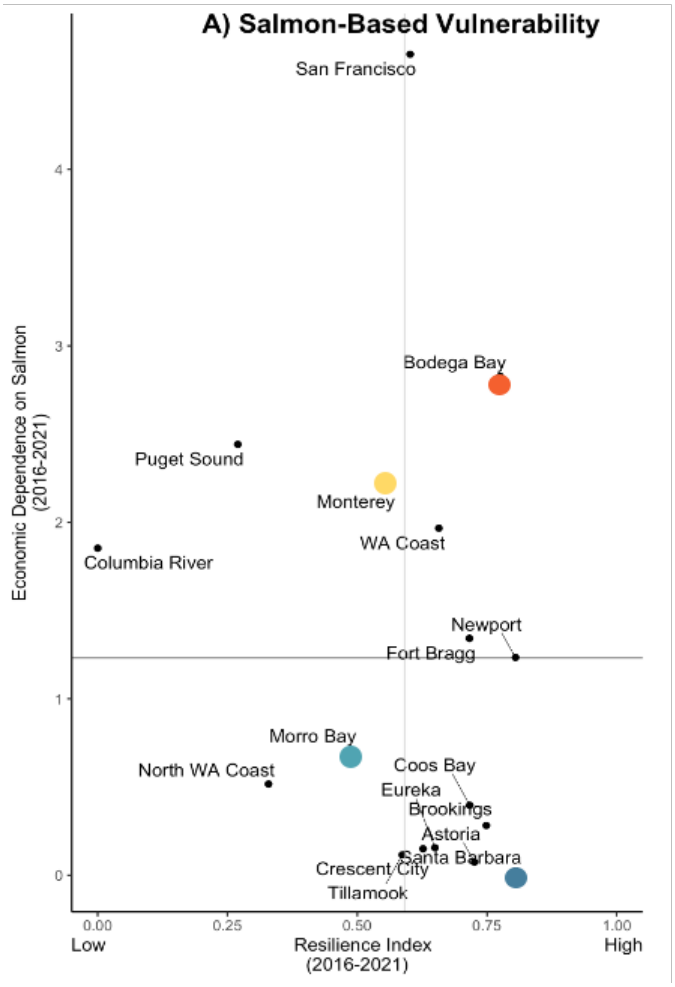

Figure U.2: Fisheries Participation Network (FPN) model metrics of overall port group fishery resilience (horizontal axis) and economic dependence on salmon (vertical axis) for IO-PAC port groups from the 2016/17 to 2021/22 fishing seasons. Ports in the upper left quadrant have relatively high economic dependence on salmon and lower overall resilience, while ports in lower right quadrant have lower dependence and high resilience. The four California ports groups presented in Figure 5.3 in the main document (Monterey, Bodega Bay, Morro Bay, Santa Barbara) are highlighted here using the same color scheme as Figure 5.3. See Harvey et al. 2023 for more information on this analysis.